

Some pages of this thesis may have been removed for copyright restrictions.

If you have discovered material in AURA which is unlawful e.g. breaches copyright, (either yours or that of a third party) or any other law, including but not limited to those relating to patent, trademark, confidentiality, data protection, obscenity, defamation, libel, then please read our [Takedown Policy](#) and [contact the service](#) immediately

**THE SEPARATION OF HYDROGEN AND
CARBON MONOXIDE USING POLYMER
MEMBRANES**

ANTHONY BERNARD HINCHLIFFE
Doctor of Philosophy

THE UNIVERSITY OF ASTON IN BIRMINGHAM
JANUARY 1991

This copy of the thesis has been supplied on condition that anyone who consults it is understood to recognise that its copyright rests with its author and that no quotation from the thesis and no information derived from it may be published without the author's prior written consent.

The University of Aston in Birmingham

SEPARATION OF HYDROGEN AND CARBON MONOXIDE USING POLYMER MEMBRANES

ANTHONY BERNARD HINCHLIFFE

Doctor of Philosophy

1991

SUMMARY

This work studies the development of polymer membranes for the separation of hydrogen and carbon monoxide from a syngas produced by the partial oxidation of natural gas. The CO product is then used for the large scale manufacture of acetic acid by reaction with methanol.

A method of economic evaluation has been developed for the process as a whole and a comparison is made between separation of the H₂/CO mixture by a membrane system and the conventional method of cryogenic distillation.

Costs are based on bids obtained from suppliers for several different specifications for the purity of the CO fed to the acetic acid reactor. When the purity of the CO is set at that obtained by cryogenic distillation it is shown that the membrane separator offers only a marginal cost advantage.

Cost parameters for the membrane separation systems have been defined in terms of effective selectivity and cost permeability. These new parameters, obtained from an analysis of the bids, are then used in a procedure which defines the optimum degree of separation and recovery of carbon monoxide for a minimum cost of manufacture of acetic acid. It is shown that a significant cost reduction is achieved with a membrane separator at the optimum process conditions.

A method of "targeting" the properties of new membranes has been developed. This involves defining the properties for new (hypothetical - yet to be developed) membranes such that their use for the hydrogen/carbon monoxide separation will produce a reduced cost of acetic acid manufacture.

The use of the targeting method is illustrated in the development of new membranes for the separation of hydrogen and carbon monoxide.

The selection of polymeric materials for new membranes is based on molecular design methods which predict the polymer properties from the molecular groups making up the polymer molecule. Two approaches have been used. One method develops the analogy between gas solubility in liquids and that in polymers. The UNIFAC group contribution method is then used to predict gas solubility in liquids. In the second method the polymer Permacor number, developed by Salame, has been correlated with hydrogen and carbon monoxide permeabilities. These correlations are used to predict the permeabilities of gases through polymers.

Materials have been tested for hydrogen and carbon monoxide permeabilities and improvements in expected economic performance have been achieved.

KEY WORDS:- Gas separation, Hydrogen, Carbon monoxide, Polymer membrane, Economic evaluation,

ACKNOWLEDGEMENTS

I would like to acknowledge all those who have helped me throughout the period of this work.

In particular I would like to thank my supervisor, Professor Ken Porter, for his help and direction.

I would also like to thank my co-supervisor Dr. Brian Tighe.

I am grateful to everyone in the Chemical Engineering and Applied Chemistry department, in particular I would like to thank Dr. Julie Pardoe.

I would like to thank Dr. Graham Pearce, formerly of B.P.Chemicals, for his help at the start of my work and Mr. Mark Carter of B.P.Chemicals who helped me greatly during the economic evaluation period of this project.

I would like to thank my family for the support they have given me, especially my mother and my sister, Tricia, for their help in word processing this thesis.

I would also like to thank B.P.Chemicals for sponsoring my work.

CONTENTS

	PAGE
SUMMARY	2
ACKNOWLEDGEMENTS	3
CONTENTS	4
LIST OF TABLES	9
LIST OF FIGURES	11
LIST OF SYMBOLS	14
INTRODUCTION	17
CHAPTER 1 LITERATURE REVIEW	22
1.1 Introduction	22
1.2 Gas separation applications for membranes	23
1.3 Alternative gas separation methods	24
1.4 Modelling of gas separation permeators and process design considerations	29
1.5 Methods of economic evaluation	39
1.6 Gas transport through polymer membranes	42
1.7 Permeability data	47
1.8 Permeability measurement	49
1.9 Conclusions	50

CHAPTER 2	APPROACH TO THE PROBLEM	51
2.1	Introduction	51
2.2	Economic evaluation	51
2.3	Optimum separation	52
2.4	Targeting	52
2.5	Molecular design of membranes	52
2.6	Permeability of membranes	53
2.7	Evaluation of chosen polymers	54
CHAPTER 3	ECONOMIC EVALUATION	55
3.1	Introduction	55
3.2	The process	56
3.3	Economic evaluation	60
3.4	Conclusions	87
CHAPTER 4	DETERMINATION OF COST PARAMETERS FOR OPTIMISATION OF MEMBRANE SEPARATION	90
4.1	Introduction	90
4.2	Effective selectivity and cost permeability	91
4.3	Crossflow model	93
4.4	Process Design	99
4.5	Correlation of bids	108
4.6	Conclusions	127

CHAPTER 5	DETERMINATION OF OPTIMUM SEPARATION BY EXISTING MEMBRANES	129
5.1	Introduction	129
5.2	Modelling the separation process	129
5.3	CO separation cost	133
5.4	Optimum separation specification	134
5.5	Conclusions	140
CHAPTER 6	TARGETING MEMBRANES FOR H ₂ /CO SEPARATION	142
6.1	Introduction	142
6.2	Targeting	143
6.3	Optimum separation specification	145
6.4	The targeting graph	154
6.5	Limiting values of effective selectivity and cost permeability	158
6.6	Conclusions	161
CHAPTER 7	MOLECULAR DESIGN OF POLYMER MEMBRANES	164
7.1	Introduction	164
7.2	Molecular design methods	166
7.3	Polymer selection	199
7.4	Consideration of other methods to improve membrane properties	200

CHAPTER 8	EXPERIMENTAL	204
8.1	Introduction	204
8.2	Polymer solutions	205
8.3	Membrane casting	205
8.4	Other polymer membranes used	207
8.5	The Davenport gas permeability apparatus	208
8.6	Experimental results	218
8.7	Conclusions	219
CHAPTER 9	EVALUATION OF MEMBRANES	220
9.1	Introduction	220
9.2	Economic evaluation	220
9.3	Correlation of permeability with Permachor number	225
CHAPTER 10	DISCUSSION	227
CHAPTER 11	CONCLUSIONS	236

CHAPTER 12	SUGGESTIONS FOR FUTURE WORK	245
12.1	Introduction	245
12.2	Membrane development	245
12.3	Consolidation	246
APPENDIX 1	ECONOMIC EVALUATION DATA	248
APPENDIX 2	SUMMARY OF SPREADSHEETS	255
APPENDIX 3	EXPERIMENTAL DAVENPORT PERMEABILITY PLOTS	270
REFERENCES		293

LIST OF TABLES

TABLE		PAGE
1.1	Advantages/disadvantages of separation processes	28
3.1	Bids for case 1	64
3.2	Bids for case 2	66
3.3	Bids for case 3	68
3.4	CO generation and separation costs for case 1	77
3.5	CO generation and separation costs for case 2	78
3.6	Comparative separation costs for case 1	80
3.7	Comparative separation costs for case 2	81
3.8	CO generation and separation costs for case 3	85
3.9	Comparative separation costs for case 3	86
4.1	Membrane area and recycle required for different process configurations and separation requirements	107
7.1	Published H ₂ and CO solubility in various liquids	169
7.2	Comparison of predicted solubility with published data for H ₂ and CO in liquids	172

7.3	GH ₂ /GCO ; SH ₂ /SCO and predicted solubility ratio of gases in polymers	172
7.4	Comparison of solubility selectivity of CO ₂ /CH ₄ with the predicted solubility ratio in liquids	174
7.5	Single group contributions for H ₂ and CO	175
7.6	Predicted solubility of groups when added to a pentyl group	177
7.7	Predicted solubilities of polymer analogues	179
7.8	Predicted and published permeabilities of H ₂ through various polymers	187
7.9	Predicted and published permeabilities of CO through various polymers	188
7.10	Polymer structures and their Permachor numbers	196
7.11	Polymers selected for testing	203
8.1	Experimentally determined permeabilities of H ₂ and CO through polymers	218

LIST OF FIGURES

FIGURE		PAGE
1.1	Permeator with perfect mixing on both sides	30
1.2	Permeator with co-current flow	31
1.3	Permeator with counter current flow	32
1.4	Crossflow permeator	33
1.5	Single stage permeator	36
1.6	Recycle permeator	37
1.7	Two stage cascade permeator	37
1.8	Series type two unit separator	38
1.9	Full continuous membrane column	38
3.1	Overall H ₂ /CO process being considered	59
4.1	Schematic diagram of asymmetric membrane	95
4.2	Differential element of crossflow permeator	95
4.3	Single stage permeator for H ₂ /CO separation	102
4.4	Single stage permeator with feed by-pass	102
4.5	Process configuration used by Suppliers B and C for high purity CO product	104
4.6	Process configuration used by Supplier A for high purity carbon monoxide product	104

4.7	Recycle permeator	106
4.8	Two stage separator without recycle	106
4.9	Two stage process with recycle used by Supplier A	112
4.10	Correlation of bids from Supplier A	115
4.11	Two unit series type permeator used by Supplier A	118
4.12	Correlation of bids from Supplier B	120
4.13	Correlation of bids from Supplier E	123
4.14	Process layout and flows for Supplier F	126
5.1	Two unit type recycle permeator	130
5.2	Comparative cost of CO sepn. Vs CO purity for Supplier A	135
5.3	Comparative cost of CO sepn. Vs CO rec. for Supplier A	136
5.4	Comparative cost of CO sepn. Vs CO purity for Supplier B	138
5.5	Comparative cost of CO sepn. Vs CO rec. for Supplier B	139
6.1	CO cost Vs CO recovery for various values of cost permeability with selectivity = 30	146
6.2	CO cost Vs CO recovery for various values of cost permeability with selectivity = 50	147
6.3	Optimum profile for CO rec. against effective selectivity	149
6.4	CO cost Vs CO purity for various values of G_c with selectivity = 30	151
6.5	CO cost Vs CO purity for various values of G_c with selectivity = 50	152
6.6	Optimum profile for CO purity against cost permeability	153

6.7	CO separation cost vs effective selectivity for various values of cost permeability	155
6.8	Targeting graph	156
6.9	Targeting graph with extended permeability range	157
6.10	Plot of CO sepn. cost Vs cost permeability showing limiting cost of separation	160
6.11	Targeting graph with Suppliers A and B marked on	162
7.1	Correlation of H ₂ permeabilities with polymer permachor number	191
7.2	Correlation of CO permeabilities with polymer Permachor number	192
7.3	Structure of Siloxy monomer used in the MMA-Siloxy co-polymer	202
8.1	Diagram of Davenport gas permeability apparatus	211
8.2	Diagram of overall process layout of equipment	212
9.1	Targeting graph showing position of PC, PMMA and PTFE	222
9.2	Targeting graph with extended permeability range showing position of MMA-Siloxy co-polymer	223
9.3	Plot of experimentally determined permeabilities for H ₂ and CO against polymer Permachor number	226
10.1	Targeting graph	232
11.1	Targeting graph	241

LIST OF SYMBOLS

Q	Flow. (sm^3/H)
Q_F, Q_R	Feed flow, retentate flow. (sm^3/H)
x_{iF}, x_{iR}	Mole fraction of component i in the feed or retentate respectively.
Y_i	Mole fraction of component i in the permeate stream.
\bar{Y}_i	Mean permeate composition. (Mol. frac.)
G	Permeability constant. ($\text{scm}^3.\text{cm}/\text{cm}^2.\text{s}.\text{(cmHg)}$)
G_i	Permeability of component i. ($\text{scm}^3.\text{cm}/\text{cm}^2.\text{s}.\text{(cmHg)}$)
G_C	Cost permeability. ($\text{sm}^3/\text{£k.H.Bara}$)
α^*	Ideal separation factor.
α_e	Effective selectivity.
l	Membrane thickness. (cm)
A	Membrane area. (cm^2)
P1	Feed pressure. (Bara)
P2	Permeate pressure. (Bara)
N	Flux. ($\text{scm}^3/\text{cm}^2.\text{s}$)
D	Diffusivity constant. (cm^2/s)
S	Solubility constant. ($\text{scm}^3/\text{cm}^3.\text{(cmHg)}$)
Ed	Activation energy for diffusion. (kJ/mol.)
ΔH_s	Enthalpy of solution of gas in polymer. (kJ/mol.)

T	Absolute temperature. (K)
R	Universal gas constant. (kJ/mol.K)
E _p	Activation energy for permeation. (kJ/mol.)
Π	Polymer Permachor number.
d	Molecular diameter for diffusion. (A)
e/k	Lennard-Jones potential. (K)
C	Unit cost of membrane plant. (£k/m ²)
C _{CH₄}	Natural gas feed cost. (£/te.CO)
C _{O₂}	Cost of oxygen. (£/te.CO)
C _{pox}	Amortised cost of POX reactor. (£/te.CO)
C _{sep}	Amortised cost of separation plant. (£/te.CO)
C _{comp}	Amortised cost of compressor. (£/te.CO)
C _g	CO generation cost. (£/te.CO)
C _{gbc}	CO generation cost for the base case. (£/te.CO)
C _p	Power cost. (£/te.CO)
C _s	CO separation cost. (£/te.CO)
C _{sc}	Comparative CO separation cost. (£/te.CO)
C _t	Total generation and separation cost. (£/te.CO)
V _{steam}	Value of steam generated. (£/te.CO)
V _{H₂}	Value of hydrogen by-product. (£/te.C)

V_p	Value of purge gas.	(£/te.CO)
C_{inst}	Fully installed cost.	(£/te.CO)
F_{inst}	Installation factor.	
F_{ind}	Indirect cost factor.	
C_Q	Quoted cost.	(£k)

INTRODUCTION

Gas separation using polymer membranes is becoming an increasingly important process. The growing interest in the field was well illustrated at the Priestley Conference in 1986. Recent developments in alternative gas separation methods has shown that they are becoming more competitive with conventional gas separation processes such as distillation and gas absorption. For example, it can be viable to use pressure swing adsorption for the separation of the permanent gases instead of using cryogenic distillation.

However, the cost effectiveness of the separation process depends on the properties of the separating material. The development of new materials for gas separation has conventionally been by intuition or by trial and error.

With advances in the molecular sciences it is conceivable that at some time in the future new materials could be designed for a particular separation process.

First, however, it is necessary to determine how the cost of the process depends on the properties of the separating material. In general, for membrane systems, it is found that membranes with high permeability have low selectivity and vice versa.

This thesis describes a method of setting targets for the selectivity and permeability of membranes to be used for the separation of hydrogen (H_2)

and carbon monoxide (CO).

The work, carried out in cooperation with B.P.Chemicals, is concerned with the separation of hydrogen and carbon monoxide from a syngas. The CO product is then used for the large scale manufacture of acetic acid by reaction with methanol.

Another area of interest is the production of acetic acid by direct combination of CO and H₂. This would lead to a requirement for the syngas ratio adjustment to an H₂:CO ratio of 1:1.

The syngas for the process is generated by the partial oxidation (POX) of natural gas in a POX reactor at approximately 850°C and 45 bara.

To achieve the successful development of new gas separation membranes for the separation of H₂ and CO which may be of commercial interest, a number of questions concerning the economics must be addressed.

How do the separating properties of membranes, the selectivity and permeability, affect the separation costs of the process? And how can different membrane systems be compared with each other and with other methods of gas separation?

Initially an economic evaluation was carried out.

The economic evaluation of the separation processes involved approaching

suppliers of membrane plant and of other separation methods, such as cryogenic distillation. The membrane system and cryogenic plant suppliers were asked to bid for various separation specifications. These bids provided a realistic source of cost data for the work that followed. This gave a comparison of capital costs and operating costs for the separation units alone, but to obtain a true comparison of each separation system the process as a whole, taking into account the process upstream (the syngas generation process) and downstream (the acetic acid production process) of the separation unit, must be considered.

The results of this study showed that membrane separation gave only a marginal advantage over the conventional cryogenic separation using the same high purity and recovery specification which is easily achieved by the cryogenic process. But the total cost of manufacturing acetic acid turned out to be lower with a membrane system in comparison with cryogenic distillation if the specification of CO purity and recovery was relaxed. This raises the question, is there an optimum separation specification for a membrane system?

New cost parameters were developed in terms of effective selectivity and cost permeability by analysing the bids in terms of a theory of membrane design and modelling the membrane separation process.

Having developed a method of evaluation which puts each system on an equal footing and having established cost parameters which characterise the membrane systems, the optimum specification could be determined for the commercial membrane systems.

The next questions to be asked are : What are the properties which a new membrane requires to be competitive? And how do you find new membrane materials with enhanced properties?

This thesis introduces the new concept of targeting, that of using economic evaluation to set targets for the properties of new (hypothetical - yet to be developed) membranes and explains how the targeting approach can be used in the development of new membranes for the separation of H₂ and CO on a commercial scale.

Combining the economic evaluation methods and modelling of the membrane process using the cost parameters at the optimum separation specification, it is possible to set targets for membrane properties. This has been done by drawing iso-cost lines on a plot of selectivity and permeability. The "targeting" approach shows the economic gains to be expected from increases in selectivity and/or permeability.

There is only a limited amount of permeability data available for hydrogen and carbon monoxide. However, methods to predict gas solubility in liquids, based on molecular groups, have been used for the development of gas absorption solvents with some success. Can molecular design methods, using molecular group contributions, be used to design and select new membrane materials with enhanced separation properties?

Ideally it would be desirable to be able to predict with confidence the selectivity and permeability of gases through polymers from molecular

structure. At this stage, however, there is no satisfactory theory for the separation of gases by polymers. The use has been made of some empirical methods to predict the transport properties of gases through polymers.

Two methods of property prediction have been used :-

1. The use of the UNIFAC group contribution method for the prediction of gas solubility in liquids, combined with the analogy that can be made between gas solubility in liquids and gas solubility in polymers.
2. The development of a correlation between the polymer "Permachor" number and the permeability of hydrogen and carbon monoxide.

Candidate polymers were selected for testing based upon the molecular design methods used above. Other polymers were selected from a knowledge of polymer structure/property relations, with the aim of combining properties using co-polymers. A number of other suggestions were also considered.

Polymer membranes were made or obtained from manufacturers and hydrogen and carbon monoxide permeability measurements taken.

The targeting analysis was then extended into a method to evaluate the new membrane materials. One of the new materials is likely to produce a significant reduction in the cost of manufacturing acetic acid by the process considered. The results of the work show in what direction future work should continue to make even larger savings.

CHAPTER 1

LITERATURE REVIEW

1.1 Introduction

The literature review was carried out from the point of view of considering three main questions.

1. Do membranes have a place in gas separation currently and what are the alternative methods of hydrogen/carbon monoxide separation available?
2. How can the hydrogen/carbon monoxide membrane separation be evaluated? This requires a knowledge of the process design and modelling of the membrane separation process as well as the methods used in economic evaluation.
3. How can new membranes be developed for the hydrogen/carbon monoxide separation? This requires an understanding of current theories of gas transport through membranes and currently available gas transport data

for hydrogen and carbon monoxide through polymeric materials.

Methods of permeability measurement are required for experimental determination of gas transport properties of polymers so these must be reviewed.

1.2 Gas Separation Applications For Membranes

Current applications for gas separation using membranes are quite limited. This is because of the intrinsically low permeability of most gases through membranes and the often low selectivity of the membranes for many commercial applications. As membranes have become more competitive over the past thirty years or so, with the advent of the asymmetric membrane and better membrane packing arrangements, they have, under certain circumstances become the most suitable separation method for some applications. This has been well demonstrated by Monsanto's "Prism" membrane.

Membrane gas separation processes are used where the gas to be separated has a high permeability when compared with the gases it is to be separated from. There are a number of examples of hydrogen separation from other gases (26,49,86,135,136); the recovery of hydrogen from hydrogenation, ammonia and methanol purge gases can produce high purity hydrogen with

recoveries of better than 90%. Helium is also a "fast" gas and membranes can be used to recover it from natural gas (165).

Membranes have also found applications for the removal of carbon dioxide from natural gas for enhanced oil recovery, and the removal of acid gases and moisture for natural gas purification (26,37,49,84,92,127,135,136).

Membranes can also be competitive with alternative methods of gas separation where only a partial separation is required. For example the oxygen or nitrogen enrichment of air (136), or in the particular case with which this thesis is concerned, the separation of carbon monoxide and hydrogen, where only syngas ratio adjustment is needed.

It is of course necessary to consider the alternative methods for gas separation to establish whether membrane separation is competitive.

1.3 Alternative Gas Separation Methods For Separation Of Hydrogen And Carbon Monoxide

Distillation is the most widely used process for the separation of industrial gases. Frequently other methods have only been considered when the separation is impossible to achieve by distillation. Distillation has many

advantages over other separation methods, such as the great economies of scale which can be made and the vast amount of experience in the design and operation of distillation processes which has been built up over the past 100 years. Distillation also has a significant advantage where the product is required at high purity (119).

The process currently used for the large scale separation of hydrogen and carbon monoxide is cryogenic separation. Before the separation can be carried out all the moisture and carbon dioxide has to be removed, otherwise these would freeze out and block the separation unit. The CO₂ is removed using a MEA wash unit which brings the CO₂ level down to 50 vpm. The remaining CO₂ and any moisture is then removed in a molecular sieve drier.

The dry, CO₂ free gas is then passed to the cold box where it is cooled by heat exchange with the outgoing products. The H₂/CO separation is achieved by successive partial condensation of the CO and the flashing of H₂ dissolved in the liquid CO. The CO is re-evaporated at low pressure and compressed to the required product pressure, which is approximately 40 bara. A high purity product is easily achieved, typically 97% pure carbon monoxide.

The cold required to operate the process is provided by the hydrogen rich tail gas which is expanded through turbines.

However, as this process needs to be operated at elevated pressure and the process streams have to be cooled to cryogenic temperatures, increasing energy costs and development in other areas could lead to new methods being more competitive.

The processes which offer competition to distillation for the H₂/CO separation include gas absorption and membrane gas separation.

1.3.1 Gas Absorption

Carbon monoxide is only slightly soluble in physical solvents even at high pressure. So the basis of the gas absorption process is that the solvent chemically absorbs the CO from the feed gas whereas it only physically absorbs other gases present.

The CO Sorb process uses Copper Aluminium Chloride in Toluene to chemically absorb the CO at elevated pressure (32). The other components in the syngas, eg. H₂, CO₂ and CH₄, are only physically absorbed with much lower bond strength.

Once the solvent has contacted the synthesis gas the solvent is flashed to a lower pressure to release H₂ and other impurities. The solvent is then

reboiled to release the CO at low pressure.

The system can produce high purity CO, but cannot tolerate water, methanol or formic acid impurities. As for the cryogenic distillation process, the CO sorb process produces a CO product at low pressure which then has to be compressed to the 40 bara pressure required.

1.3.2 Membrane Separation

The separation of hydrogen and carbon monoxide using a membrane, takes a feed at high pressure and passes it on one side of a thin polymer film or hollow fibre.

The hydrogen permeates through the membrane faster than the CO. Thus the permeate, which is at low pressure, is enriched in hydrogen and the retentate, at high pressure, is enriched in CO.

To produce a high purity product recompression and the use of more than one stage is required.

The CO product from this process is produced at high pressure.

TABLE 1.1**Advantages/Disadvantages of Separation Processes**

PROCESS	ADVANTAGES	DISADVANTAGES
Cryogenic	Easily achieved separation for high purity CO product. Large amount of experience in this field.	Requires removal of all moisture and CO ₂ . CO product has to be compressed.
Chemical Absorption. (CO Sorb.)	High purity product can be obtained.	License for process has to be bought. High solvent and utility costs CO product has to be compressed. Moisture removal is required. Process is difficult to operate.
Membranes.	Simple process. Process can tolerate moisture (above dew point) and CO ₂ . CO product produced at high pressure.	Difficult to achieve high purity without recycle. Uncertain membrane life, may be only about 5 years.

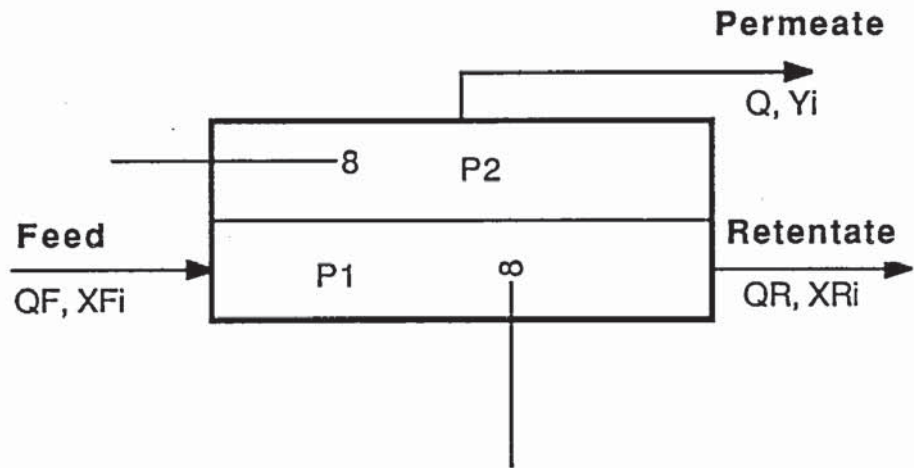
1.4 Modelling of Gas Separation Permeators and Process Design Considerations

In order to be able to carry out the design of gas separation membrane modules it is necessary to be able to model what happens inside the permeator. Initial studies made many assumptions about the flow patterns in permeator modules. Permeator performance was modelled assuming perfect mixing on both sides of the membrane, co-current, counter current and crossflow patterns (25,28,59,62,104,146,161,165). The assumption of perfect mixing on both sides of the membrane yields a simple solution to the governing mass transfer equations. However it is unlikely ever to be true in any practical case.

Figures 1.1 to 1.4 show diagrams of permeators with perfect mixing, co-current, counter current and crossflow patterns.

FIGURE 1.1

Permeator With Perfect Mixing on Both Sides of the Membrane



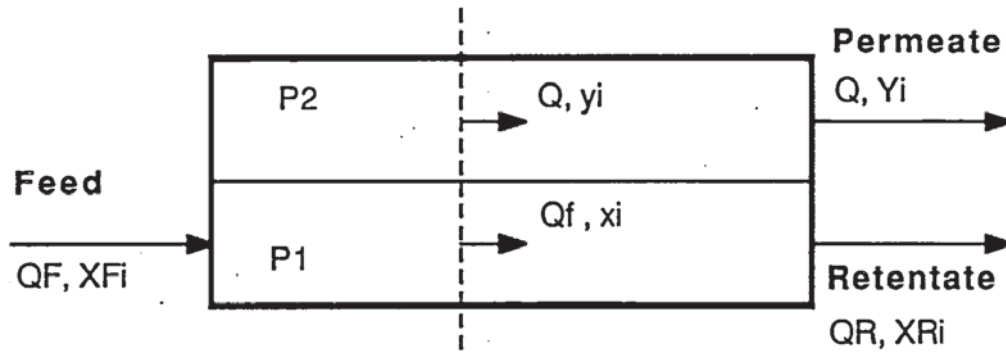
For a binary mixture :-

$$Q_F \cdot X_{Fi} - Q_R \cdot X_{Ri} = (G_i/l) \cdot A \cdot (P_1 \cdot X_{Ri} - P_2 \cdot Y_i) = (Q_F - Q_R) \cdot Y_i$$

$$Q_F \cdot (1 - X_{Fi}) - Q_R \cdot (1 - X_{Ri}) = (G_j/l) \cdot A \cdot (P_1 \cdot (1 - X_{Ri}) - P_2 \cdot (1 - Y_i)) \\ = (Q_F - Q_R) \cdot (1 - Y_i)$$

FIGURE 1.2

Permeator With Co-current Flow



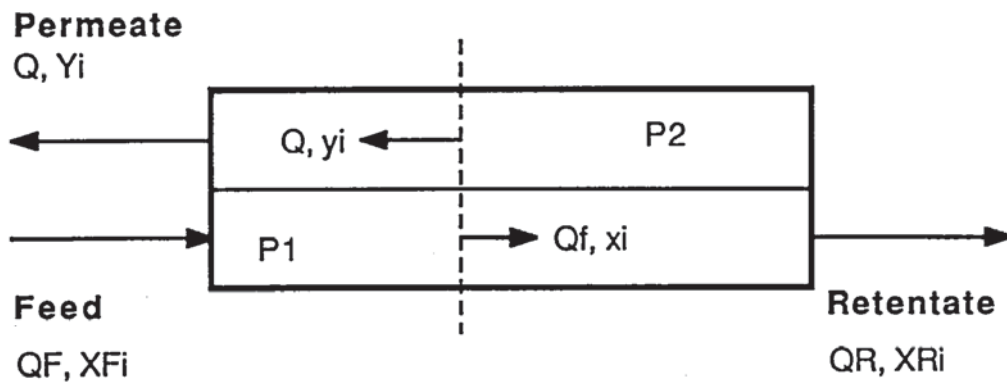
For a binary mixture :-

$$\frac{-d(Qf \cdot xi)}{dA} = \frac{Gi \cdot (P1 \cdot xi - P2 \cdot yi)}{l} = \frac{d(Q \cdot yi)}{dA}$$

$$\frac{-d(Qf(1 - xi))}{dA} = \frac{Gj \cdot (P1(1 - xi) - P2 \cdot (1 - yi))}{l} = \frac{d(Q(1 - yi))}{dA}$$

FIGURE 1.3

Permeator With Counter Current Flow



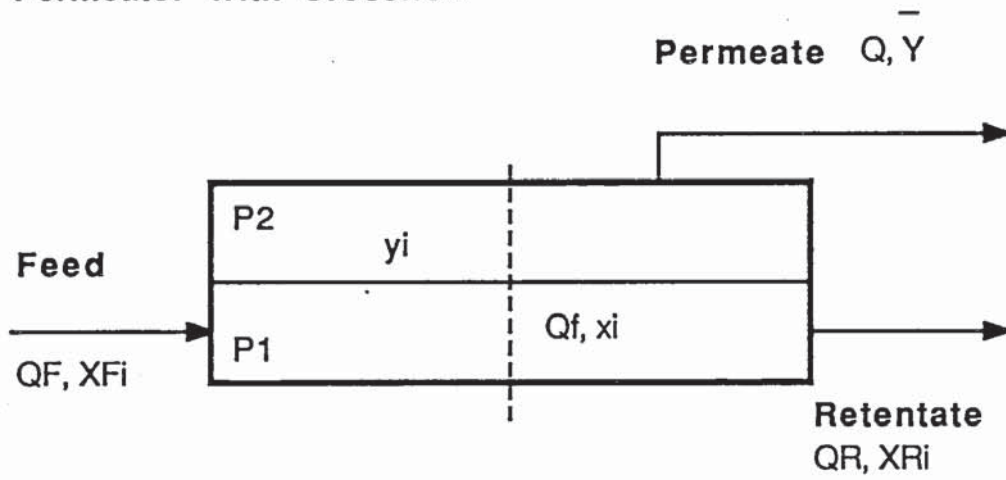
For a binary mixture :-

$$\frac{-d(Qf.xi)}{dA} = \frac{Gi.(P1.xi - P2.yi)}{l} = \frac{-d(Q.yi)}{dA}$$

$$\frac{-d(Qf(1 - xi))}{dA} = \frac{Gj.(P1(1 - xi) - P2.(1 - yi))}{l} = \frac{-d(Q(1 - yi))}{dA}$$

FIGURE 1.4

Permeator With Crossflow



For a binary mixture :-

$$\frac{-d(Qf.xi)}{dA} = \frac{G_i.(P1.xi - P2.yi)}{l} = \frac{d(Qy_i)}{dA}$$

$$\frac{-d(Qf(1 - xi))}{dA} = \frac{G_j.(P1.(1 - xi) - P2.(1 - y_i))}{l} = \frac{d(Q(1 - y_i))}{dA}$$

Modelling the permeator on co-current, counter current or crossflow patterns yield more complex mathematical problems, and all the references sited above (25,28,59,62,104,146,161,165), required the use of numerical methods to solve the ruling differential equations. Walawender and Stern developed the problem further by considering parametric analysis of co-current and counter current models (161).

Currently membrane gas separation is achieved using asymmetric or ultrathin composite polymer membranes. In this type of membrane it is generally thought that the flow pattern for separation will be crossflow, regardless of the overall directions of flow in the module, as long as the dense (active) layer of the membrane is on the high pressure side. Here the gas permeating through the membrane is forced to travel perpendicular to the membrane surface, through the porous support layer (130). Also recently (Saltonstall, 1987) an analytical solution to the mass balance equations for the crossflow model has been achieved (130). This allows savings in computer time and contributes to a greater insight into the separation process.

Many studies have concentrated on the modelling of hollow fibre membrane modules as this packing arrangement allows the largest membrane area per unit volume. Models have been developed by Pan and Habgood which incorporate the effects of permeate pressure drop (111) and by Thorman and Hwang which considers the deformation of polymer fibres (154), which are

particular areas of concern in hollow fibre permeators. More general models limit their scope to process and design variables (7,34,110,155).

As most commercial separations have to be carried out by multiple stage membrane processes, another question which has to be addressed is:- which is the best process layout for a particular gas separation? This question has largely been considered on the basis of each individual separation, comparing different process layouts (52,64,88,91,109,124). A number of different process layouts have been considered, and these include the following.

FIGURE 1.5

Single Stage Permeator.

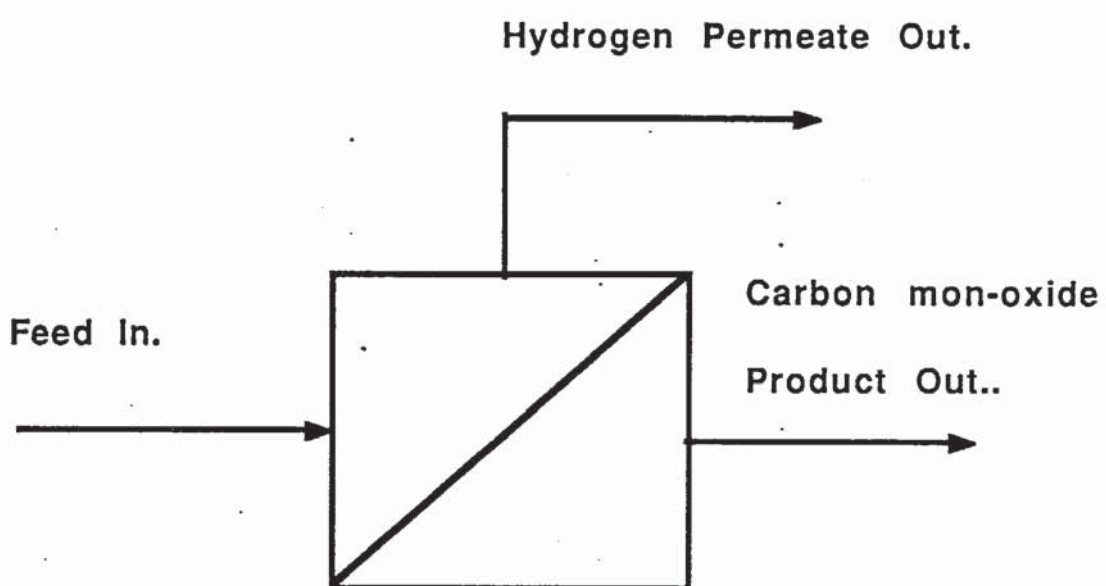


FIGURE 1.6
Recycle Permeator.

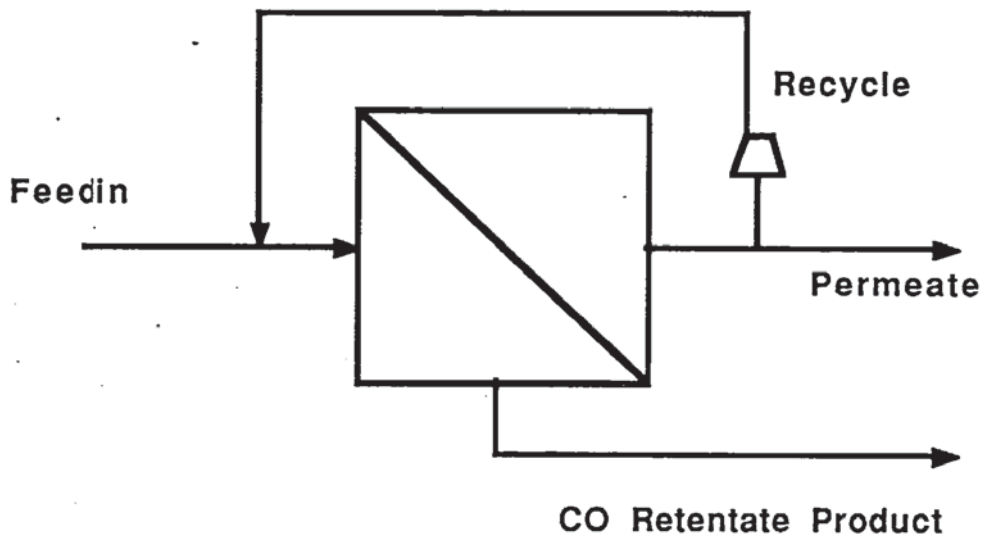
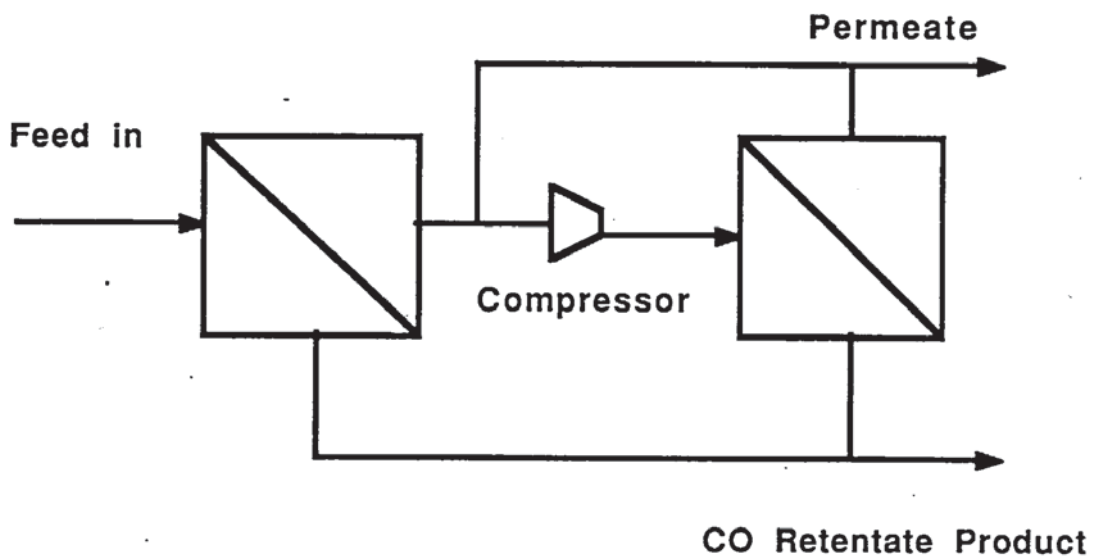


FIGURE 1.7
Two Stage Cascade Permeator



The same process layouts are considered by many workers to consider different separations, making the same conclusions. None of the above have considered three unit separators except for the straight forward serial fed separator, which requires more than one compression stage. Also general strategies for process design have not been developed. Further consideration of this question for carbon monoxide and hydrogen separation will be given in chapter 4 of this thesis.

To compare different methods to separate hydrogen and carbon monoxide or different process layouts, the economics of the process must be considered.

1.5 Methods of Economic Evaluation

Economic evaluation of projects is carried out so that a comparison can be made between different processes to manufacture a product and to assess the cost of the product.

The evaluation can be carried out with varying degrees of accuracy, depending upon what the evaluation is being made for and how much information is available about the processes under consideration. The economic estimates will never be totally accurate because between 25 and 40% of the costs involved are indirect costs and are very difficult to quantify.

The economic evaluation can be presented in various ways. The projects can be viewed in terms of profitability, showing the expected rate of return on investment. Alternatively, a minimum acceptable rate of return can be used to calculate the cost of manufacture of the product.

For continuous processes the fixed investment cost is usually the major factor influencing the manufacturing cost (117). Estimates of the fixed investment can be obtained from various sources. Order of magnitude cost estimates, which provide complete plant costs from detailed information of previous projects, can be obtained to within 10 - 50%. Study estimates are used to assess the economic feasibility of a project before any major expenditure is undertaken. These estimates are usually to within 30%. Budget cost estimates are more accurate than study estimates and hence require more detailed information. Budget cost estimates calculate costs to within 20% error. Where more detailed information is available a project control estimate can be made and is to within 10%. The most accurate costing is a "firm" estimate which requires the total detailing of the project.

Other factors which influence the manufacturing cost are raw material costs, utility costs, labour costs and maintenance costs as well as the previously mentioned indirect costs.

From this data the manufacturing cost or transfer price of the product can be

calculated.

Simple and quick methods for evaluating projects and new processes, without the necessity for detailed design and costing have been developed (2,120,142,169,173).

Ingeleby, Rossiter and Douglas (68) considered the economic tradeoffs which may exist between the reactor and recycle. This is of particular interest to this work, which takes into account the process as a whole, and where there are a number of tradeoffs which can be made.

Economic evaluations usually evaluate existing processes and systems to establish whether they are economically competitive. An alternative approach has been taken in this work. The evaluation has been carried out to consider the properties which are required by the membrane gas separation process for the hydrogen / carbon monoxide separation, such that the process will be competitive with other separation methods.

The Process Evaluation Group at B.P. Chemicals in Hull has a great deal of cost data and reports relevant to this project which have been referred to (30 - 32 and 113). This included the capital cost of the POX reactor for the generation of hydrogen/carbon monoxide syngas and the composition of the syngas. The cost of raw materials and services. Cost correlations for

compressors and scale up formulae for plant and equipment. Also made available was the mass balance for the cryogenic separation process for hydrogen and carbon monoxide used on B.P.Chemicals A5 project. (See appendix 1).

1.6 Gas Transport Through Polymer Membranes

The permeation of gases through polymer films is understood to be a solution/diffusion process. That is, initially the gas dissolves in the polymer and then diffuses through the polymer matrix (125).

For rubbery polymers the sorption of gases obeys Henry's law, such that there is a linear relationship between the gas partial pressure and concentration in the solid. The diffusion of the gas through the polymer also bears a linear relationship to the concentration of the gas at the membrane interfaces, as Fick's law states.

Thus the steady state flux, N , can be stated as :

$$N = \frac{D.S.(P_1 - P_2)}{l} \quad (1.9)$$

D = Diffusion coefficient .

S = Solubility Coefficient.

P₁, P₂ = Partial pressure of gas on the high and low pressure sides of the membrane respectively.

l = Membrane thickness.

$$G = D.S \quad (1.10)$$

G = Permeability constant.

Hence :-

$$G = \frac{N.l}{(P_1 - P_2)} \quad (1.11)$$

The sorption and diffusion of gases through rubbery polymers has been compared to the absorption and diffusion of gases through liquids (76).

The permeability of gases through glassy polymers shows some deviation from predictions based on Henry's law for solubility and Fick's law of diffusion.

Theories have been developed to explain these deviations, for example (14-17 and 42). The theories which are largely accepted and provide the most useful means of predicting permeability behaviour at various pressures, are the dual mode sorption theory, and the partial immobilisation theory of diffusion. Many studies carried out by Barrer, Barrie, Koros and others strongly support these theories (8,13,35,75,77,78,97,98,147,160,170).

Further deviations from the simple solution/diffusion mechanism of permeation

occur when there are mixed gases. Here the gases may have to compete for solution sites. These deviations have also been explained in terms of the dual mode theories (35,73,74,132). The effect of orientating polymers, upon permeability and separating properties has been studied (159).

The effect of temperature upon the permeability of gases through polymers is an Arrhenius type relationship. This is governed by the enthalpy of solution of the gas in the polymer, ΔH_s , and the activation energy for diffusion, E_d (123,148).

$$D = D_0 \cdot \exp - ((E_d) / R.T) \quad (1.12)$$

$$S = S_0 \cdot \exp - ((\Delta H_s) / R.T) \quad (1.13)$$

$D_0, S_0 = \text{constants.}$

$R = \text{Universal gas const.}$

$T = \text{absolute temperature.}$

Let :

$$G_0 = S_0 \cdot D_0 \quad (1.14)$$

And :

$$E_p = \Delta H_s + E_d \quad (1.15)$$

Then :

$$G = G_0 \cdot \exp - ((E_p) / R.T) \quad (1.16)$$

The separation of gases using polymer membranes can be achieved because different gases permeate through polymers at different rates (75). This means that a gas mixture is enriched in the fast permeating gas on the low pressure, permeate, side of the membrane and enriched in the slow permeating gas on the high pressure, retentate, side.

An initial measure of how good a membrane is at separating two gases is the ideal separation factor, α^* . The ideal separation factor is the ratio of the permeability of the fast permeating gas to that of the slow permeating gas.

$$\alpha^* = G_a / G_b \quad (1.17)$$

G_a, G_b = permeability of the fast and slow gases respectively.

Gas separation using polymer membranes was an unattractive method until the integrally skinned asymmetric and ultrathin supported membranes were developed (48,141). This allowed the active layer to be made much thinner

than had previously been possible with dense homogeneous polymer membranes (149). The flux achievable was consequently increased by a factor of around twenty. Further improvements were made in the packing arrangements of membranes with the development of spiral wound and hollow fibre membranes. With the significant advances in producing reliable asymmetric membranes, concentration has turned to the improvement of selectivity and permeability of membranes by modifying the molecular structure of the polymer. Studies have been carried out making systematic modifications to the polymer structure (33,51,76,150).

The enhancement of properties of polymers for gas separation has been considered by studying the solubility and diffusivity of gases in polymers separately. One method which has been used is to draw the analogy between the solubility of gases in liquids and the sorption of gases in polymers. The magnitude of gas solubility in polymers is much less than in liquid (75). However, the solubility selectivity of a liquid to two gases is remarkably close to that of the analogous polymer. It is useful to be able to use this analogy because there is much more information available for gas solubility in liquids (21 - 23,54,55,71,164,167,168), than in polymers.

A large amount of data on the solubility of gases in liquids has been collected by Wilhelm and Battino. Also reliable methods for the prediction of gas solubility in liquids based upon the UNIFAC group contribution method have

been developed by Sanders et al (134). Work carried out by Sithioth at Aston University using methods based upon the UNIFAC group contribution method to design a solvent for gas absorption also proved to be successful (140).

A method for predicting the gas permeability of polymers has also been developed using group contributions. This method by Salame,(128) incorporates the cohesive energy density and specific volume of the polymer and the condensability and the molecular diameter of the gas. The data required for the polymer groups has been built up by Salame and the gas properties are available in the literature (58,118).

1.7 Permeability Data

Relatively abundant data are available for oxygen, nitrogen and carbon dioxide permeabilities through many polymers, this being the information required about barrier materials.

Permeability data for H_2 has been reported by Barrer and Chio, van Amerongen, Simril and Herschberger, and Yasuda and Rosengren. CO permeability data has been reported by Michaels and Bixler. With this information it is frequently possible to find the permeability for either H_2 or CO but seldom for both.

McCandless (89) and Henis and Tripodi (56) have carried out measurements for both H₂ and CO on a range of polymers.

McCandless's data on fourteen polymers shows a dramatic drop in the selectivity to H₂/CO when the temperature is raised above the glass transition temperature of the polymer.

Permeability data for H₂ and CO is also available for most of the commercially marketed membranes.

The permeability of hydrogen through metals (69) is also of interest, and a study of gas permeability through Palladium coated Poly(ethyleneterephthalate) has been carried out by Mercea et al. (96). This showed the metal coated membrane to be a very good barrier to helium, carbon dioxide, nitrogen and argon, reducing the permeability considerably when compared with the uncoated film. The permeability of the hydrogen through the metal coated film was virtually unchanged.

The amount of permeability data available for hydrogen and carbon monoxide is limited. A knowledge of currently used techniques for the measurement of gas permeability will be needed for new membranes.

1.8 Permeability Measurement

There are basically three ways that pure gas permeabilities are measured directly:- 1. Pressure is held constant, and the volume is variable as in the Linde cell.

2. Volume is constant and the pressure is allowed to vary, as in the Dow cell and the Davenport cell (41).

and 3. Where both the pressure and volume are constant and a carrier gas is used to "sweep" the permeate gas away (125).

Gas permeability can also be measured indirectly by measuring thermal conductivity (172) and electrical properties. Several methods of measuring mixed gas permeabilities and high pressure equipment have been described, e.g. by K.C.O'Brien et al (107).

Using data from the transient period of the experimental methods above (125) it is possible to calculate the solubility of the gas in the polymer and hence obtain values for the solubility and diffusivity separately. Other methods have been used to obtain solubility data alone, such as the method used by L.Iler (67). Here an isolated sample of polymer is exposed to the desired penetrant at a controlled pressure and the solubility characteristics are measured gravimetrically.

1.9 Conclusions

There is a need to assess the currently available membrane gas separation systems for the hydrogen/carbon monoxide separation being considered.

For membrane development it would be appropriate to target the properties required by new membranes, such that they would be economically competitive, before carrying out membrane development work.

The available hydrogen/carbon monoxide permeability data is useful and can assist the use of the molecular design methods based on molecular groups for the permeability prediction of polymers.

CHAPTER 2

APPROACH TO THE PROBLEM

2.1 Introduction

The approach described below was developed at different times during the research work. Nevertheless it is appropriate at this point to summarise the different stages in the work that follows.

2.2 Economic Evaluation

An economic evaluation of the use of commercially available membranes to separate hydrogen and carbon monoxide in a plant for the production of acetic acid was carried out. This was done under the auspices of B.P. Chemicals and was based on achieving the same degree of separation as that obtained in other plants using cryogenic distillation.

2.3 Optimum Separation

The whole process from hydrogen/carbon monoxide syngas generation to the acetic acid production is optimised for the process using a membrane separator. The optimisation is carried out in terms of optimum degree of separation and loss of product, to produce the lowest cost. This requires the defining of commercially available membranes in terms of cost factors for selectivity and permeability.

2.4 Targeting

The development of a method for "targeting" the properties for new (hypothetical - yet to be developed) membranes such that using them for the separation of hydrogen and carbon monoxide will produce a reduced cost of acetic acid manufacture. The targeting method indicates the best direction for membrane development.

2.5 Molecular Design Of Membranes

The selection of polymers has been made using methods to predict the properties of polymers. Two methods, both based on molecular groups, have been used. These methods have been used for the molecular design of new

polymer membranes.

The first method used was to take the analogy of gas solubility in liquids with gas solubility in polymers. And with methods already developed to predict gas solubility in liquids, the solubility selectivity is predicted for a liquid and this is extended to the analogous polymer.

The second method used was to build up a correlation based upon the Permachor method used by Salame, to predict the permeabilities of hydrogen and carbon monoxide through polymers. This method allows the permeability and selectivity to be predicted for polymers from groups contained in the repeat unit. Molecular design of polymers with the required properties can then be carried out.

2.6 Permeability of Membranes

Membranes were made from polymers which had been chosen on the basis of the molecular design methods and the permeabilities of hydrogen and carbon monoxide were measured on the Davenport gas permeability apparatus. This yielded the pure gas permeability of the polymer and the ideal separation factor.

2.7 Evaluation of Chosen Polymer

The evaluation of new polymer membrane materials was made by locating the experimentally determined separation factor and permeability on the targeting graph developed previously. This gives an estimated cost for the separation of CO from the syngas using the new membrane.

CHAPTER 3

ECONOMIC EVALUATION

3.1 Introduction

To carry out an economic evaluation of the separation of hydrogen and carbon monoxide it is necessary to have some knowledge of the overall process being considered.

The economic evaluation was carried out to establish what membrane separation systems are available and whether they are economically competitive with the currently used cryogenic separation process.

To ensure that the information obtained from suppliers was commercially valid, the enquiries were made under the auspices of B.P. Chemicals.

To get an understanding of the factors which influence the economics of the separation process a comparison of capital cost and power requirements is made from bids. However, how do we find out which are the factors which affect the process as a whole? consideration must be given to the separation

specification required and to the properties of the membrane plant which affect the process economics.

3.2 The Process

Production of Acetyls within B. P. Chemicals is presently based upon reactions between CO and Methanol. This means there is a need for large scale production of CO.

Active research is also being carried out to produce Acetic Acid and other acetyls by direct reaction between CO and H₂. Whilst this is not feasible at the moment, there is still a great deal of interest in being able to produce a syngas with H₂:CO ratio of 1:1.

Currently the methods of producing CO available are either by reforming or partially oxidising a feedstock of natural gas or oil (113).

These processes produce a syngas of H₂ and CO as well as impurities, which depends on the type of feedstock used. To obtain pure CO or a syngas with H₂:CO ratio of 1:1, the gas has to be cleaned and then separated to the required purity.

Various processes exist to separate H₂ and CO and these include:-
Cryogenic separation, Chemical absorption, and Membrane separation.

This evaluation is concerned with comparing membrane separations with competing processes and evaluating the commercially available membrane systems for the separation of H₂ and CO.

For the purposes of the evaluation a feed from a non-catalytic partial oxidation (POX) reactor with a natural gas feedstock was used. The POX reactor operates at about 850°C and 45 bars. The typical specification from the POX reactor is as follows:-

H ₂	0.626 mol. frac.
CO	0.337 mol. frac.
CO ₂	0.031 mol. frac.
CH ₄	0.003 mol. frac.
N ₂	0.003 mol. frac.

The figures above are on a dry gas basis and the gas is saturated at 45°C and 40 bara (30).

The feed syngas is then pretreated as required before going to the H₂/CO separation process. The by-product of the separation is a hydrogen rich

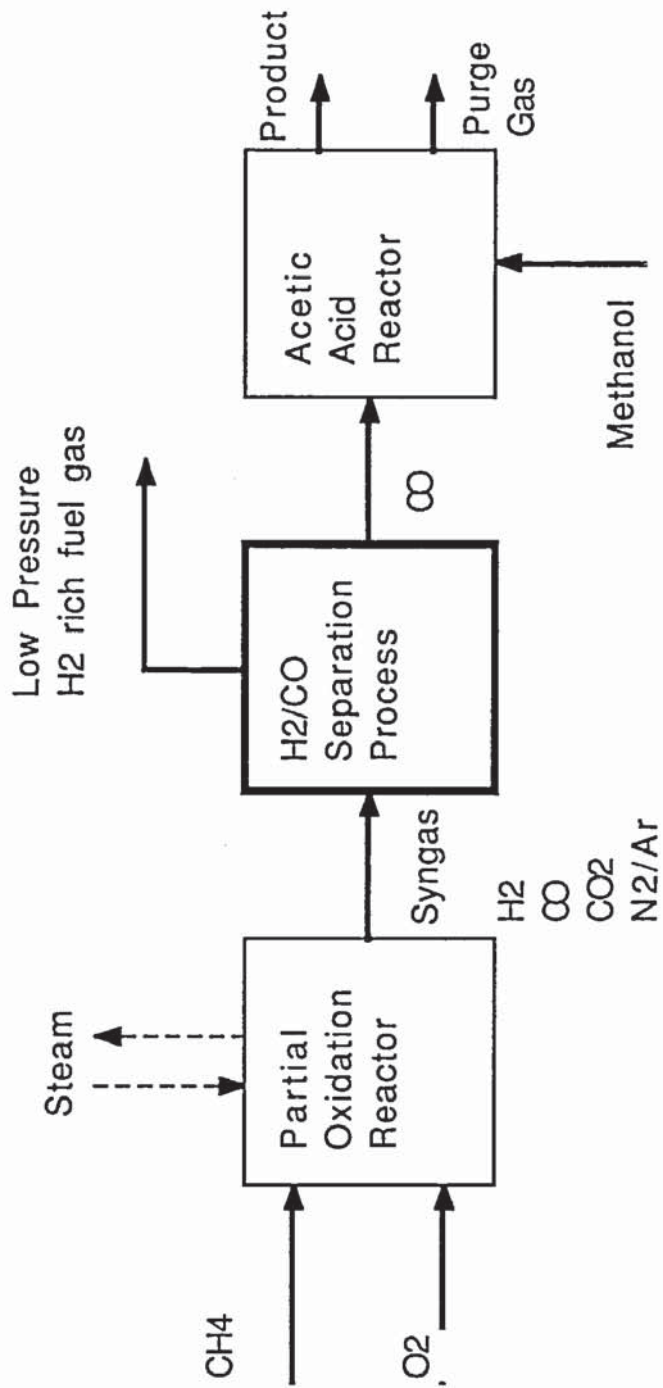
stream which is used as a fuel gas.

The CO product, which is required at a pressure of around 40 bara, is then used as a reactant in the downstream acetic acid reactor.

Figure 3.1 illustrates the process as a whole.

Figure 3.1

The Overall Process



3.3 Economic Evaluation

3.3.1 Separation Specification

The economic evaluation was carried out to compare commercially available membrane separation systems and to compare membrane systems with cryogenic separation systems. In order to ascertain as much information as possible the enquiries were kept very broad. And so suppliers were asked to consider three separation specifications.

CASE 1. Plant to supply 100,000 Tonnes per annum of 97% pure CO at a pressure of circa 40 bara.

CASE 2. Plant to supply 100,000 Tonnes per annum of 95% pure CO at a pressure of circa 40 bara.

CASE 3. Plant to supply syngas of an H₂:CO ratio of 1:1 at a CO flow of 100,000 Tonnes per annum and at a pressure of circa 40 bara.

As mentioned previously, the feed gas for all three cases is based on that from a POX reactor with a natural gas feed. The following was specified.

The following suppliers were approached:-

Cryogenic Systems :-

L'air Liquide

Linde

Membrane Systems :-

DuPont	Hollow fibre Polyamide membrane
Monsanto	Hollow fibre Polysulphone membrane
W. R. Grace	Spiral wound Cellulose Acetate membrane
Cynara	Hollow fibre Cellulose Acetate membrane
Ube	Hollow fibre Polyimide membrane
Air Products	Spiral wound Cellulose Acetate membrane

To honour commercial confidentiality the membrane system suppliers will be referred to as : supplier A, supplier B, supplier C and supplier F not respectively. The membranes used by the suppliers will be referred to as : Membranes A - F and will correspond to suppliers A - F.

3.3.3 The Bids

The results of the bid enquiry are summarised in the tables, 3.1 to 3.3.

All the different plants and processes supplied from the enquiry had differing CO recovery rates, because this had been left open to the suppliers

depending upon the capability of their systems. The CO recovery rates varied from 44% to 98%.

Case 1. (97% CO purity, 100,000 TePA of CO product).

By referring to table 3.1 overleaf it can be seen that the capital cost of membrane plant is less than the cost of the cryogenic separation plant. For supplier A, with a 40 bara feed and 96.7 % CO recovery the membrane plant cost is 35% less than the cryogenic plant. For supplier B, with a 40 bara feed and 96% CO recovery the membrane plant cost is more than 50% less than the cost of the cryogenic plant for the same separation. However, in both the cases for membrane suppliers the compression power required for recycle is three times as great as the power required by the cryogenic process. This also means that the capital cost of the compressor required for the membrane plant will be twice that required by the cryogenic process.

Broadly the capital cost of the membrane separation systems is approximately 80% of the cryogenic separation process for the equivalent separation, (97% CO purity, 96% CO recovery and 100,000 TePA of CO product) but uses three times as much power in its operation.

TABLE 3.1

Bids For Case 1. (97% pure CO)

Supplier	Feed Pressure Bara	CO Recovery %	Separation Plant Cost £k	Compression Power KW
Cryogenic	40	95.8	3533	1330
A	30	96.2	3760	3132
	40	96.9	2278	3362
	40	90.3	1889	932
	40	85.6	1846	365
	40	81.2	1824	231
	50	97.3	1606	3684
	B	30	96.0	2440
30		93.0	2070	2280
30		90.0	1910	1470
40		96.0	1520	4200
40		93.0	1280	2090
40		90.0	1180	1300
50		96.0	1090	4220
50		93.0	910	2040
50		90.0	840	1250
C	40	46.3	4565	-
	40	73.1	3696	1450
D	30	84.9	1760	1370
	40	85.0	1340	1110
	50	85.1	1090	1200

Noting the bid from supplier B for a 40 bara feed pressure and a CO recovery of 90% (table 3.1) the compression power has reduced to approximately the same as for the cryogenic process . However, the capital cost of the membrane plant is only one third of the capital cost of the cryogenic process. It can be seen, therefore, that significant cost reductions can be made by reducing the CO recovery.

Case 2. (95% CO purity, 100,000 TePA of CO product).

In case 2 the specified CO purity was relaxed to 95%. The bids received from this enquiry are given in table 3.2.

The cost of a cryogenic separation process for this specification would be virtually the same (99%) as for the cryogenic process in case 1 (97% CO purity, 96% CO recovery and 100,000 TePA).

Referring to the bids from supplier B in tables 3.1 and 3.2 the effect of the relaxation in specification from 97% CO purity to 95% CO purity can be illustrated. For a feed pressure of 40 bara and a CO recovery of 96% the capital cost of the membrane plant was reduced by 30% and the compression power was reduced by 24%. Similar capital cost and compression power reductions were made in bids with different CO recoveries and feed pressures.

TABLE 3.2**Bids For Case 2. (95% pure CO)**

Supplier	Feed Pressure Bara	CO Recovery %	Separation Plant Cost £k	Compression Power KW
A	30	92.3	1667	805
	40	92.9	1442	837
	40	90.7	1391	485
	40	85.9	1356	192
	40	80.2	1174	-
	50	93.3	1037	772
B	30	96.0	1670	3270
	30	93.0	1390	1570
	30	90.0	1280	920
	40	96.0	1060	3210
	40	93.0	880	1480
	40	90.0	810	830
	50	96.0	780	3280
	50	93.0	640	1480
	50	90.0	600	810
C	40	66.5	2044	-
	40	77.4	1913	430
D	* 30	84.4	1270	970
	40	85.0	1220	1030
	50	85.2	1020	1210

* CO purity of 93.4% only achieved.

Again it can be seen from table 3.2 that a reduction in the CO recovery yields a considerable reduction in capital cost and compression power required.

It should also be noted, generally, that the higher the feed pressure the lower the cost of membrane plant and compression power required.

Case 3. (1:1, H₂:CO syngas ratio, 100,000 TePA of CO flow).

The specification of the 1:1 ratio of H₂:CO was chosen for a different application from that of cases 1 and 2 above. Here it is the direct reaction of hydrogen and carbon monoxide to produce acetic acid which is of interest.

The syngas ratio adjustment to a 1:1 ratio represents only a partial separation of the feed syngas. As can be seen from table 3.3 the separation can be achieved easily by the membrane systems in one stage. (ie. No recompression power is required). The capital cost of the membrane plants is as low as 10% of the capital cost of the cryogenic plant.

The clear conclusion here, is that membrane gas separation has great advantages over cryogenic separation where only a partial separation is required.

TABLE 3.3**Bids For Case 3. (1:1, H₂:CO Syngas ratio)**

Supplier	Feed Pressure Bara	CO Recovery %	Separation Plant Cost £k	Compression Power KW
Cryogenic	40	95.8	2767	660
A	30	97.6	343	
	40	97.8	245	
	50	97.8	191	
B	30	97.0	300	
	40	97.0	230	
	50	97.0	200	
C	40	96.0	426	
E	30	96.9	447	
	40	97.1	387	
	50	97.2	353	

3.3.4 Cost Of Production For High Purity CO (97% or 95% pure CO)

Whilst the basic analysis of the bids carried out in the previous section is useful, it is inadequate in that direct comparisons can not be made from one bid to another unless all the specification parameters (CO purity, CO recovery and CO production rate) are the same.

To take account of the variations in CO purity and recovery the process as a whole must be considered. The cost of producing 100,000 TePA of CO can be calculated and hence a price per tonne of CO can be calculated for each specified separation system.

By evaluating the cost of CO production in this way the real significance of a reduction in CO recovery and/or purity can be quantified in economic terms.

Lowering the CO purity requires an increase in purge gas from the downstream reactor and a lower CO recovery requires more CO generation to compensate for the greater loss of CO to the permeate stream.

In order to build up the cost of CO production, for the production of acetic acid equivalent to that from 100,000 TePA of 97% pure CO, we need to take into account the cost of CO generation in the partial oxidation (POX) reactor, the cost of separating the syngas into a CO product and a hydrogen rich fuel gas, either by cryogenic or membrane separation, and the effect upon the cost of the acetic acid reactor process.

CO Generation. (POX reactor)

The generation of CO is achieved by the partial oxidation of natural gas to produce a syngas of hydrogen and carbon monoxide plus impurities.

To produce 100,000 TePA of 97% pure CO at a recovery of 95.8%, which is the separation currently achieved by the cryogenic separation process, a POX reactor of a specified size will be required and with it the required amounts of natural gas feed and oxygen.

If, however, the separation specification is changed such that a lower CO purity is achieved then the POX reactor will have to be increased in size because more syngas would have to be produced to compensate for additional CO being purged from the acetic acid reactor. As well as the increased capital cost there would also be an increase in the natural gas feed and oxygen costs.

If the CO recovery achieved in the separation process was lowered then again the size of the POX reactor would have to be increased along with the variable costs associated with it. This is because more of the CO would be passed into the waste (hydrogen rich) stream of the separation process.

CO Separation. (Membrane/Cryogenic separation process).

The purpose of the CO separation unit is to separate the H₂/CO syngas to provide a high pressure, approximately 40 bara, high purity CO product to supply the downstream, acetic acid reactor.

Where a membrane separation process is used for the separation, savings can be made by lowering the separation specification below that used by the current cryogenic process. (ie. 97% CO purity, 96% CO recovery for 100,000 TePA of CO product).

If the CO purity specification is lowered then the capital cost of the membrane plant may be reduced. Also the associated recycle compression power and hence compressor capital cost can be reduced.

On the other hand, the lowering of the CO purity means that more syngas has to be processed to provide the additional purge gas required by the downstream acetic acid reactor. This of course will result in an increase in the capital and operating costs of the membrane separation process.

If the CO recovery specification is lowered then the capital cost of the membrane plant may be reduced. The required recycle may also be reduced, meaning a lower compressor capital cost and lower compression power.

As well as the reduction in costs because of the less rigorous separation, there would be an increased quantity of hydrogen rich permeate produced which could be used as fuel.

Downstream Reaction. (Acetic Acid Reactor).

The process considered here involves the production of CO for the manufacture of acetic acid by reaction with methanol. The production rate considered is for the production of acetic acid which can be made from

100,000 TePA of CO at a purity of 97%.

If the purity of the CO product supplied to the acetic acid reactor is lowered then additional purge gas is required from the reactor. This means that additional syngas has to be produced and separated. However, the increase in capital cost associated with the downstream reactor is considered to be negligible and is assumed to be zero in this analysis.

The additional CO purged from the reactor can be used as a fuel gas.

If the CO recovery is lowered the cost of the acetic acid process is unaffected.

Calculation Of CO Cost

To calculate the production cost of CO we use the cryogenic separation process as the base case for comparison. That is the separation specification of 97% CO purity, 95.8% CO recovery and 100,000 TePA of CO product.

Where the CO recovery is reduced the POX reactor process will be increased and the separation process will be sized so that 100,000 TePA of 97% pure CO product is still produced.

Where the CO purity is reduced to 95% the POX reactor process and the separation process will be increased to make up for the additional purge required by the downstream reactor.

The economic evaluation was carried out as follows:-

Steam value	V_{STEAM}
Hydrogen rich fuel value	V_{H2}
Purge gas value	V_P

The feed gas, steam generated from the process, the hydrogen rich permeate and any additional purge gas from the downstream reactor are costed from their thermal value. The cost of oxygen is the current price of oxygen supplied "over the fence" for the process.

Both the credit for the hydrogen rich permeate and any additional purge gas are made to the CO generation process, as the origin of these products is the POX reactor.

$$CO \text{ Generation Cost } (C_g) = C_{POX} + C_{CH_4} + C_{O_2} - V_{STEAM} - V_{H_2} - V_P \quad (3.1)$$

CO Separation.

Capital cost	Amortised separation plant cost .	C_{SEP}
	Amortised compressor cost.	C_{COMP}

Variable cost	Membrane replacement cost.	C_{MR}
	Power cost.	C_P

$$CO \text{ Separation Cost } (C_S) = C_{SEP} + C_{COMP} + C_{MR} + C_P \quad (3.2)$$

$$Total \text{ Generation and Separation Cost } (C_t) = C_g + C_S \quad (3.3)$$

To obtain a comparative cost for the separation of CO the currently used Cryogenic process is used as the base case for comparison.

Cost of CO generation for the Base Case = C_{gbc}

Hence the comparative separation cost (C_{SC}) is :-

$$C_{SC} = C_g + C_S - C_{gbc} \quad (3.4)$$

As a measure of comparison of the membrane separation with the cryogenic separation the ratio of the comparative separation cost (C_{SC}) and the base case separation cost (C_{sbc}) is used as a comparison index. $= C_{SC}/C_{sbc}$.

Further details of the methods used in the economic evaluation and the

spreadsheets used to build up the costs are given in appendices 1 and 2 respectively.

The following tables 3.4 and 3.5 give the calculated CO generation cost (C_g), the calculated CO separation cost (C_s) and the total production cost (C_t) for cases 1 and 2 (97% pure CO and 95% pure CO) respectively. The costs are compiled for each of the instances where bids were supplied.

TABLE 3.4

CO Generation and Separation Costs for Case 1

Supplier	Feed Pressure Bara	CO Recovery %	Generation Cost £/Te	Separation Cost £/Te	Total Cost £/Te
Cryogenic	40	95.8	80.99	52.39	133.38
A	30	96.2	81.62	72.06	153.68
	40	96.9	79.74	50.12	129.86
	40	90.3	84.09	37.58	121.67
	40	85.6	87.10	35.86	122.96
	40	81.2	89.59	36.06	125.65
	50	97.3	81.53	40.86	122.39
B	30	96.0	80.79	56.00	136.79
	30	93.0	82.46	43.15	125.61
	30	90.0	84.09	37.60	121.69
	40	96.0	80.79	41.21	122.00
	40	93.0	82.46	30.33	112.79
	40	90.0	84.09	25.71	109.80
	50	96.0	80.79	34.68	115.47
	50	93.0	82.46	24.47	106.93
	50	90.0	84.09	20.29	104.38
C	40	46.3	134.26	70.03	204.29
	40	73.1	95.76	64.98	160.74
D	40	85.0	85.35	28.59	113.94
	40	80.0	88.56	27.79	116.35

TABLE 3.5

CO Generation and Separation Costs for Case 2

Supplier	Feed Pressure Bara	CO Recovery %	Generation Cost £/Te	Separation Cost £/Te	Total Cost £/Te
A	30	92.3	88.94	33.15	122.09
	40	92.9	87.95	29.47	117.42
	40	90.7	89.14	27.34	116.48
	40	85.9	92.51	26.33	118.84
	40	80.2	96.96	22.35	119.31
	50	93.3	87.61	22.45	110.06
B	30	96.0	86.18	42.20	128.38
	30	93.0	87.95	31.31	119.26
	30	90.0	89.75	26.70	116.45
	40	96.0	86.18	32.21	118.39
	40	93.0	87.95	22.77	110.72
	40	90.0	89.75	18.74	108.49
	50	96.0	86.18	27.97	114.15
	50	93.0	87.95	18.92	106.87
C	40	66.5	109.18	32.76	141.94
	40	77.4	99.37	34.26	133.63
D	40	85.0	93.20	27.37	120.57
F	40	91.0	89.14	36.59	125.73

The reductions in cost due to the different separation systems and different separation specifications are illustrated in tables 3.6 and 3.7, for cases 1 and 2 respectively (case1: 97% pure CO and case 2: 95% pure CO). The comparative separation cost (C_{SC}) allows the separation systems to be compared with the base case cryogenic separation and with each other by adding to the actual cost of membrane separation, the cost penalties associated with lower CO purity or lower CO recovery. As stated previously,

$$C_{SC} = C_g - C_{gbc} + C_s \quad (3.4)$$

The proportion of the cost of membrane separation to the base case cryogenic separation is given by the ratio :-

$$C_{SC} / C_{sbc} \quad (3.5)$$

This shows the cost of the membrane system, at different separation specifications, relative to the cryogenic separation.

TABLE 3.6**Comparative CO Separation Costs for Case 1**

Supplier	Feed Pressure Bara	CO Recovery %	Comparative CO Separation Cost £/Te
Cryogenic	40	95.8	52.39
A	30	96.2	72.69
	40	96.9	48.87
	40	90.3	40.68
	40	85.6	41.97
	40	81.2	44.66
	50	97.3	41.40
B	30	96.0	55.80
	30	93.0	44.62
	30	90.0	40.70
	40	96.0	41.01
	40	93.0	31.80
	40	90.0	28.81
	50	96.0	34.48
	50	93.0	25.94
	50	90.0	23.39
C	40	46.3	123.30
	40	73.1	79.75
D	40	85.0	32.95
	40	80.0	35.36

TABLE 3.7

Comparative CO Separation Costs for Case 2

Supplier	Feed Pressure Bara	CO Recovery %	Comparative CO Separation Cost £/Te
A	30	92.3	41.10
	40	92.9	36.43
	40	90.7	35.49
	40	85.9	37.85
	40	80.2	38.32
	50	93.3	29.07
B	30	96.0	47.39
	30	93.0	38.27
	30	90.0	35.46
	40	96.0	37.40
	40	93.0	29.73
	40	90.0	27.50
	50	96.0	33.16
	50	93.0	25.88
	50	90.0	24.04
C	40	66.5	60.95
	40	77.4	52.64
D	40	85.0	39.58
F	40	91.0	44.74

3.3.5 Cost Of CO For Case 3 (H₂/CO ratio of 1:1, CO flow of 100,000 TePA)

In the case of H₂ : CO syngas ratio adjustment to 1:1, the separation can be achieved quite easily in one stage by membrane separation whilst maintaining a high CO recovery.

As the application for the syngas of H₂ : CO ratio of 1:1 is different to that of the pure CO cases (acetic acid is produced by direct reaction of hydrogen and carbon monoxide) there is no penalty associated with the production of the lower purity CO. Also in this separation process much less hydrogen rich permeate will be produced because much of the hydrogen is retained in the high pressure syngas product stream. Here the economics of the process as a whole are only affected by the CO recovery, which will determine the size of the POX reactor required for the given separation process to produce a CO flow of 100,000 TePA.

The basis for comparison of the separation processes will again be the cryogenic separation process. The cryogenic process for the syngas ratio adjustment to a 1:1, H₂ : CO ratio produces a CO flow of 100,000 TePA with a CO recovery of 97.9%.

Analogous cost equations to those for cases 1 and 2 can be derived. For this

case the equations have no reference to purge gas from the acetic acid reactor.

Calculation of CO Cost.

CO Generation.

Capital cost	Amortised POX reactor cost	C_{POX}
Variable costs	Natural gas feed cost	C_{CH4}
	Oxygen cost	C_{O2}
	Steam value	V_{STEAM}
	Hydrogen rich fuel value	V_{H2}

$$\text{CO Generation Cost } (C_g) = C_{POX} + C_{CH4} + C_{O2} - V_{STEAM} - V_{H2} \quad (3.6)$$

CO Separation.

Capital cost	Amortised separation plant cost .	C_{SEP}
Variable cost	Membrane replacement cost.	C_{MR}

$$\text{CO Separation Cost (C}_s\text{)} = \text{C}_{\text{SEP}} + \text{C}_{\text{MR}} \quad (3.6)$$

$$\text{Total Generation and Separation Cost (C}_t\text{)} = \text{C}_g + \text{C}_s \quad (3.7)$$

The comparative separation cost (C_{sc}) remains the same as before except the value of C_{gbc} is for the base case in the production of H₂ : CO syngas of a 1:1 ratio.

Thus :-

$$C_{sc} = C_g - C_{gbc} + C_s \quad (3.8)$$

The comparison index is also defined as before, as :-

$$C_{sc}/C_{sbc} \quad (3.9)$$

Table 3.8 gives the calculated CO generation and separation costs for cryogenic and membrane separation plant. Table 3.9 illustrates the comparative cost of CO separation as defined above.

TABLE 3.8**CO Generation and Separation Costs for Case 3**

Supplier	Feed Pressure Bara	CO Recovery %	Generation Cost £/Te	Separation Cost £/Te	Total Cost £/Te
Cryogenic	40	97.9	98.04	40.67	138.71
A	30	97.6	98.05	5.26	103.31
	40	97.8	97.92	3.76	101.68
	50	97.8	97.92	2.93	100.85
B	30	97.0	98.42	4.60	103.02
	40	97.0	98.42	3.53	101.95
	50	97.0	98.42	3.07	101.49
C	40	96.0	98.65	6.53	105.18
E	30	96.9	98.10	6.86	104.96
	40	97.1	98.09	5.98	104.07
	50	97.2	98.09	5.41	103.50

TABLE 3.9

Comparative CO Separation Costs for Case 3

Supplier	Feed Pressure Bara	CO Recovery %	Comparative Cost of Separation £/Te
Cryogenic	40	97.9	40.67
A	30	97.6	5.27
	40	97.8	3.64
	50	97.8	2.81
B	30	97.0	4.98
	40	97.0	3.91
	50	97.0	3.45
C	40	96.0	7.14
E	30	96.9	6.92
	40	97.1	6.03
	50	97.2	5.46

3.4 Conclusions

General observations can be made from the bids received from the enquiries made.

For the equivalent separation to the cryogenic separation, (97% CO purity, 96% CO recovery, 100,000 TePA CO product) the membrane separation capital cost is around 80% of the cryogenic capital cost, but the membrane system requires three times as much power.

Capital cost and power reductions can be made by relaxing the separation specification by either lowering the required CO purity or CO recovery.

Partial separation of the feed syngas (for example the syngas ratio adjustment to an H₂ : CO ratio of 1:1 considered in case 3) can be achieved easily by membrane plants and have great advantages over the cryogenic separation. The capital cost of the membrane systems are as low as 10% of the capital cost of the cryogenic separation process.

The economic analysis carried out allows a comparison of the membrane separation systems and the cryogenic separation system to be made in terms of the process as a whole. The comparison being made in terms of the amount of acetic acid which can be produced from 100,000 TePA of 97% pure

carbon monoxide.

A comparison index can be used to compare the membrane systems with the cryogenic separation process. This is the ratio of the comparative cost of membrane separation to the base case cost of cryogenic separation.

From the economic analysis for the cryogenic separation specification, (97% CO purity, 96% CO recovery and 100,000 TePA of CO product) the cost of the membrane separation process is between 80 - 93 % of the cryogenic cost.

The relaxation of the separation specification yields large cost reductions when the process is considered as a whole. The results calculated for supplier A show that a minimum cost is achieved when the CO recovery is lowered. The results show that the separation cost is lower at 95% CO purity than for 97% CO purity.

Minimum costs are not reached for the other membrane suppliers.

Each membrane system must have a different optimum separation specification which will give the minimum cost of CO separation for that particular membrane plant.

The minimum values found for the system supplied by Supplier A indicates an

optimum CO recovery value, but the optimum CO purity has not been found.

The specifications chosen for the economic evaluation were somewhat arbitrary. It is necessary to determine the optimum separation specification of the particular membrane systems.

CHAPTER 4

DETERMINATION OF COST PARAMETERS FOR THE OPTIMISATION OF MEMBRANE SEPARATION

4.1 Introduction

To find the optimum separation specification for any particular membrane plant the parameters which determine the cost of the membrane separation system must be defined.

If the cost parameters for the membrane systems can be defined then a model could be used to simulate the membrane gas separation process and calculate the cost of the membrane separation.

From the bids received from the economic evaluation enquiries and modelling of the membrane separation process, can the bid information be correlated with cost parameters?

If a correlation of the bid information is possible, then the membrane systems can be characterised.

4.2 Effective Selectivity and Cost Permeability

An intrinsic measure of how good a membrane is at separating two gases is its selectivity. This is the relative permeability of the membrane to the two gases being separated, in this case hydrogen and carbon monoxide. The selectivity determines how much recycle will be required to achieve a given separation. The membrane area required for a given separation is determined from the permeability of the faster permeating gas, hydrogen. These two properties can be used as the basis of the definition of the cost parameters for membrane gas separation systems.

In models used to simulate gas separation using membranes, certain assumptions are usually made.

It is assumed that there is no pressure drop on the high or low pressure side of the permeator. This is largely adequate for spiral wound permeators where pressure drops are generally low. However, hollow fibre units may have a more significant permeate pressure drop where the ratio of fibre length to diameter is high and where the permeate collects on the inside of the fibre.

The models also assume that there will be no interaction between permeating components. This may be accurate for permeation at low pressure but deviations have been observed where high pressure systems are used.

In the simulation of the membrane separation process an Effective Selectivity, α_e , is used such that the actual separation achieved in a commercial scale separator is predicted. This is a useful way of accommodating the assumptions made in the crossflow model used in this analysis.

The permeability of the faster permeating gas through the membrane determines the area required for a given separation.

Membrane separation plant are built in a modular form. This means that if the size of a membrane plant is to be doubled, it simply has twice as many membrane modules. This implies that the capital cost of a modular membrane separation plant is very close to being directly proportional to the membrane area.

Proportionality is assumed in this analysis for large scale plant.

Thus, if capital cost = C.A (4.1)

C = Unit cost of membrane
plant in £k/m² say.

A = Membrane area in m².

We can define a Cost Permeability, G_C , Where :-

$$G_C = G_a/C \quad (4.2)$$

G_a = Actual membrane permeability in $\text{sm}^3/\text{m}^2 \cdot \text{H} \cdot \text{bara}$.

G_C = Cost permeability in $\text{sm}^3/\text{£k} \cdot \text{H} \cdot \text{bara}$.

Use of the effective selectivity and cost permeability of a membrane separation system in a model to simulate the membrane separation process will mean that the capital cost of the membrane plant and the recycle flow required for a given separation can be calculated.

Furthermore if these parameters are approximately constant for a particular process condition it should be possible to calculate them from an analysis of plant operating data. In the absence of such data, values may be determined from analysis of suppliers bids. This is described in the next section.

4.3 Crossflow Model

A correlation of supplier information may be obtained by comparing the capital and power costs with the area and separation achieved for a membrane of a particular permeability and selectivity. By comparing bids for several different

specified separations it is possible to calculate the cost permeability and effective selectivity for that suppliers membrane.

An asymmetric polymer membrane can be considered to carry out crossflow gas separation no matter which type of permeator is used. Figure 4.1, overleaf, illustrates the flows on either side of the membrane. As can be seen, for membranes where the support layer is on the low pressure side, which is usually the case, once gases have permeated across the active layer they are forced to flow perpendicular to the feed flow through the porous support layer.

FIGURE 4.1
Schematic Diagram Of Asymmetric Membrane

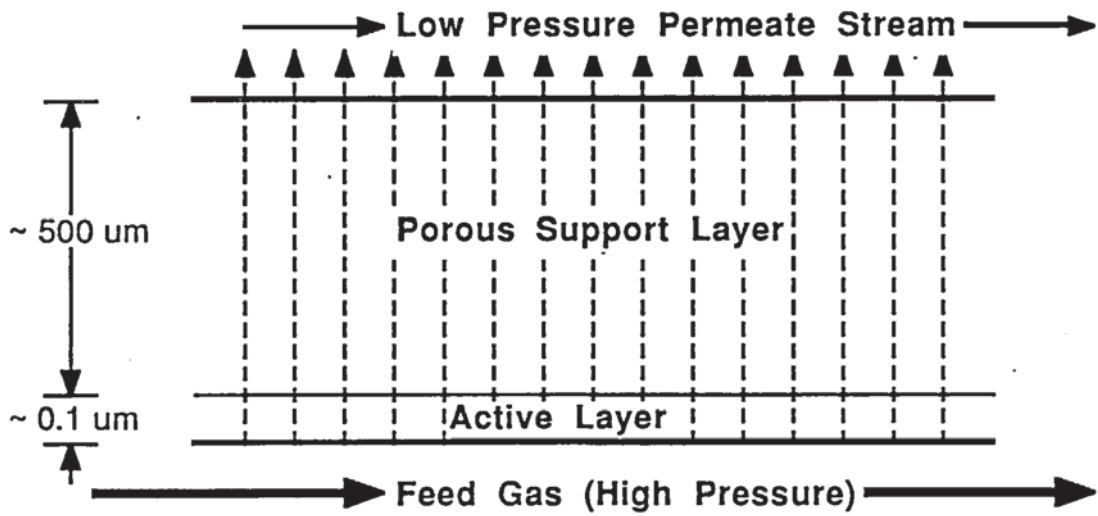
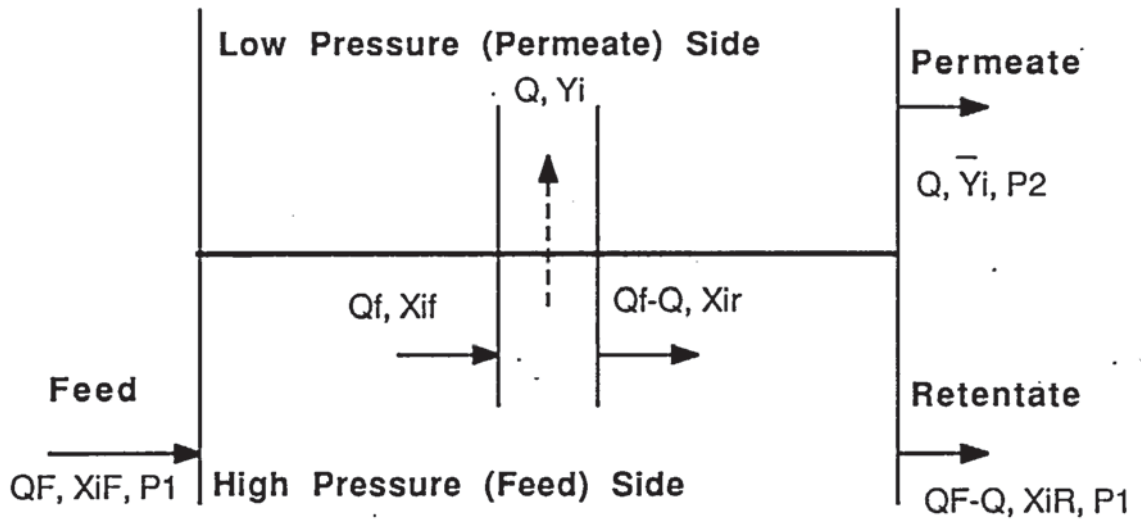


FIGURE 4.2
Differential Element Of Crossflow Permeator



An analytical solution to the mass transfer equations for a crossflow permeator has been obtained by C.W.Saltonstall (130). The model used in this analysis assumes that there is no pressure drop on the high or low pressure side of the permeator.

For a binary gas mixture the gas concentrations vary along the membrane, with the relation between gas concentration on the high pressure and low pressure side of the membrane given by:-

$$Y_1^2 - Y_1 - d(\beta - 1)Y_1 - d.X_1.Y_1 + \beta.d.X_1 = 0 \quad (4.3)$$

$$d = P_1/P_2 \quad (4.4)$$

$$\beta = \alpha/(\alpha - 1) \quad (4.5)$$

P_1 = Feed pressure.

P_2 = Permeate pressure.

α = Selectivity.

Y_1 = Permeate composition of component 1.

X_1 = Retentate composition of component 1.

The permeate composition at the entrance and exit of the permeator (Y_{1F} and Y_{1R}) can be calculated from equation (4.3). Integrating over the membrane area gives the characteristic equation relating product flow to the feed flow, separation and membrane properties.

$$\frac{Q_R}{Q_F} = \frac{\beta - Y_{1R} (1 - Y_{1R})^a (Y_{1R})^b}{\beta - Y_{1F} (1 - Y_{1F}) (Y_{1F})} \quad (4.6)$$

$$a = (1 - \beta.d)/(d - 1) \quad (4.7)$$

$$b = \beta.d/(d - 1) - 1 \quad (4.8)$$

Q refers to flow.

F refers to feed point.

R refers to residue (exit) point.

The average permeate composition, \bar{Y}_1 , can then be calculated from the overall mass balance:-

$$\bar{Y}_1 = \frac{X_{1F} - \left(\frac{Q_R}{Q_F}\right) X_{1R}}{1 - \left(\frac{Q_R}{Q_F}\right)} \quad (4.9)$$

And the membrane area is given by:-

$$A = \frac{(QF - QR)(\beta - Y_1)}{P_2 G_1 (d - 1)(\beta - 1)} \quad (4.10)$$

To simulate a single stage crossflow permeator for the separation of H₂ and CO a spreadsheet was written based on the above equations. A description of the spreadsheet is given in appendix 2. The inputs required are as follows:-

Feed composition	XH ₂ F	(mol. frac.)
Retentate composition	XH ₂ R	(Mol. frac.)
Permeability of H ₂	GH ₂	(SM ³ /H.M ² Bar.)
Selectivity	α	
Feed pressure	P1	(Bara.)
Permeate pressure	P2	(Bara.)
Feed flow	QF	(SM ³ /H)

From this information b and d are calculated. Then YH₂F and YH₂R are calculated from equation (4.3). There are two solutions to the quadratic equations but only one has any physical meaning.

The exponents a and b are next calculated and the value of Q can be determined. \bar{Y}_{H_2} is then calculated from the overall mass balance.

The results are then summarised:-

Feed Flow. (SM³/H)

Retentate Flow. (SM³/H)

Permeate Flow. (SM³/H)

% CO Recovery.

CO in Permeate. (Mole fraction CO)

Retentate (product) Purity. (Mole fraction CO)

Membrane Area. (M²)

4.4 Process Design of Membrane Separations

The basis for the process layout of a membrane separation unit is to achieve the given separation at the required product recovery using the minimum membrane area and minimum recycle flow. Thus producing the system with minimum capital and power costs.

Both of these objectives can be achieved by, wherever possible, maximising the driving force of the faster permeating gas in the separation modules. This can be done in two ways. Firstly by keeping the degree of separation in any module to a minimum, i.e. if the separation can be achieved with only partial separation, do not make a purer product than required.

Secondly, the recycle stream should be reintroduced at a point which will increase the concentration of the fast gas in the feed where possible. This will have the effect of increasing the driving force across the membrane for the fast gas.

4.4.1 H₂ : CO Syngas ratio of 1:1

The separation of the hydrogen and CO syngas can be achieved in one stage if only a syngas ratio adjustment is needed, to say, an H₂ : CO ratio of 1:1. The process designs proposed by membrane plant suppliers for this case were of two different types, as illustrated in figures 4.3 and 4.4.

For the single stage process considered in figure 4.4, more membrane area is required by producing a smaller quantity of a pure product and then mixing it with the feed to produce an H₂ : CO ratio of 1:1, than processing all the feed and separating it until a 1:1 ratio is attained, as in figure 4.3.

A reduction in the separator cost of 20% could have been achieved if the

layout in figure 4.3 had been adopted instead of the figure 4.4 process layout.

FIGURE 4.3

Single Stage Permeator.

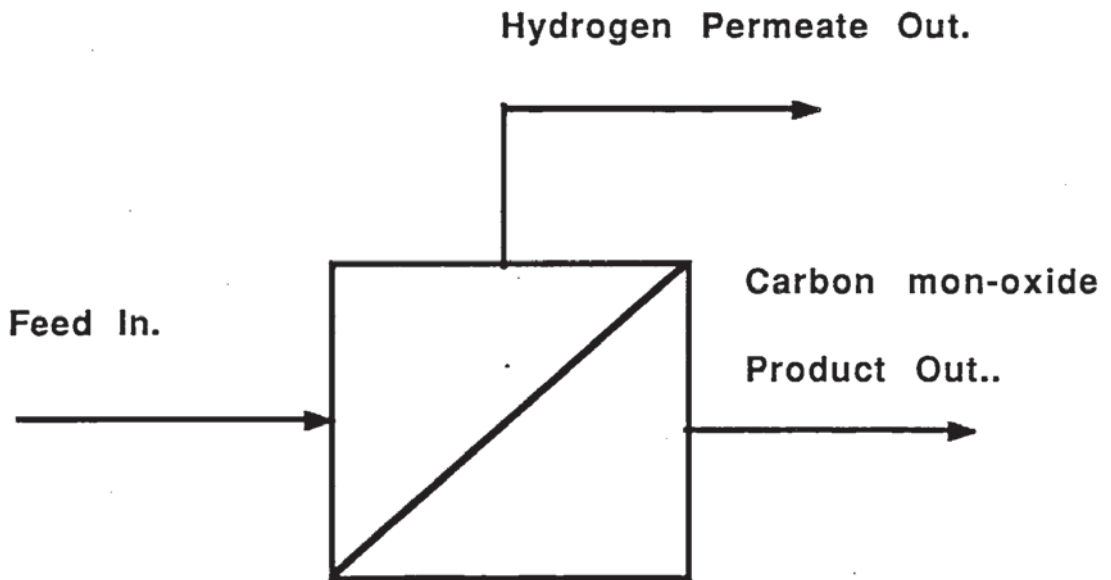
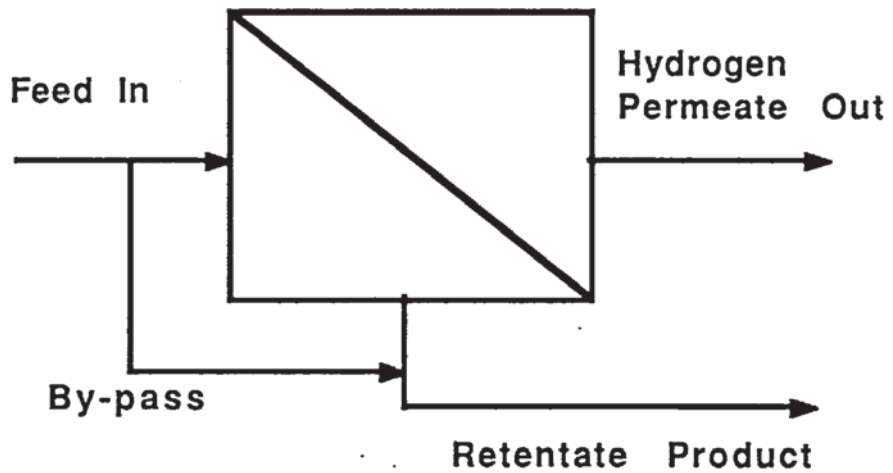


FIGURE 4.4

Single Stage Permeator With By-pass.



4.4.2 Pure CO Product

Where a pure CO product is required, as in the cases 1 and 2 (97% and 95% pure CO product respectively) a two stage process with recycle is used to achieve the required purity at an acceptable CO recovery rate. Again the process designs proposed by the membrane plant suppliers were of two different layouts. See figures 4.5 and 4.6 overleaf.

Of the commercial suppliers, suppliers B and C proposed the two unit recycle permeator layout (figure 4.5) and supplier A proposed the three unit recycle permeator process layout (figure 4.6).

Suppliers D and F did not indicate which process design they had used and supplier E did not provide any proposals for the pure CO product separations.

For separations with a relatively low recycle, the two unit recycle permeator layout (figure 4.5) gives the minimum area and compression power requirement. As the amount of recycle required to achieve the separation increases the three unit recycle permeator (figure 4.6) becomes the most efficient of the two.

For the correlation of bid data from suppliers and for further analysis in this thesis the two unit recycle permeator process was modelled on the basis of the crossflow model previously explained.

FIGURE 4.5

Two Unit Recycle Permeator

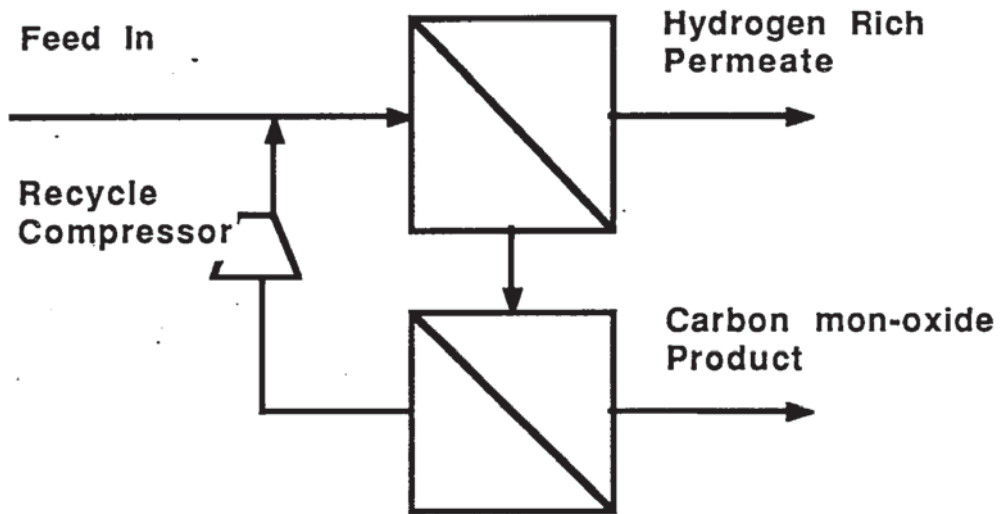
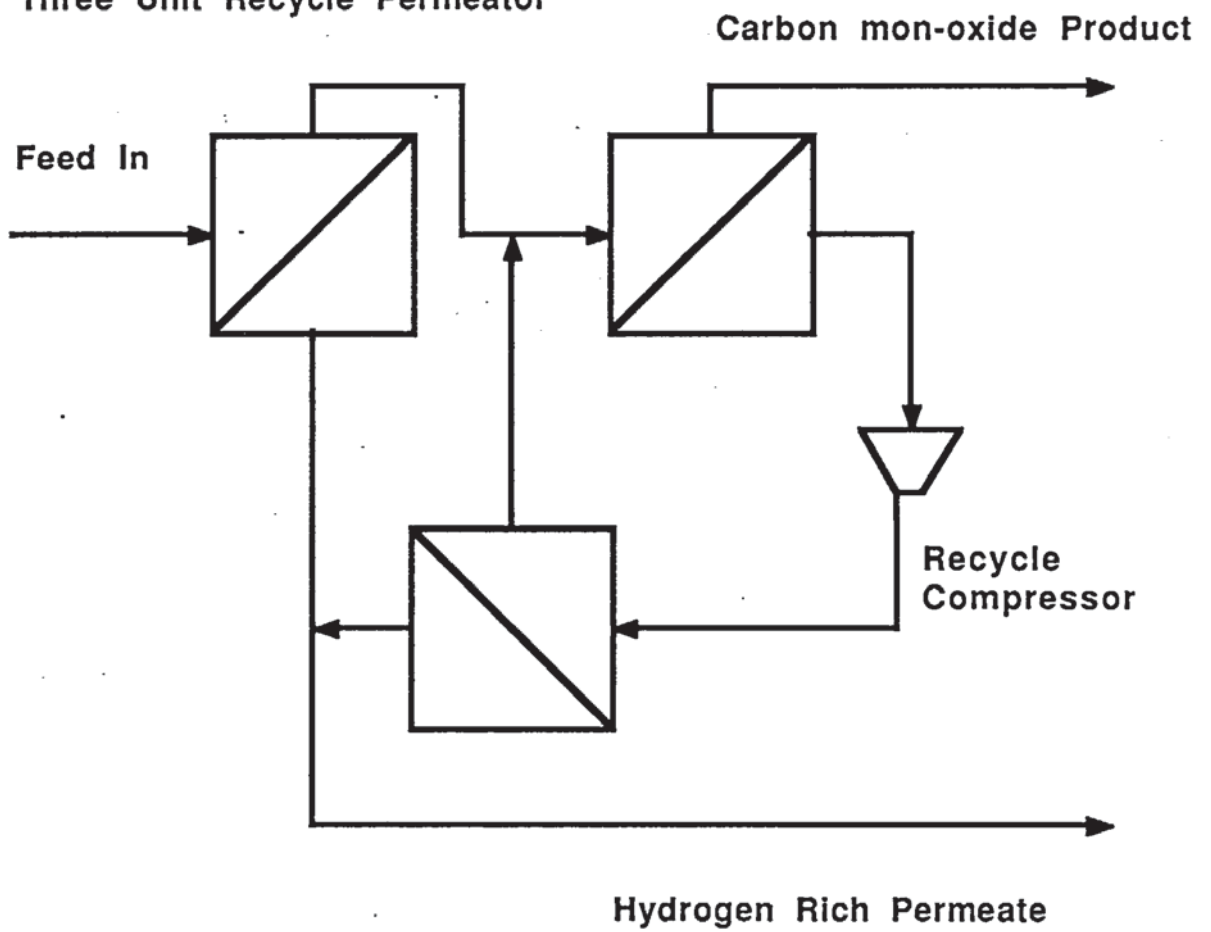


FIGURE 4.6

Three Unit Recycle Permeator



The two unit recycle permeator is adopted because it is the most efficient process layout for many of the separation requirements and also, most of the suppliers have proposed this layout in their bids.

A comparison of two other process layouts with the two unit recycle permeator was also made. The other process layouts being the recycle permeator shown in figure 4.7 and the two stage permeator without recycle, figure 4.8.

The comparison between the three process designs was made for four product specifications separating a binary feed of H₂ and CO (65% H₂ ; 35% CO), to a CO product of 95% and 97% purity at 90% and 95% CO recovery.

The selectivity and permeability used for the membrane were $\alpha = 30$;

$G_{H_2} = 0.324 \text{ sm}^3/\text{m}^2.\text{H.bara}$. Table 4.1 shows that the area and power requirements are lowest for the two unit recycle permeator in each of the four cases considered.

FIGURE 4.7
Recycle Permeator.

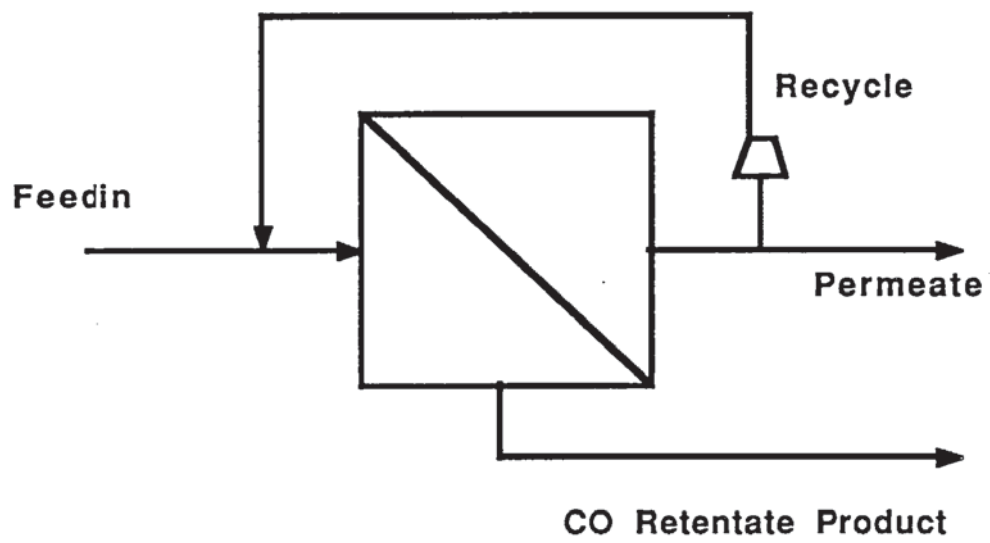


FIGURE 4.8
Two Stage Permeator Without Recycle

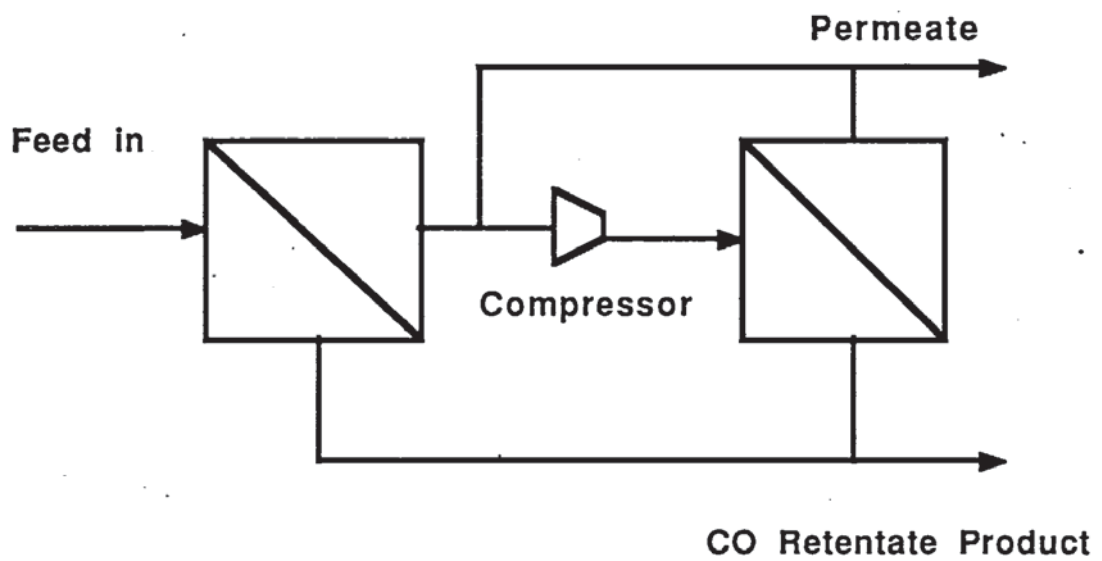


TABLE 4.1

**Membrane Area and Compression Power Required
For Different Process Configurations and
For a Number of Different Separation Duties**

For separation of a binary mixture of H₂ and CO (65% H₂; 35% CO)

Selectivity = 30 ; Permeability, GH₂ = 0.324 sm³/m².H.Bara.

Process Layout	Product Specification							
	1. 95% CO @ 90% recovery 10,000sm ³ /H		2. 95% CO @ 95% recovery 10,000sm ³ /H		3. 97% CO @ 90% recovery 10,000sm ³ /H		4. 97% CO @ 95% recovery 10,000sm ³ /H	
	Area (m ²)	Power (KW)						
1 Stage Recycle	7310	2072	11930	8500	9530	3470	15080	11390
2 Stages Without Recycle	6370	1146	6970	2190	7870	1660	8370	2560
2 Stages With R'cl.	5700	222	6220	1010	6890	345	7510	1240

4.5 Correlation Of Bids

The general approach taken to correlate the bid information from suppliers was to consider the syngas ratio adjustment to an H₂ : CO ratio of 1;1. This separation, being able to be carried out in one stage made it quite straight forward to calculate the effective selectivity of the suppliers membrane plant. This was done by using the one stage crossflow model and by successive approximation of the effective selectivity in the model, match the calculated data with the suppliers mass balance data or the separation specification. At this stage an arbitrary cost permeability is used and the calculated membrane plant cost is ignored until the mass balance data calculated corresponds with the suppliers data.

Once the effective selectivity has been calculated this can be checked by calculating the mass balance data for the other one stage processes of the same supplier. In all the cases, excepting for data from supplier C, the mass balance data calculated, matched to within 2% of the suppliers data.

Having confidence in the calculated effective selectivity for the membrane plants, the cost data could be correlated.

This was achieved by initially setting the cost permeability used in the model to an arbitrary value, usually 1.0 sm³/£k.H.bara, but if the units of flow used by the suppliers were different to sm³/H, different, arbitrary cost permeability units

were used for convenience.

Inserting the arbitrary cost permeability into the model, yields an arbitrary "cost" which is proportional to the area of the membrane used in the membrane plant.

The same effective selectivity and arbitrary cost permeability were used for each of the bid cases. Where the pure CO product cases were considered the two unit recycle permeator process layout was simulated to calculate the membrane arbitrary cost and recycle flow.

The capital cost of the membrane plant from the suppliers bid was then plotted against the arbitrary cost. From the correlations obtained the actual membrane plant cost permeability is calculated.

The information from all the membrane plant suppliers was considered. The calculation of the effective selectivity and cost permeability was possible in all cases except for membrane plant C, which did not yield a consistent value for the effective selectivity, and membrane plant D, where insufficient information was supplied to obtain a correlation.

4.5.1 Supplier A

The effective selectivity was matched with the mass balance data for the

single stage, case 2 (95% CO purity bid, with an 80.2% CO recovery).

An effective selectivity of 31 yielded the following results :-

	Calculated value	Supplier A value
CO recovery (%)	80.19	80.2
CO flow (M3)	6978	6979
H2 flow (M3)	17614	17613
H2 purity (%)	90.51	90.38

In both cases the CO purity was 95.0%.

To confirm that the effective selectivity calculated was correct the mass balances from other bids were matched where detailed information was available. Mass balance data was available for the case 3 (syngas ratio of 1:1) bids and for the case 2 (95% CO purity) bid with 40 bara feed and 85.9% CO recovery, which is a two stage separation process with recycle, as shown in figure 4.9.

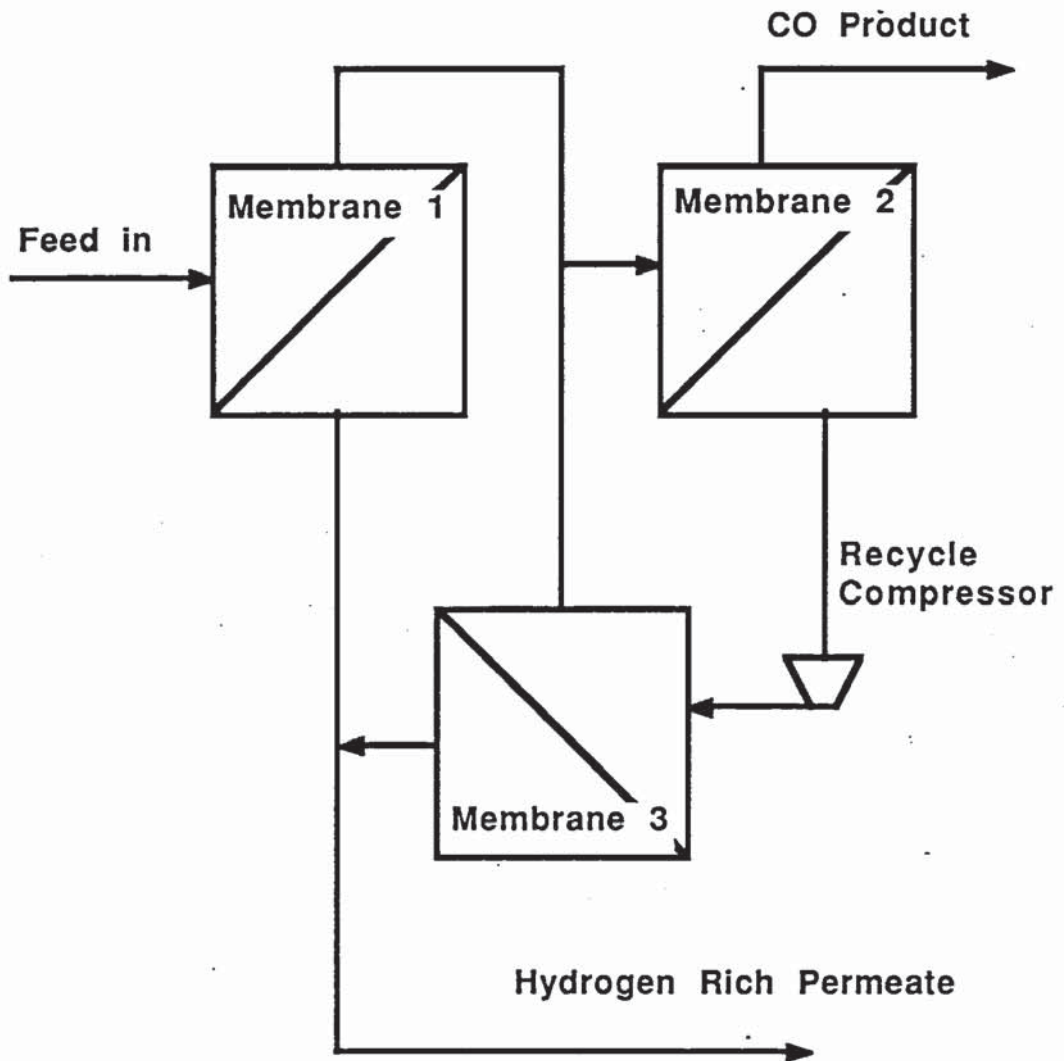
	Calculated value	Supplier A value
Case 3. 50 Bara Feed.		
CO recovery. (%)	97.8	97.8
H ₂ purity. (%)	97.6	97.7
Case 3. 40 Bara Feed.		
CO recovery. (%)	97.5	97.6
H ₂ purity. (%)	97.8	97.8
Case 3. 30 Bara Feed.		
CO recovery. (%)	97.7	97.6
H ₂ purity. (%)	97.4	97.6

Case 2. 40 Bara Feed. 85.9% CO recovery, Two stages with recycle.

The process layout used by Supplier A is as shown in figure 4.9.

FIGURE 4.9

Process Layout Used By Supplier A



	Calculated value	Supplier A value
Membrane 1		
H ₂ purity. (%)	92.9	92.9
Retentate flow. (sm ³ /H)	7809	7820
Permeate flow. (sm ³ /H)	16782	16772
Membrane 2		
H ₂ purity. (%)	44.1	43.5
Retentate flow. (sm ³ /H)	7464	7441
Permeate flow. (sm ³ /H)	1372	1394
Membrane 3		
H ₂ purity. (%)	92.9	92.9
Retentate flow. (sm ³ /H)	1016	1015
Permeate flow. (sm ³ /H)	378	379

Good agreement was achieved between the calculated and quoted mass balance data.

The crossflow model was then used to simulate the two unit type recycle membrane process, as previously described in figure 4.5, to correlate all the

bids. The following graph, figure 4.10, plots the quoted capital cost of the plant against an arbitrary, area proportional, cost using a cost permeability of 1.0 mscf/£k.D.Bara:

The data correlates very well. Deviations from the correlation which are seen for the two stage processes can be explained by the difference between the two unit type recycle permeator, used in the simulation, and the three unit type recycle permeator thought to be adopted by supplier A.

Where the data points appear above the line, the two unit type recycle permeator is the more efficient process layout in terms of membrane area. Where the data points are below the line the three unit type recycle permeator is the more area efficient layout.

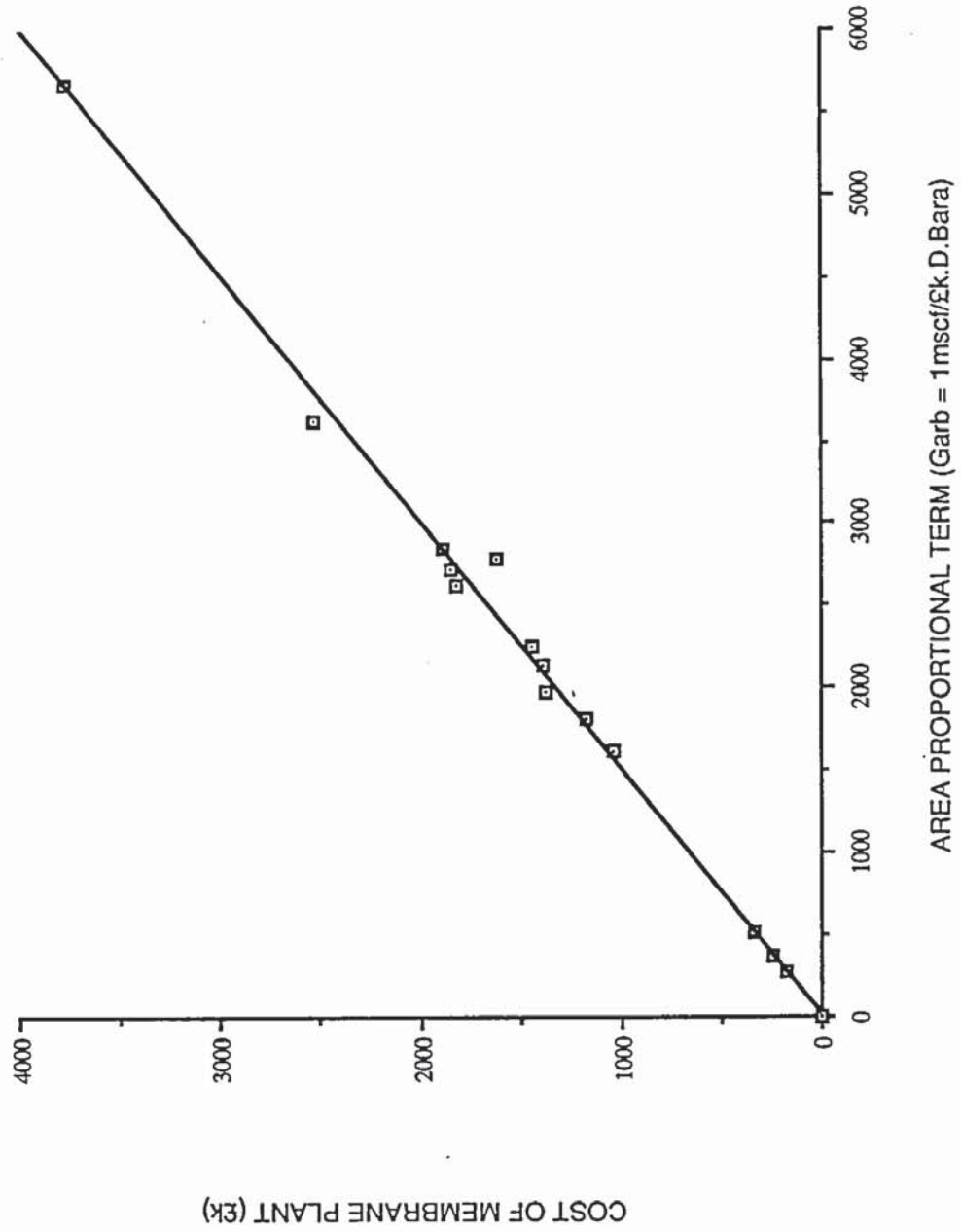
The extremely good correlation achieved shows that there is little difference in the required area using the two or three unit type recycle permeator.

From figure 4.10 the actual cost permeability, G_c , which is used to calculate the area proportional cost, can be calculated.

FIGURE 4.10

Correlation of bid information from supplier A

to determine cost permeability for membrane plant A.



For Supplier A.

$$G_C = G_{arb} / (\text{slope of graph})$$

$$G_{arb} = 1.0 \text{ mscf}/\text{£k.D.Bara.}$$

$$= 1.17975 \text{ sm}^3/\text{£k.H.Bara.}$$

$$\text{Slope} = 0.662.$$

Hence :-

$$G_C = 1.78 \quad \text{sm}^3/\text{£k.H.Bara.}$$

The correlation is of the form :-

$$\text{Membrane Plant Cost (£k).} = C.A.$$

C = Cost per unit area of membrane
plant. (£k/m²).

A = Membrane Area. (m²).

C.A. is calculated using the crossflow model with an effective selectivity of 31 and a cost permeability of 1.78 sm³/£k.H.Bar.

4.5.2 Supplier B

Supplier B supplied a large amount of data for the different cases considered. Where a pure CO product (cases 1 and 2) was required they used the two unit type recycle permeator process shown in figure 4.11.

An effective selectivity of 22 was calculated by matching mass balance data from the two cases where enough mass balance data was provided.

FIGURE 4.11

Process Layout Used By Supplier B

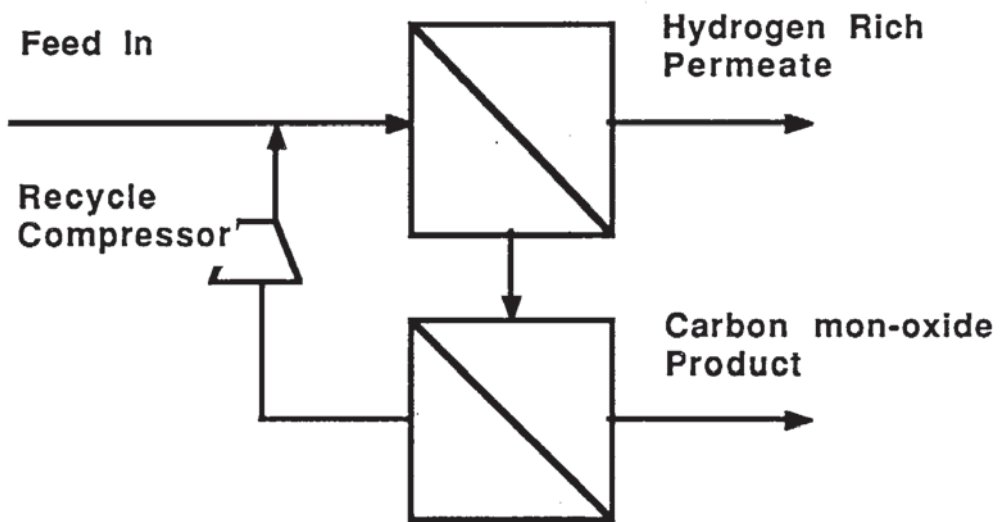


Figure 4.12 plots the capital cost of supplier B's bids against the arbitrary, area proportional, cost using $G_{arb} = 1.0 \text{ Nm}^3/\text{£k.H.Bara}$.

Again the method yielded an excellent correlation of the bid data.

From figure 4.12 two cost correlations can be calculated which both have the same cost permeability, G_C , which is used to calculate the area proportional cost.

$$G_C = G_{arb}/(\text{slope})$$

$$G_{arb} = 1.0 \text{ Nm}^3/\text{£k.H.Bara}$$

$$\text{Slope} = 0.443$$

Hence :-

$$G_C = 2.26 \quad \text{Nm}^3/\text{£k.H.Bara}$$

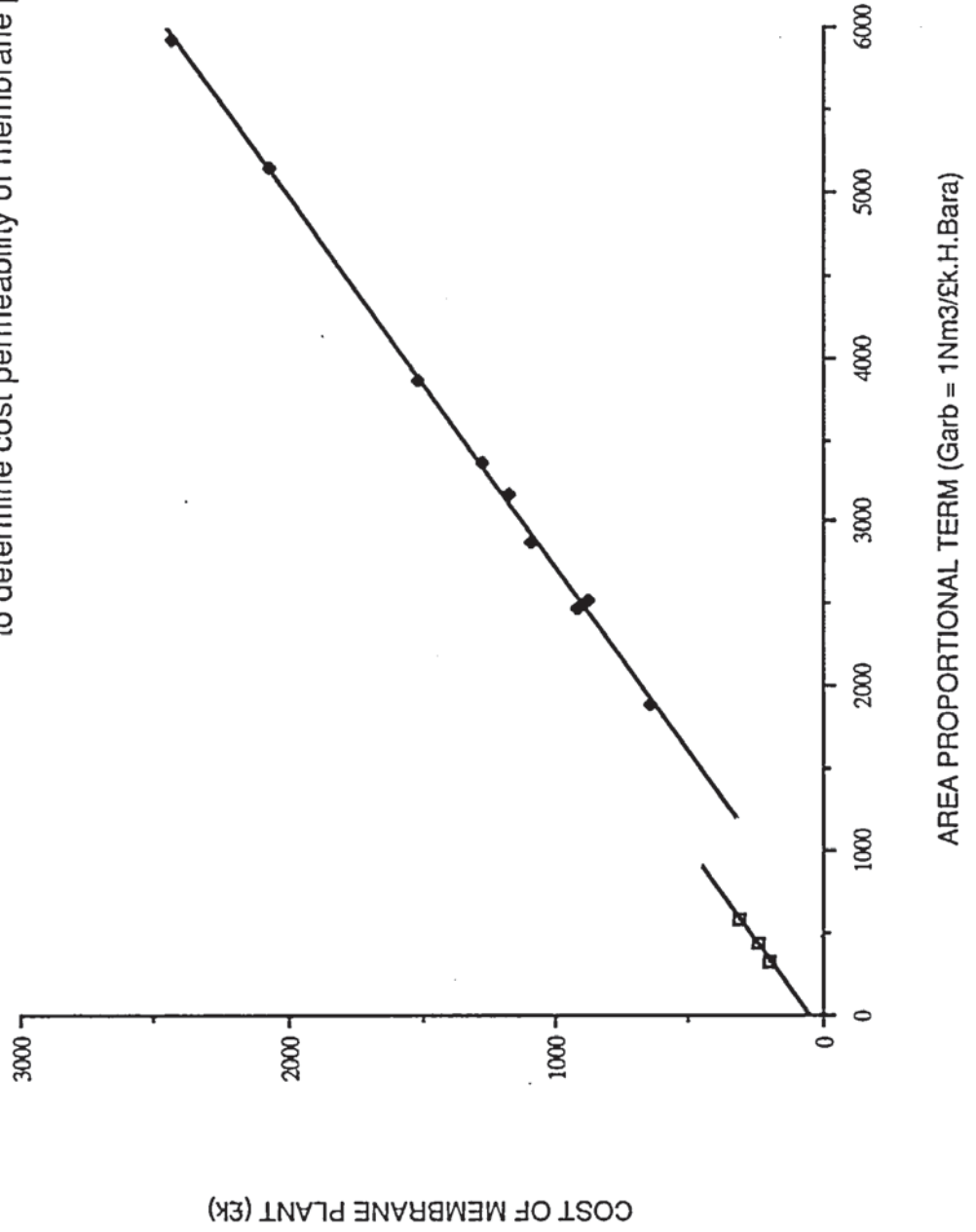
$$= 2.37 \quad \text{sm}^3/\text{£k.H.Bara}$$

Generally, we can say,

Membrane Plant Cost = Area Proportional Cost + Fixed Cost.

FIGURE 4.12

Correlation of bid information from supplier B
to determine cost permeability of membrane plant B.



And for Supplier B,

For Small Single Stage Membrane Plant, we have :-

$$\text{Membrane Plant Cost (£k).} = C.A + 50.$$

C = Cost per unit area of membrane
plant. (£k/m²).

A = Membrane area (m²).

For Large Two Stage Membrane Plant, we have :-

$$\text{Membrane Plant Cost (£k).} = C.A - 209.$$

C.A is calculated using the crossflow model with an effective selectivity of 22 and a cost permeability of 2.37 sm³/£k.H.Bar.

4.5.3 Supplier C

The mass balance data supplied by supplier C gave conflicting values for the effective selectivity when the analysis was carried in this case. Therefore the method could not be used to correlate the bids from supplier C.

4.5.4 Supplier D

Supplier D gave bids for cases 1 and 2, the pure CO product cases. These all require two stage processes for the separation and there was no detailed mass balance data provided apart from the CO recovery for the given specification.

Simulation of the process using the crossflow model of a two unit type recycle permeator showed that the effective selectivity of membrane plant D was significantly lower than the other membrane plants. This appeared to be in the range of 14 to 16.

In the absence of sufficient data a reliable correlation could not be made.

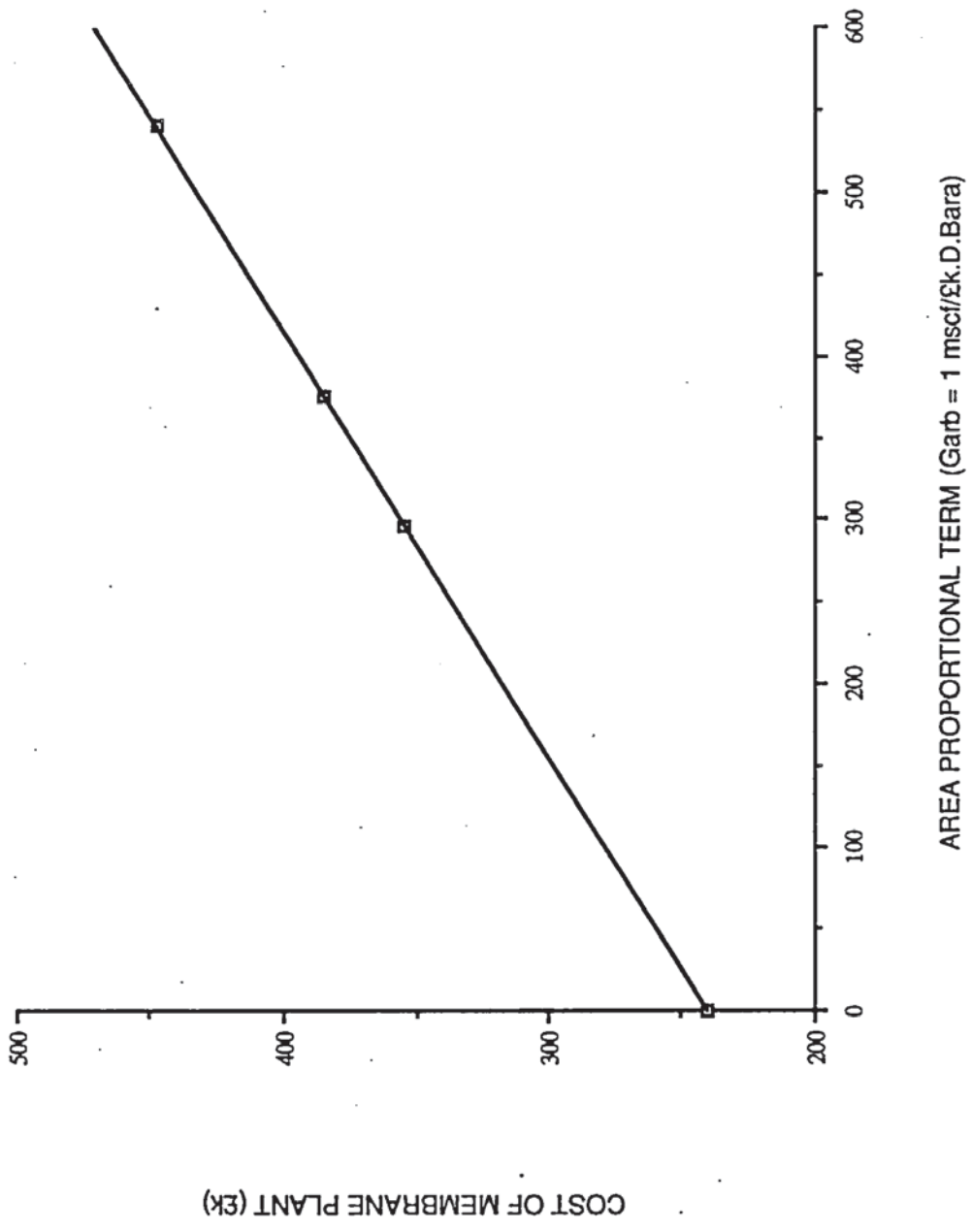
4.5.5 Supplier E

Supplier E provided bids for the syngas ratio adjustment to H₂:CO ratio of 1:1 (case 3) only. They gave data for the 30,40 and 50 bara feed cases.

The mass balance data was matched using the single stage crossflow model and an effective selectivity of 25 was calculated. This effective selectivity was then used to correlate the bids.

Figure 4.13 shows the plot of membrane plant cost against the arbitrary area

FIGURE 4.13 . . . Correlation of bid information from supplier E
to determine cost permeability for membrane plant E.



proportional cost, using $G_{arb} = 1.0 \text{ mscf/}\text{£k.D.Bara}$. As can be seen, the correlation fits very well and is of the same form as for suppliers A and B. This correlation, of course, can only be used for small, single stage membrane plant.

$$G_C = G_{arb}/(\text{slope}).$$

$$G_{arb} = 1.0 \text{ mscf/}\text{£k.D.Bara}.$$

$$\text{Slope} = 0.3868.$$

Thus :-

$$G_C = 3.05 \quad \text{sm}^3/\text{£k.H.Bara}.$$

And :-

$$\text{Membrane Plant Cost (}\text{£k)} = C.A + 240.$$

C = Cost per unit area of membrane plant (£k/m^2).

A = Membrane area (m^2).

$C.A$ is calculated using the crossflow model with an effective selectivity of 25 and a cost permeability of $3.05 \text{ sm}^3/\text{£k.H.Bar}$.

4.5.6 Supplier F

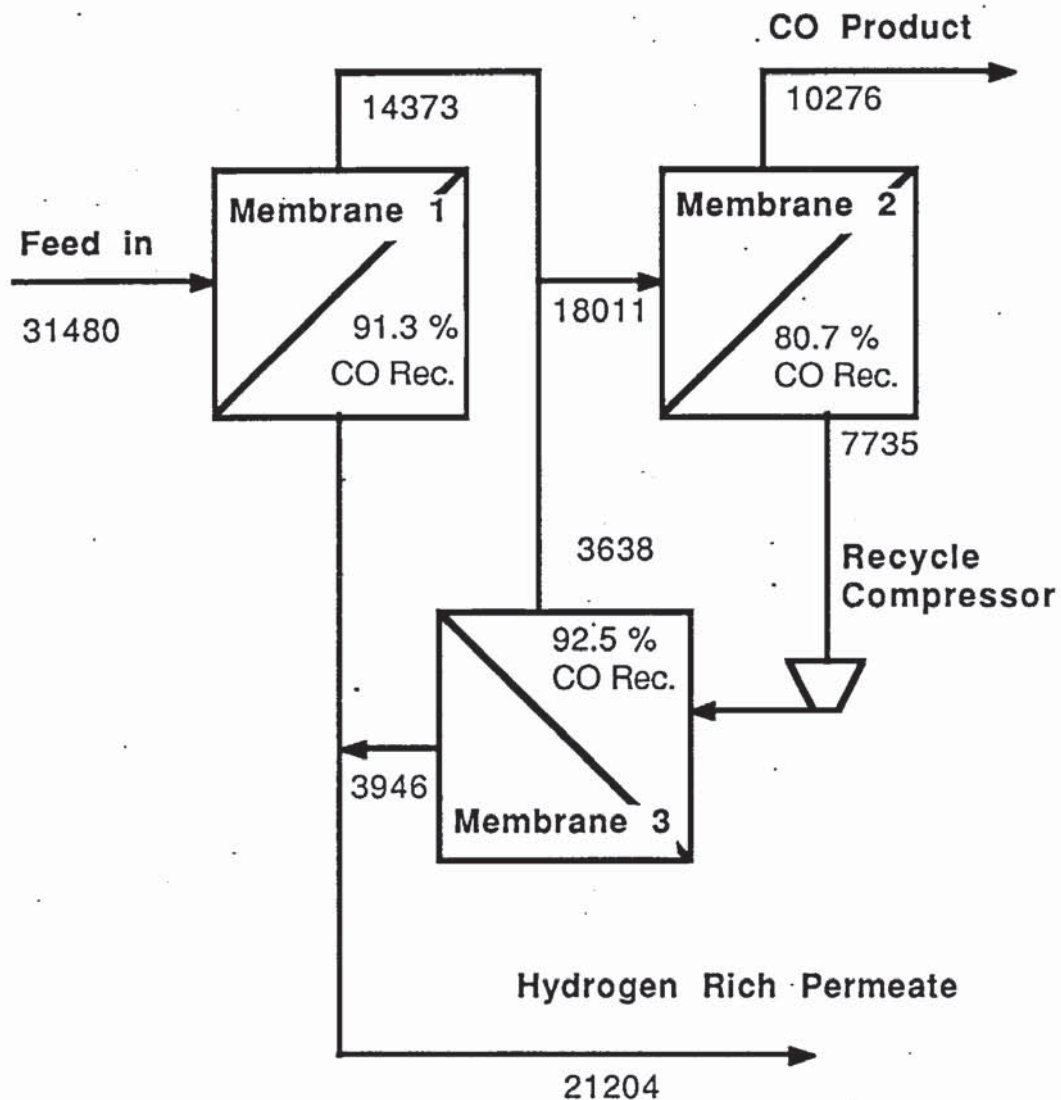
Supplier F submitted only one quotation. It was, therefore, not possible to verify the calculation of effective selectivity by correlation with other data. However, it was possible to establish the probable process layout which was used, and the internal process mass balance from overall mass balance data.

The effective selectivity was calculated to be 19.

The calculated process flow and mass balance is given in figure 4.14.

FIGURE 4.14

Process Layout and Flows For Supplier F
(All Flows in sm³ /H)



4.6 Conclusions

1. The cost parameters, Effective Selectivity, α_e , and Cost Permeability, G_C , have been defined to describe the properties of membrane separation systems.
2. A model of the crossflow membrane permeator can be used with the effective selectivity and cost permeability to simulate the membrane separation process.
3. The correlation of information from suppliers, where enough information was obtained, has allowed the calculation of the effective selectivity, α_e , and the area proportional, cost permeability, G_C , of some commercially available membrane systems.

With the use of the cost correlations obtained, and α_e and G_C , the cost of the membrane separation can be calculated for any separation specification.

Effective Selectivity and Cost Permeability of Membrane Separation Plant.

Supplier.	Effective Selectivity α_e	Cost Permeability G_C (£k.H.Bara)
A	31	1.73
B	22	2.37
E	25	3.05
F	19	-

4. Having correlated the suppliers information it is possible to predict the suppliers membrane plant costs for other specifications. This in turn has provided useful information for B.P. Chemicals without reference to the supplying companies.

5. With the calculation of the effective selectivity and cost permeability for the commercial membrane plants and the available cost correlations, it will now be possible, using the crossflow model, to calculate the optimum separation specification which gives the minimum overall cost of CO for the H₂/CO separation.

CHAPTER 5

DETERMINATION OF OPTIMUM SEPARATION BY EXISTING MEMBRANES

5.1 Introduction

From the economic analysis carried out in chapter 3 it was seen that, by changing the separation specification a reduction in the cost of CO separation could be achieved.

There must therefore be a separation specification which will give the minimum cost of CO separation. So, what is the optimum separation specification for any particular membrane?

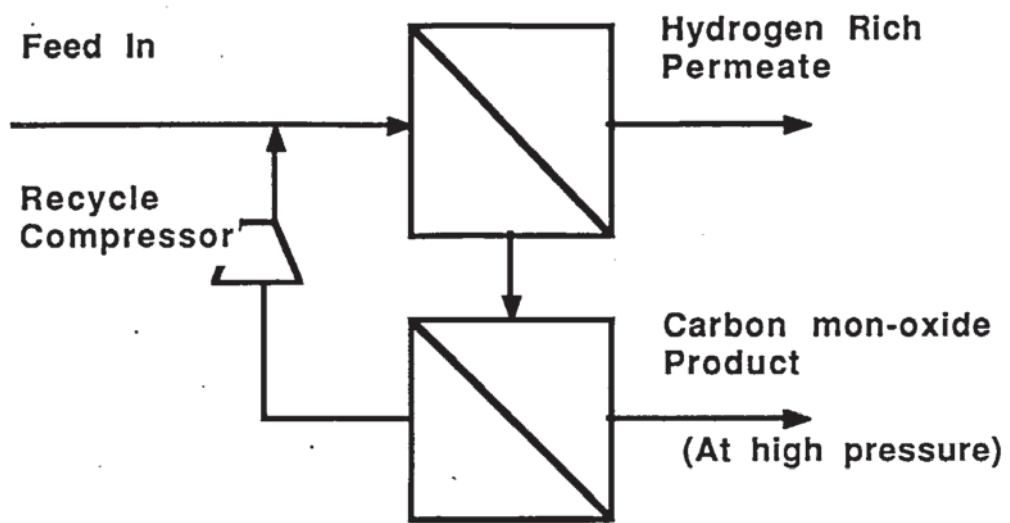
In this chapter the optimum separation specification for some of the commercially available membrane systems will be considered.

5.2 Modelling The Separation Process

As in the previous chapter, the crossflow model of a permeator was used to simulate the membrane separation process. If the required separation can not be achieved in one stage then the separation was carried out using the two

FIGURE 5.1

Two Unit Recycle Permeator



unit type recycle permeator process layout. Figure 5.1 shows the process flowsheet.

The two unit type recycle permeator process is adopted because many of the suppliers use this arrangement and it is consistent with the cost correlations derived in chapter 4.

The process will be modelled on the basis of a binary mixture. Although the feed is a multicomponent syngas, the binary model can be used with acceptable accuracy because the impurities in the syngas are small. The assumption made, is to say that any H₂O or CO₂ in the feed, permeates through the membrane at the same rate as H₂. And any N₂ or CH₄ in the feed, permeates through the membrane at the same rate as the CO.

The feed specification of :-

H ₂	0.626	mol. frac.	
CO	0.337	"	"
CO ₂	0.031	"	"
CH ₄	0.003	"	"
N ₂	0.003	"	"

becomes:-

H ₂	0.657 mol. frac.
CO	0.343 " "

To take account of impurities remaining in the product, the model is used with a higher purity in the model than actually specified. This value is arrived at by consideration of actual multicomponent mass balances from the commercial membrane system suppliers. For example if a 95% CO purity is specified, then the purity used in the crossflow model will be 97% CO purity and for a specified CO purity of 97%, a value of 99% is used in the crossflow model.

To simulate the separation process carried out by existing commercial membranes the effective selectivity and the cost permeability of the particular membrane, which have been calculated, are used in the crossflow model.

Here, only the optimum separation specification for membrane plants A and B will be determined.

The simulation of the separation process yields the capital cost of the membrane plant when combined with the appropriate cost correlation, the required compression power for the recycle stream and a complete mass balance.

5.3 CO Separation Cost

The cost of the separation of CO from the H₂/CO syngas is calculated in the same way as the economic analysis carried out in chapter 3.

The capital cost of the membrane plant and the mass balance data from the process simulation is used to build up the capital and variable costs of the POX process and separation process. The recycle compression power is used to calculate the capital cost of the compressor and the power cost.

This economic analysis produces the cost of CO generation and CO separation which in turn yields a comparative CO separation cost for the particular separation specification being considered.

$$C_{CS} = C_g + C_s - C_{gbc} \quad (5.1)$$

5.4 Optimum Separation Specification

The cost of CO separation is calculated for a range of CO separation specifications (CO purity and CO recovery). Graphs can be drawn to determine the optimum CO purity and the optimum CO recovery.

5.4.1 Supplier A

The graphs in figures 5.2 and 5.3 refer to the comparative separation cost of CO using supplier A's membrane plant. The plots of comparative CO separation cost against CO product purity show that the minimum cost is at a purity of between 95 and 96% CO even for different CO recoveries from 85 to 97% shown.

In the region of the optimum purity the graph is quite shallow, but CO separation cost increases very rapidly above 97% purity.

Figure 5.3 shows a plot of the comparative separation cost against CO recovery. The optimum CO recovery is found for the case of 95% CO purity, which is the optimum product purity.

Again the optimum recovery does not vary significantly with changing purity. The optimum CO recovery for this membrane plant is 90%.

As the required recovery increases above 94% the CO separation cost rapidly increases. The separation cost increases more gently for CO recovery rates of less than 90%.

FIGURE 5.2

Comparative cost of CO separation Vs CO purity for supplier A's membrane plant.

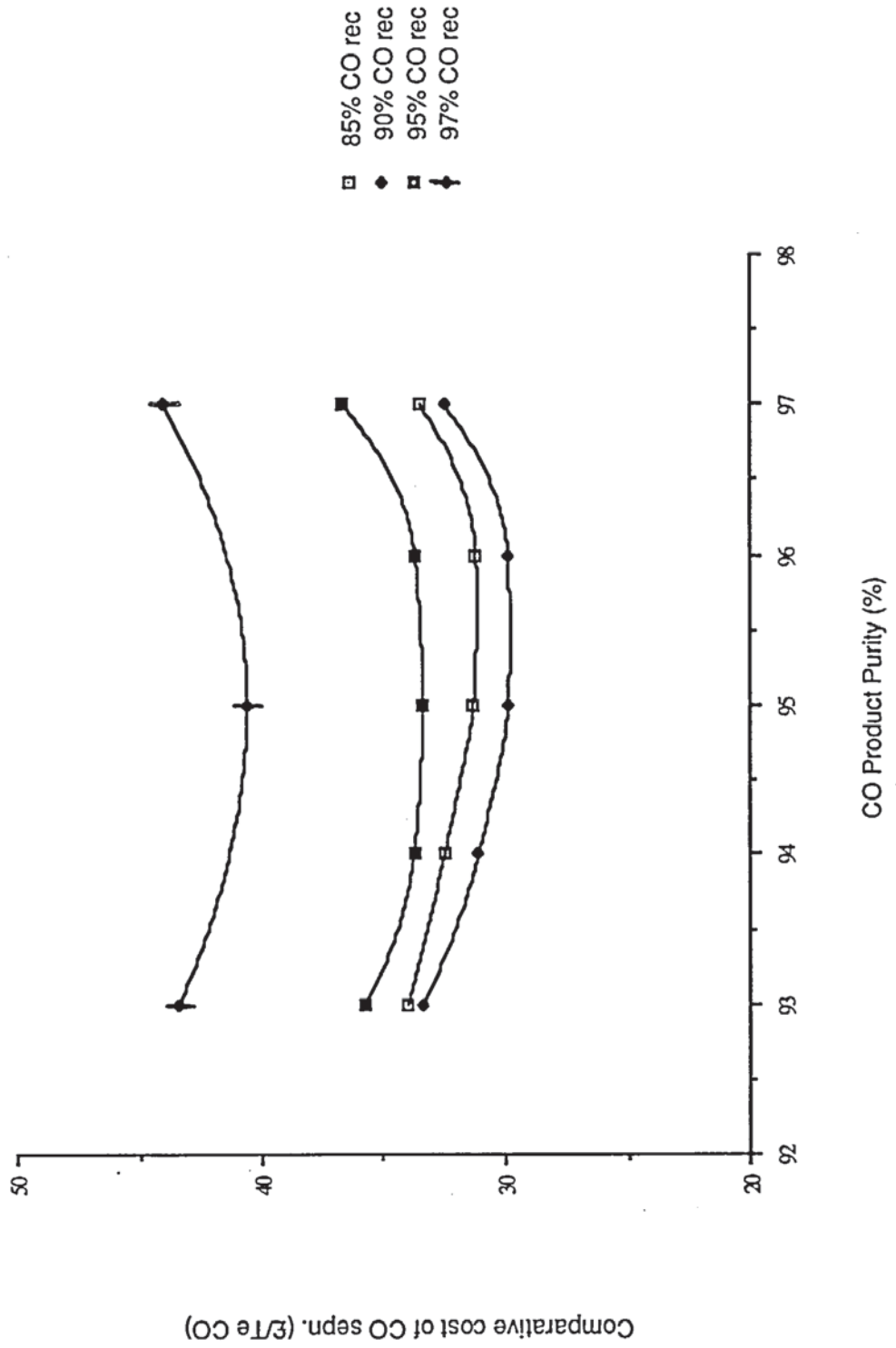
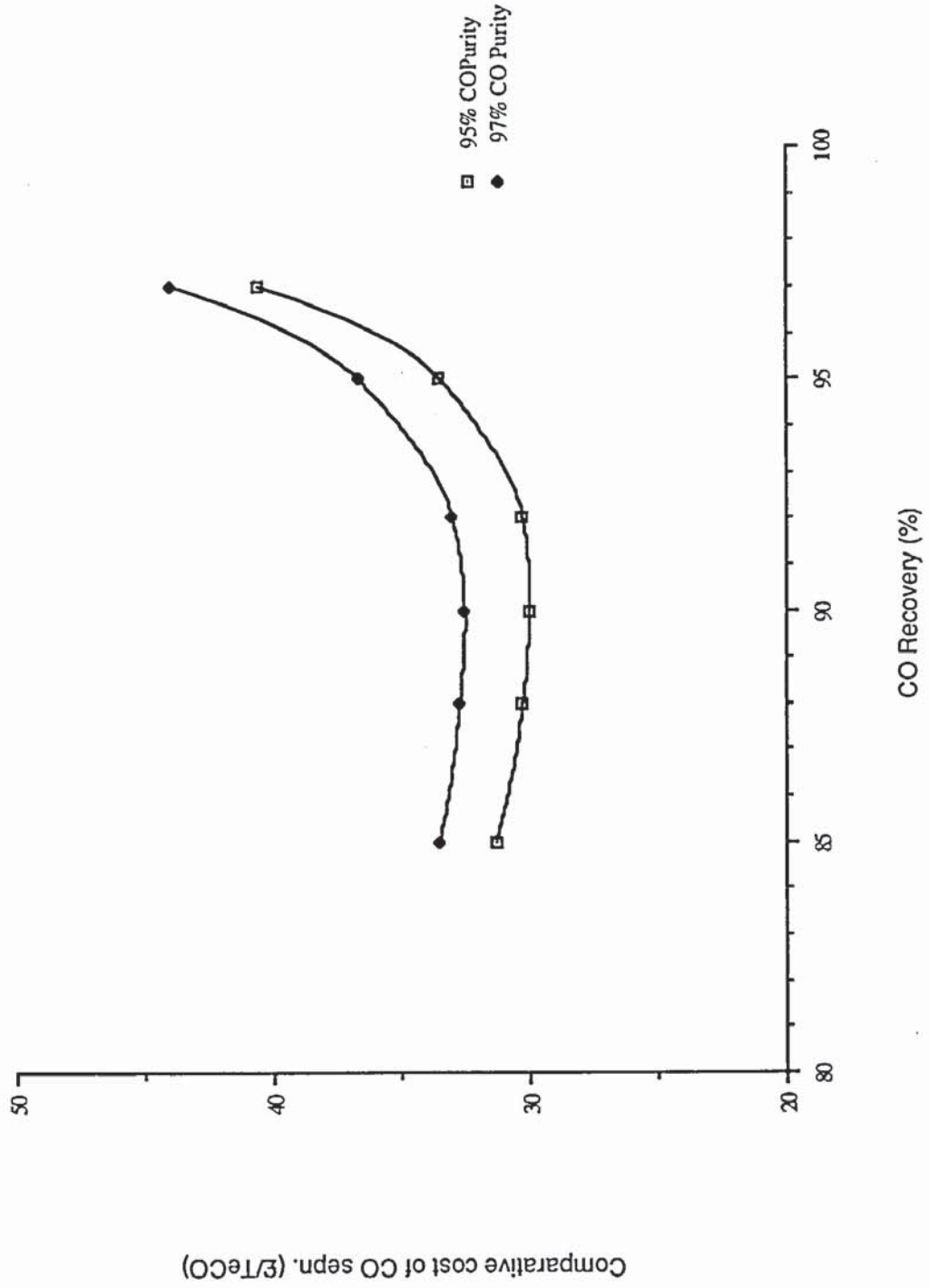


FIGURE 5.3 Comparative cost of separation of CO Vs CO recovery for supplier A's membrane plant to establish optimum recovery.



5.4.2 Supplier B

Figure 5.4 shows graphs of the comparative CO separation cost against CO product purity, at different CO recoveries, for membrane plant B. The minimum cost again lies between 95 and 96% CO purity.

The plots in figure 5.5 show the comparative CO separation cost against the CO recovery at a number of CO purities. The optimum CO recovery is at 88% for the optimum purity.

Comparative cost of separation of CO using membrane plant B
Vs CO product purity, to establish optimum purity.

FIGURE 5.4

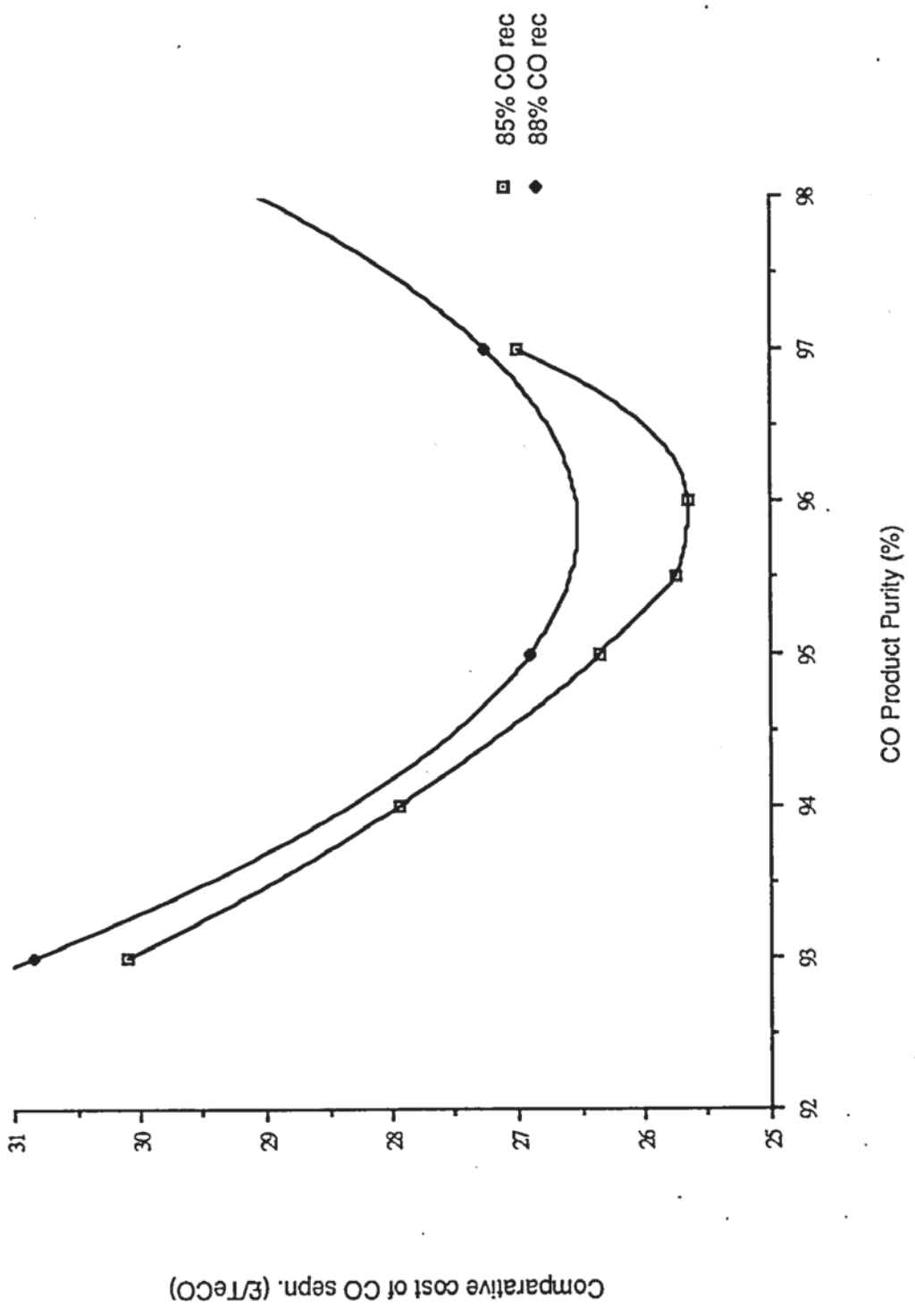
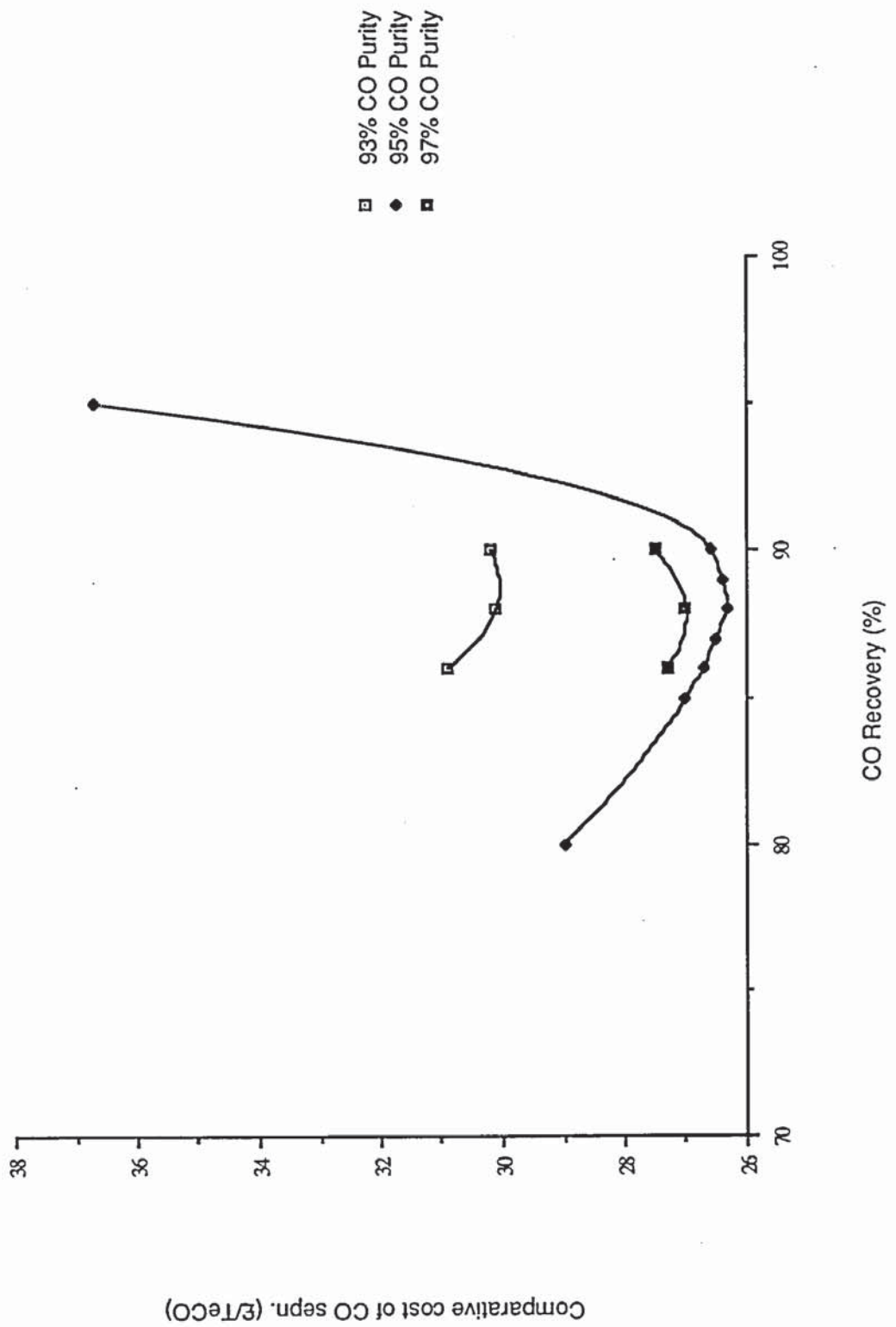


FIGURE 5.5 Comparative cost of separation of CO Vs CO recovery for membrane plant B, to establish optimum recovery.



5.5 Conclusions

1. If there is enough information about suppliers membrane plant to characterise the properties of the membrane in terms of effective selectivity and cost permeability, then the optimum separation specification can be found.
2. The optimum separation specification for the membrane plants of suppliers A and B have been determined.

Supplier A :

$$\alpha_e = 31$$

$$G_C = 1.78 \text{ sm}^3/\text{£k.H.Bar.}$$

Optimum CO purity = 95%.

Optimum CO recovery = 90%.

Supplier B :

$$\alpha_e = 22$$

$$G_C = 2.37 \text{ sm}^3/\text{£k.H.Bar.}$$

Optimum CO purity = 95.5%.

Optimum CO recovery = 88%.

3. The cost of CO separation using the optimum specification has been reduced considerably from that of the cryogenic separation specification. For supplier A the comparative cost is £32/te.CO and for supplier B the

comparative cost is £27/te.CO. This represents a reduction to 52% of the cryogenic separation cost (cryogenic separation cost = £52.40/te.CO) for membrane plant B.

4. The competitive position of membrane separation for the H₂/CO separation process considered has therefore been radically changed from being on a par with cryogenic separation, using the cryogenic separation specification, to being very much more competitive than cryogenic separation if the process as a whole is optimised.

A comparative separation cost of CO to less than 60% of the cryogenic separation is equivalent to a cost reduction of the process as a whole [POX reactor + Separation process + Acetic acid reactor] of the order of 10%.

CHAPTER 6

TARGETING MEMBRANES FOR H₂/CO SEPARATION

6.1 Introduction

It has been shown previously that membrane separation of H₂ and CO can be competitive with cryogenic separation if the optimum separation specification is chosen.

The development of new membranes requires improvements in performance over existing membranes. How do we know which properties of the membrane should be improved to provide the best improvements in economic performance?

We know that it is important to establish the optimum separation specification for any particular membrane. If the effective selectivity of the membrane is changed this will alter the recycle requirements and compression costs of the separation process and if the cost permeability is changed, this will affect the capital cost of the membrane plant. And changes in one or both of the properties may also have an effect upon the optimum separation specification.

As effective selectivity is increased, then, ultimately it would be expected that

the separation would be able to be achieved without any recycle (ie. a one stage process).

As cost permeability increases, it would be expected that the capital cost of the membrane plant would become increasingly negligible.

This chapter describes the "targeting" method now proposed to provide direction for the development of new membranes, including consideration of the limiting values of effective selectivity and cost permeability.

It is suggested that the concept of targeting (developed here for the H₂/CO separation in the acetic acid process) may be usefully employed to guide development of membranes for other processes.

6.2 Targeting

Targeting is the procedure used to define the properties of membranes such that membrane gas separation will be economically competitive with other methods of separating gases. The case considered here is the separation of H₂ and CO to produce a pure CO product for the large scale manufacture of acetic acid.

The properties of the membrane which affect its economic performance are

the effective selectivity to H₂ and CO and the cost permeability of the faster permeating gas, H₂.

It has been shown in the previous chapter that for any particular combination of effective selectivity and cost permeability there is an optimum separation and a minimum cost process.

It is possible that the same cost of CO separation will result from many combinations of effective selectivity and cost permeability. The cost of CO separation can be calculated for a range of values of effective selectivity and cost permeability at the optimum separation specification.

The cost data can then be represented graphically as plots of comparative CO separation cost against effective selectivity for various values of cost permeability. From these curves, iso-cost lines can be constructed on a plot of effective selectivity and cost permeability.

These iso-cost lines form the "targeting" graph which may be used in the development of improved membrane gas separators. The targeting graph shows the economic gains to be expected from increases in effective selectivity and/or permeability.

The range of properties considered to obtain the targeting graph was an effective selectivity range of 5 to 60 and a cost permeability range of 1.0 to

20.0 sm³/£k.H.Bar.

6.3 Optimum Separation Specification

A techno-economic analysis was carried out using the membrane separation models and economic evaluation methods explained in previous chapters.

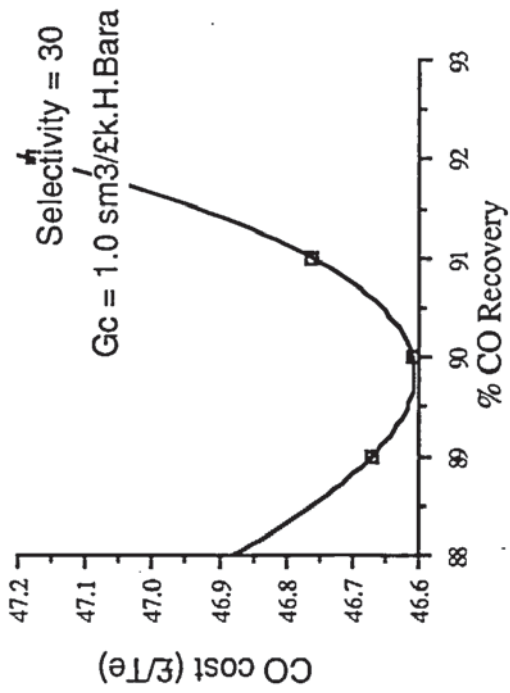
This analysis determined the comparative cost of CO separation for the range of membrane properties being considered. The results are represented graphically in figures 6.1 to 6.6

The CO recovery is considered in figures 6.1 and 6.2. Here the cost of separation is plotted against the CO recovery. In figure 6.1 the effective selectivity of the membrane is 30. The four graphs show that through the range of cost permeabilities of $G_c = 1.0$ to $G_c = 5.0$ sm³/£k.H.Bar the optimum CO recovery varies only from 89.75 to 90.75. Also the graphs are very shallow in this region, thus the optimum recovery could be considered constant over the range of cost permeabilities from 1.0 to 5.0 sm³/£k.H.Bar.

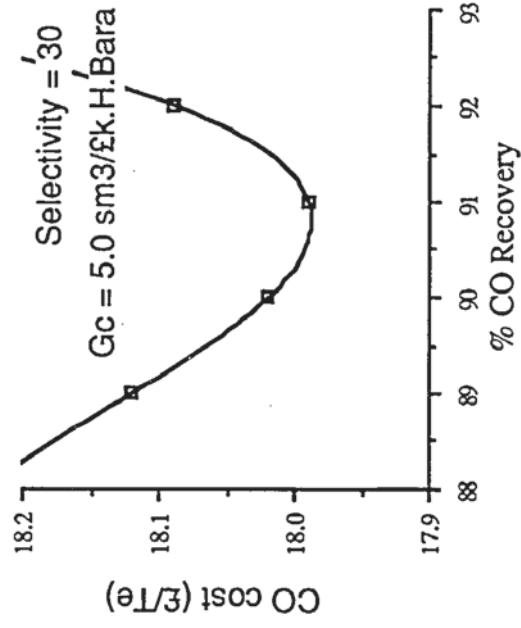
If the permeability is increased to very high values, say 10.0 or 20.0 sm³/£k.H.Bar, the lower two graphs in figure 6.1 show that the optimum CO recovery has remained in the region of 91%.

Figure 6.2 shows a similar picture to figure 6.1. Only here $\alpha_e = 50$.

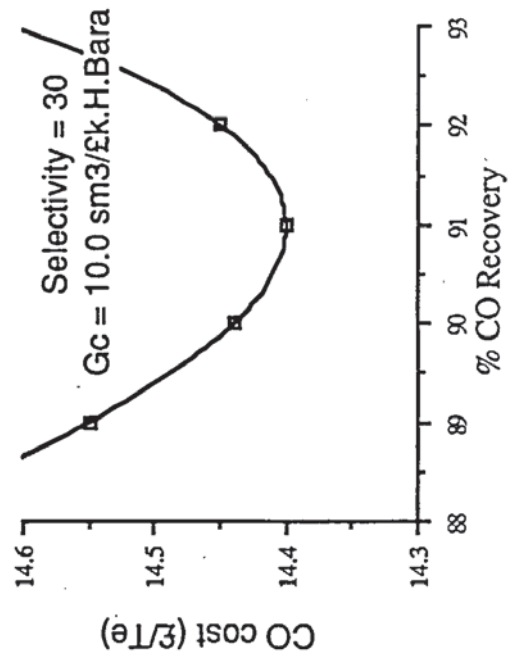
FIGURE 6.1 CO Cost vs CO Recovery



CO Cost vs CO Recovery



CO Cost vs CO Recovery



CO Cost vs CO Recovery

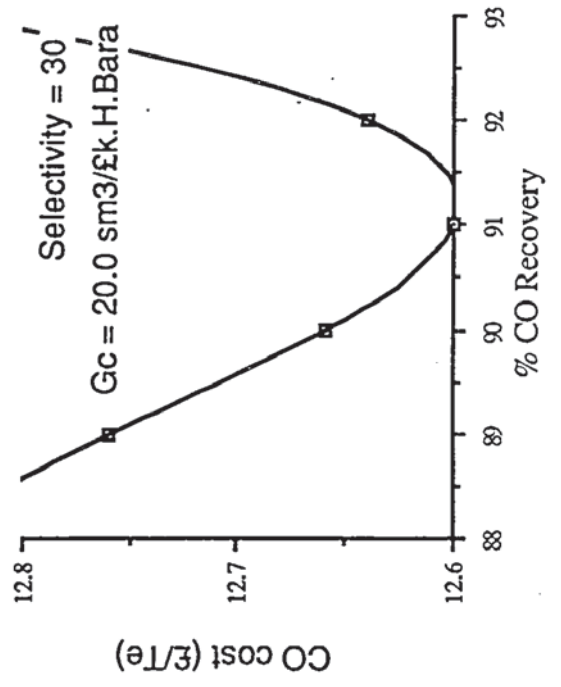
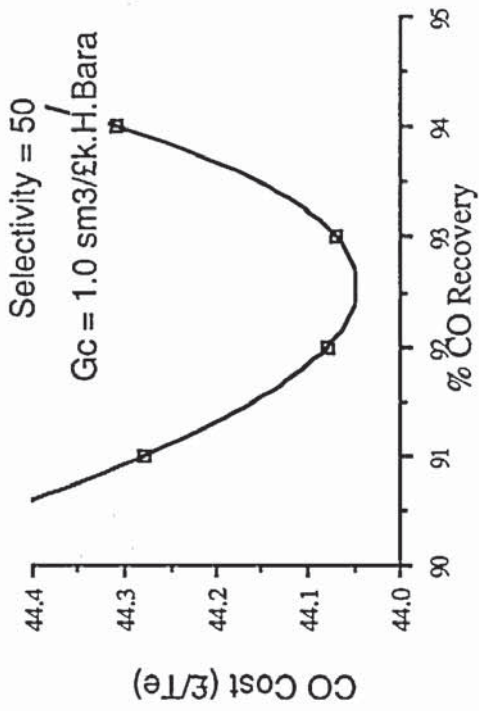
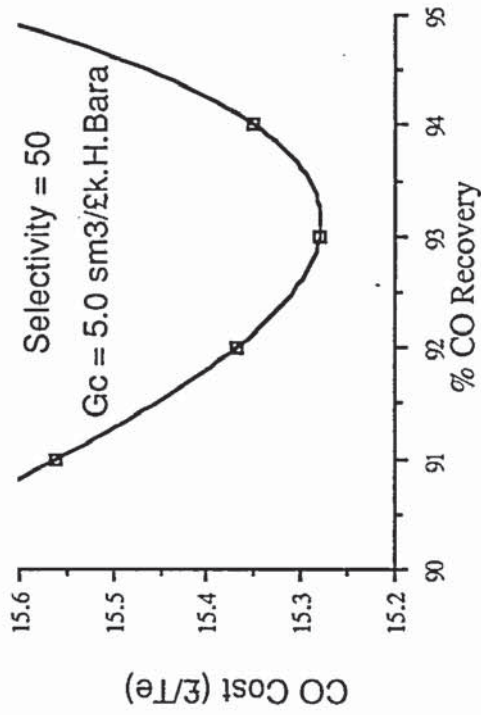


FIGURE 6.2

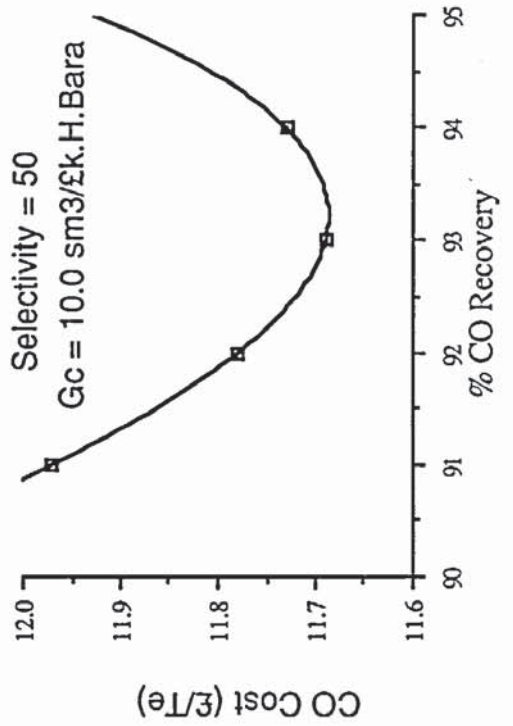
CO Cost vs CO Recovery



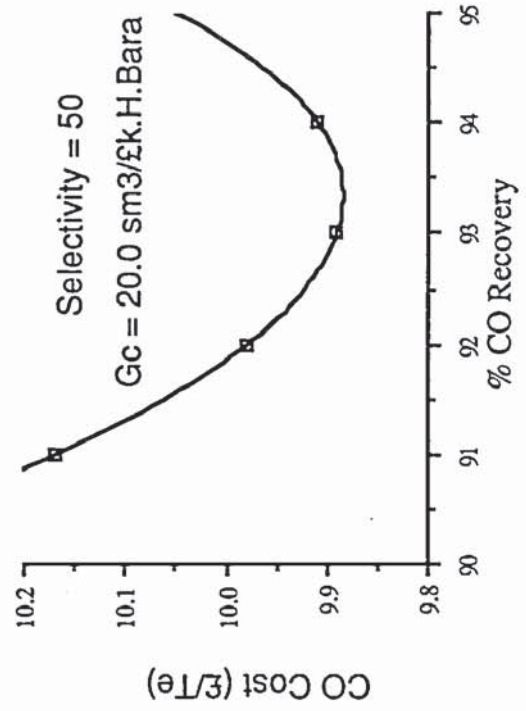
CO Cost vs CO Recovery



CO Cost vs CO Recovery



CO Cost vs CO Recovery

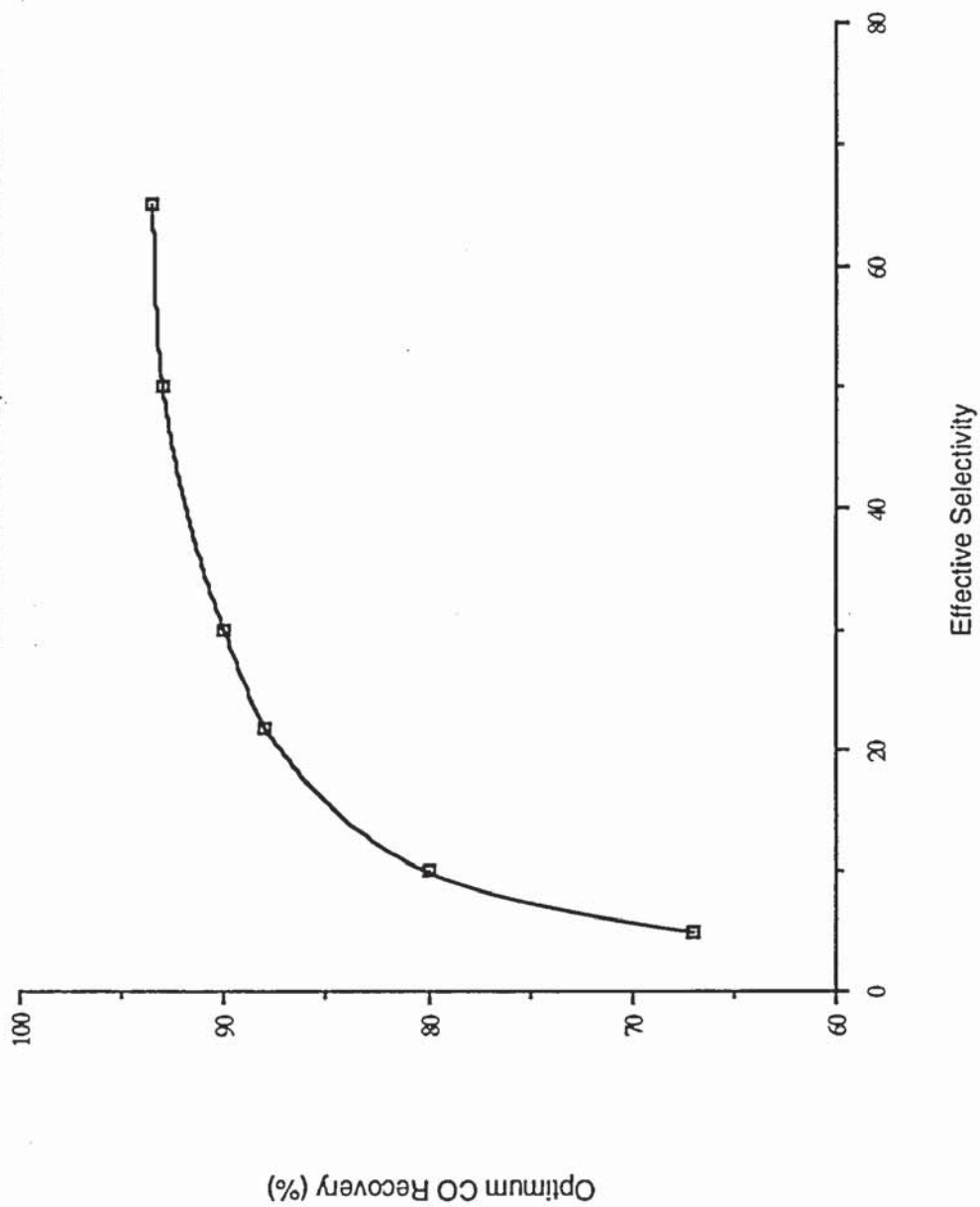


The graphs show the comparative CO separation cost versus the CO recovery for different values of membrane cost permeability. The four graphs show that the optimum CO recovery is between 92 and 93% for the range of cost permeabilities from 1.0 to 20.0 $\text{sm}^3/\text{£k.H.Bar}$. Again the curves are very shallow at the minimum point so it is taken that the optimum CO recovery is constant at 93%.

Further calculations of the optimum CO recovery for different effective selectivities were made. From these it could be seen that the optimum CO recovery is largely dependent upon effective selectivity, but varies little with the cost permeability. So, for the purposes of this analysis the optimum CO recovery is taken to be independent of the cost permeability for a given effective selectivity for the range of permeabilities under consideration.

Figure 6.3 shows a plot of the optimum CO recovery against the effective selectivity of the membrane separator which has been used in the techno-economic analysis.

FIGURE 6.3 Plot of optimum CO recovery against effective selectivity for membrane separation of H₂ and CO.



The CO purity is considered in figures 6.4 and 6.5. Figure 6.4 considers the H₂/CO separation using a membrane of effective selectivity of 30. The graphs show that as the cost permeability is increased the optimum CO purity increases. For cost permeabilities close to that of existing membrane systems is within the range of 94.5 to 96%. In the analysis to build up the targeting graph a 95% CO purity is used. This is assumed to be adequate because the graphs are shallow close to the minimum point. Where higher values of cost permeability, between 5.0 and 20.0 sm³/£k.H.Bar, are considered, the optimum purity is between 96 and 97.5%. Calculations made for high values of permeability use the appropriate optimum CO purity.

Comparing figure 6.4 with figure 6.5, which plots CO separation cost against CO purity at an effective selectivity of 50, it can be seen that the optimum CO purity is very close to that of the case where the effective selectivity is 30. It is taken that the optimum CO purity will be largely independent of effective selectivity in the range of interest. So the CO purity is varied only with the cost permeability.

Figure 6.6 shows the optimum CO purity for variations in membrane cost permeability.

FIGURE 6.4 Cost of CO separation, for a range of cost permeabilities, against CO product purity.

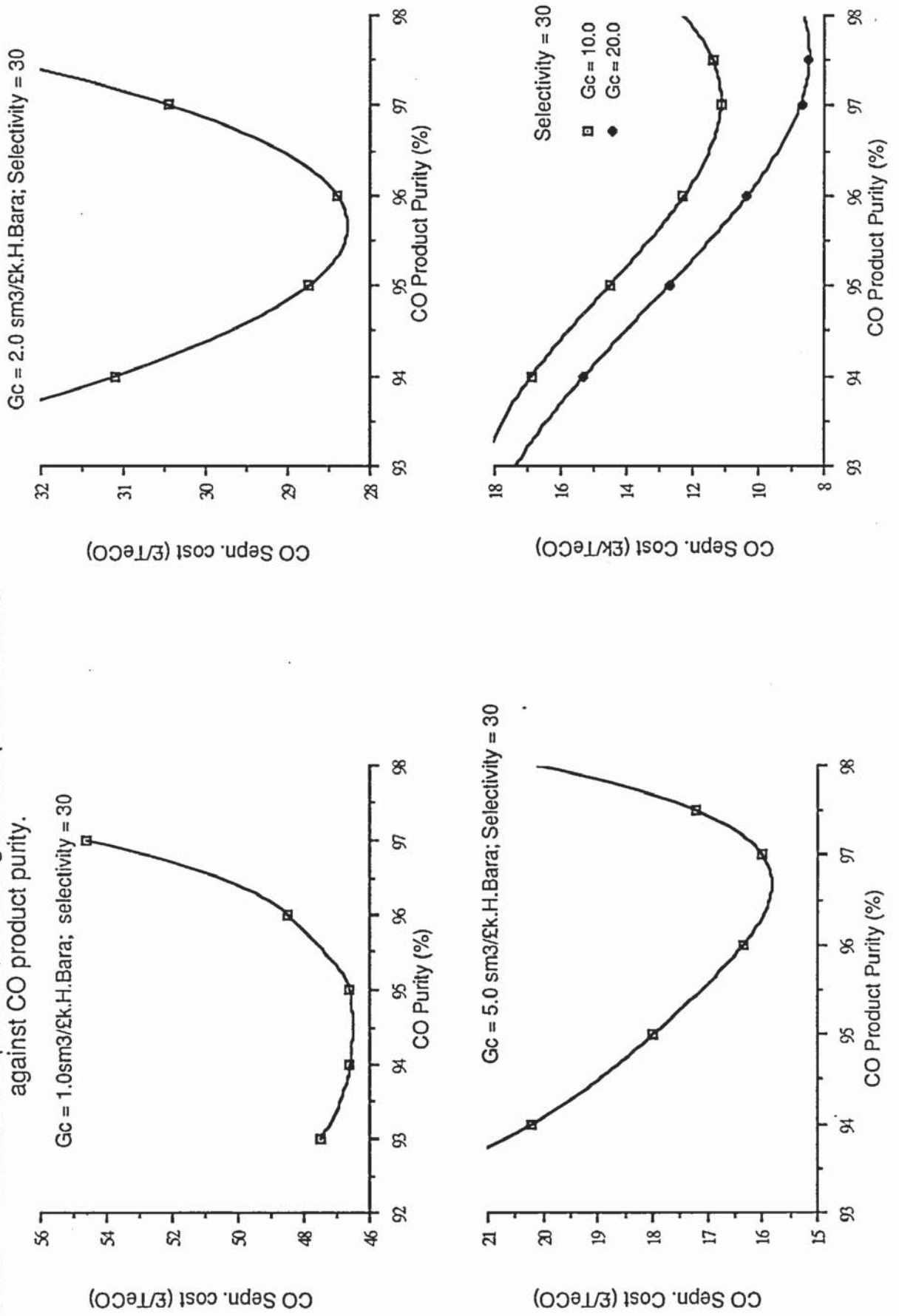


FIGURE 6.5 CO Separation cost, for a range of cost permeabilities, against CO product purity.

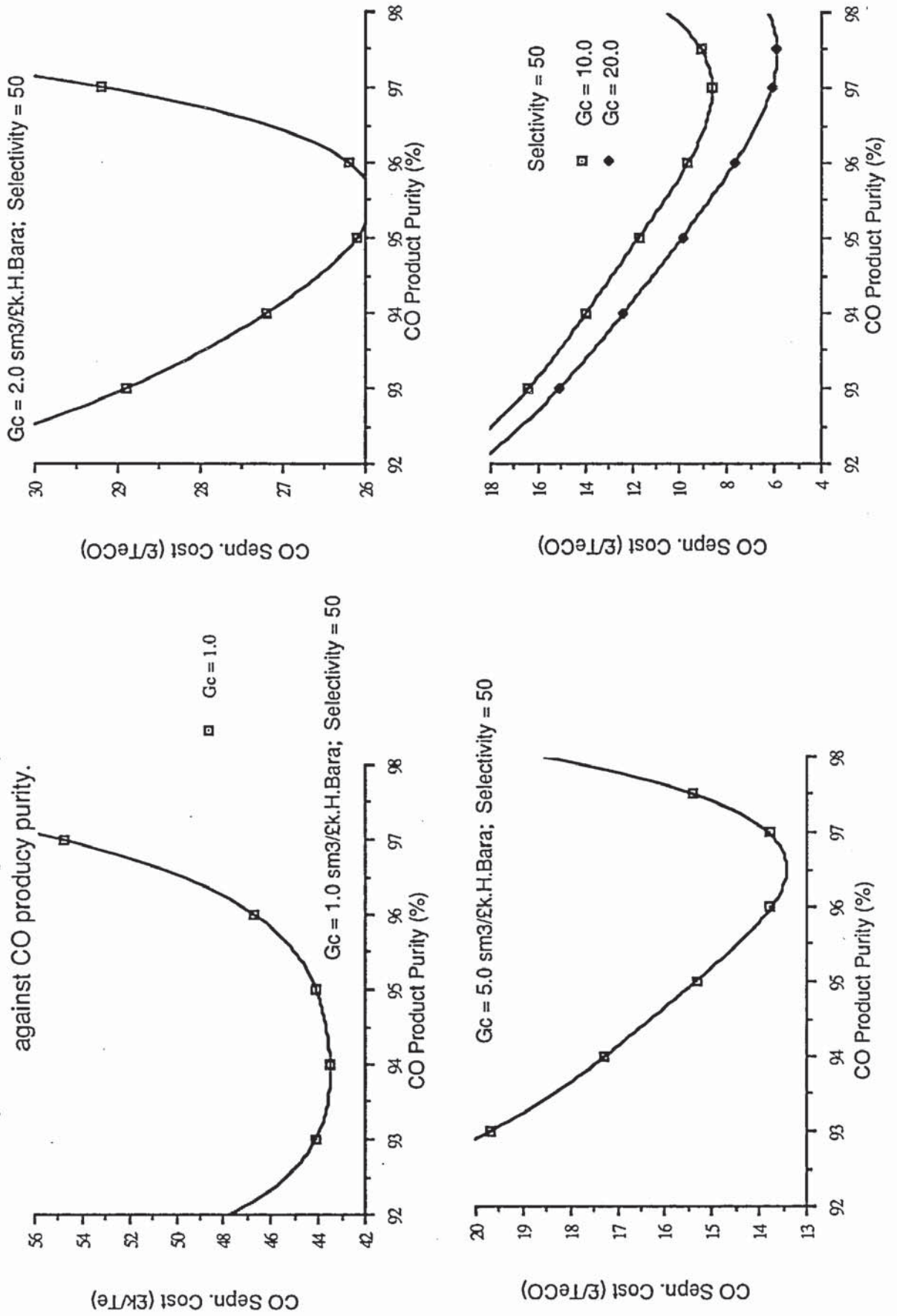
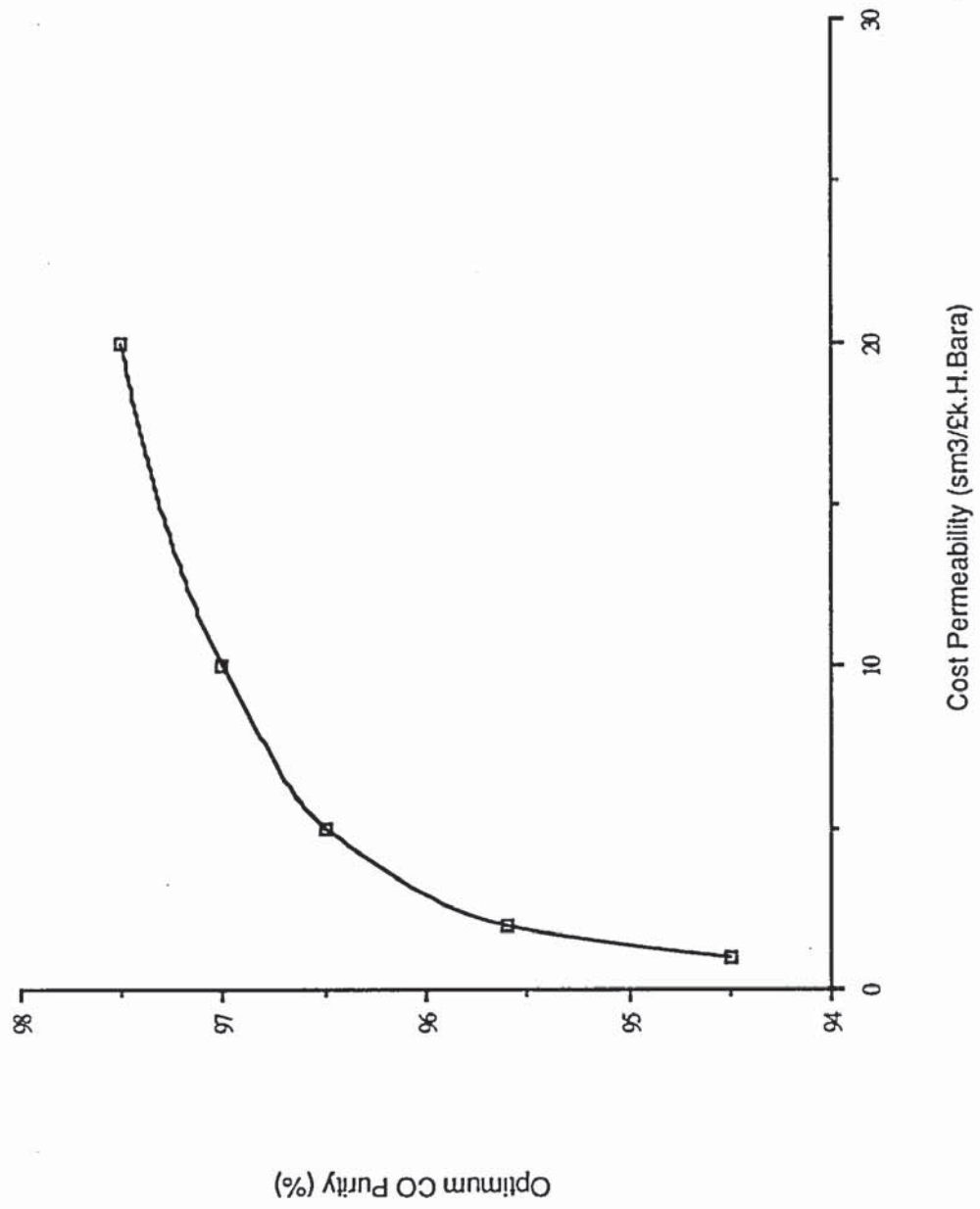


FIGURE 6.6

Plot of optimum CO product purity against cost permeability

for the membrane separation of H₂ and CO.



6.4 The Targeting Graph

Using the optimum CO recovery at various membrane effective selectivities and the optimum CO purity at various cost permeabilities, the comparative cost of CO separation is calculated.

Figure 6.7 shows the cost of CO separation plotted against effective selectivity for different values of cost permeability. By drawing lines of constant cost, figure 6.7 was used to construct iso-cost lines on a plot of effective selectivity versus cost permeability, shown in figure 6.8, the targeting graph.

These curves become the basis for targeting membrane development.

Figure 6.9 shows the targeting graph for an extended range of permeability, up to 20.0 $\text{sm}^3/\text{k.H.Bar}$.

FIGURE 6.7

Cost of CO separation Vs selectivity

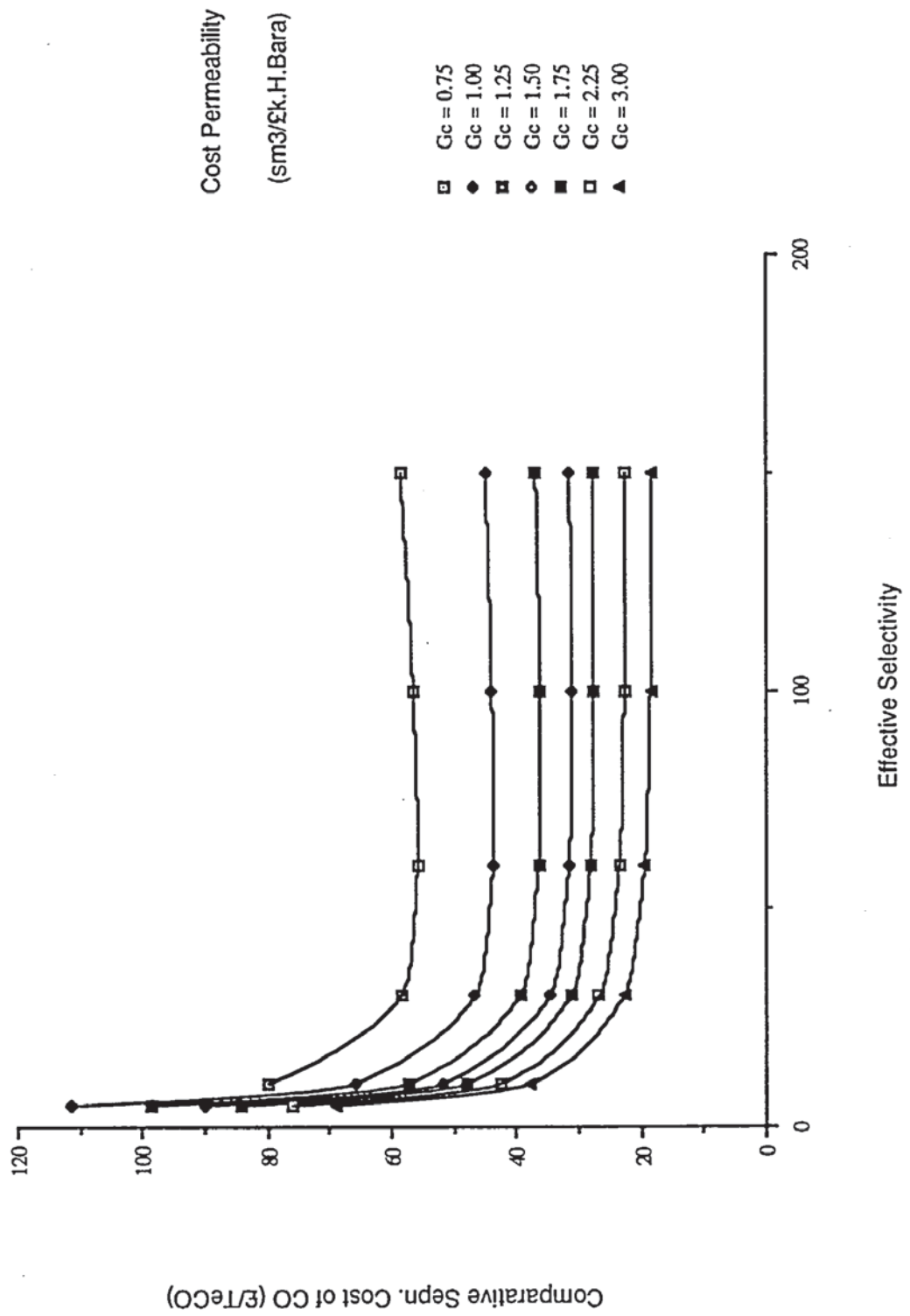


FIGURE 6.8

TARGETTING GRAPH

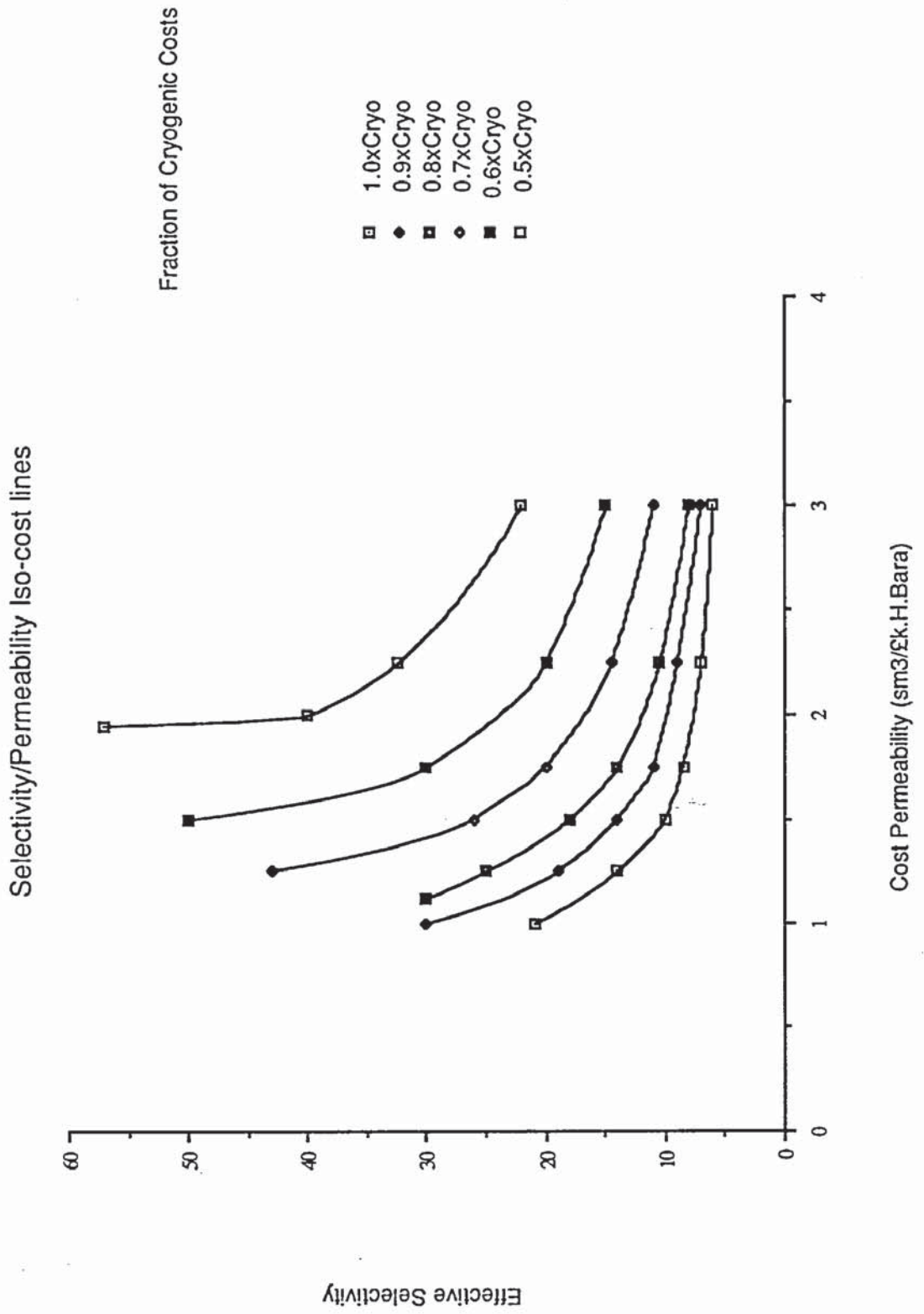
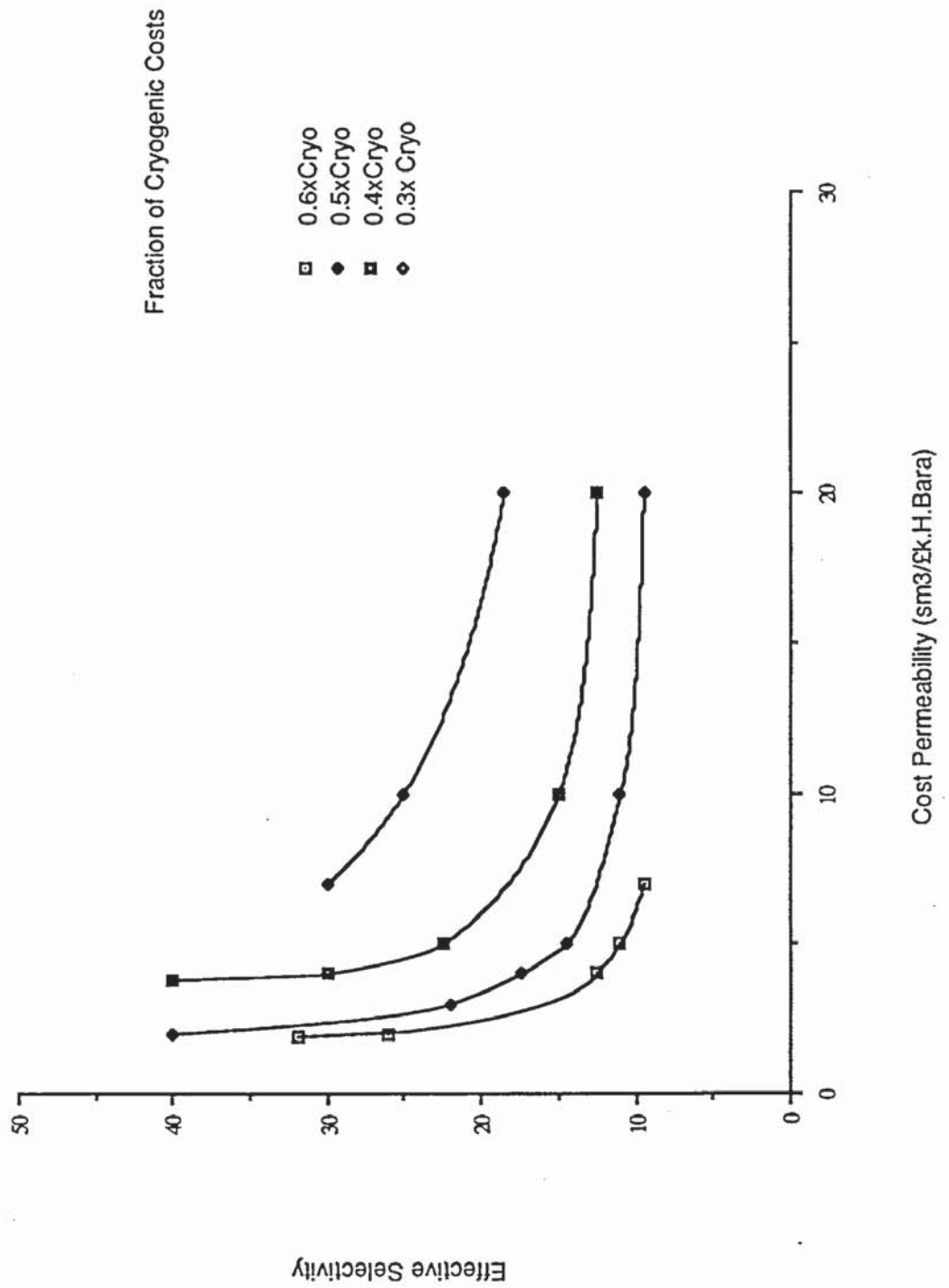


FIGURE 6.9

Iso-cost curves for an extended permeability range



6.5 Limiting Values Of Effective Selectivity And Cost Permeability

The effective selectivity of a membrane separation system determines the amount of recycle required to achieve a particular separation. As the effective selectivity of the membrane is increased, the amount of recycle required will decrease. Eventually, as the selectivity is increased, the required separation will be able to be achieved in a one stage process.

Further increases in the selectivity will yield a higher quality CO product, but not necessarily a reduction in the cost of CO separation in terms of the process as a whole.

At an effective selectivity of 60 to 70 a pure CO product can be produced at close enough to the optimum recovery in one stage.

The cost permeability of membrane separators determines the capital cost of the membrane plant. As the cost permeability increases the capital cost of the plant reduces. This implies that as the cost permeability tends to infinity, the membrane plant cost will tend to zero.

$$G_c \rightarrow \infty ;$$

$$\text{Membrane plant cost} \rightarrow 0$$

The CO separation cost equation is :-

$$C_s = C_{sep} + C_{comp} + C_{mr} + C_p$$

C_s = Cost of separation.

C_{sep} = Amortised cost of
separation plant.

C_{comp} = Amortised cost of
compressor.

C_{mr} = Membrane
replacement cost.

C_p = Power cost.

As $G_c \rightarrow \infty$

$$C_s \rightarrow C_{comp} + C_p$$

Therefore the cost of separation will be determined by the compression requirements which will determine the upstream and downstream costs depending upon the CO recovery and purity. These are in turn dependent upon the effective selectivity. Thus there is a minimum CO separation cost for a given effective selectivity where an increase in cost permeability will make no difference to the cost of separation.

FIGURE 6.10

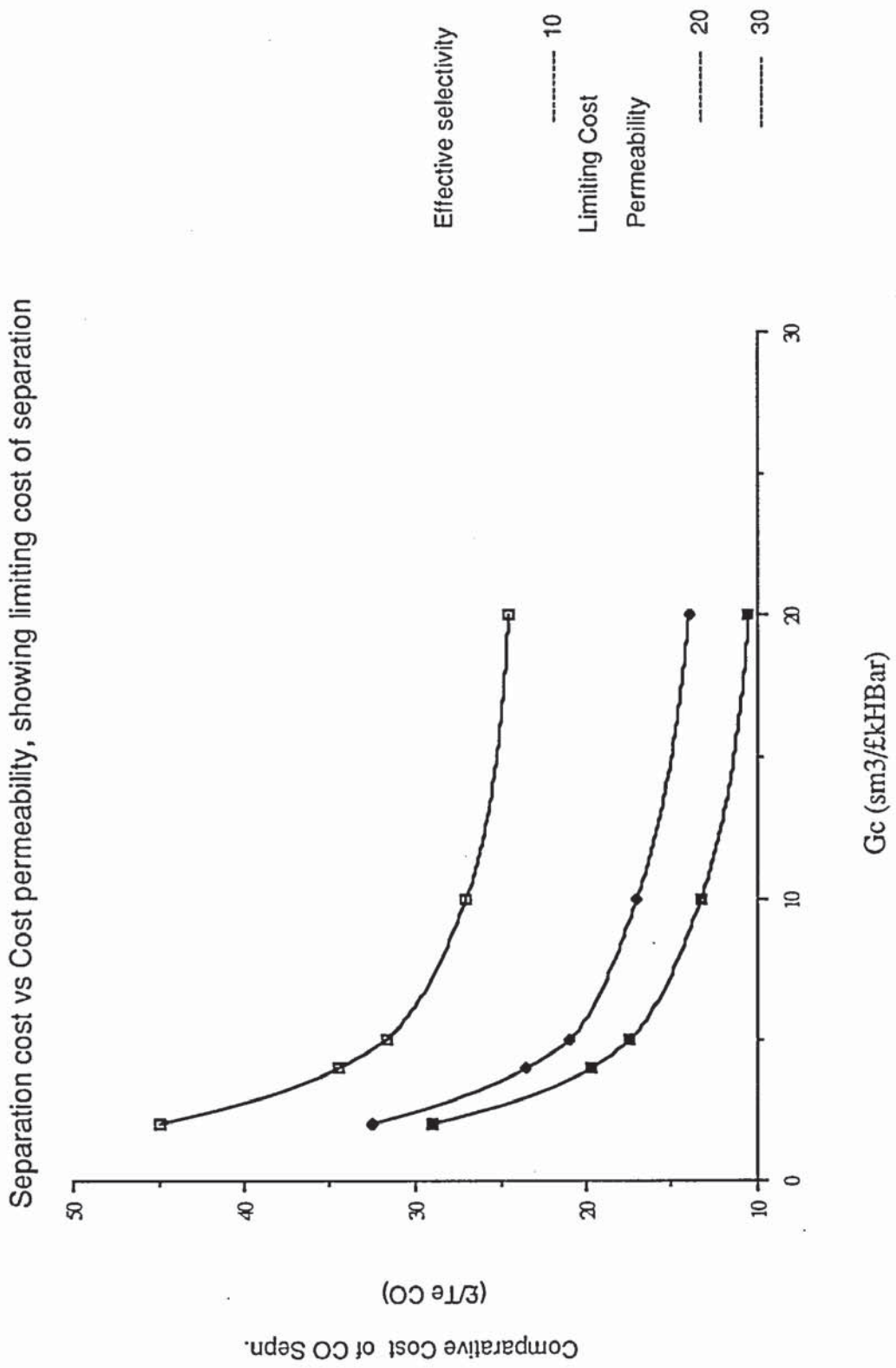


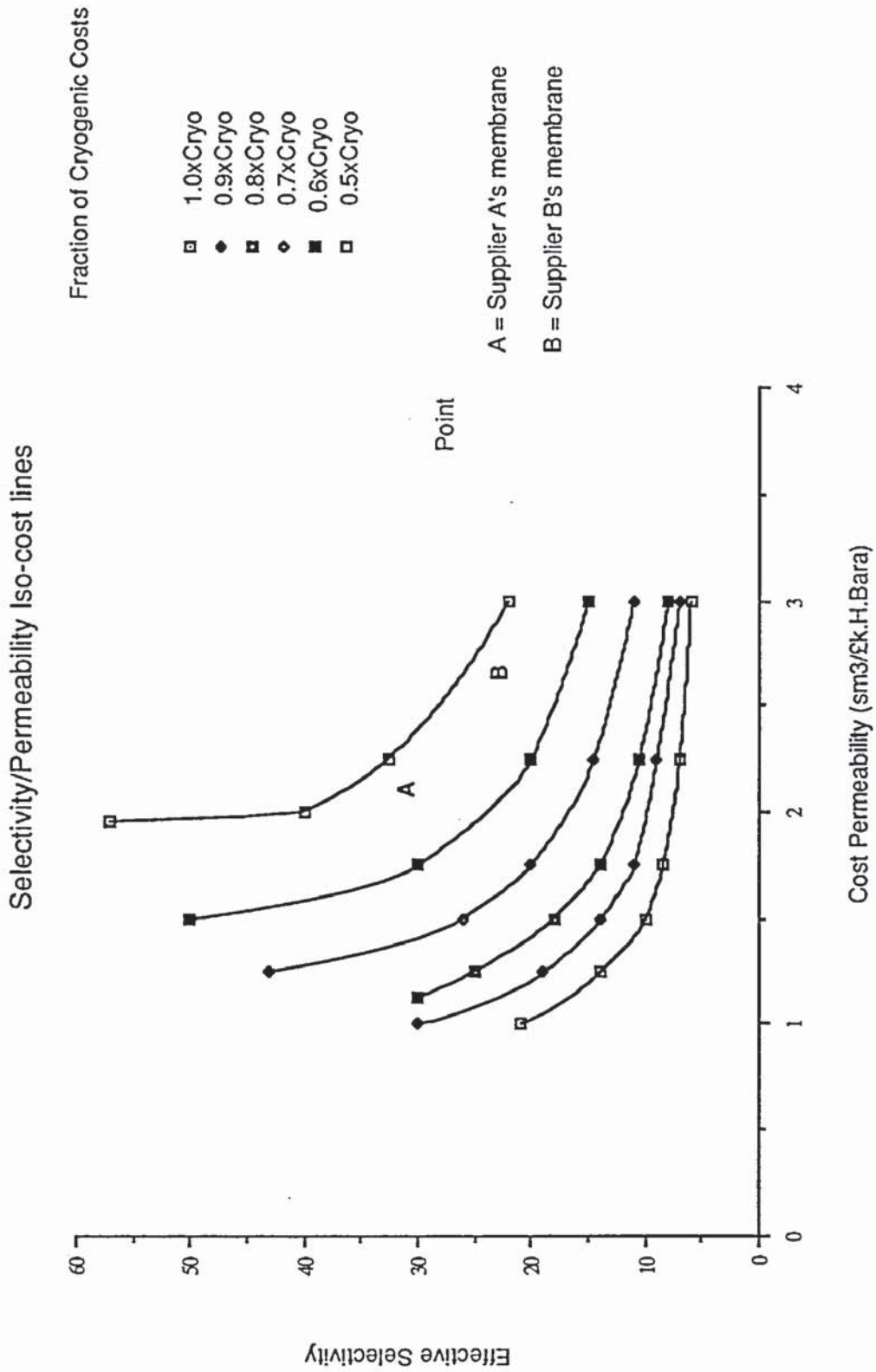
Figure 6.10 shows plots of comparative CO separation cost against cost permeability showing the limiting separation cost for various values of effective selectivity.

6.6 Conclusions

1. The targeting graph shows the economic gains to be expected from increases in effective selectivity and/or cost permeability. Thus providing a target to aim at for those engaged in membrane research and development.
2. Existing commercial membranes can be pin-pointed on the graph to show the current position. (See figure 6.11).
3. Newly developed membranes can be plotted on the graph to give a very quick economic appraisal of the new membrane.
4. A target in terms of selectivity is an effective selectivity of 60 to 70 where a one stage process could be used for the separation.
5. Large gains can be made by increasing cost permeability before increasing effective selectivity because the currently used membranes are of low permeability. However, the gains become less significant above a cost permeability of about $10.0 \text{ sm}^3/\text{£k.H.Bar}$.

FIGURE 6.11

TARGETTING GRAPH



6. There is a minimum cost of separation for each effective selectivity, where increases in the cost permeability will not yield a reduction in separation cost.

7. The use of the targeting method can be extended to other separations and may also eventually provide an indication as to which method of separation is appropriate for a given process.

CHAPTER 7

MOLECULAR DESIGN OF POLYMER MEMBRANES

7.1 Introduction

The targeting analysis carried out in the previous chapter has shown that the greatest economic gains can be made by improving the permeability of the gas separation membranes, because currently used membranes are of low permeability.

Once the permeability of the membrane gets close to the limiting value then a worthwhile target is an effective selectivity of 60. The hydrogen / carbon monoxide separation can then be carried out in one stage.

A number of different approaches could be considered for the selection of new membrane materials. We know that there is only limited permeability data available for hydrogen and carbon monoxide. Therefore, can molecular design methods, based upon molecular group contributions be used to design and select polymer materials with enhanced separation properties?

Here, two empirical methods which use molecular group contributions to predict properties are used to select membrane materials for the separation of

hydrogen and carbon monoxide.

The first method combines the prediction of gas solubility in liquids using the UNIFAC group contribution method (134) with the use of the analogy of gas solubility in liquids with gas solubility in polymers (76). Taking the repeat structure of the polymer to be analogous to the liquid molecular structure, a measure of the solubility selectivity can be calculated.

The second approach uses a correlation based on the Permachor method (128) for the prediction of gas permeability through polymers.

Both the UNIFAC group contribution method and the Permachor correlation are based on molecular groups and whilst being able to predict properties for many molecular structures a limiting factor is the available number of molecular groups which can be used in the methods.

Candidate polymers have been selected using the molecular design methods as well as other methods considered for the improvement of membrane properties.

7.2 Molecular Design Methods

7.2.1 Approach 1. UNIFAC Group Contribution Method

Enhancement of Solubility and Solubility Selectivity

The process of gas permeation through polymer membranes is the product of the solubility of the gas in the polymer and the rate of diffusion, of the gas, through the polymer.

To obtain polymer structures which have good separating properties for the separation of hydrogen and carbon monoxide, the permeability of hydrogen through the membrane must be as high as possible and the selectivity of hydrogen to carbon monoxide must also be as high as possible. To produce polymers which may have enhanced separation properties the solubility and diffusivity of hydrogen and carbon monoxide in the polymer can be considered separately.

If the solubility of hydrogen and the solubility selectivity of one polymer can be increased over another it would be expected that the membrane separation properties would be enhanced, as long as there was no deterioration in the diffusivity of the membrane.

There is of course, only limited data available for the solubility of gases in polymers. There is much more data for the solubility of H₂ and CO in liquids and accurate solubility prediction methods are available.

Analogy Between Gas Solubility In Liquids With That In Polymers

The sorption and diffusion of gases through rubbery polymers has been compared to the absorption and diffusion through liquids (76). The magnitude of gas solubility in polymers is much less than that in liquids, but if the polymer repeat unit is taken to be analogous to the liquid structure then the ratio of gas solubility of two gases in the polymer is remarkably close to that of the solubility ratio in the liquid.

Whilst this analogy can only strictly be used for rubbery polymers, it may be able to be used to identify groups which will enhance the solubility properties of polymers for the hydrogen / carbon monoxide separation.

Solubility of H₂ and CO In Liquids

The following table, table 7.1, shows the solubility of H₂ and CO in various liquids. Several observations can be made, but one is that there is only a

small amount of experimentally determined solubility data for H₂ and CO in liquids.

TABLE 7.1**Experimentally Determined Solubility of H₂ and CO in Liquids**

Solvent	Mol. Frac. H ₂ X 10 ⁴	Mol. Frac. CO X 10 ⁴	Ratio of H ₂ /CO
Ethanol	2.067	4.843	0.427
Cyclohexane	4.142	9.91	0.418
Chlorobenzene	2.609	6.468	0.403
n-Heptane	6.859	17.24	0.398
Toluene	3.171	8.11	0.391
Acetone	2.996	7.719	0.388
Benzene	2.580	6.680	0.386
Tetrachloromethane	3.349	8.763	0.382
Perfluoro-n-heptane	14.03	38.75	0.362

The range of solubility ratio of $H_2 : CO$ is from 0.362 to 0.427. It would be expected that polymers based on the liquids with high solubility ratio, (H_2/CO), would have high solubility selectivity.

It should also be noted that the fluoroheptane shows a considerably higher solubility than any of the other liquids in the table. This may indicate a way of enhancing the solubility of hydrogen although the solubility selectivity may not necessarily be enhanced.

Prediction Of Gas Solubility In Liquids

Despite the lack of available published solubility data for hydrogen and carbon monoxide in liquids, the polymer analogy approach can still be used. The prediction of gas solubility in liquids using the UNIFAC group contribution method has been previously used successfully for the molecular design of solvents for CO_2 absorption (140).

The solubility of liquids is predicted by building up empirical data based upon the groups present in the liquid molecular structure. Thus many combinations can be used providing a much larger number of liquid solubilities than is available in the literature. The limiting factor is still, however, the number of groups in the prediction method.

To ensure that the prediction of the solubility data was reliable for hydrogen and carbon monoxide in liquids, the predicted value was compared with experimentally determined solubility data. Table 7.2 shows that an extremely good agreement is obtained, 100% accuracy to two significant figures in most cases. Where total agreement was not achieved the maximum error was 9%.

Comparison Of Predicted Solubility Ratios With Available Solubility Selectivity For Various Polymers

An attempt to compare available solubility and permeability data for polymers with the predicted solubility in the repeat unit of the polymer was made. The comparison was limited for two reasons, 1. the available permeability data which is broken down into the solubility and diffusivity contributions is limited and 2. of the polymers where data is available only a limited number of polymer repeat units could be predicted.

Table 7.3 demonstrates that the trend followed by the solubility selectivity for polybutadiene, natural rubber and polyethylene is predicted by the analogy with liquid structure. However, the solubility selectivity is a long way out for butyl rubber.

TABLE 7.2**Predicted and Measured Solubilities for H₂ and CO**

Solvent	H ₂ Solubility		CO Solubility	
	Mol. Frac. X 10 ⁴		Mol. Frac. X 10 ⁴	
	Predicted	Expr. Data	Predicted	Expr. Data
Cyclohexane	4.2	4.142	9.9	9.91
n-Heptane	6.3	6.859	17.5	17.24
Toluene	3.0	3.171	8.1	8.11
Benzene	2.6	2.580	6.7	6.680

TABLE 7.3**Comparason of Predicted Solubility Ratios with****Actual Polymer Selectivities**

Material	Actual Relative Permeability	Actual Solubility Selectivity	Predicted Solubility Ratio
CO ₂ /N ₂			
Natural rubber	16.22	-	12.43
Butyl rubber	15.99	-	7.66
Polystyrene	13.33	-	10.20
O ₂ /N ₂			
Butyl rubber	3.94	2.19	1.49
Polybutadiene	2.74	2.14	2.83
Natural rubber	2.96	2.03	1.96
Linear Polyethylene	2.93	1.60	1.91

The CO₂/N₂ permeability data shows that a trend can not be assumed from predicted solubility data, as the diffusivity of the gases will vary from one polymer to the next. A great deal more data is required to draw any firm conclusions as to whether the method used can be extended usefully to predict the trends followed by the solubility selectivity of polymers. Published data usually gives permeability data only and where it is available as solubility and diffusivity coefficients, only a few structures can be predicted. The previous analysis was calculated from references (76,118 and 158).

The method gives very good agreement for the solubility selectivity of gases in liquids as shown by table 7.4. This would suggest that where the analogy of liquids to polymer can be made with certainty, the prediction method should be able to be extended to polymers to indicate a trend at least.

Thus the molecular groups which will enhance polymer solubility selectivity and the magnitude of the solubility of H₂ in the polymer could be identified. However, the effect which these groups have on the diffusivity of the gases would not be known. It would be expected that the diffusivity would be affected in some way.

Table 7.4

Solvent	Solubility Selectivity	Predicted Solubility
	CO ₂ /CH ₄	Ratio CO ₂ /CH ₄
n-Hexane	2.4	2.36
n-Heptane	3.47	2.37
Toluene	4.19	4.04
Benzene	4.68	4.76
Ethanol	5.12	5.04
Methanol	7.36	6.55

Molecular Design Of Polymer Membrane By UNIFAC Group Contribution Method

Using software developed by Sithioth (140) using the UNIFAC group contribution method, hydrogen and carbon monoxide solubility contributions of each of the available molecular groups were calculated. Table 7.5 shows the predicted solubility of H₂ and CO for molecular groups and the ratio of the H₂ : CO solubility.

Table 7.5 Single group contributions for H₂ and CO

Group	Solubility. (Mol. Frac.)		Ratio H ₂ /CO
	H ₂	CO	
CH ₃	0.00066	0.00339	0.195
CH ₃ (CH)	0.00050	0.00281	0.178
CH ₃ (C)	0.00047	0.00265	0.177
CH ₂	0.00016	0.00059	0.271
CH ₂ (Cy)	0.00021	0.00077	0.273
CH	Negligible solubility		
ACH	0.00014	0.00061	0.230
ACCH ₃	0.00021	0.00101	0.208
ACCH ₂	0.00011	0.00054	0.204
ACCH	Negligible solubility		
OH	Negligible solubility		
CH ₂ CO	0.0010	0.00023	0.438

To assess which groups would be expected to enhance either the solubility selectivity or the magnitude of the H₂ solubility a comparison is made between the solubility of H₂ and CO in a pentyl group alone and then the solubility in the pentyl group with different molecular groups added to it. If the ratio of the H₂/CO solubility has been increased above that of the pentyl group

alone, then it would be expected that this group would be a favourable group to enhance the solubility selectivity. If the magnitude of the H₂ solubility has been increased above that of the pentyl group alone then it would be expected that this group would enhance the H₂ solubility.

From table 7.6, overleaf, the groups which yield an H₂/CO ratio of significantly greater than 0.360 (pentyl group alone) are:

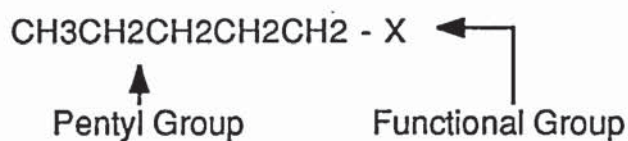
CH ₂ (Cy)	0.375
CH	0.441
ACH	0.368
OH	0.441
CH ₂ CO	0.390

Of the above groups, the CH₂(Cy), CH and ACH groups increase the magnitude of the H₂ solubility. It can therefore be inferred that the CH₂(Cy), CH and ACH groups would increase the solubility selectivity and enhance the solubility of H₂ if they were present in a polymer structure.

The OH group would be expected to enhance the solubility selectivity but may reduce the overall H₂ solubility. There may also be disadvantages of having OH groups in the polymer from a moisture susceptibility point of view.

TABLE 7.6

Predicted Solubility of Groups Added to a Pentyl Group



Functional Group	Solubility (Mol. Frac.)		Ratio H ₂ /CO
	H ₂	CO	
CH ₃	0.00063	0.00182	0.346
CH ₃ (CH)	0.00057	0.00169	0.337
CH ₃ (C)	0.00057	0.00167	0.341
CH ₂	0.00048	0.00181	0.265
CH ₂ (Cy)	0.00048	0.00128	0.375
CH	0.00045	0.00102	0.441
C	0.00041	0.00113	0.363
ACH	0.00046	0.00125	0.368
ACCH ₃	0.00048	0.00134	0.358
ACCH ₂	0.00044	0.00122	0.361
ACCH	0.00039	0.00109	0.358
OH	0.00030	0.00068	0.441
CH ₂ CO	0.00041	0.00105	0.390

AC = Aromatic carbon; (Cy) = Cyclic;

CH₃(CH) = CH₃ group attached to CH group;

CH₃(C) = CH₃ group attached to a C group.

The CH₂CO group would appear to have properties which would enhance the solubility selectivity with a slight reduction in the H₂ solubility.

To find structures of polymers which may prove to be good at separating H₂ and CO, polymer repeat units were formulated maximising the molecular groups which should enhance the solubility properties. The solubility of the repeat unit was then predicted to see if the solubility properties would be favourable. Polymer chain length was also considered to see whether the increase in chain length would increase the solubility selectivity.

Table 7.7 shows a number of solvent groups and polymer repeat units considered. The table shows that polymers with a high content of CH groups, such as in polyacetylene, have high H₂/CO solubility and that polyisoprene should have a favourable solubility selectivity with a high hydrogen solubility.

This method can not be used in isolation to select polymers because it does not take into account the effect of the gas diffusivity through the polymer. However, it may be used in conjunction with other methods.

TABLE 7.7

Predicted Solubilities

Solvent/Repeat Unit	Solubility (Mol. Frac.)		Ratio H2/CO
	H2	CO	
Cyclopentane	0.00038	0.00092	0.41
Cyclohexane	0.00042	0.00099	0.42
Cyclooctane	0.00049	0.00111	0.441
H3CCHCHCH3	0.00051	0.00111	0.460
H3C(CH)4CH2	0.00046	0.00058	0.79
CH2(CH)8CH2	0.00043	0.00028	1.5
Polyisoprene			
CH2(CH3)CHCH2	0.00030	0.00066	0.46
(CH2C(CH3)CHCH2)2	0.00043	0.00087	0.49
Polybutadiene			
CH2CHCHCH2	0.00020	0.00023	0.87
(CH2CHCHCH2)2	0.00029	0.00029	1.00
Polyacetylene			
CHCH	0.00010	0.00010	1.0
CHCHCHCH	0.00012	0.00010	1.2
Polystyrene			
CH2CH 	0.00024	0.00048	0.5
CHC 	0.00017	0.00032	0.53
C  C 	0.00024	0.00052	0.46

7.2.2 Approach 2. Gas Permeability Prediction Using Permachor Number

The Permachor method by Salame published in 1986 proposes that gas permeability through polymers can be related to two properties of the polymer and two properties of the permeating gas.

The cohesive energy density of the polymer, which is a measure of how tightly the polymer chains are bound together, and the free volume between polymer chains, which is a measure of the voidage which is present that gas molecules could readily diffuse through are the parameters used to calculate segmental Permachor values for the components in the polymer repeat unit. The characteristic Permachor number of a polymer is calculated by adding the component Permachor values for all the molecular segments in the polymer repeat unit.

The parameters used to describe the permeating gas are the molecular diameter for diffusion, which is a measure of how easily the molecule can be "sieved", and the Lennard - Jones potential for solubility, which is a measure of the ability of the gas to condense or dissolve into the polymer.

The basic predictive equation relating permeability to the Permachor number is :-

$$G = W \exp(-S.\pi) \quad (7.1)$$

Where W and S are constants dependent only upon the gas properties for a constant temperature.

G = Gas permeability.

π = Permachor number of the polymer.

Salame calculates the equations for oxygen, nitrogen and carbon dioxide, and plots experimental data against his predictive equations to get a very good correlation.

The Permachor method was used to predict the permeabilities of hydrogen and carbon monoxide. The required molecular diameters were obtained from reference (118) and the Lennard - Jones potentials from reference (58).

Permachor equation:

$$G = W \exp(-S.\pi) \quad (7.1)$$

$$W = A' \lambda^2 \gamma \exp \left(- \left[\frac{1}{R.T} - B' \right] \omega . d^2 + \frac{26.5(e/k) - \Delta H_o}{R.T} - 0.013(e/k) \right) \quad (7.2)$$

$$S = \left(\frac{1}{R.T} - B' \right) v + \beta' \quad (7.3)$$

$$v = 0.473.l.d^2 \quad (7.4)$$

d = Molecular diameter for diffusion

The parameters in the above equations are constants for the permeating gas dependent upon whether the polymer is in the "glassy" or "rubbery" state. The following table gives the values of the constants required to calculate W and S in equations (7.1)

Constant	Units	Glassy Polymers	Rubbery Polymers
A'	(cm ² /s.A)	1.3 X 10 ⁻⁶	1.3 X 10 ⁻⁷
B'	(mol/cal)	7 X 10 ⁻⁴	1.1 X 10 ⁻³
λ	(A)	15	26
γ	(cc/cc(cmHg))	4.2 X 10 ⁻⁴	6.8 X 10 ⁻³
β'	(cc/cal)	0.030	0.030
ω	(cal/mol.A ²)	460	500
ΔH ₀	(cal/mol)	900	3100

R is the Universal gas constant.

We also have :-

Lennard - Jones potentials (e/k) :-

For H₂ e/k = 37 K

For CO e/k = 110K

Molecular diameters :-

For H₂ d = 2.89 Å

For CO d = 3.76 Å

From the above data the Permachor equations for the permeability of H₂ and CO can be calculated.

For glassy polymers at 303 K we have :-

For Hydrogen.

$v = 59.3$ (cc/mol)

$S = 0.0864$

$W = 2.24 \times 10^{-9}$

Hence.

$$GH_2 = 2.24 \times 10^{-9} \cdot \exp(-0.0864 \cdot \pi) \quad (7.5)$$

For Carbon Monoxide.

$$v = 100.3 \quad (\text{cc/mol})$$

$$S = 0.126$$

$$W = 1.68 \times 10^{-9}$$

Hence.

$$G_{CO} = 1.68 \times 10^{-9} \cdot \exp(-0.126 \cdot \pi) \quad (7.6)$$

For rubbery polymers at 303 K we have :-

For Hydrogen.

$$v = 102.7 \quad (\text{cc/mol})$$

$$S = 0.0867$$

$$W = 1.11 \times 10^{-9}$$

Hence.

$$GH_2 = 1.11 \times 10^{-9} \cdot \exp(-0.0867 \cdot \pi) \quad (7.7)$$

For Carbon Monoxide.

$$v = 173.9 \quad (\text{cc/mol})$$

$$S = 0.126$$

$$W = 2.13 \times 10^{-9}$$

Hence.

$$G_{CO} = 2.13 \times 10^{-9} \cdot \exp(-0.126 \cdot \pi) \quad (7.8)$$

The above Permachor equations for H₂ and CO were used to predict the gas permeabilities of polymers where experimental data was available and where a value of the Permachor number could be calculated. The following tables give a comparison of the predicted values with the experimentally determined values. All the experimental values obtained from the literature were measured at 303K or were adjusted to 303K by the activation energy for permeation. The glass transition temperature of the polymers is listed in the tables. Where the glass transition temperature is greater than 303K then the

equation for glassy polymers was used and where it is lower than 303K the equation for rubbery polymers was used.

Table 7.8 shows clearly that the Permachor method predicts the permeability of hydrogen through polymers with a wide range of errors. The actual measured value ranging from as much as 67 times the predicted value down to a predicted value which was only half the actual measured permeability.

Although the range of errors for the prediction of carbon monoxide permeabilities, shown by table 7.9 (except for the predicted value of the PVC permeability), is less than that for the prediction of H₂ permeabilities, the errors are still substantial.

TABLE 7.8

Predicted Permeability of Hydrogen Through Various Polymers

Polymer	Permachor Number	Glass Transition Temp. (K)	Gas Permeability		% Error $\left[\frac{\text{Expr.} - \text{Pred.}}{0.01 \text{ Expr.}} \right]$
			Expr.	Predicted	
Silicone rubber	- 23	150	520	82	84
Polybutadiene	6		50.4	6.6	87
TPX	7		136	6.1	96
PPO	13		112.8	7.3	94
Polyethylene	15	188	20	3.0	85
Polypropylene	15		69	3.0	96
Polystyrene	27	373	11	2.2	80
PTFE	30		11.28	1.7	85
PEO	33	206	1.8	0.64	64
PVF	50	313	0.6	0.3	50
PET	59	342	1.3	0.14	89
PVC	61	354	8.0	0.12	99
Nylon 6	64	320	1.5	0.089	94
PTFCE	64		1.42	0.089	94
PAN	110	378	0.1	0.0017	98
Polyvinylalcohol	135		0.009	0.00019	98

TABLE 7.9

**Predicted Permeability of Carbon monoxide
Through Various Polymers**

Polymer	Permachor Number	Glass Transition Temp. (K)	Gas Permeability		% Error $\left[\frac{\text{Expr.} - \text{Pred.}}{0.01 \text{Expr.}} \right]$
			Expr.	Predicted	
Silicone rubber	- 23	150	250	386	- 54
Polyethylene	15	188	3.77	3.2	15
Polystyrene	27	373	0.92	0.56	39
PEO	33	206	0.419	0.33	21
PVF	50	313	0.009	0.031	-244
PET	59	342	0.0188	0.0099	16
PVC	61	354	0.62	0.0077	99
Nylon 6	64	320	0.013	0.053	59
PAN	110	378	0.0001	0.000016	84

Correlation of H₂ and CO Permeabilities with Permachor Number

The contributory reasons as to why such large errors are apparent using the Permachor method for hydrogen and carbon monoxide which are not present for oxygen, nitrogen and carbon dioxide could be :-

1. Carbon monoxide is a non-symmetrical molecule which also possesses a dipole moment. This may mean that the use of the molecular diameter and Lennard - Jones potential to describe the CO molecule is not as meaningful, as for totally symmetrical molecules.

2. The values of the parameters, A', B', λ , γ , β , W, and ΔH_0 (taken to depend only on whether the polymer is glassy or rubbery) may not be constant. It may be that they change for different gases.

If point 2 above is largely the case then a correlation of the gas permeability against the polymer Permachor number may be made. The form of the correlation would still be of the form :-

$$G = W \cdot \exp(-S\pi) \quad (7.1)$$

but the constants, W and S, would be determined empirically from

experimental data.

The following graphs in figures 7.1 and 7.2 have been constructed from available experimental permeability data for hydrogen and carbon monoxide.

The graphs show quite a good correlation of permeability against the polymer Permachor number. The graphs can be used to calculate the following relationships at 303K.

For Hydrogen

$$G_{H_2} = 99.5 \times 10^{-10} \cdot \exp(0.0677 \cdot \pi) \quad (7.9)$$

For Carbon Monoxide

$$G_{CO} = 18.5 \times 10^{-10} \cdot \exp(-0.113 \cdot \pi) \quad (7.10)$$

FIGURE 7.1
Correlation of Hydrogen Permeability of
Polymers with Polymer Permachor Number.

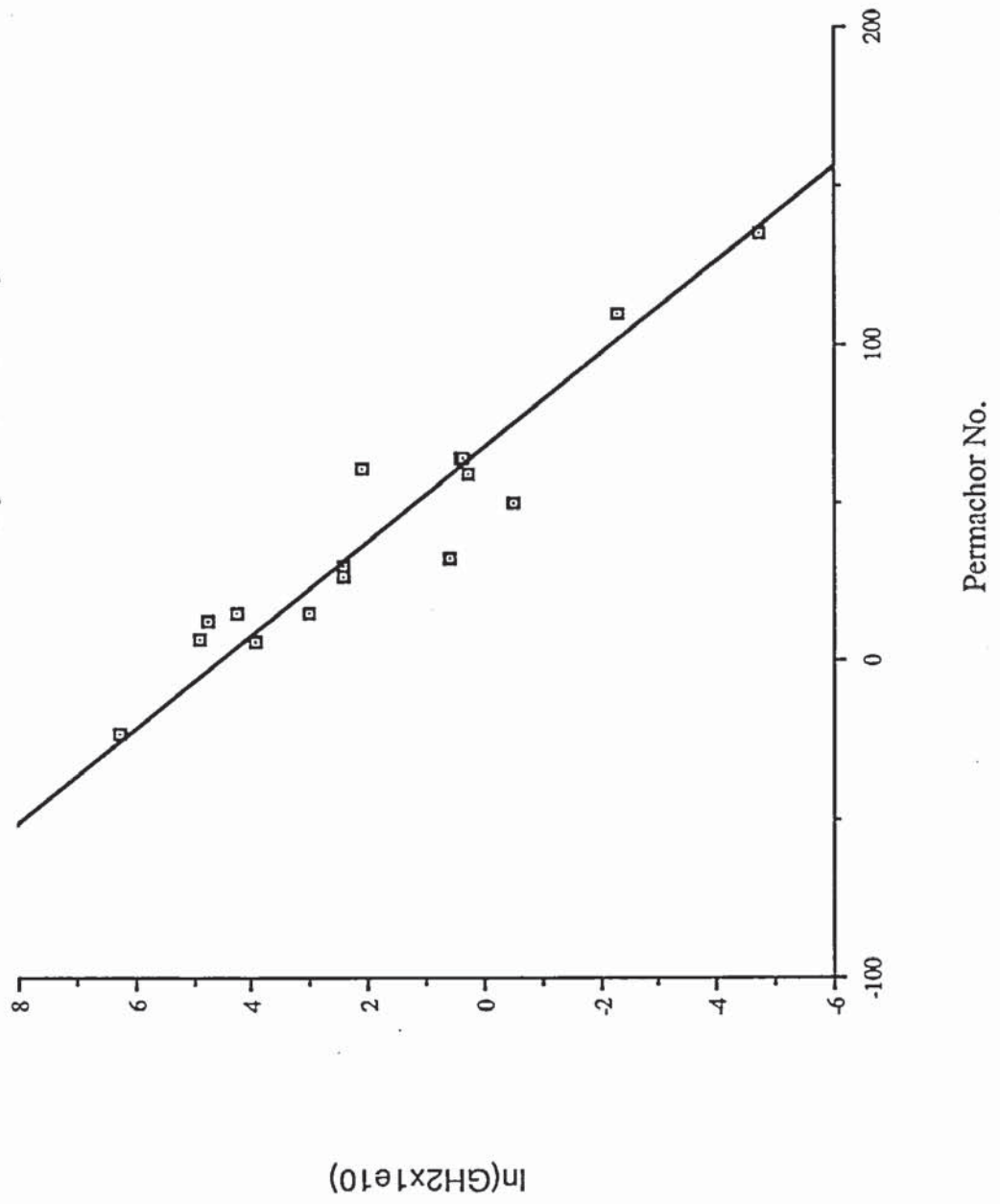
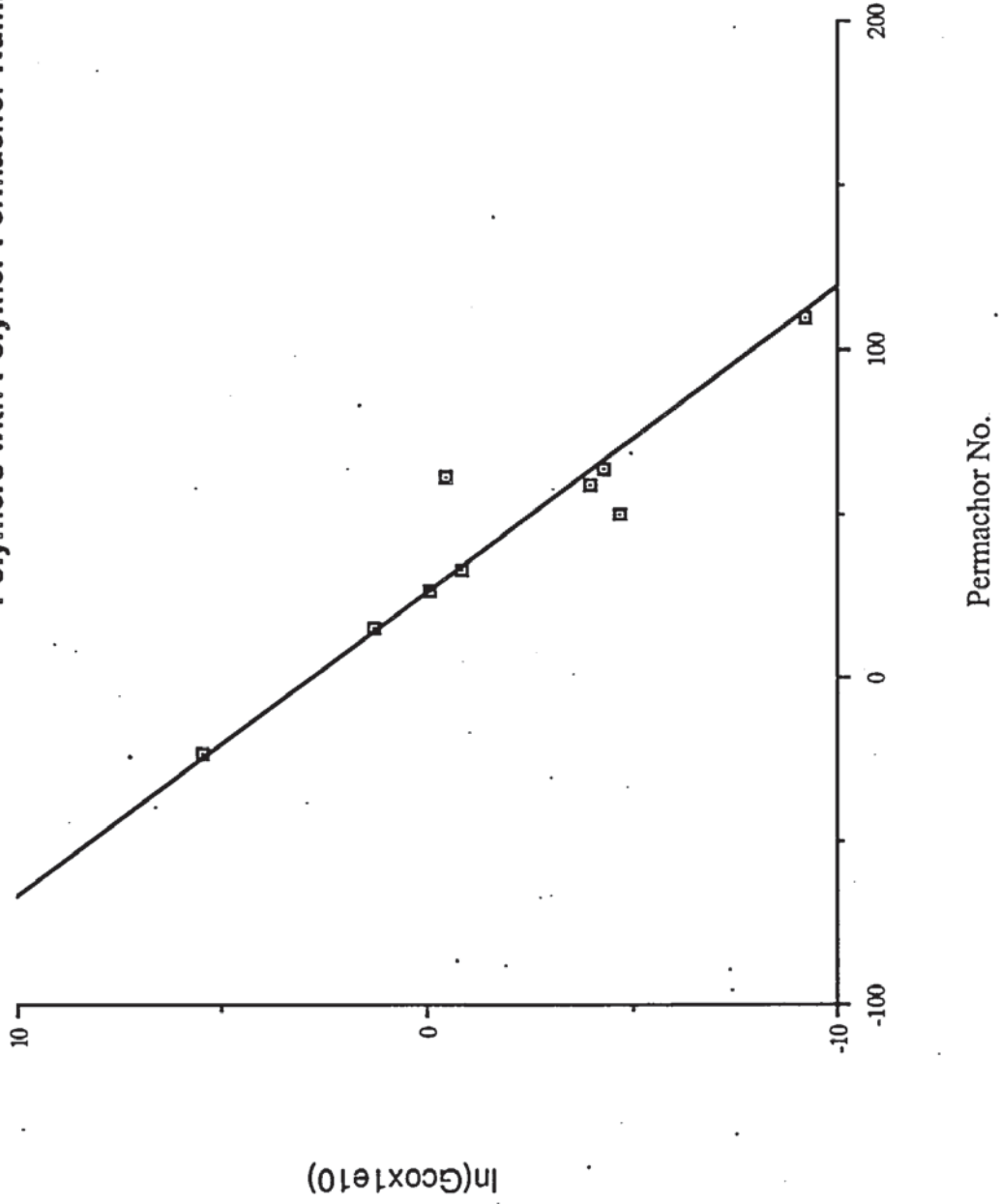


FIGURE 7.2

Correlation of Carbon mon-oxide Permeability of

Polymers with Polymer Permachor Number.



Hence we can say :-

$$\alpha_{(H_2/CO)} = 5.38 \cdot \exp(0.0453 \cdot \pi) \quad (7.11)$$

Selection of Appropriate Permachor Number.

Commercially a new membrane would have to be able to compete with Cellulose acetate membranes.

From my experimental work the permeability and selectivity of Cellulose acetate are as follows :-

$$G_{H_2} = 6.21 \times 10^{-10} \text{ scm}^3 \cdot \text{cm}/\text{cm}^2 \cdot \text{s} \cdot (\text{cmHg})$$

$$\alpha_{(H_2/CO)} = 25$$

Therefore it is required that a polymer should have a Permachor number which will yield:-

$$G_{H_2} > 6.21 \times 10^{-10} \quad \text{scm}^3 \cdot \text{cm}/\text{cm}^2 \cdot \text{s} \cdot (\text{cmHg}) \quad (7.12)$$

G_{H_2} given by :-

$$\ln G_{H_2} = \ln(99.5 \times 10^{-10}) - 0.0677 \cdot \pi \quad (7.13)$$

Hence.

$$\pi < 41$$

$$\text{For } \pi < 41 ; G_{H_2} > 6.21 \times 10^{-10} \quad (7.14)$$

With a Permachor number of 41, which gives a permeability equal to that of Cellulose acetate, the selectivity of the polymer must be better than that for cellulose acetate for an improvement to be made. The separation factor to be expected from a polymer with a Permachor number of 41 is:-

$$\pi = 41 ; \alpha_{(H_2/CO)} = 34.5 \quad (7.15)$$

To maintain a separation factor as good as that for cellulose acetate a minimum value of the Permachor number can be calculated. This is:-

For $\alpha_{(H_2/CO)} > 25$

)

) (7.16)

$\pi > 34$

)

The selection of polymers for membrane development using the Permachor correlation was based upon selecting polymers with Permachor numbers in the range 30 - 40.

The number of groups available in the Permachor method is quite large and there are many structures which can be made with Permachor numbers of between 30 and 40. Listed in table 7.10 there is a sample of those considered.

In selecting polymers for testing, three considerations were made.

1. Groups which were indicated as having enhanced solubility properties from the UNIFAC group contribution method analysis should be incorporated in the polymer structure if possible.

2. The polymer Permachor number was in the range 30 to 40.

- and 3. The polymer would be expected to be a glassy polymer at the temperature of operation, so that the strength of the polymer would be expected to be satisfactory.

TABLE 7.10

Some Polymer Structures With Permachor Numbers
Between 25 and 50

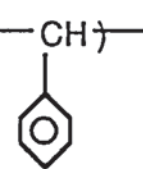
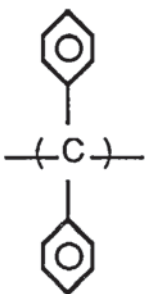
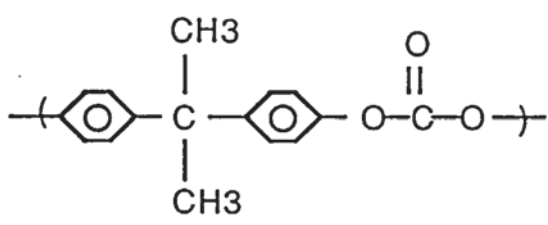
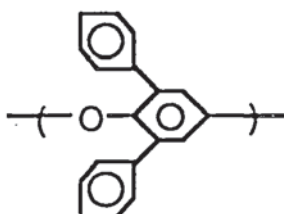
Polymer Repeat Structure	Permachor No.
1. Polystyrene $\text{-(CH}_2\text{-CH)-}$ 	27
2. 	28
3. $\text{-(CH}_2\text{-C}_6\text{H}_4\text{-CH}_2\text{)-}$ 	30
4. PTFE $\text{-(CF}_2\text{-CF}_2\text{)-}$	30
5. Polycarbonate 	31
6. PEO $\text{-(CH}_2\text{-CH}_2\text{-O)-}$	33

TABLE 7.10 cont.

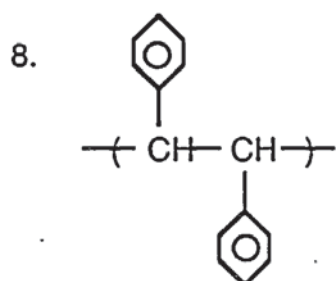
Polymer Repeat Structure

Permachor No.

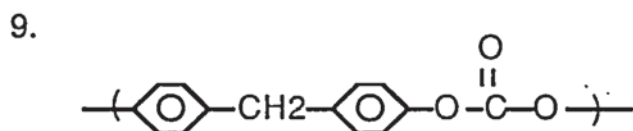
7. Poly(oxy-2,6-diphenyl-1,4-phenylene)



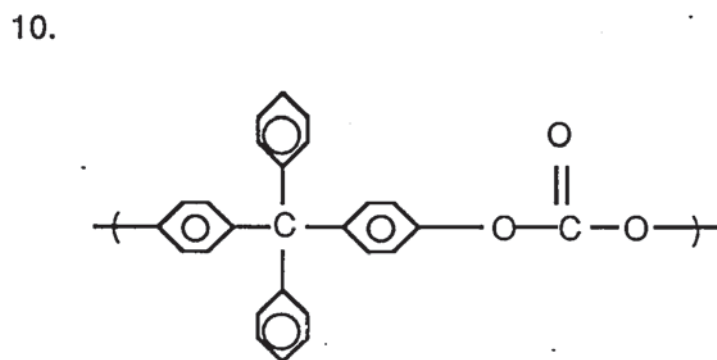
37



39



40



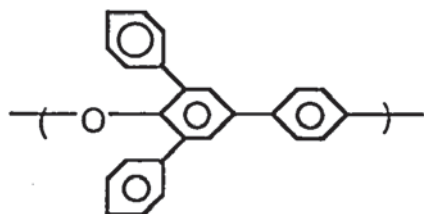
43

TABLE 7.10 cont.

Polymer Repeat Unit

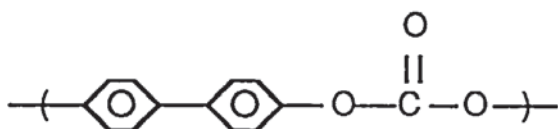
Permachor No.

11.



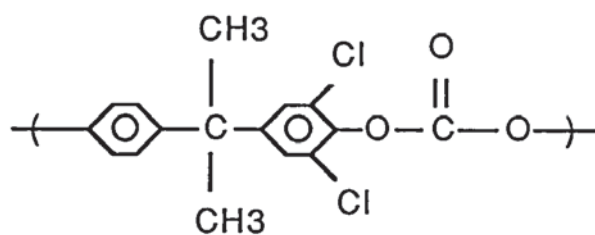
45

12.



48

13.



51

7.3 Polymer Selection

Suitable materials were chosen for testing based mainly on the Permachor correlation, but also selecting materials which contain high proportions of groups which are predicted to have good solubility properties. The polymers selected have the additional advantage of being readily available.

Polycarbonate has a Permachor number of 31 and contains aromatic rings and carboxyl groups, both of which may enhance the solubility selectivity. PTFE which has a Permachor number of 30 is a highly fluorinated polymer. It was noted previously that highly fluorinated solvents had a much higher solubility for hydrogen and carbon monoxide.

Other polymers were selected to obtain further data to test the Permachor correlation.

Also currently used membrane polymers, such as cellulose acetate and polyimide were tested as benchmarks.

7.4 Consideration Of Other Methods To Improve Membrane Properties

1. Using a polymer membrane for the separation of H₂ and CO, the polar nature of the CO molecule could be exploited by applying a non-uniform electric field across the membrane. The molecular rotation of the CO molecule would be reduced when inside the polymer membrane structure. Applying an electric field would thus retard the progress of the CO through the membrane, enhancing the natural properties of the membrane. H₂ not having any dipole would be unaffected by the electric field.

2. The properties of polymers which have very high selectivities to H₂ and CO but very low permeabilities, rendering them uneconomic in their own right, could be combined with polymers which have low selectivity but extremely high permeability. The polymers could be combined in co-polymers and the best membrane properties would be achieved by selecting the best co-polymer mix.

3. The property of molecular hydrogen to split into atomic hydrogen on the surface of some metals could be exploited, as this then allows the atomic hydrogen to diffuse through the metal. Metals are virtually impermeable to all other gases. To facilitate the permeability of gases a very fine layer of metal

(10 - 20 Å) is deposited on the surface of a polymer film. The metal with the highest hydrogen permeability is Palladium, but many metals display the same property to a lesser extent (69,96).

Polymers were selected for testing based upon the ideas explained in paragraphs 2 and 3 above.

A co-polymer (of methyl methacrylate and a highly permeable siloxy group) was selected to see if an enhancement could be made of the permeability of the polymethylmethacrylate alone, without too much reduction in the selectivity. The co-polymer has a 50 : 50 mix of each polymer group.

Figure 7.3 shows the structure of the siloxy monomer used in the co-polymer.

Polymethylmethacrylate films were also made for testing.

Aluminium coated polyethyleneterephthalate was tested to see if enhanced selectivity could be achieved.

FIGURE 7.3

Siloxy Monomer used in the MMA - Siloxy Co-polymer

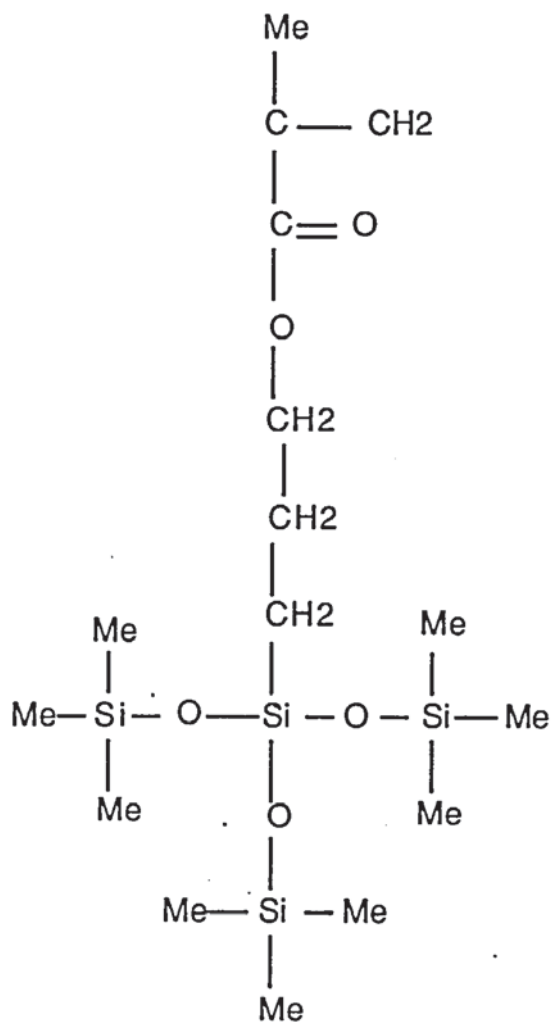


Table 7.11 Polymers Selected For Testing

Polymer	Permachor No.	Predicted Permeability ($\times 10^{10} \text{scm}^3 \text{cm/cm}^2 \text{s}(\text{cmHg})$) (@30°C)		Reason for Selection
		H2	CO	
Cellulose diacetate	-	-	-	Currently used membrane material.
Polyimide	-	-	-	Currently used membrane material.
Polybutadiene	6	66	9.4	Support for Permachor Correlation.
Polyisoprene	15	36	3.4	"
Polyethylene	15	36	3.4	"
PTFE	30	13	0.62	Candidate membrane material.
Polycarbonate	31	12	0.56	"
Co-polymer of MMA and Siloxy monomer	-	-	-	Possible high permeability membrane.
Al coated PET	-	-	-	Possible high selectivity membrane.

CHAPTER 8

EXPERIMENTAL

8.1 Introduction

Gas permeability measurements were carried out in this work to establish how the newly Chosen membrane materials would compare with membrane materials currently used in commercial membrane systems. Where the permeability and selectivity of the polymer had been predicted these results may provide support for the Permachor correlation for polymer permeability.

The experimental work carried out in this project has involved the production of thin dense homogeneous polymer membranes and the measurement of H₂ and CO permeabilities of the membranes made and of manufactured films obtained.

Films were made by several methods of solvent casting, some membranes used were polymerised in-situ.

The measurement of gas permeability through the membranes was achieved using the Davenport Gas Permeability Apparatus (41). This equipment is durable, easy to use and gives repeatable results. Other methods of

permeability measurement may provide quicker results, but these rely upon indirect methods of measurement (172).

8.2 Polymer Solutions

Polymer solutions were made up from polymers selected for suitable membranes. The solvents were selected from the Polymer Handbook (29), or from solubility parameter tables (173). Solutions were made up between 5-10 wt% such that the solution would flow easily. To produce a solution it was usually necessary to have the polymer finely divided and to either continuously stir or shake the mixture.

8.3 Membrane Casting

Three methods have been used to make membranes.

1. Doctor blade :-

A doctor blade is a stainless steel channel formed by two parallel struts separated by an adjustable blade. The Doctor blade is placed on a piece of plate glass and the blade is adjusted so that the required thickness of polymer solution is cast. The reservoir between the struts is filled with the polymer solution. The whole Doctor blade is then moved slowly and continuously over the glass plate laying down a uniform thickness of solution. The glass plate is covered to prevent dust settling on it and the solvent is allowed to evaporate.

The drying time will vary depending on the thickness of the film and the type of solvent used. Once the solvent has evaporated the polymer film can be peeled off the glass plate. Very thin membranes can be transferred to porous supporting membranes.

2. Channel :-

This method for membrane making is essentially the same as using the Doctor blade. It allows larger and thicker films to be made. A channel is formed on a glass plate by layers of plastic tape. The channel width is the width of the required film plus approximately 4 cm. The height of the channel is that which will produce the required thickness of film. To ensure a uniform film the channel walls are measured using a micrometer at several points on each side.

Another glass plate, which is wider than the channel, is used as a blade. This glass plate must be "dead" straight and be smooth edged.

The polymer solution is poured onto the glass plate at one end of the channel.

The blade is then moved slowly and continuously along the channel walls, filling the channel with polymer solution. The solvent is then allowed to evaporate.

Once the film has been formed it is cut away from the channel walls and peeled from the glass plate.

For polymers which adhere strongly to glass the glass plate is pretreated with "Repelcote".

3. Spinning Disc :-

Here the polymer solution is applied to a disc of Melenex which is then rotated at 200-2500 rpm. The film thickness can be varied by varying the speed of rotation and the concentration of the polymer solution. The membrane can be simply peeled off the Melenex disc.

Membranes the correct size for the Davenport Gas Permeability Apparatus are punched out with a stainless steel punch made for the purpose. This gives membranes of known cross-sectional area and allows the thickness of the membrane to be measured accurately gravimetrically. If the membrane is thick enough (>0.1 mm) it can be measured using a micrometer.

8.4 Other Polymer Membranes Used

8.4.1 Membranes Polymerised In-situ

The methyl methacrylate - Siloxy co-polymer membrane was polymerised in-situ between glass plates by colleagues in the Applied Chemistry section of the department. The membrane used was approximately 1 mm in thickness.

8.4.2 Films Obtained From Manufacturers

- Polyethylene. The sample of Polyethylene used was generally available low density polyethylene film with a measured thickness of 85 μm .
- Polyetherurethane. The sample of film used was manufactured by Wolff Walsrode as Walopur 2201 film. The film thickness was 500 μm . The manufacturer would not divulge the molecular structure of the polymer.
- Cellulose Diacetate. The cellulose acetate film was manufactured by Courtaulds as Clarifoil. Film thickness = 50 μm .
- Vacuum Metallised Polyester. Film manufactured by Van Leer. 12 μm polyester film metallised with aluminium on one side.
- PTFE. Extruded PTFE film supplied and manufactured by Fluorocarbon.

8.5 The Davenport Gas Permeability Apparatus

The apparatus has two main interconnecting parts; a stainless steel cell and a

manometer. The cell unit is connected through a capillary tube to a manometer and a vacuum system. For ease of operation, the complete apparatus is fitted to a vertical mounting (see figure 8.1).

The cell unit has two main parts. The unit is made leak free by using a rubber "O" ring to form a seal between the two cell parts which are clamped together by six vertical studs and nuts.

The lower part of the cell opens into a glass capillary tube of 1.5mm bore. This forms part of the manometer which is connected to a vacuum system. Mounted vertically behind the capillary is a scale 10cm long graduated in divisions of 1cm and sub-divisions of 1mm. Sufficient mercury is stored in the reservoir to fill the manometer to a level just above the bottom of the enlarged side tube.

A small bore glass capillary tube forming one arm of a manometer is partially filled with mercury. This tube is connected to the lower part of a stainless steel cell unit. The test specimen, of known area, is supported horizontally on a steel insert fitted inside the lower part of the cell.

The upper part of the cell is fitted to the lower and one atmosphere of the test gas is fed into the upper cell component. The air in the cell cavity and the manometer is evacuated so that there is a differential pressure of approximately one atmosphere between the top and bottom surfaces of the

test specimen.

FIGURE 8.1

Davenport Gas Permeability Apparatus

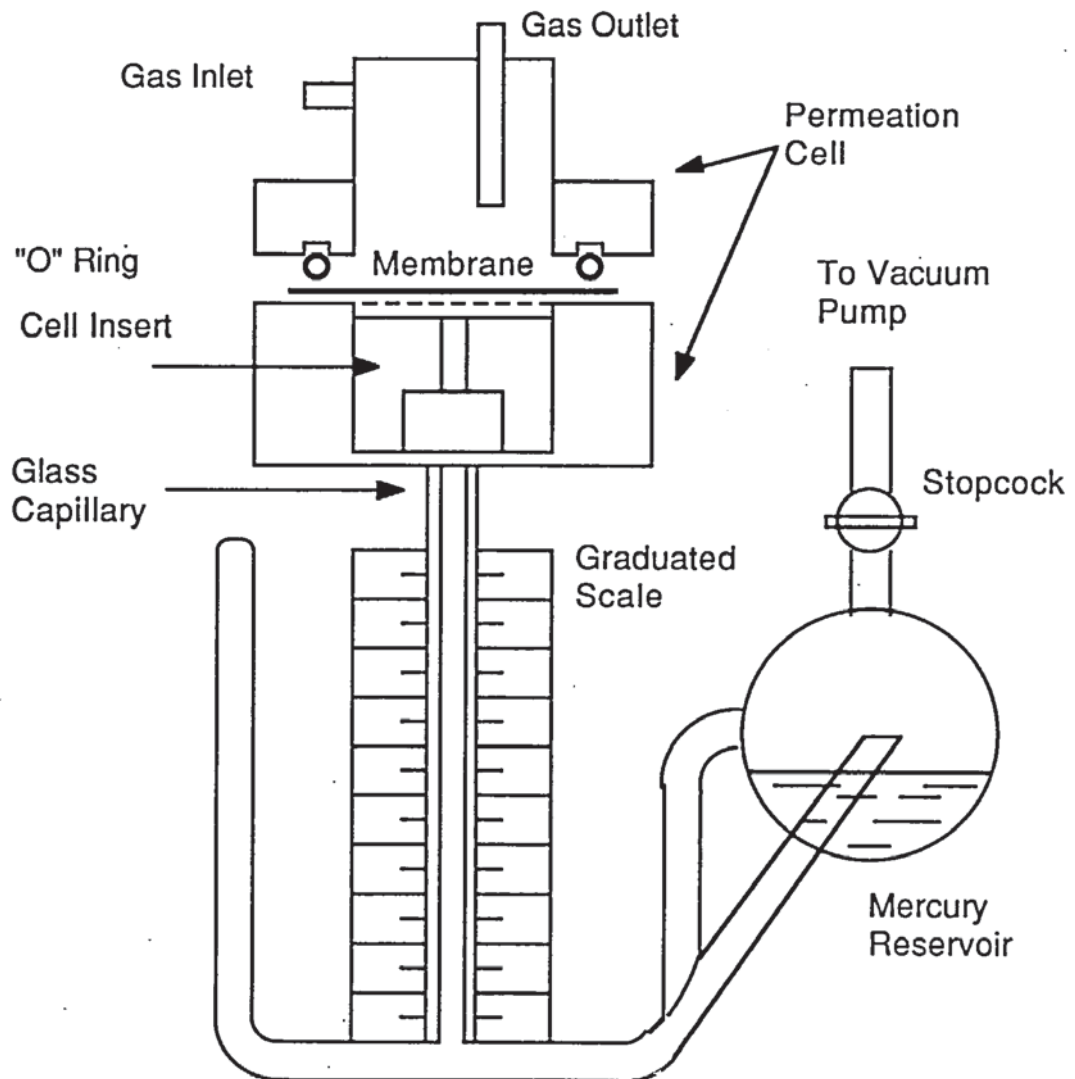
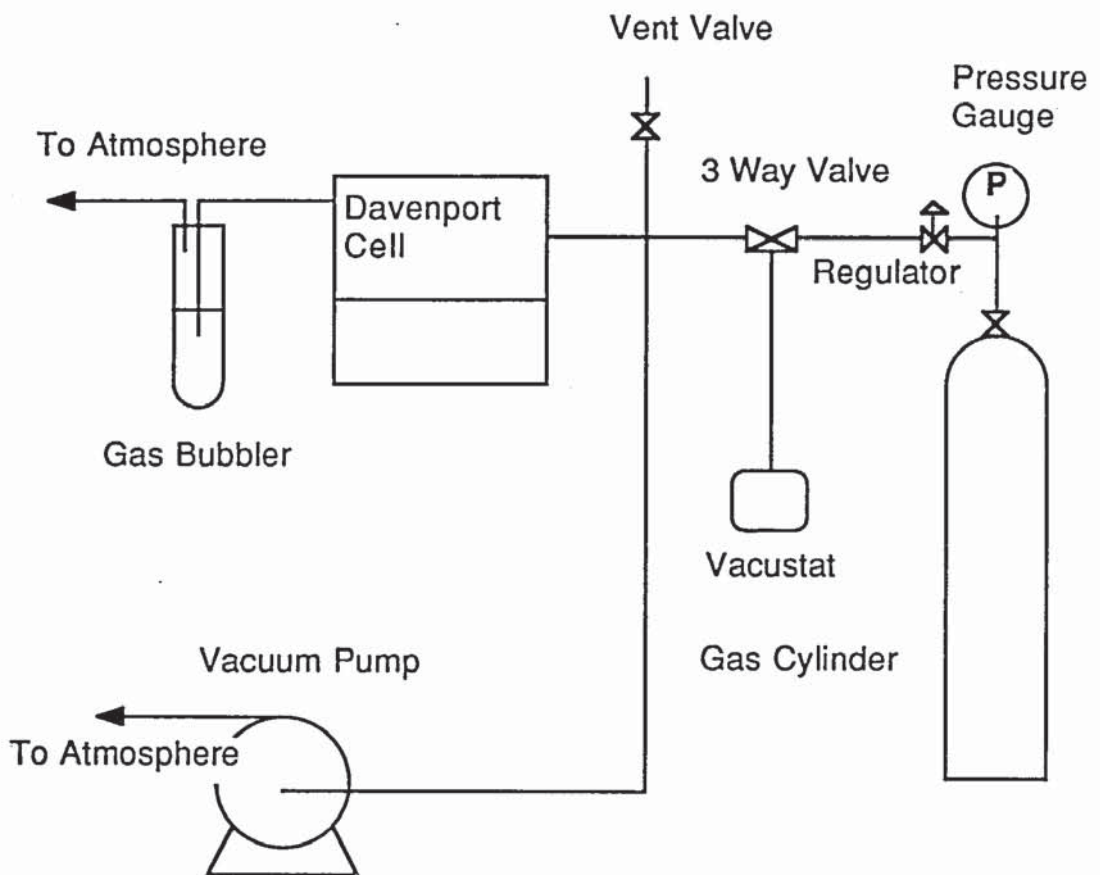


FIGURE 8.2

Diagram of Experimental Layout



The apparatus is left in this condition and the change in the height of mercury in the capillary tube is observed and plotted against time. When the plot shows that a steady state has been established, the transmission rate is calculated.

The Davenport apparatus, vacuum pressure gauge and gas bubbler are used in a fume cupboard to prevent the build up of any poisonous gases or of an explosive mixture.

The hydrogen for the experiments was supplied by BOC Ltd in high pressure cylinders at a purity of 99.99%. The carbon monoxide was supplied similarly at high pressure by Air Products Ltd at a purity of 99.9%. The gases were let down to a pressure just above atmospheric pressure by regulators (BOC Saffire 230 (BS 5741) and ESAB model A0441100) and piped through copper pipe to the inlet of the Davenport cell.

From the outlet of the cell the gas is piped to a gas bubbler bottle so that the rate of gas flow can easily be seen and regulated to the required amount. From there the gas is piped to the outside of the building.

The manometer side of the Davenport apparatus is connected to a vacuum pump (Edwards Speedivac 2) and mercury vacuum gauge (BOC Vacustat) by a valving arrangement. The vacuum pump could produce a vacuum of down to 0.2 mmHg., which is quite satisfactory for the permeability test. The

exhaust from the vacuum pump was piped back to the fume cupboard. Figure 8.2 shows, schematically, the experimental apparatus as a whole.

8.5.1 Experimental Procedure

The test specimen and filter paper are dried in a vacuum oven for two hours.

The cell is fitted with the appropriate free volume insert. (5, 10, 15 or 20 cm³).

Place the pre-dried no.1 Whatman filter centrally on top of the lower half of the cell.

Place the test specimen flatly and centrally over the filter paper and screw the parts of the cell together, tightening the nuts evenly. Ensure that the stop cock is properly greased with non-silicone vacuum tap grease and then closed.

Fill the upper cell component with the test gas so that the gas is at atmospheric pressure in this part of the cell.

Open the stop cock and evacuate the lower cell unit and the manometer to a pressure of less than 0.4 mm of Hg. Measure this reduced pressure on the mercury Vacustat incorporated in the vacuum system.

Close the stop cock and then tilt the whole apparatus so that the mercury is transferred from the reservoir and fills the manometer.

Return the apparatus to the vertical.

Readings of the mercury level are assisted by the use of a times 5 magnifying glass clamped in front of the manometer scale.

Record the height of mercury by reading the graduated scale. Also record the time. Record as frequently as possible the change in height of mercury and the corresponding time interval. Continuously plot the readings until six consecutive readings show a linear correlation.

8.5.2 Temperature Control

The temperature at which the permeability tests were carried out was the prevailing laboratory ambient temperature. This was measured at the start and finish of each test and did not vary by more than 1°C. The temperature of the experiments was in the range of 16-24°C.

8.5.3 Safety

The gases being tested were Carbon monoxide and Hydrogen. Carbon monoxide being flammable and poisonous, and Hydrogen being highly flammable the permeability tests were carried out in a fume cupboard. The gas was supplied from high pressure cylinders through appropriate regulators

and let down to just above atmospheric pressure. The gases were piped to the Davenport apparatus and then piped outside the building so the gases would not enter the fume cupboard unless there was an inadvertent leak.

Overalls, gloves and safety glasses were worn when required and the University safety regulations (142) were followed.

8.5.4 Calculation of Transmission Rate

The gas transmission rate, TR., can be calculated for each specimen from the following equation:-

$$TR = 273.P.V/(T.A(P_1 - P_2)) \quad (8.1)$$

$$G = TR.I \quad (8.2)$$

P = Rate of pressure change in manometer: (cmHg/s.)

V = Total volume between the test specimen and the mercury level in the capillary tube. (cm³.)

This is the sum of the volume of the insert, (either 5, 10, 15 or 20 cm³) the volume of the capillary above the mercury level halfway through the test, (Cross sectional area of capillary is 0.018 cm²) and the free space volume in the filter paper. (cmHg.)

T = Temperature of the test.	(K)
A = Area of the specimen under test.	(23.77 cm ²)
(P1-P2) = Pressure difference across the specimen	(cmHg)
l = Membrane thickness.	(cm)

A spreadsheet was written which calculates the permeability of the polymer sample from experimental readings. The spreadsheet is contained on the disc at the back of this thesis and is called 'DAVENPORT'.

8.5.5 Experimental Repeatability and Accuracy

Initially permeability measurements were carried out for oxygen and nitrogen through polyisoprene and polybutadiene to establish that good repeatability was obtained. The results obtained from these tests agreed with published values of the permeabilities to within 4% of my results.

8.6 Results

TABLE 8.1

Experimental Results

Polymer	Membrane Thickness (mm)	Temp. (deg C)	Permeability		Separation Factor
			H2	CO	
			(Barrer)		
Polyisoprene (Solvent cast)	0.35	24	59.8	17.2	3.5
Polybutadiene (Solvent cast)	0.15	20	33.1	2.3	14
Polyethylene (Manufactured)	0.085	21	6.35	0.88	7.2
Polyetherurethane (Walsroder films)	0.50	20	6.22	0.91	6.8
Polycarbonate	0.31	20	7.05	0.28	25
Polyimide (Ube industries)	0.05	19	0.52	0.016	33
Cellulose di-acetate (Solvent cast)	0.05	18	6.21	0.25	25
PTFE (Fluorocarbon)	0.09	20	11.9	1.1	10
MMA-Siloxo Copolymer (Polymerised in-situ)	1.05	19	70.3	3.2	22
PMMA (Solvent cast)	0.085	16	6.9	0.25	27
Al coated PET *	0.012	22	0.046	0.025	1.8

* Transmission rate quoted (10e-10.scm³/cm².s.(cmHg))
(1 Barrer = 10e-10.scm³.cm/cm².s.(cmHg))

8.7 Conclusions

The Davenport gas permeability apparatus is durable and easily operated, the results obtained are generally accurate and reliable.

However, where transmission rates are very low it was more difficult to get consistent results. It would also have been desirable for the equipment to have been operated in a temperature controlled environment.

CHAPTER 9

EVALUATION OF MEMBRANES

9.1 Introduction

The evaluation of membranes has been considered in two ways. The first is to position the membrane on the iso-cost curves to evaluate its economic competitiveness. The second is to establish whether the properties of the membrane support the correlation between permeabilities of H₂ and CO and the polymer Permachor number.

9.2 Economic Evaluation

To assess the economic results of the polymers chosen to be used as membrane materials for the separation of hydrogen and carbon monoxide, the cost permeability and selectivity of the membrane can be positioned on the targeting graph.

As yet there is no clearly established relationship between the ideal separation factor and pure gas permeability as measured in the laboratory, with the effective selectivity and cost permeability of a membrane in service.

To overcome this, the assumption that the ideal separation factor and the effective selectivity are equal is made. To relate the permeability of hydrogen and the cost permeability it is assumed that the membrane production costs will be the same no matter which polymer is used. The cost permeability is then taken to be the ratio of the new membrane permeability to the permeability of cellulose acetate and multiplied by the cost permeability of the membrane used by Supplier A.

ie.

$$G_c(\text{New Membrane}) = \frac{G_{H_2}(\text{New Membrane})}{G_{H_2}(\text{Cell. Acetate})} \cdot G_c(\text{Supplier A}) \quad (9.1)$$

Figure 9.1 shows the relative positions of polycarbonate (PC), polymethylmethacrylate (PMMA) and polytetrafluoroethylene (PTFE) on the targeting graph. The position of the most competitive commercial membranes, supplier A and supplier B, is also shown. The targeting graph shows that the cost of CO separation using polycarbonate and polymethylmethacrylate membranes would be less than 60% of the cost of cryogenic separation. This puts these membranes on a par with suppliers A and B.

The PTFE membrane, whilst having a higher permeability than currently used

FIGURE 9.1

TARGETTING GRAPH

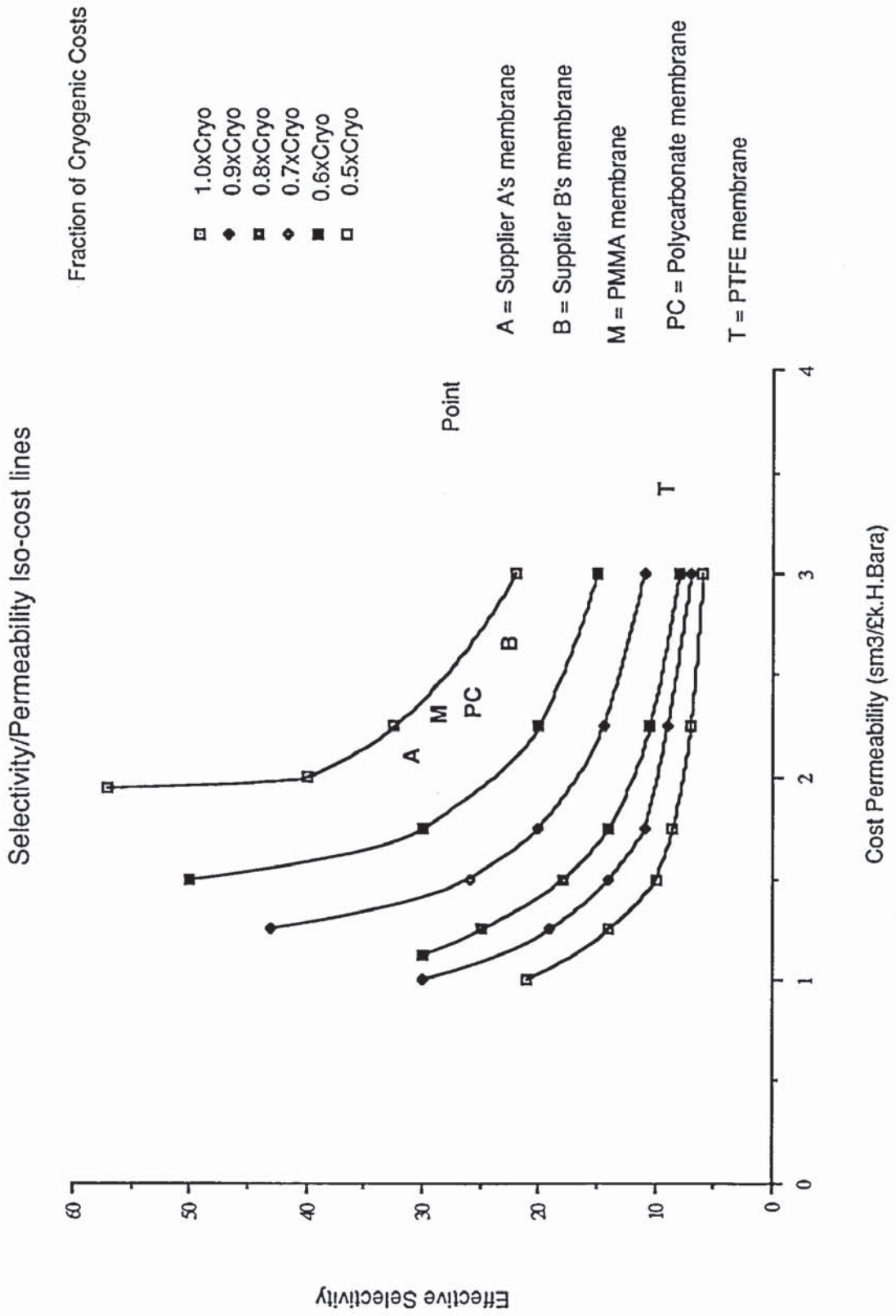
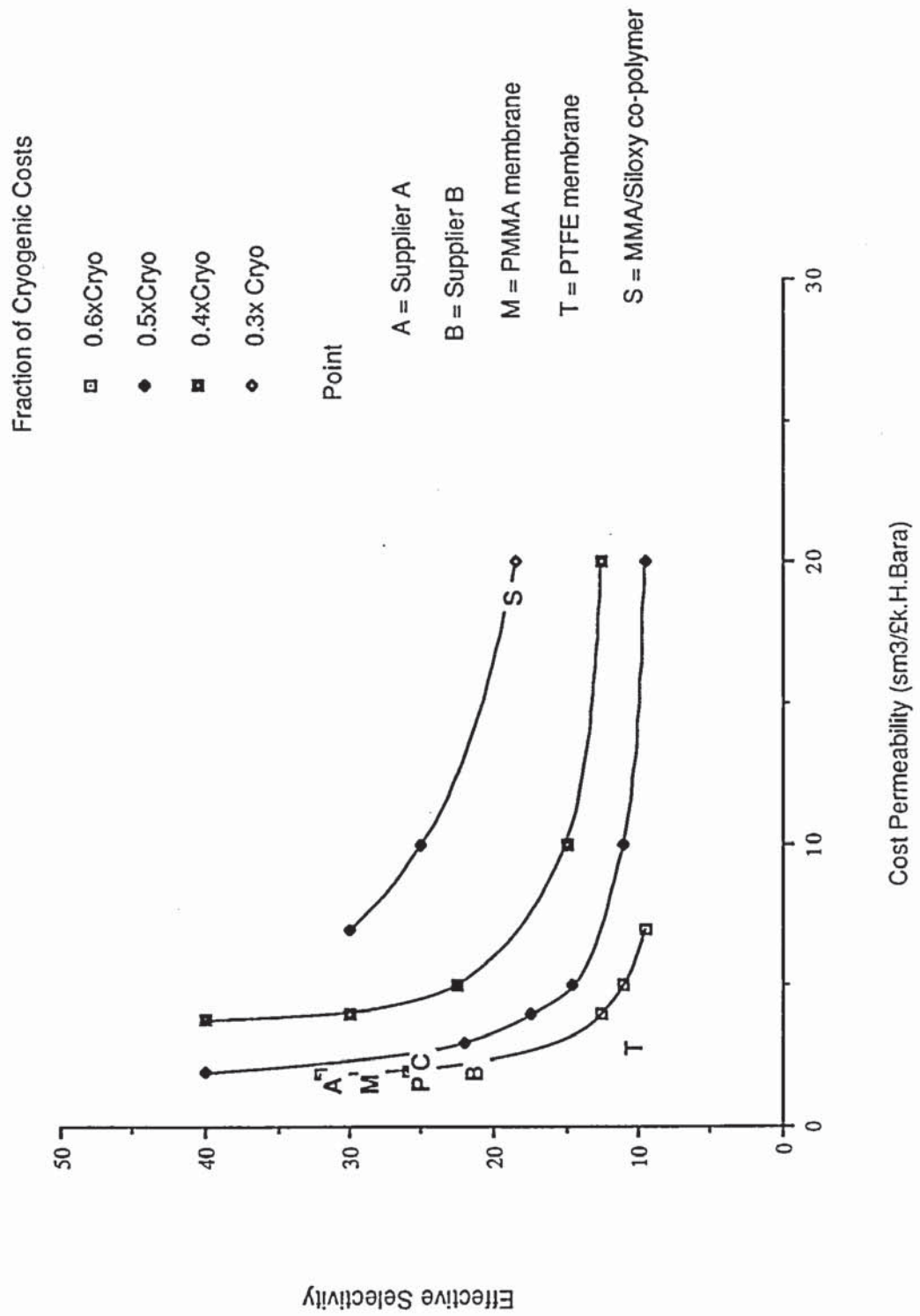


FIGURE 9.2

Iso-cost curves for an extended permeability range



membranes, has a lower selectivity. The cost of CO separation using a PTFE membrane would be 70% of the cost of cryogenic separation.

In order to show the position of the co-polymer of methylmethacrylate (MMA) and siloxy group figure 9.2 was constructed. This graph extends the permeability range of the targeting graph to 20.0 $\text{sm}^3/\text{k.H.Bar}$. In this region limiting values of separation cost are to all intents and purposes reached at low values of selectivity.

On the left hand side of the figure, at low values of cost permeability, the positions of membranes A, B, PC, PMMA and PTFE are again marked.

The permeability of the 50 : 50 MMA-Siloxy co-polymer is about one order of magnitude higher than the other membranes. The cost of CO separation would be further reduced by using this membrane and it would give a cost of less than 50% of the cost of cryogenic separation.

The high permeability of this polymer has meant that it is virtually at the limiting point in terms of separation cost for a selectivity of 22. It is thought that further separation cost reductions could be made by using different co-polymer blends which may have lower permeability but higher selectivity.

It may be expected that the selectivity could be enhanced by increasing the proportion of MMA. The proportion of MMA could be increased until the cost

permeability became a significant factor.

9.3 Correlation of Permeability with Permachor Number

The permeability measurements made were at temperatures of about 20°C. This has meant that they can not be plotted on figures 5.1 and 5.2 which show plots of permeability at 30°C.

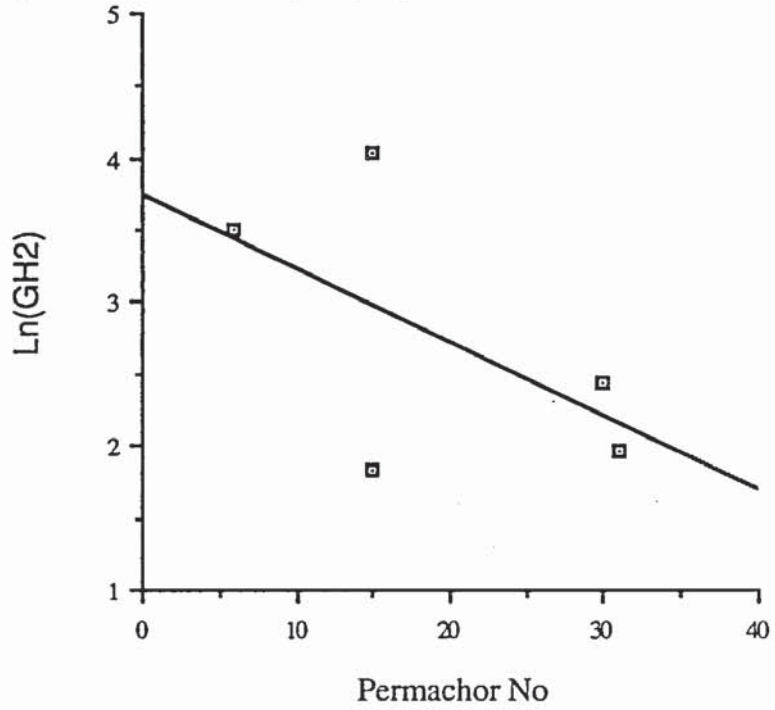
The data which has been obtained at 20°C can, of course, be plotted in its own right along with other data which is available at 20°C.

The results show broadly that as the Permachor number is increased the gas permeability decreases. The experimental results lie either side of a line which would support the Permachor correlation, however there is a large amount of scatter, particularly in the results for CO permeabilities, to strongly back up the Permachor correlation. See figure 9.3.

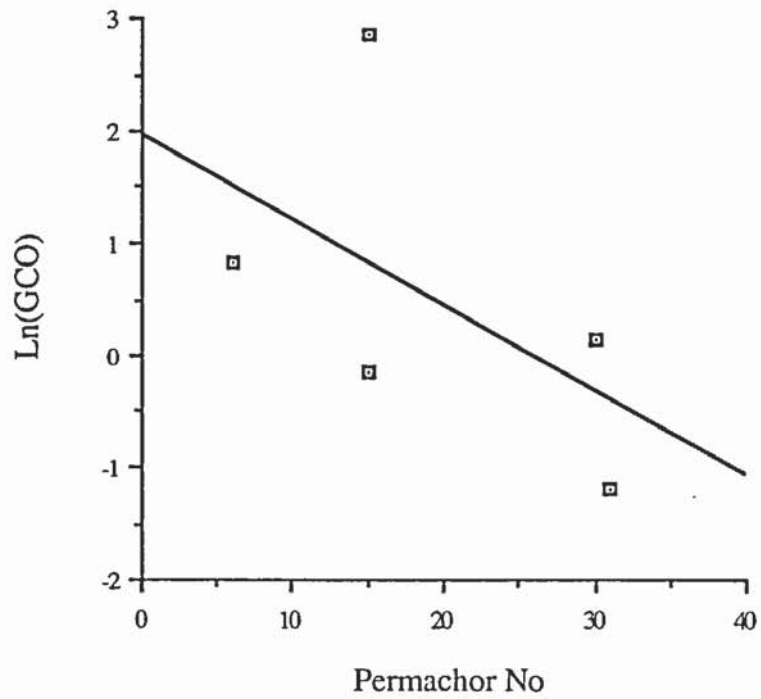
The low permeability obtained for polyethylene might be explained by the fact that this is not a completely amorphous polymer.

FIGURE 9.3

Log of H₂ permeability of polymers at 20 C vs Permachor number



Log of CO permeability of polymers at 20 C vs Permachor number



CHAPTER 10

DISCUSSION

To develop membranes for the separation of CO from an H₂/CO syngas it is necessary to know what membranes are available and what the competing processes are. An economic evaluation was carried out where suppliers of membrane separation systems and cryogenic plant were approached. They were asked to provide quotes for various CO separations from H₂/CO syngas. To ensure the credibility of the evaluation, it was carried out under the auspices of B. P. Chemicals.

The information received from suppliers quoted different product recovery rates for the different separation cases. To analyse the information on a comparable basis an economic evaluation method was developed which takes into account the effects upstream and downstream of the separation unit. Clearly if the CO recovery is low, more feed will have to be processed to produce the same amount of product. Also there is a greater purge required if the CO purity is low.

The process currently used for this separation is cryogenic distillation. Gas

absorption and membrane separation are among the competing processes.

Membrane process suppliers produce both hollow fibre and spiral wound systems using various types of membrane materials. The polymers used include: Cellulose acetate, Polysulphone, Polyimide and Polyamide.

In this process the syngas is supplied at high pressure which is a considerable advantage for the membrane separation which supplies the product at high pressure. The cryogenic process produces a low pressure product which then requires compressing. Another advantage the membrane systems have over the cryogenic is that carbon dioxide and moisture (above its dew point) can be tolerated. If CO₂ and moisture are allowed into the cryogenic separation unit they would freeze and cause blockages.

The modular nature of the membrane systems means that the cost is almost directly proportional to the throughput. This means that membrane systems do not benefit from the economies of scale as does the cryogenic process, which closely follows the six tenths rule. However, there are benefits to be gained from easier installation. With the relatively limited experience of membrane gas separation systems in the field, questions of membrane life and reliability arise. Although the process is a simple one plants have only been operating for five years or so. As yet the membrane systems appear to be problem free. Five years, then, is taken to be the membrane life. The

membrane replacement cost is quite significant being approximately two thirds of the membrane plant cost.

The membrane separation process proves to be very competitive when only a partial separation is required. To produce a syngas of H₂:CO ratio of 1:1 the cost of membrane separation was as low as 10% of the cryogenic cost. And the separation can be achieved in one stage.

High degrees of separation and recovery are less favourable in one stage because, as the feed passes along the membrane module the driving force (partial pressure difference) for mass transfer of H₂ reduces. Thus very large amounts of area are required for relatively small amounts of permeation. A point will be reached where additional membrane area will not contribute to the separation. To produce high purity CO a two stage membrane process with recycle is required, and the cost is of the same order as cryogenic separation for a CO product of 97% purity and 96% CO recovery.

Further analysis of the information from suppliers was carried out by modelling the membrane separation process using the solution to the crossflow mass transfer equations produced by C. W. Saltonstall. (130). To overcome complications due to the difference between the selectivity achieved in a commercial scale module and the Ideal separation factor, an Effective Selectivity is used in the model such that the actual separation achieved is

predicted.

The other characteristic property of the membrane plant is the membrane permeability. This is considered in cost terms in the model, such that the Cost Permeability, when used, predicts the actual membrane plant cost. This is possible because for large membrane plants the cost can be assumed to be directly proportional to the membrane area. Thus the commercial membrane systems can be characterised by their membrane effective selectivity and cost permeability. This was justified by the success in correlating bids for different separation specifications in these terms.

As previously mentioned the CO product purity and recovery have cost implications upstream and downstream of the separation unit. To produce targets for development of membranes it was necessary to carry out cost optimisation of the process as a whole for the many combinations of membrane properties possible. Broadly speaking, permeability affects the size of the membrane unit and the selectivity affects both the size of the membrane unit and the amount of recycle required to achieve the separation.

For each membrane separator of given selectivity and permeability there is an optimum product purity and recovery which will give the lowest overall cost of CO production.

By characterising the membrane systems of existing commercial suppliers in terms of effective selectivity and cost permeability it is possible to obtain the

optimum separation specification for these systems. A significant cost reduction is achieved for the H₂/CO separation by operating at this optimum point. The separation cost is reduced to less than 60% of that for cryogenic separation for some of the commercial systems.

The same cost of separation is obtained with many combinations of permeability and selectivity. Iso-cost lines can be drawn on a plot of permeability and selectivity as in figure 10.1. The cost of separation is expressed as a proportion of the cost of separation by cryogenic distillation. The positions of two commercially available membrane separators are shown on the iso-cost curves.

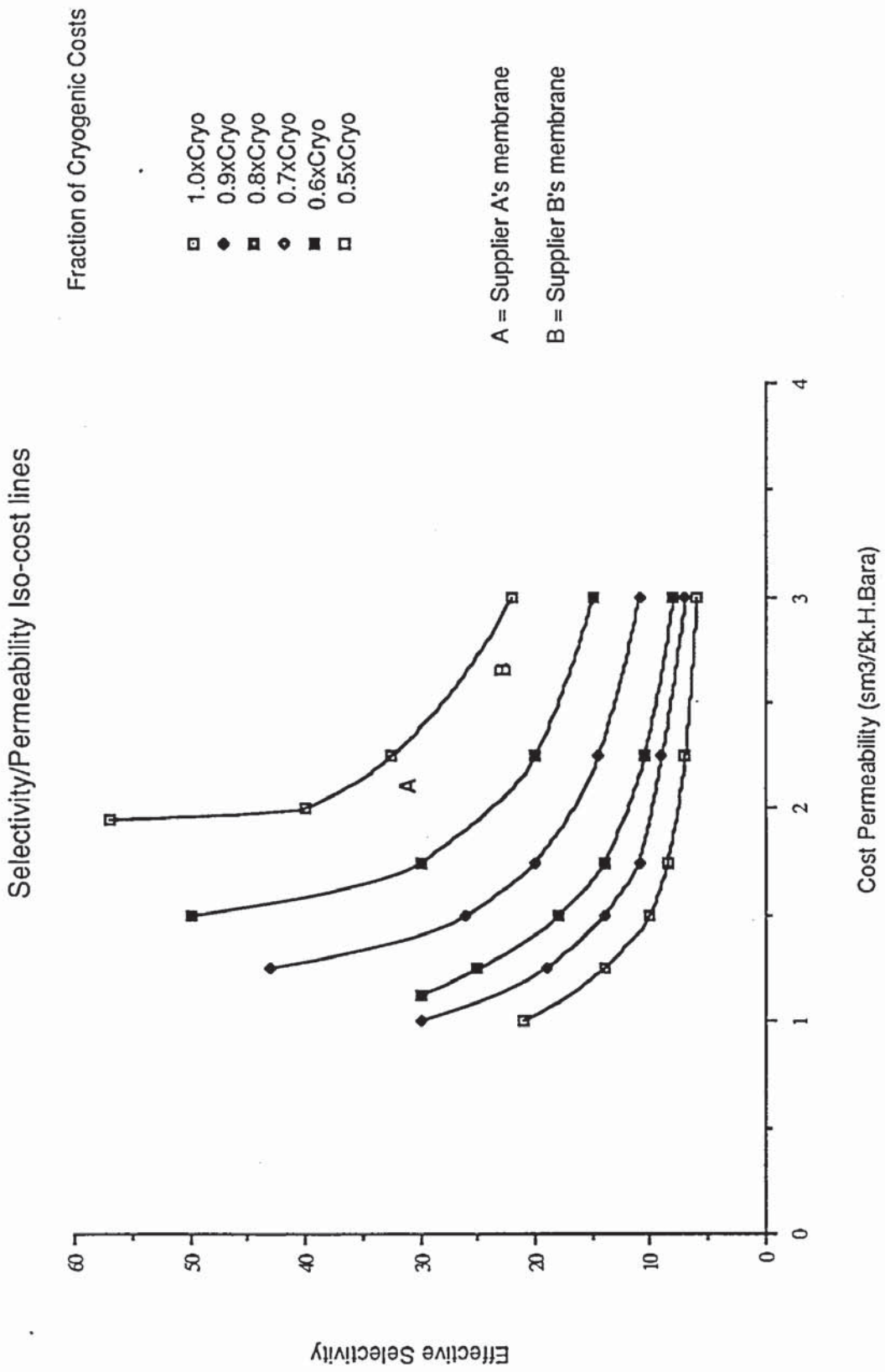
The targeting graph may be used to assist in the development of improved membrane gas separators. It shows the economic gains to be expected from increases in selectivity and/or permeability. Thus providing a "target" to aim for.

The targeting analysis may also assist in choosing between membrane separators and other methods of separation and provide a useful quantitative approach to separation process design.

For the production of a rich CO product from an H₂/CO syngas as considered in this thesis the targeting graph shows that clear advantages are to be made

FIGURE 10.1

TARGETTING GRAPH



by improving the membrane permeability. It can be seen that permeability reaches a limiting value where no further advantage is to be gained. At this permeability the cost of separation is governed solely by the selectivity. This should be used as the target for membrane permeability.

The target for selectivity should be such that the separation can be achieved in one stage. For the case considered in the evaluation this is an effective selectivity of approximately 60. Above this point the separation cost would be governed primarily by the permeability of the membrane.

Commercially available membranes whilst offering competition to the currently used cryogenic process, still have a great deal of scope for further development.

Prediction methods have been employed at Aston University to good effect for the molecular design of gas absorption solvents (140). Here Sithiosoth used the method developed by Sanders et al (134). This type of approach to development of gas separation polymers is also very useful.

The analogy between gas solubility in liquids and in polymers is understood to be valid for rubbery polymers. However, the selectivity achieved by rubbery polymers is low and thus limits the extension of S. Sithiosoth's approach to this problem.

Many of the deviations of gas permeability through polymers have been explained in terms of the dual mode sorption and transport theories, but these do not allow predictions on a molecular basis. The Permachor method developed by M. Salame (128) uses a molecular group contribution method to predict the permeabilities of O₂, N₂ and CO₂ through polymers. The method uses the cohesive energy density and free volume of polymers and the diameter (for diffusion) and Lennard-Jones potential of the gas.

The Permachor method when used for the prediction of H₂ and CO permeabilities gives rise to very large errors. However, available permeability data correlates well with the characteristic polymer Permachor number used by Salame. This correlation has been used to provide a guide to the selection of polymers for H₂/CO gas separation.

There are notable exceptions where the permeability deviates from the correlation. It is thought that this is due to polymers having highly polar groups present which interact with the gases.

The correlation is best used as a guide to the selection of polymers rather than a definitive prediction of polymer selectivity and permeability. Even though the correlation of the log of permeability is within about 10%, inaccuracies can be compounded when predicting selectivity. Polymers with a low Permachor number have higher permeability than polymers with high permachor

numbers, but they tend to be less selective.

The polymers selected and tested have aimed for enhanced permeability. polycarbonate and polymethylmethacrylate have slight advantages over existing cellulose acetate membranes, but a significant improvement has been made with the use of a co-polymer of methylmethacrylate and a siloxy group.

This co-polymer would be expected to achieve the H₂/CO separation at less than 50% of the cost of the cryogenic separation process..

An alternative approach could also be considered to select less permeable materials which can be used at high temperatures. This would mean that selectivity may be enhanced and permeability increased as well by operating at high temperature.

This work has selected a polymer which has a considerable enhancement of permeability and its position on the iso-cost curve is beyond the value where permeability yields any economic benefits. This should therefore be a good starting point for the enhancement of selectivity based upon this polymer. Selectivity could be enhanced at the expense of some permeability which would not damage its economic performance.

CHAPTER 11

CONCLUSIONS

1. In a process for the production of acetic acid the cost of the CO separation for the membrane process is on a par with the cryogenic process for the separation specification used in the cryogenic process (CO product purity = 97%; CO product recovery = 96%; CO product pressure = 40 Bara). The capital cost of membrane separation plant for the H₂/CO separation is about 80% of that for cryogenic separation. However, the membrane plant requires three times as much power to achieve the same separation specification as for the cryogenic process.
2. Capital cost and power reductions can be made in the membrane separation process by relaxing the separation specification, by either lowering the CO product purity or the CO product recovery.
3. For a membrane plant of any given separation properties there is an

optimum separation specification which gives the minimum cost of H₂/CO separation. The optimum separation specification is dependent upon the separating properties of the membrane plant.

4. At the optimum separation specification the cost of CO separation using membranes has been reduced considerably below that of the cost for cryogenic separation.

At the optimum specification for supplier A the comparative separation cost is £32/te.CO and for supplier B the comparative separation cost is £27/te.CO. This represents a reduction to 52% of the cryogenic separation cost (cryogenic separation cost = £52.40/te.CO) for membrane plant B.

5. The competitive position of the membrane separation for the hydrogen / carbon monoxide separation process has therefore been radically changed. From appearing to cost about the same as for cryogenic separation, to being very much more competitive than cryogenic separation by using the optimum separation specification.

6. Economic analysis methods were developed to allow each of the separation systems considered to be compared directly with each other on an equal basis. This was achieved by considering the whole process upstream and downstream of the separation unit. The comparison being made in terms

of the amount of acetic acid which can be produced using 100,000 tePA of 97% pure CO.

7. Newly developed cost parameters, the effective selectivity (α_e) and cost permeability (G_c), have been defined to characterise the separating properties of membrane gas separation systems.

8. A model of a crossflow membrane permeator has been used with the effective selectivity and cost permeability to simulate the membrane process.

9. The calculation of the effective selectivity and cost permeability of some commercial membrane systems was achieved by correlating information from the membrane suppliers.

Supplier	Effective Selectivity. α_e	Cost Permeability G_c (sm ³ /£k.H.Bar)
A	31	1.78
B	22	2.37
E	25	3.05
F	19	-

10. It is possible, knowing the effective selectivity and cost permeability of commercial membrane systems, to predict the suppliers membrane plant costs. This has provided useful information for B.P.Chemicals without reference to the supplying companies.

11. If there is enough information about suppliers membranes to characterise the membrane plant in terms of effective selectivity and cost permeability, then the optimum separation specification can be determined.

12. The optimum separation specification for membrane plants of suppliers A and B have been determined.

Supplier A $\alpha_e = 31.$ Gc = 1.78
sm³/£k.H.Bar.

Optimum CO purity = 95%.

Optimum CO recovery = 90%.

Supplier B $\alpha_e = 22.$ Gc = 2.37
sm³/£k.H.Bar.

Optimum CO purity = 95.5%.

Optimum CO recovery = 88%.

13. The same cost of separation can be obtained with many combinations of effective selectivity and cost permeability.

A method for targeting membrane properties has been developed. "Targeting" means defining the properties required by the membrane such that a membrane gas separation plant will be economically competitive with other membrane plants and with other methods of gas separation.

Iso-cost lines on a plot of effective selectivity and cost permeability have been drawn. The costs are expressed as a proportion of the cost of separation by cryogenic distillation.

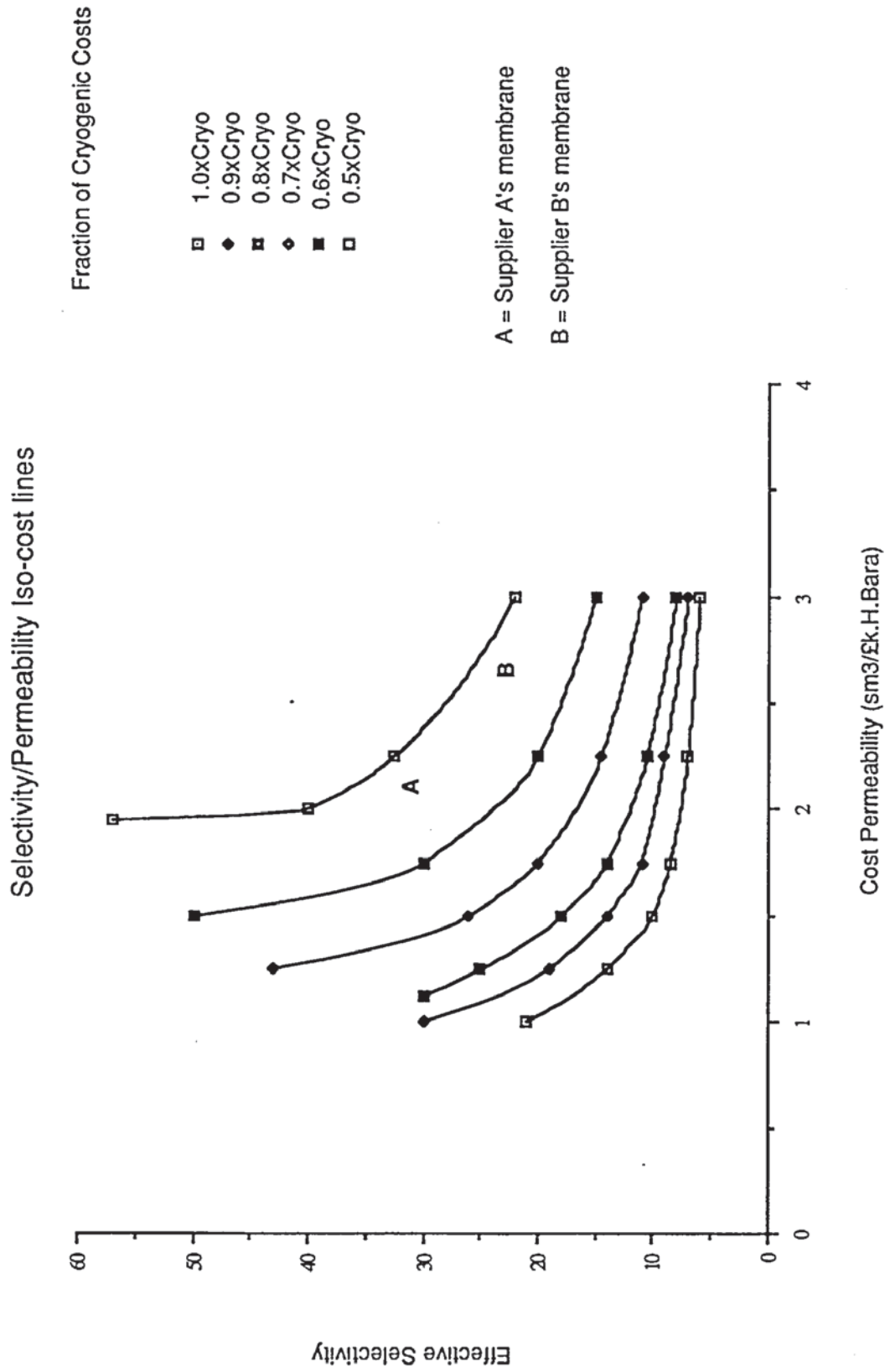
Existing commercial membrane plants can be pin-pointed on the graphs to show the current position. (See figure 11.1).

14. Figure 11.1 may be used to assist in the development of improved membrane gas separators. It shows the economic gains to be expected from increases in selectivity and/or permeability. It thus provides a "target" to aim at for those engaged in membrane research and development.

15. A target in terms of selectivity is an effective selectivity of 60 where a one stage process can be used for the separation.

FIGURE 11.1

TARGETTING GRAPH



16. Large gains can be made by increasing permeability, before improving selectivity, because currently used membranes are of very low permeability. However economic gains become less significant above a cost permeability of $10.0 \text{ sm}^3/\text{£k.H.Bar}$.
17. There is a minimum cost of separation associated with each effective selectivity where increases in the cost permeability will not yield a reduction in separation cost.
18. Newly developed membranes can be plotted on the targeting graph to give a very quick economic appraisal of the new membrane.
19. The use of the targeting method can be extended to other separations. It may also assist in choosing between membrane separators and other separation methods.
20. Methods to predict material properties based upon molecular groups can be used in the design and selection of new polymer membrane materials.
21. The UNIFAC group contribution method for the prediction of gas solubility in liquids has been used to identify molecular groups which will have high H_2/CO solubility ratio.

22. A correlation between the hydrogen and carbon monoxide permeabilities of polymers and the polymer Permachor number has been made.

The Permachor number is built up from the molecular groups contained in the polymer repeat unit.

The correlation has been used to predict polymer permeabilities and selectivities which in turn have been used to select candidate polymers for the separation of hydrogen and carbon monoxide.

23. The co-polymer of 50 : 50 methylmethacrylate and siloxy group proved to have a very high permeability, about 10 times that of currently used membranes. This polymer is much better than currently used membranes. The comparative separation cost would be about 30% of the separation cost for the cryogenic process.

24. It may be expected that further improvements in membrane properties could be made based on the methylmethacrylate / siloxy co-polymer by adjusting the co-polymer ratio. By increasing the proportion of methylmethacrylate the selectivity should increase, giving an improvement in the economic performance of the membrane, but the consequent reduction in permeability would have to be quite large before it started to affect the performance adversely.

25. Other membrane materials selected, such as polycarbonate and PTFE are on a par, economically, with the currently used membranes of suppliers A and B.

26. Whilst following the general trend expected by the Permachor correlation, there was insufficient experimental data obtained from this project to strongly support the Permachor correlation which was developed.

CHAPTER 12

SUGGESTIONS FOR FUTURE WORK

12.1 Introduction

Further work is required following on from this project to achieve two main aims. Firstly, to take advantage of the work already carried out and where positive progress has been made. And secondly, to provide further information to improve upon the methods used in this work.

12.2 Membrane Development

An area which may prove to be able to yield relatively high selectivity membranes, whilst maintaining high permeability is to combine the properties of highly selective polymer materials with those of highly permeable polymers.

For example a co-polymer could be synthesised combining Polyacrylonitrile,

which has an ideal separation factor = 110 and a permeability of $0.1 \text{ cm}^3 \cdot \text{cm} / \text{cm}^2 \cdot \text{s} \cdot (\text{cmHg})$, and a highly permeable polymer such as the siloxy compound used in this work. As a measure of the properties of silicone materials it is known that silicone rubber has a selectivity of 2 and a permeability of $520 \text{ cm}^3 / \text{cm}^2 \cdot \text{s} \cdot (\text{cmHg})$.

Making a number of co-polymer blends would lead to a relationship between selectivity, permeability and the proportions of the co-polymer. The optimum composition should be able to be made to get the best of both worlds.

Throughout this work several ideas have arisen for the separation of hydrogen and carbon monoxide, such as the use of a non-uniform electric field applied across a membrane, and these may be worthy of further development.

12.3 Consolidation

Further work is required to establish the relationship between the laboratory measured pure gas permeabilities and ideal separation factors and the concepts of effective selectivity and cost permeability developed in this thesis. This could be done by testing membrane modules. It may be that the effective selectivity and cost permeability can be enhanced by improved membrane module design.

Another area which may lead to useful developments for membrane

separation is the use of polymer membranes at elevated temperatures. If permeability data is obtained at different temperatures for hydrogen and carbon monoxide a correlation between the polymer Permachor number, permeability and temperature should be able to be made in the form:-

$$G = A \cdot \exp(B \cdot p) \cdot \exp(-((C+D \cdot p)/T)) \quad (12.1)$$

A, B, C & D are constants. T = Absolute temperature.

If high temperature polymers are used for the hydrogen / carbon monoxide separation the gains in permeability associated with high temperature operation may significantly outweigh the losses in selectivity. If a permachor number could be defined for a polymer at an elevated temperature then likely polymer candidates could be selected.

The process considered in this thesis would lend itself to separation at high temperature because the syngas is initially produced at 850°C from the POX reactor.

APPENDIX 1

ECONOMIC EVALUATION DATA

Introduction

Much of the information used in the economic evaluation is specific to B.P. Chemicals. Capital costs, scale up methods and variable costs were agreed with the Process Evaluation Group at B.P. Chemicals at the time the calculations were made.

Capital Cost

The capital costs quoted by suppliers of plant and equipment is the cost before installation and any other costs.

Factors are used, based on experience, to calculate the fully installed cost of plant ready for operation.

$$C_{inst} = (1 + F_{inst}) \cdot C_Q \quad (A1.1)$$

C_Q = Quoted cost.

F_{inst} = Installation factor.

C_{inst} = Fully installed cost.

Additional costs not directly associated with the installation of the plant, such as overheads and engineering consultancy costs, also have to be taken into account. Again, experience factors are used to calculate these indirect costs.

$$C_{inst+ind} = (1 + F_{ind}) \cdot C_{inst} \quad (A1.2)$$

$C_{inst+ind}$ = Total installed and indirect cost.

F_{ind} = Indirect cost factor.

The indirect and installation factors can be combined so that the Total installed and indirect cost can be calculated from the quoted cost directly.

$$C_{inst+ind} = (1 + F_{inst})(1 + F_{ind}) \cdot C_Q \quad (A1.3)$$

Capital cost of POX reactor :-

$$C_{\text{inst+ind}} = \text{£ } 10.64 \text{ m}$$

This value is for the base case production of syngas which will produce 100,000 tePA of 97% pure CO at a recovery of 95.8%.

This figure was obtained from B.P. Chemicals' Process Evaluation Group.

The scale up of the POX reactor cost is as follows :-

$$\text{New POX reactor cost} = \left[\frac{[\text{New Feed Flow}]^{0.67}}{[\text{Old Feed Flow}]} \right] \cdot \text{Old POX reactor cost.} \quad (\text{A1.4})$$

Capital cost of cryogenic plant :-

The factor for the total installed and indirect cost for a cryogenic separation unit is between 4 and 4.5 based on experience. For the purposes of this evaluation the following has been used.

$$C_{\text{inst+ind}} = 4.5 \cdot C_Q \quad (\text{A1.5})$$

Capital cost of membrane plant :-

Experience of installing this type of plant is limited. The fully installed and indirect costs are based upon experience of installing skid mounted PSA plant.

$$C_{\text{inst}} = 2 \cdot C_Q \quad (\text{A1.6})$$

$$C_{\text{ind}} = 2 \cdot C_{\text{inst}} \quad (\text{A1.7})$$

ie. $C_{\text{inst+ind}} = 4 \cdot C_Q \quad (\text{A1.8})$

Because of the limited experience of costing in this field, further information is required to obtain a more accurate installation cost. It may be that the installation cost would be lower than that assumed above because of the modular nature of membrane plant.

Capital cost of compressors :-

The capital cost of compressors has been calculated on the basis of power consumption using the following cost correlation for centrifugal compressors of above 170 kw.

$$C_Q = \frac{575 \cdot 6100 \cdot P^{0.6}}{383.7} \quad (A1.9)$$

Where the compressor power has been calculated a 70% compressor isothermal efficiency is assumed.

Variable Costs

Process streams were costed from their fuel value. A thermal value of £0.21/therm was used.

Natural gas.

Calorific value of CH₄ = 474 therms/te.

Hydrogen.

Calorific value of H₂ = 1137 therms/te.

Carbon monoxide. Calorific value of CO = 97.2 therms/te.

Cost of oxygen = £ 23.00 / te.

Cost of electricity = £ 0.02 / kWh.

Membrane replacement cost :-

The long term reliability of membrane plants is not known due to the limited number of plants in operation and the age of the plants. So far it appears that the plants are reliable and there have been no major failures of membranes, even in environments of corrosive gases. However, a cautious approach to this aspect was thought to be best and a membrane life of five years is assumed.

The cost of replacement membrane modules was quoted to be two thirds of the quoted cost of the membrane plant. This cost is spread linearly over five years.

Hence :-

$$\text{CMR} = 0.67 \cdot \text{Quoted cost of membrane plant} / 5 \quad (\text{A1.10})$$

Calculation of Purge Gas Penalty

For every 1% reduction in CO purity an extra 2.57 moles of CO has to be purged from the downstream, acetic acid, reactor.

Exchange Rates

$$\text{£ } 1.00 = \$ 1.50 = \text{DM } 3.00 = \text{JY } 230.00$$

APPENDIX 2

SPREADSHEETS

Introduction

The spreadsheets used have been written on the Supercalc 3 spreadsheet programme which is IBM compatible. The disc at the back of this thesis contains a copy of the Supercalc 3 spreadsheet and the three spreadsheets described in this appendix. To load the spreadsheet programme type SC3 at the prompt a>. To load a spreadsheet, type /L and then the spreadsheet name.

Basically two spreadsheets have been used for the economic evaluation of membrane systems and for the modelling of the membrane separation process.

The economic evaluation spreadsheet will evaluate any membrane system from the required input data. The crossflow model of a membrane permeator

has been used for the modelling spreadsheet and this programme has been combined in various ways to simulate a single stage permeator, a recycle permeator, a two stage series type permeator and a two unit type recycle permeator. The output from the modelling spreadsheets has then been combined with the economic evaluation spreadsheet.

A spreadsheet was also written to plot a graph of experimental data from the Davenport permeability test and to calculate the membrane permeability between any two desirable points.

Economic Evaluation Spreadsheet

Spreadsheet name :- ECONOMEM

The following printout is the full listing of the economic evaluation spreadsheet. The calculation formulae are listed after the printout. The letters and numbers refer to the cell location in the spreadsheet.

```

1  A  || B  || C  || D  || E  || F  || G  ||
11: EVALUATION OF MEMBRANE SEPARATION SYSTEMS TO SEPARATE CO FROM SYNGAS
2: -----
3:
4: This Spreadsheet calculates the cost of producing CO using membrane
5: separation. The feed is syngas supplied from a non-catalytic FOX
6: reactor. The programme takes into account the CO recovery achieved,
7: the purity of the CO product, but does not make any adjustments for
8: varying feed pressure.
9:
10:
11: The inputs required are:
12:
13:                                     NAME OF SUPPLIER
14:                                     SIZE OF PLANT (TONNES/ANNUM )
15:                                     % CO PURITY
16:                                     % CO RECOVERY
17:                                     QUOTED COST OF MEMBN. SEPN. PLA
18:                                     QUOTED COST OF COMPRESSOR
19:                                     EXCHANGE RATE OF CURRENCY QUOTE
20:                                     POWER REQUIRED (KW.)
21:                                     THE CO AND H2 FLOWS IN THE PERM
22:
23:
24: It may be required to change other factors to look at sensitivity,
25: these are listed separately.
26: The factors which can be changed are:
27:
28: FACTOR TO OBTAIN INSTALLED COST OF MEMBRANE PLANT FROM QUOTED COST
29: FACTOR FOR MAINTENANCE COST OF CAPITAL
30: FACTOR FOR DEPRECIATION OF CAPITAL
31: FACTOR FOR RETURN ON INVESTMENT
32: COST OF ELECTRICITY (POUNDS/KWH)
33: COST OF OXYGEN (POUNDS/TONNE)
34: THERMAL VALUE (POUNDS/THERM)
35:
36:
37:
38: Enter inputs in column "F" using the units indicated.
39:
40: NAME OF SUPPLIER. >
41:
42: SIZE OF PLANT (TONNES/ANNUM) > 100000
43:
44: % CO PURITY > 95
45:
46: % CO RECOVERY > 80
47:
48: QUOTED COST OF MEMBN. SEPN. PLANT > 1395000
49:
50: EXCHANGE RATE > 1
51:
52: POWER REQUIRED (KW) > 0
53:
54: H2 FLOW IN PERMEATE STREAM (M3/HR) > 21534
55:
56: CO FLOW IN PERMEATE STREAM (M3/HR) > 2366

```

	A	B	C	D	E	F	G
62	The other factors are listed below and can be changed if desired.						
63							
64	FACTOR TO OBTAIN INSTALLATION COST OF						
65							2
66	MEMBRANE SEPARATION PLANT						
67	FACTOR TO OBTAIN INSTALLED COST OF COMPRESSOR						
68							1.3
69	FACTOR TO OBTAIN INDIRECT COST OF COMPRESSOR						
70							1.8
71	CURRENT COST INDEX						
72							575
73	MAINTENANCE COST OF CAPITAL						
74					>		.05
75	DEPRECIATION OF CAPITAL						
76					>		.1
77	RETURN ON INVESTMENT						
78					>		.2
79	COST OF ELECTRICITY (POUNDS/KWH)						
80					>		.02
81	COST OF OXYGEN (POUNDS/TONNE)						
82					>		23
83	THERMAL VALUE (POUNDS/THERM)						
84					>		.21
85	-----						
86							
87	A table showing the results starts on row 124, after the calculation						
88	section.						
89							
90	-----						
91							2/80/40
92	-----						
93							
94	CO GENERATION			CO SEPARATION			
95							
96							
97	FACTOR 1	1.1975			POWER		0
98							
99	FACTOR 2	1.054185			MEMBRANE		
100	REPLACEMENT						
101	FACTOR 3	1			COST >	1.8693	
102							
103	FEED COST	84.83238			PLANT COST		20.47988
104							
105	O2 COST	26.70072			COMPRESSOR COST		0
106							
107	FUEL COST	6.393675					
108							
109	STEAM CREDIT	21.57197			CO PURGE CREDIT		1.106027
110							
111	H2 CREDIT	41.82659					
112							
113	POX COST	43.53200	37.24				
114							
115							
116	-----						

I	A	B	C	D	E	F	G	
124	RESULTS SECTION					2/80/40		
125								
126								
127	ITEM	:						COST (POUNDS/TONNE)
128	-----	:	-----					-----
129	CO GENERATION	:						
130	-----	:						
131	VARIABLE COSTS	:						117.93
132	STEAM, H2 AND CO PURGE CREDITS	:	-					64.5
133	POX REACTOR COST	:						43.53
134	-----	:	-----					-----
135	TOTAL CO GENERATION COST	:						96.96
136		:						
137	CO SEPARATION	:						
138	-----	:						
139	VARIABLE COSTS	:						1.87
140	CAPITAL COST : MEMBRANE PLANT	:						20.48
141	: COMPRESSOR	:						0
142	-----	:	-----					-----
143	TOTAL CO SEPARATION COST	:						22.35
144		:						
145	=====	:	=====					=====
146	GROSS TOTAL COST	:						119.31
147	=====	:	=====					=====

$$\begin{aligned}
\text{Factor 1} &= 95.8/F46 \\
\text{Factor 2} &= 100/(100 - (97 - F44) * 2.57) \\
\text{Factor 3} &= F42/100,000 \\
\text{Feed cost} &= 6720000*B97*B99*B101/F42 \\
\text{O2 cost} &= 2115098*B97*B99*B101/F42 \\
\text{Fuel cost} &= 506475.2*B97*B99*B101/F42 \\
\text{Steam credit} &= 1708824*B97*B99*B101/F42 \\
\text{H2 credit} &= (F54*1137*8000*F83/(11118*F42)) \\
&\quad + (F56*97.2*8000*F83/(800*F42)) \\
\text{POX cost} &= ((F73 + F75 + F77) + 10640000*(B97*B99*B101)**0.67)/F42 \\
\text{Power} &= F52*F79*8000*B99/F42 \\
\text{Membrane replacement cost} &= 0.67*F48*0.2/(F42*F50) \\
\text{Plant cost} &= ((F73 + F75 + F77)*F48*2*F65*B99)/(F42*F50) \\
&\quad ((F73 + F75 + F77)*6100*(F52*B99)**0.6*F67*F69*F71) \\
\text{Compressor cost} &= \frac{\text{Plant cost}}{(F42*383.7)} \\
\text{CO purge credit} &= B99*1000*(97 - F44)*2.57*97.2*F83/F42
\end{aligned}$$

Results section.

CO Generation.

Variable costs = Round(B103 = B105 + B107,2)

Steam, H2 and CO purge credits = Round(C109 + C111 + G109,2)

POX reactor cost = Round(B113,2)

Total CO generation cost = F131 + F133 - F132

CO Separation.

Variable costs = Round(F97 + F101,2)

Capital cost : Membrane plant = Round(G103,2)

Capital cost : Compressor = Round(G105,2)

Total CO separation cost = F139 + F140 + F141

Gross total cost = G135 + G143

Crossflow Model Spreadsheet

Spreadsheet name : CROSSFLO

The following printout is the full listing of the single stage crossflow model of a permeator spreadsheet . Formulae for the spreadsheet are written out following the printout.

```

 1 | A | B | C | D | E | F | G |
11|This spreadsheet will calculate the membrane area required for
21|a single stage permeator separating two components. It assumes
31|a crossflow configuration and the solution is based upon the
41|the solution to the governing differential equations provided
51|by C.W.Saltonstall, J Mem Sci 32(1987)185-193.
61
71
81
91
10|INPUTS                                ENTER INPUTS IN COLUMN "D"
11|
12|
13|XH2F                                .65
14|XH2R                                .565
15|RH2                                1.219
16|ALPHA                              31
17|P                                    40
18|p                                    2
19|QF                                28944.20
20|
21|
22|
23|
24|
25|CALCULATIONS
26|
27|
28|BETA = 1.033333
29|D = 20
30|
31|Calculation of YH2F                 Calculation of YH2R
32|a = 1                               a = 1
33|b = -14.6667                       b = -12.9667
34|c = 13.43333                       c = 11.67667
35|
36|YH2F = .9816057                    YH2R = .9736197
37|
38|
39|Calculation of Q
40|
41|A = -1.03509
42|B = .0877193
43|
44|TERM1 = 1.154385
45|TERM2 = .6885092
46|TERM3 = .9992837
47|
48|Q = 5955.697
49|
50|
51|Calculation of permeate purity,  $\bar{Y}H2$ 
52|
53|
54| $\bar{Y}H2$  = .9780931
55|
56|
57|Calculation of area
58|
59|
60|AREA = 213.0699

```

I A II B II C II D II E II F II G I

61!
62!
63!
64!
65!
66!
67!
68!
69!
70!
71!
72!
73!
74!
75!
76!
77!
78!
79!

RESULTS.

FEED FLOW (M3)	28944.20
RAFFINATE FLOW (M3)	22988.51
PERMEATE FLOW (M3)	5955.697
% CO RECOVERY	98.71209
PERMEATE PURITY (MOL FRAC CO)	.0219069
RAFFINATE PURITY (MOL FRAC CO)	.435
MEMBRANE AREA (M2)	213.0699

Calculations

$$\text{Beta} = D16/(D16 - 1)$$

$$D = D17/D18$$

For YH2F :-

$$a = 1$$

$$b = 1 - B29*(B28 - 1) - B29*D13$$

$$c = B28*B29*D13$$

$$YH2F = (-B33 - (B33**2 - 4*B32*B34)**0.5)/(2*B32)$$

For YH2R :-

$$a = 1$$

$$b = 1 - B29*(B28 - 1) - B29*D14$$

$$c = B28*B29*D14$$

$$YH2R = (-E33 - (E33**2 - 4*E32*E34)**0.5)/(2*E32)$$

Calculation of Q :-

$$A = (1 - B28*B29)/(B29 - 1)$$

$$B = B28*B29/(B29 - 1) - 1$$

$$\text{Term 1} = B28 - E36/(B28 - B36)$$

$$\text{Term 2} = ((1 - E36)/(1 - B36))**B41$$

$$\text{Term 3} = (E36/B36)**B42$$

$$Q = D19 - B44*B45*B46*D19$$

$$\bar{Y}_{H2} = ((D13 - D14) * D19 / B48) + D14$$

$$\text{Area} = B48 * (B28 - B54) / (D18 * D15 * (B29 - 1) * (B28 - 1))$$

Results

$$\text{Feed flow} = D19$$

$$\text{Retentate flow} = D19 - B48$$

$$\text{Permeate flow} = B48$$

$$\% \text{ CO Recovery} = 100 * (1 - D14) * (D19 - B48) / ((1 - D13) * D19)$$

$$\text{Permeate purity} = 1 - B54$$

$$\text{Retentate purity} = 1 - D14$$

$$\text{Membrane area} = B60$$

Gas Permeability Test Spreadsheet

Spreadsheet name : DAVENPORT

The following printout is the full listing of the spreadsheet for the pressure/time plot for the Davenport gas permeability test. The formulae for the calculation of the membrane permeability are written out following the printout.

The pressure / time plots for all the carbon mon-oxide and hydrogen permeability tests are printed out in appendix 3.

```

 1 A  2 B  3 C  4 D  5 E  6 F  7 G  8
1!This spreadsheet graphs the data from a permeability test and
2!calculates the gas permeability for the given polymer film.
3!
4!DATA REQUIRED.
5!-----
6!Gas used.
7!Polymer used.
8!Film thickness. (mm)
9!Initial pressure. (mmHg)
10!Temperature. (deg C)
11!Cell insert used. (cm3)
12!Hg. height (cm) vs. Time (mins) data.
13!
14!
15!
16!ENTER INPUTS IN COLUMN C.
17!-----
18!Gas      :      HYDROGEN.
19!Polymer  :      PMMA-SILOXY
20!Film thickness :      1
21!Initial pressure :      .3
22!Temperature :      19
23!Insert used :      20
24!
25!Enter 1st and last      Time Hg Height
26!points to be used      10      0
27!in C25 and C26      0      0
28!
29!
30!Time (min)      0      5      10      15      20      25
31!Hg height
32!
33!
34!
35!Hg Drop (cm) =      0
36!Time (s) =      -600
37!Volume (cm3) =      20.582
38!
39!Transmission rate (cm3/cm2.s.(cmHg)) =      0
40!Gas Permeability (cm3.mm/cm2.s.(cmHg))=      0 1e-10cm

```

$$\text{Hg Drop} = D25 - D26$$

$$\text{Time} = 60 * (C26 - C25)$$

$$\text{Volume} = C23 + 0.24 + 0.018 * (19 - D25 + (C35/2))$$

$$\text{Transmission rate} = (273 * C35 * C37 * 10) / ((C22 + 273) * C36 * 76 * 23.77 * (760 - C21))$$

$$\text{Gas permeability} = F39 * C20 * E10 * 10^{-10}$$

APPENDIX 3

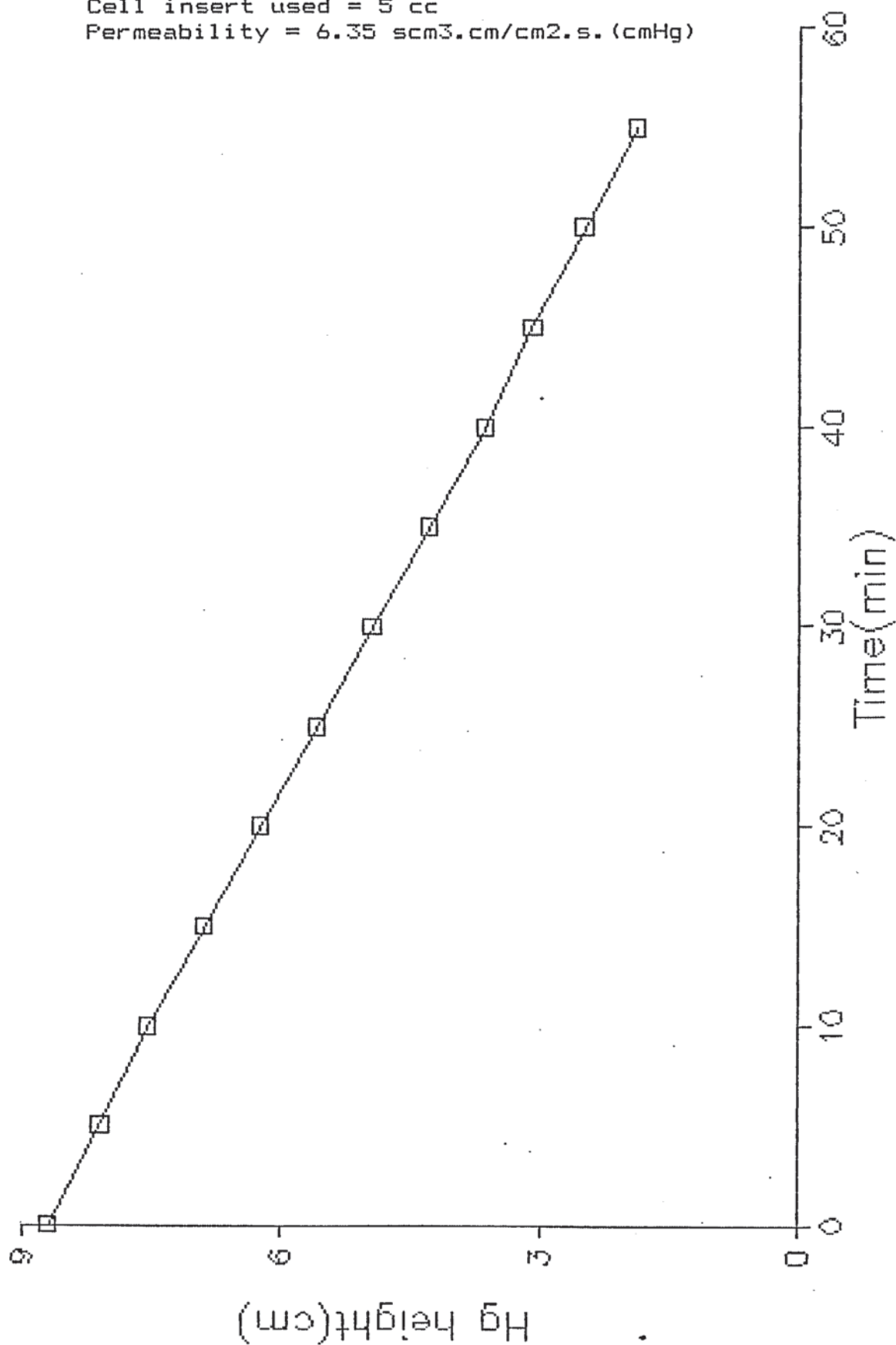
EXPERIMENTAL PERMEABILITY PLOTS

Introduction

The following graphs are the pressure versus time plots obtained for membranes in the Davenport gas permeability apparatus. The permeating gases used were hydrogen and carbon monoxide.

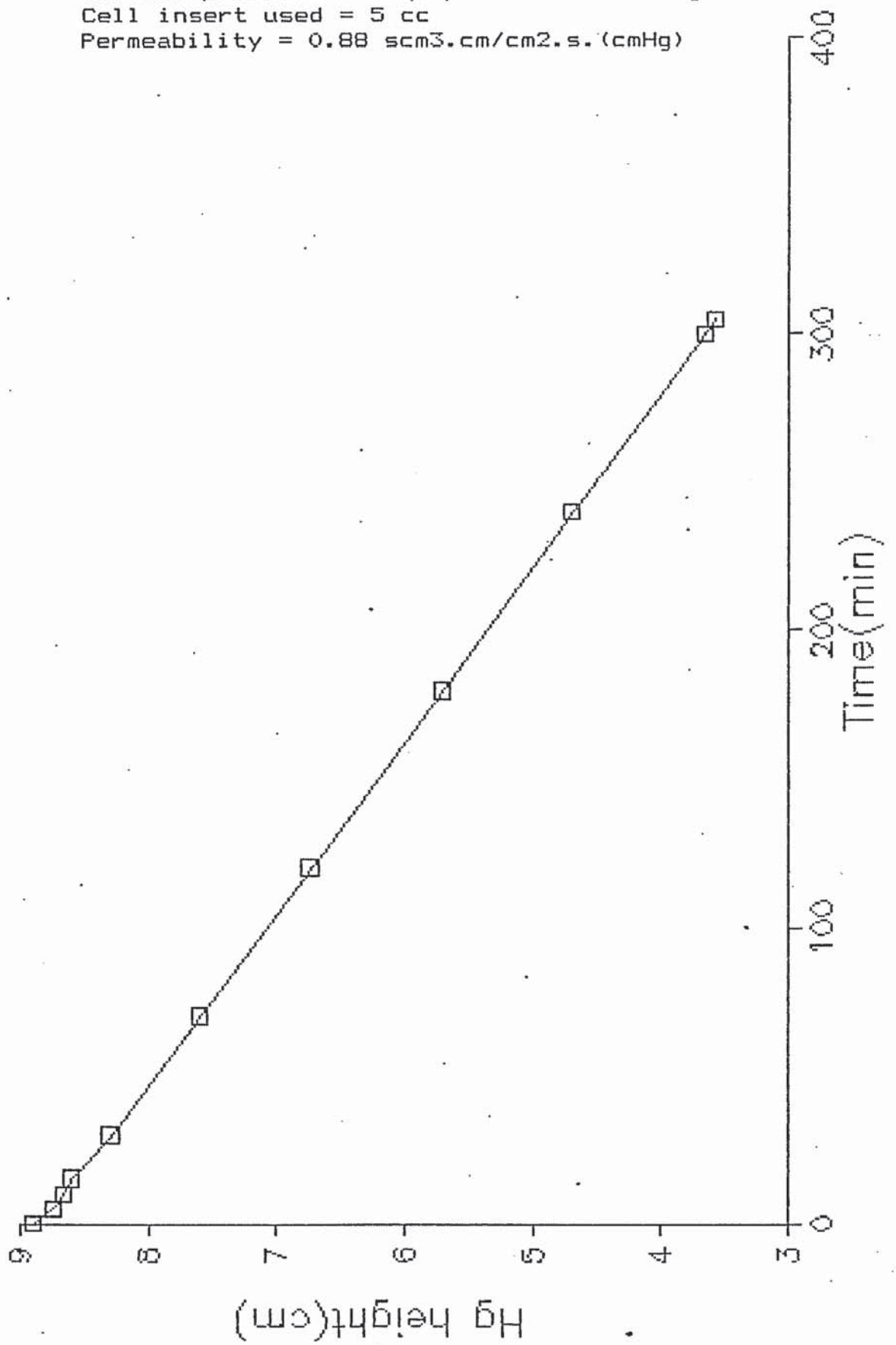
Membrane thickness = 0.085mm
Temperature of experiment = 21 C
Initial pressure of equipment = 0.45 mmHg
Cell insert used = 5 cc
Permeability = 6.35 scm³.cm/cm².s.(cmHg)

HYDROGEN/POLYETHYLENE



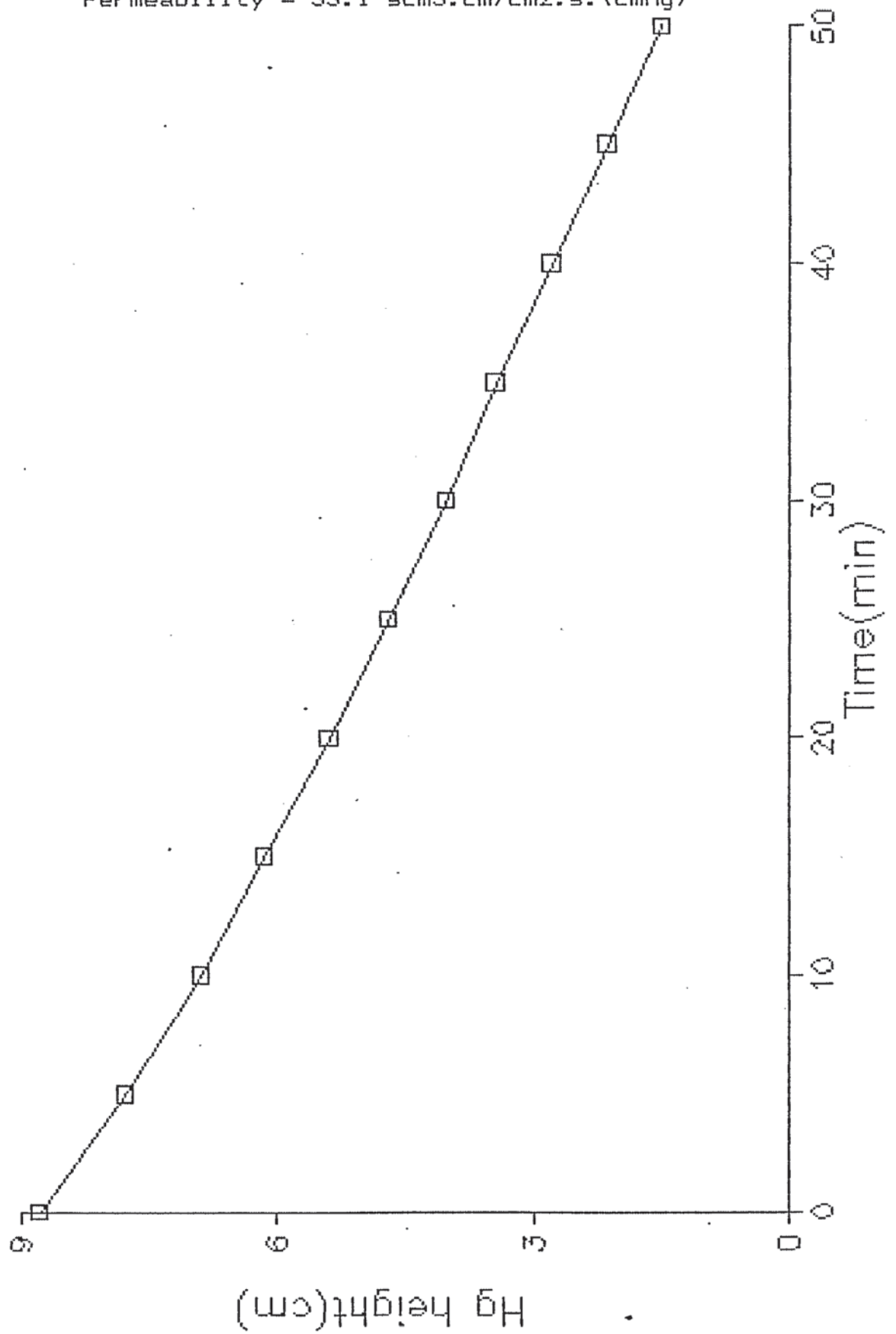
CARBON MON-OXIDE/POLYETHYLENE

Membrane thickness = 0.085mm
Temperature of experiment = 20 C
Initial pressure of equipment = 0.35 mmHg
Cell insert used = 5 cc
Permeability = 0.88 scm³.cm/cm².s.(cmHg)



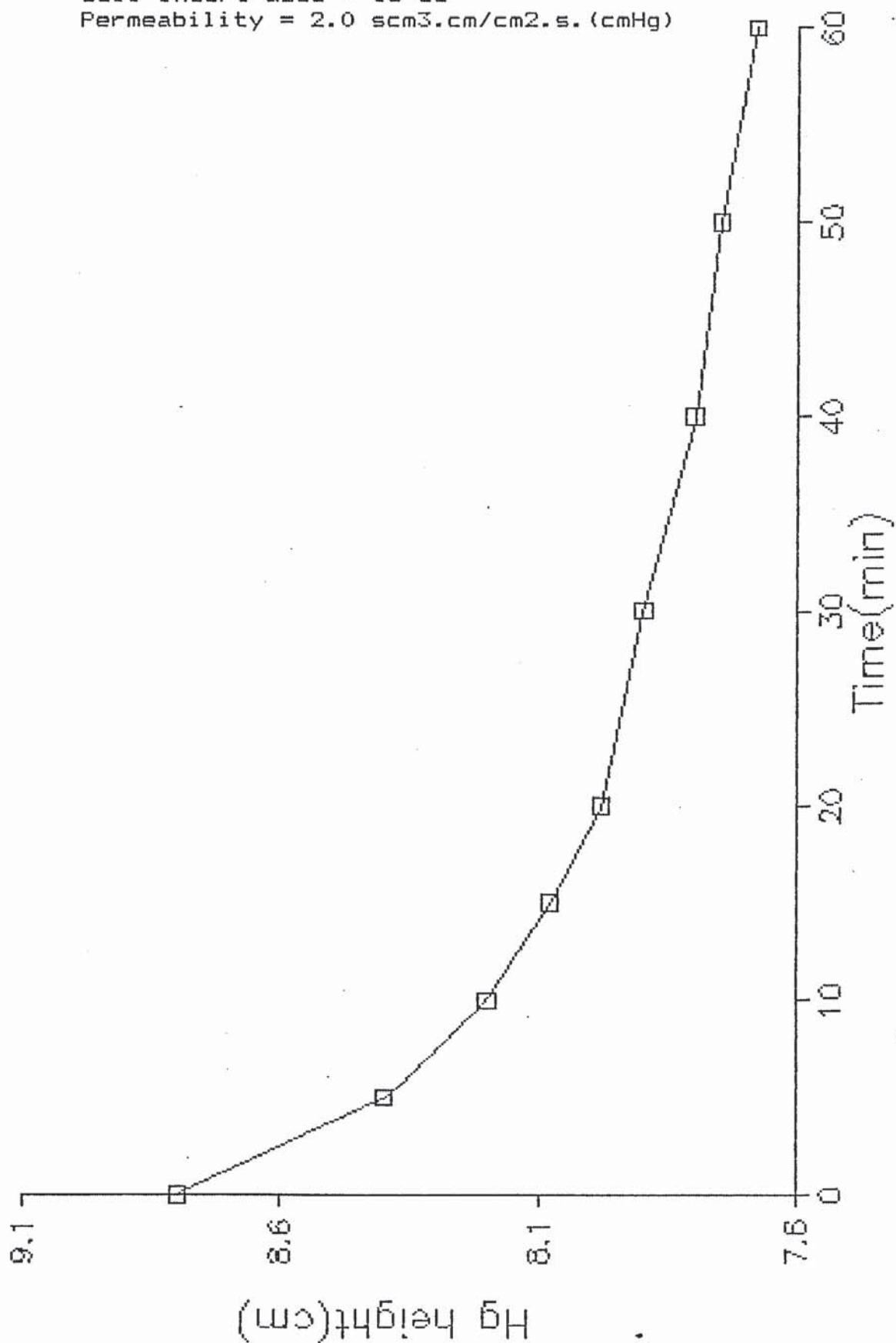
Membrane thickness = 0.15mm
Temperature of experiment = 20 C
Initial pressure of equipment = 0.25 mmHg
Cell insert used = 15 cc
Permeability = 33.1 scm³.cm/cm².s.(cmHg)

HYDROGEN/POLYBUTADIENE



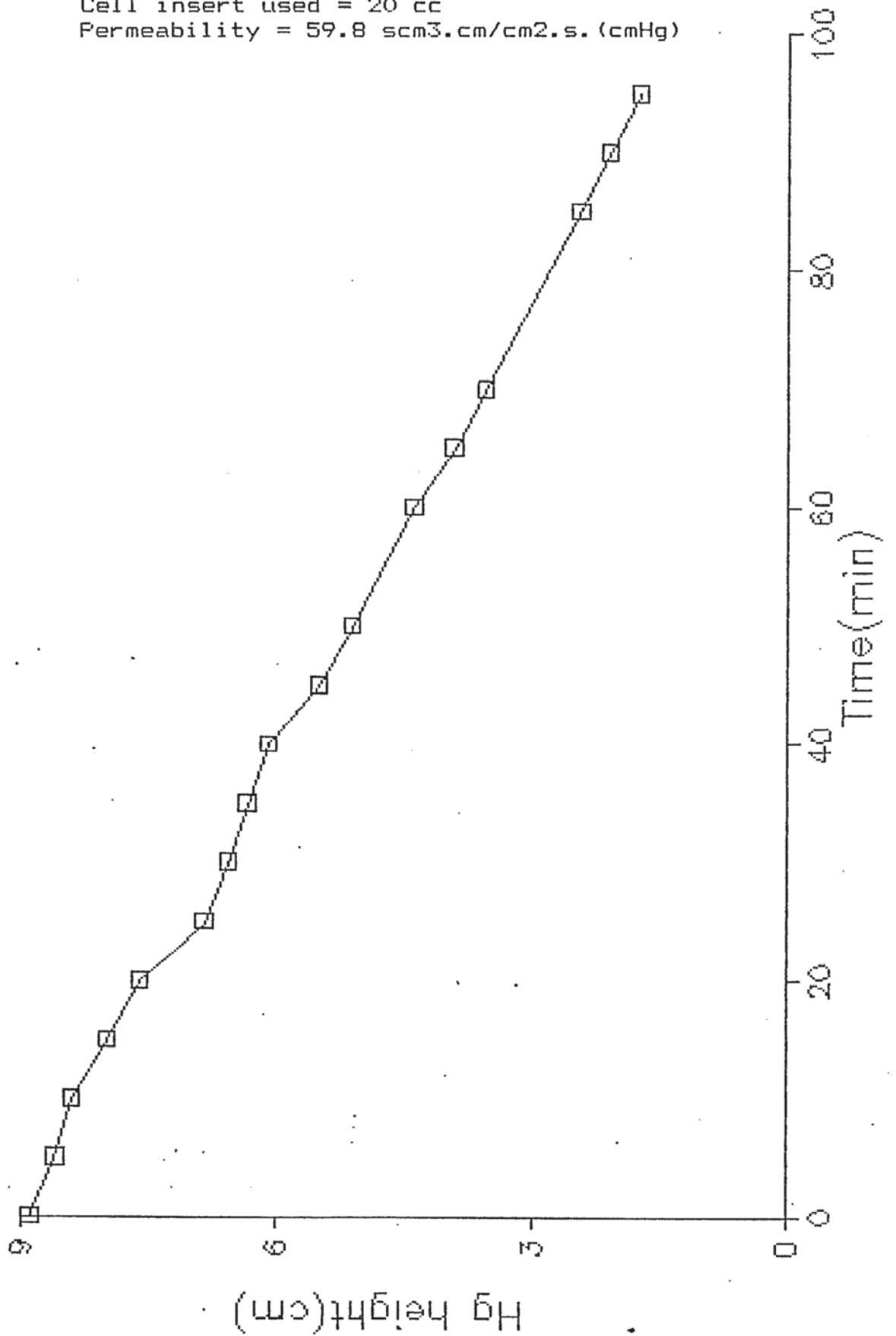
CARBON MON-OXIDE/POLYBUTADIENE

Membrane thickness = 0.15mm
Temperature of experiment = 21 C
Initial pressure of equipment = 0.25 mmHg
Cell insert used = 15 cc
Permeability = 2.0 scm³.cm/cm².s. (cmHg)



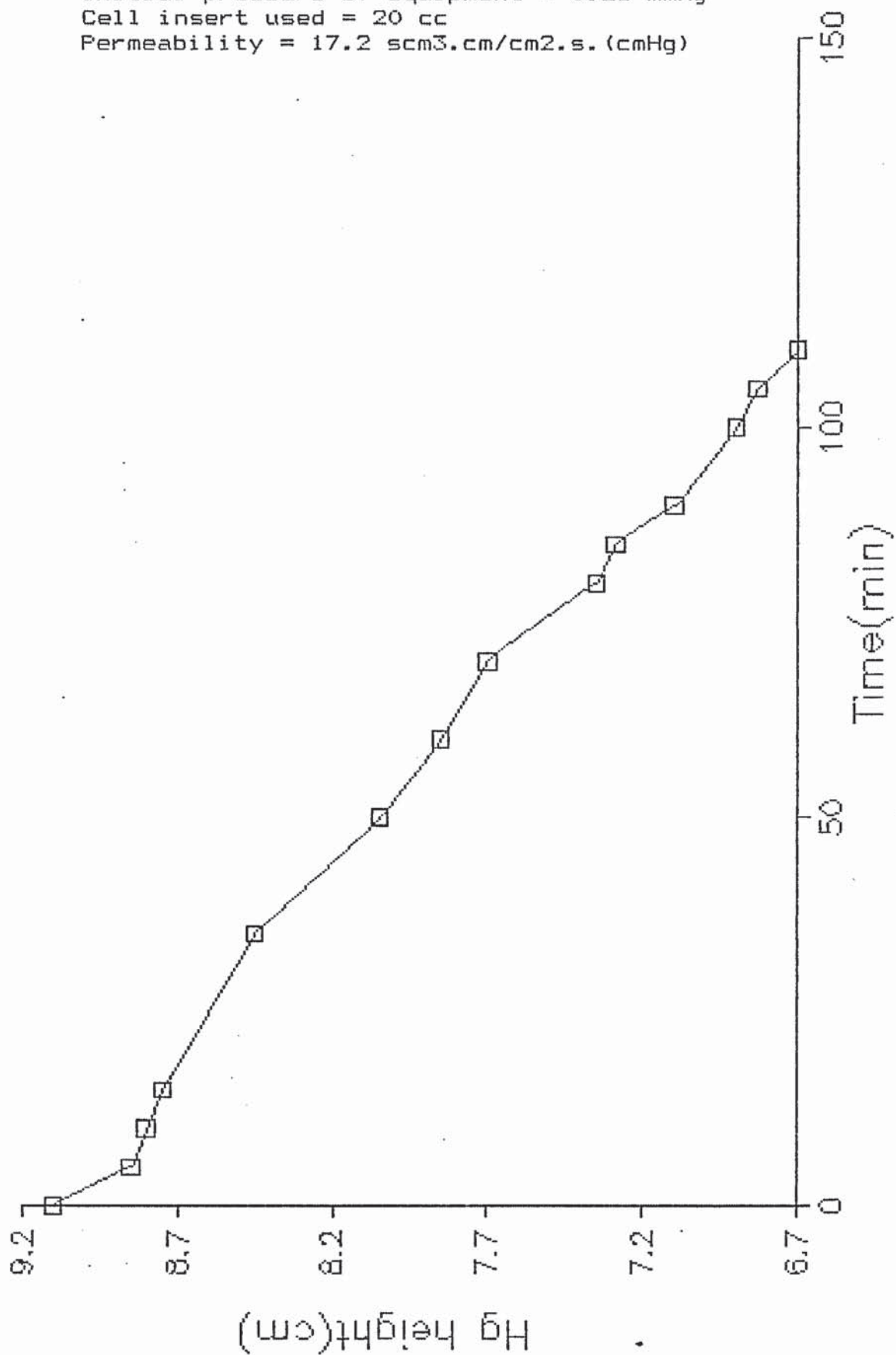
Membrane thickness = 0.35mm
Temperature of experiment = 24 C
Initial pressure of equipment = 0.30 mmHg
Cell insert used = 20 cc
Permeability = 59.8 scm³.cm/cm².s.(cmHg)

HYDROGEN/POLYISOPPRENE



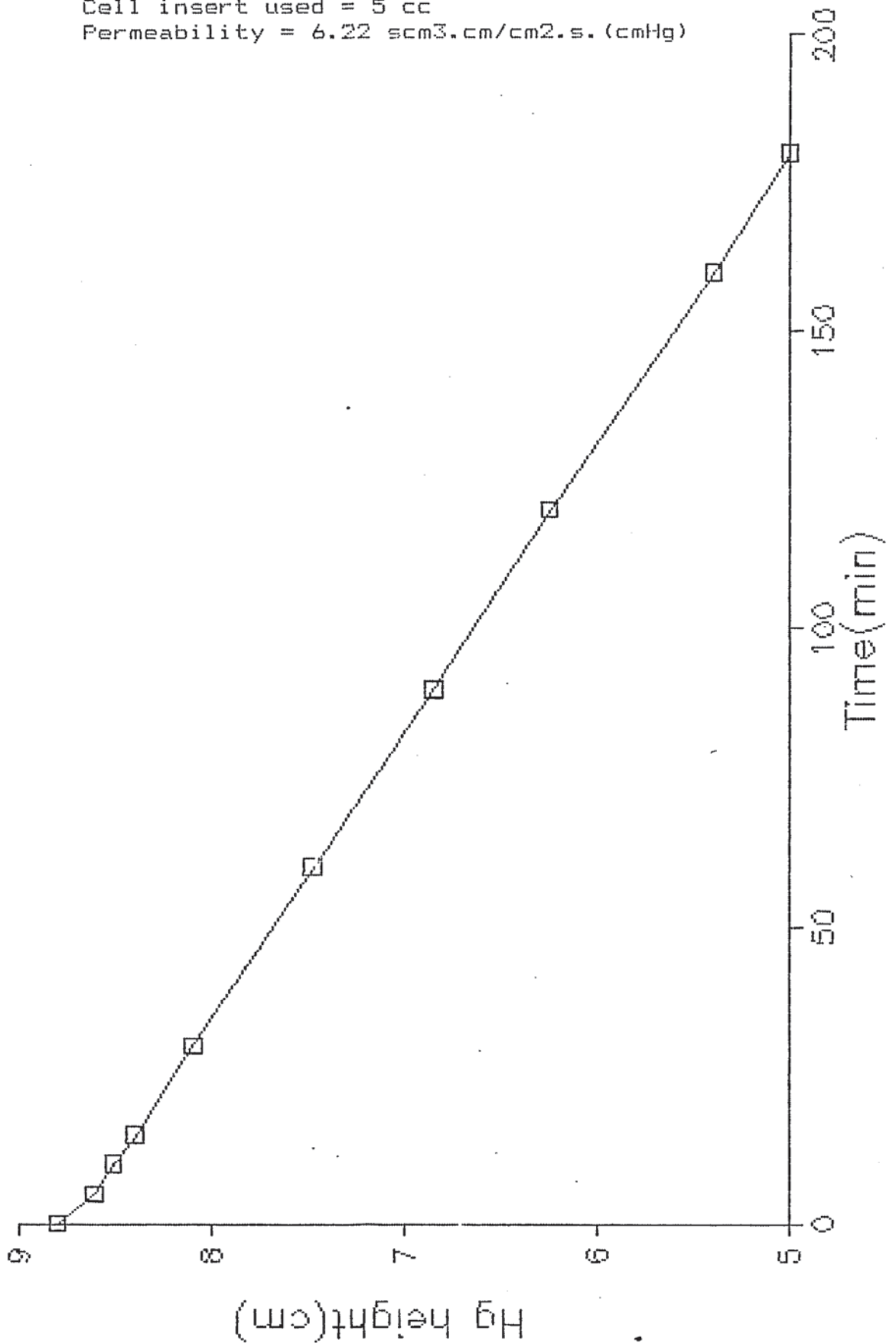
CARBON MON-OXIDE/POLYISOPPRENE

Membrane thickness = 0.35mm
Temperature of experiment = 23 C
Initial pressure of equipment = 0.25 mmHg
Cell insert used = 20 cc
Permeability = 17.2 scm³.cm/cm².s. (cmHg)



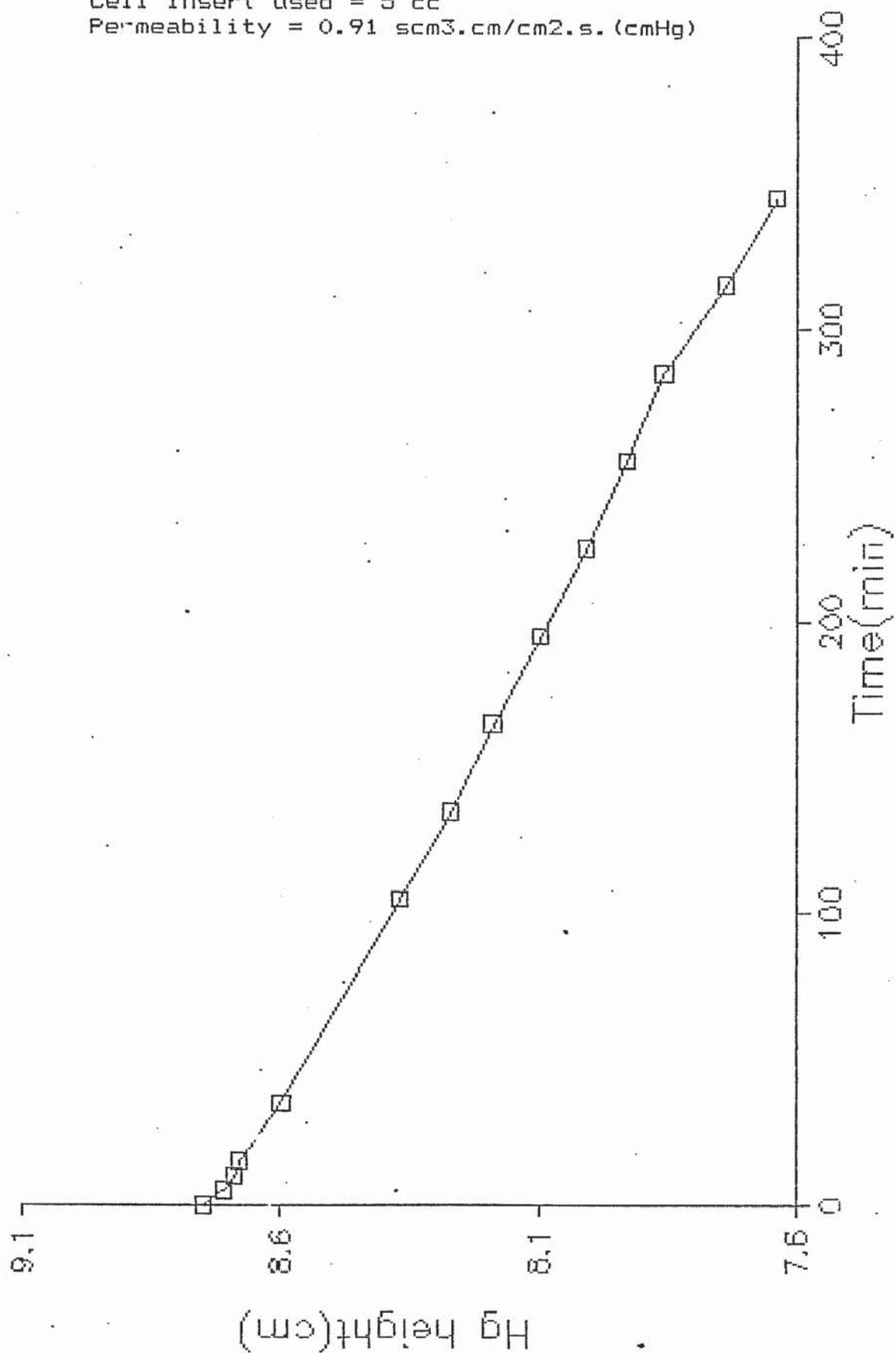
HYDROGEN/POLYETHERURETHANE

Membrane thickness = 0.50mm
Temperature of experiment = 20 C
Initial pressure of equipment = 0.40 mmHg
Cell insert used = 5 cc
Permeability = 6.22 scm³.cm/cm².s.(cmHg)



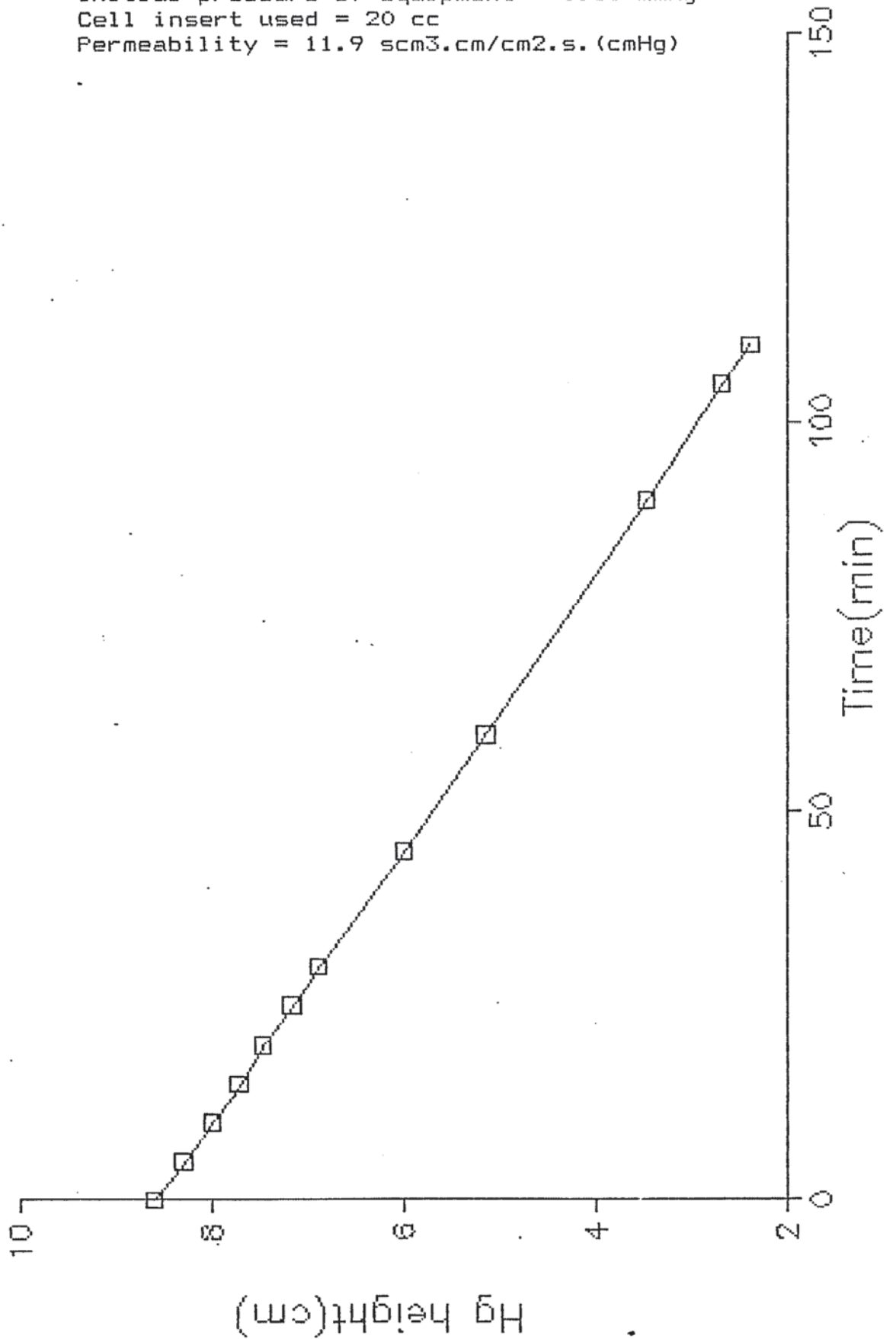
CARBON MON-OXIDE/POLYETHERURETHANE

Membrane thickness = 0.50mm
Temperature of experiment = 20 C
Initial pressure of equipment = 0.25 mmHg
Cell insert used = 5 cc
Permeability = 0.91 scm³.cm/cm².s.(cmHg)



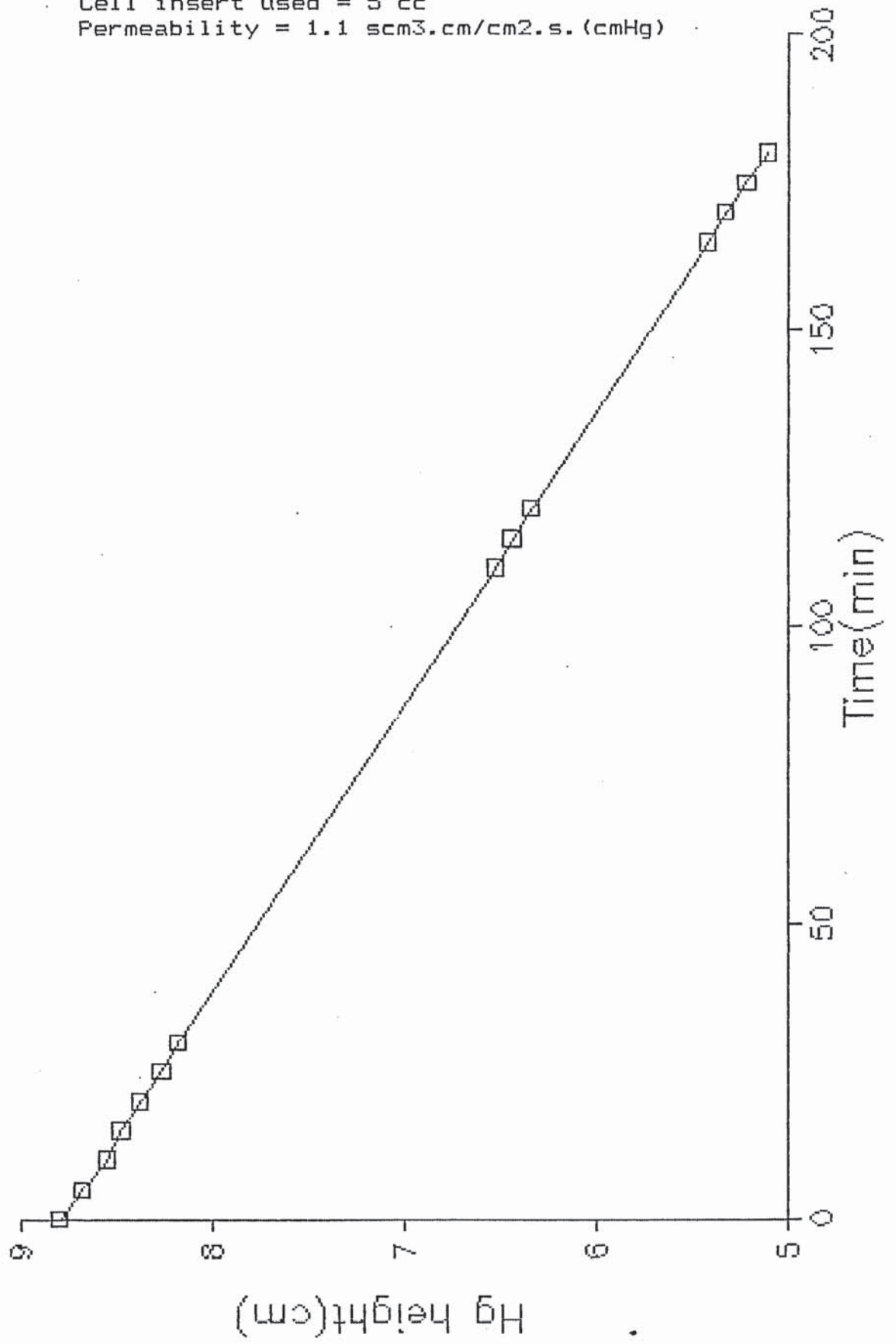
Membrane thickness = 0.09mm
Temperature of experiment = 20 C
Initial pressure of equipment = 0.30 mmHg
Cell insert used = 20 cc
Permeability = 11.9 scm³.cm/cm².s.(cmHg)

HYDROGEN/PTFE



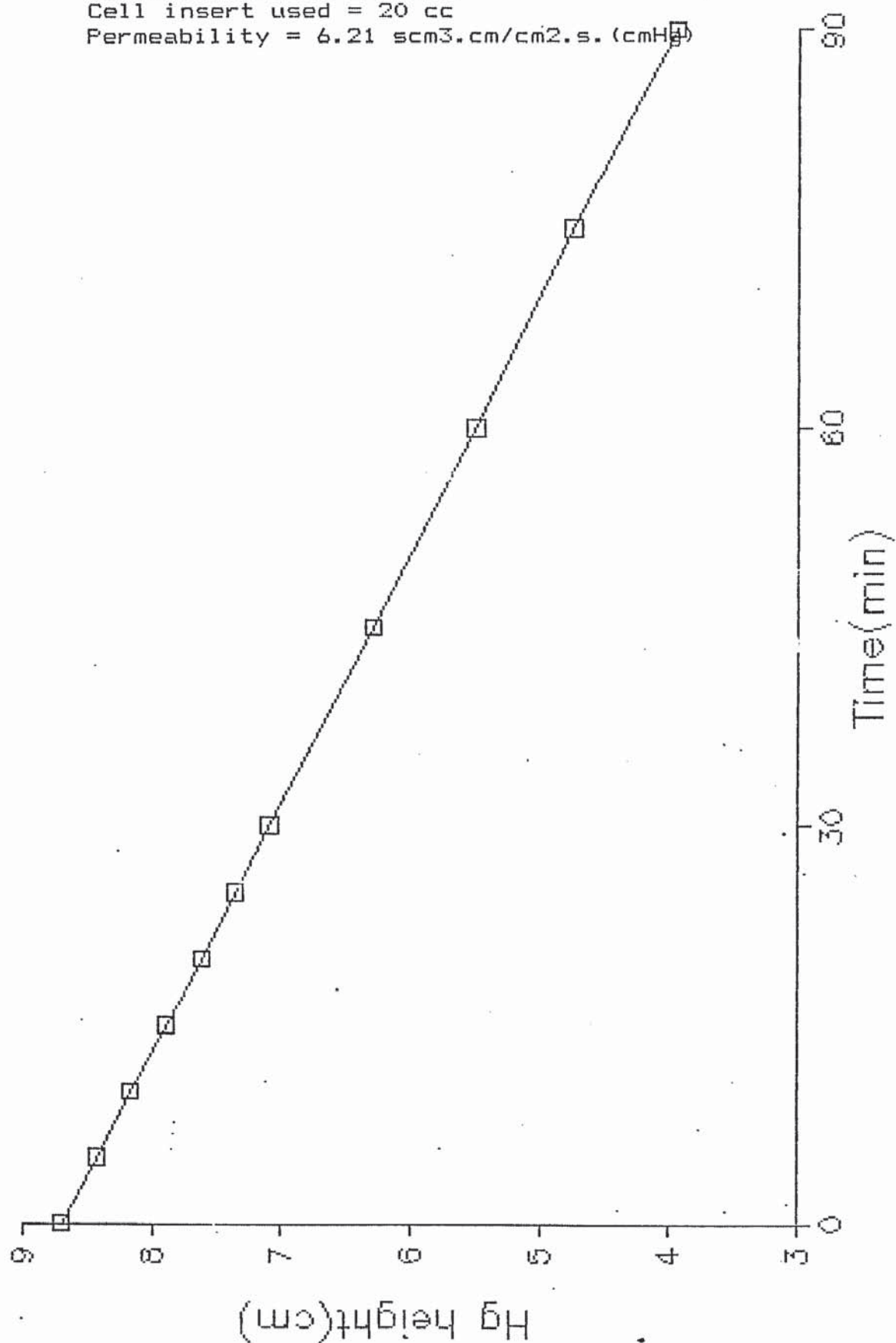
Membrane thickness = 0.09mm
Temperature of experiment = 18 C
Initial pressure of equipment = 0.30 mmHg
Cell insert used = 5 cc
Permeability = 1.1 scm³.cm/cm².s.(cmHg)

CARBON MON-OXIDE/PTFE



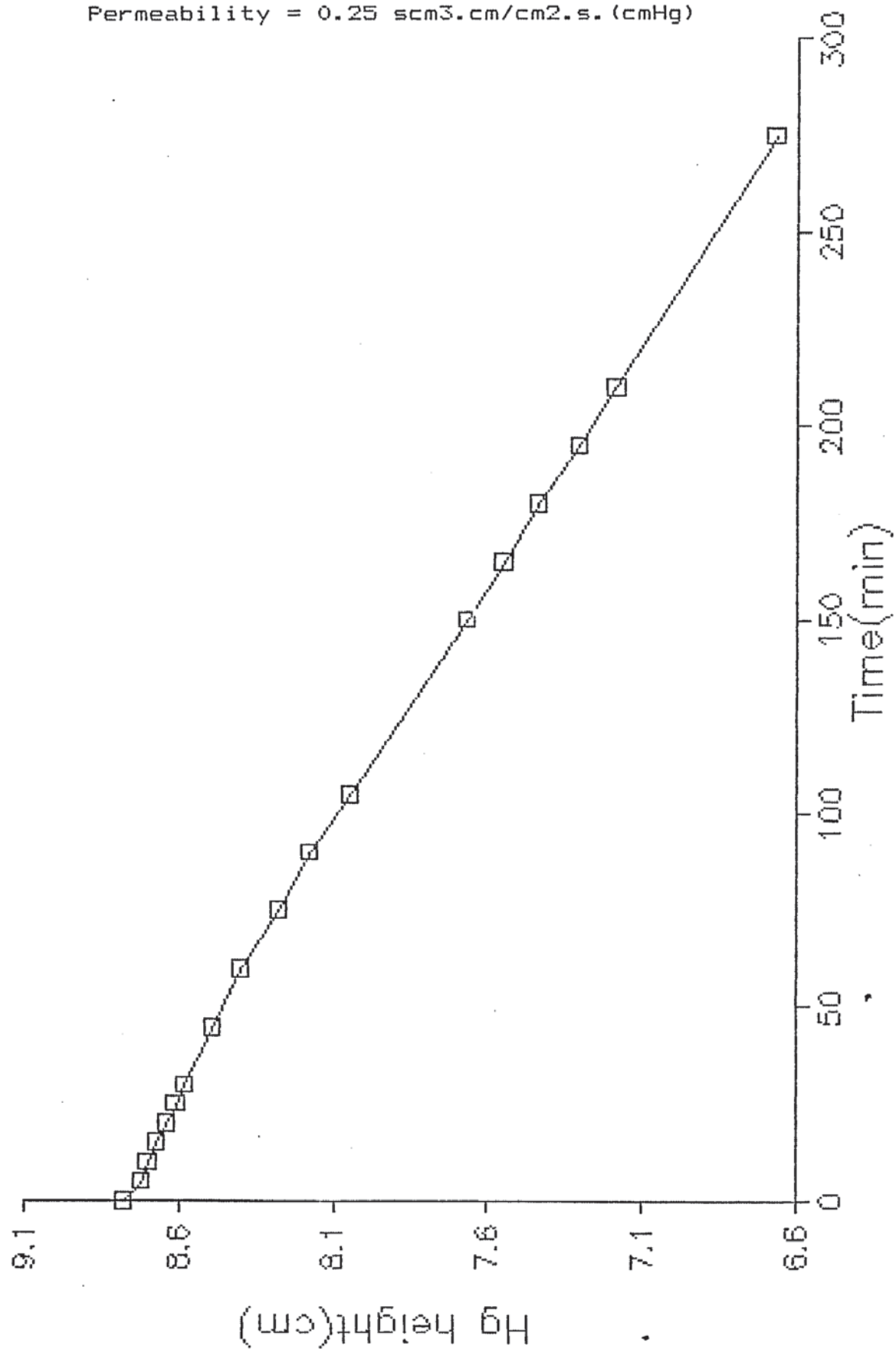
Membrane thickness = 0.05mm
Temperature of experiment = 18 C
Initial pressure of equipment = 0.20 mmHg
Cell insert used = 20 cc
Permeability = 6.21 scm³.cm/cm².s.(cmHg)

HYDROGEN/CELLULOSE DIACETATE



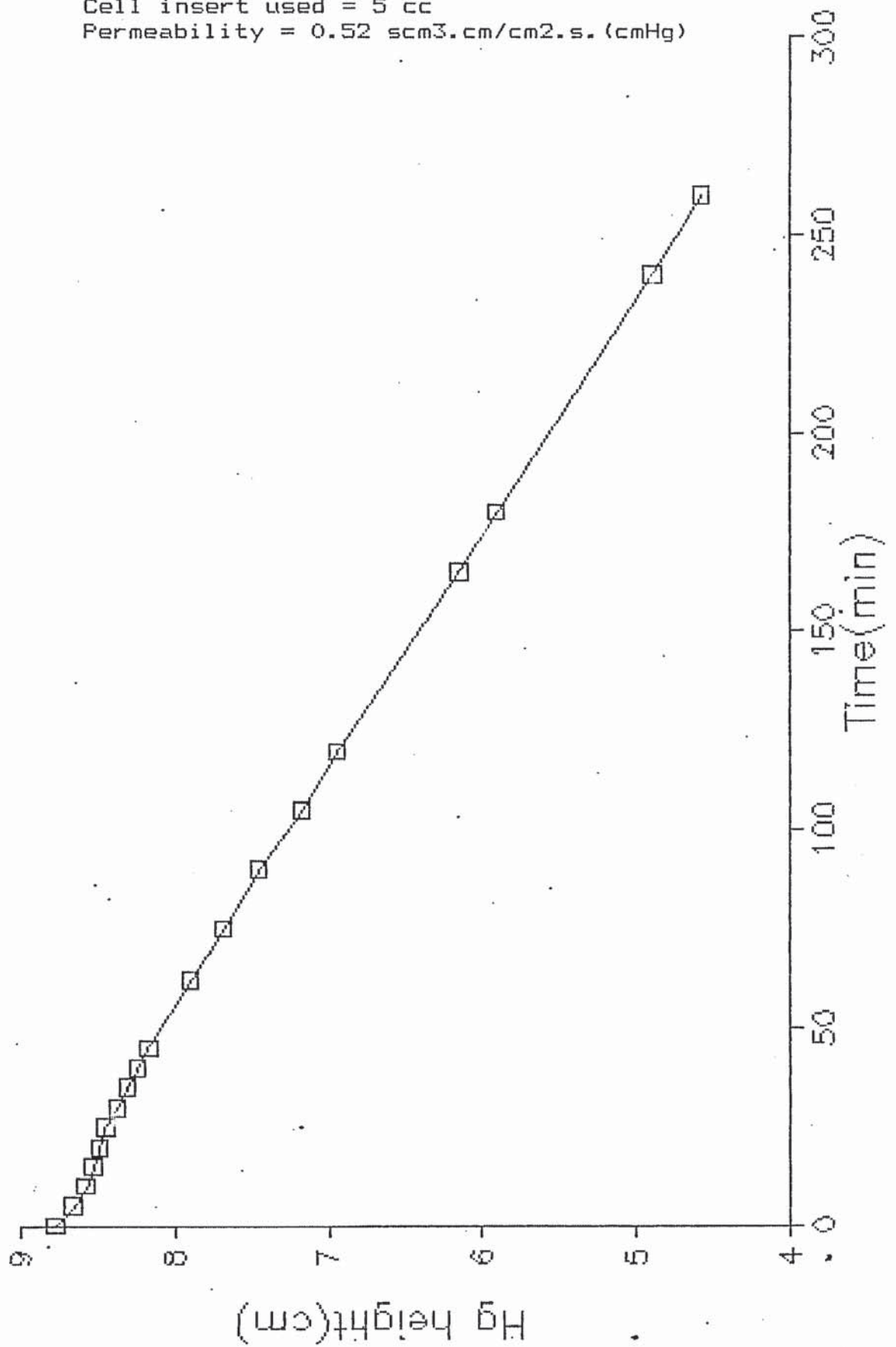
CARBON MON-OXIDE/CELLULOSE DIACETATE

Membrane thickness = 0.05mm
Temperature of experiment = 18 C
Initial pressure of equipment = 0.25 mmHg
Cell insert used = 5 cc
Permeability = 0.25 scm³.cm/cm².s.(cmHg)



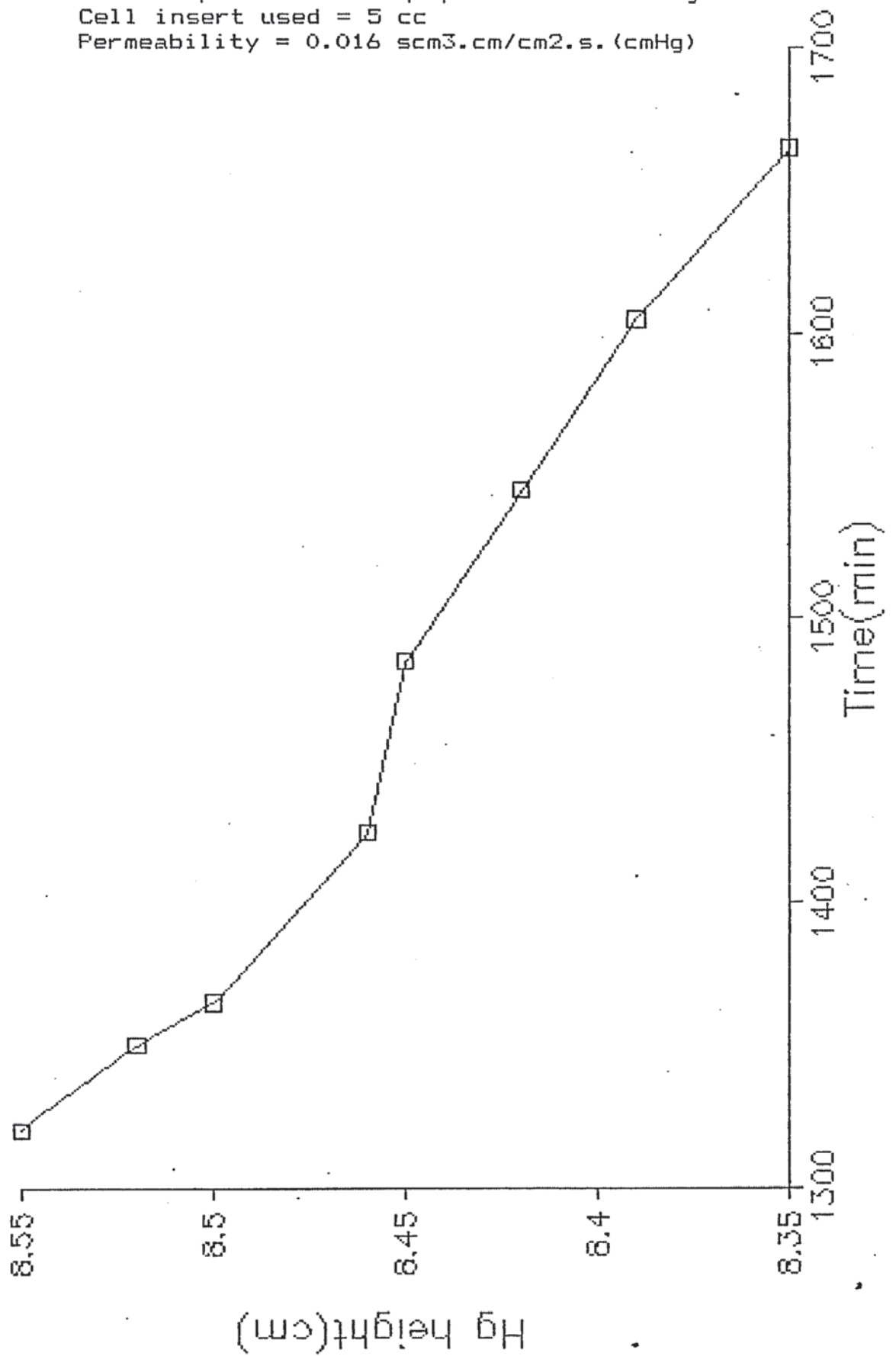
HYDROGEN/POLYIMIDE(TYPE R)

Membrane thickness = 0.05mm
Temperature of experiment = 19 C
Initial pressure of equipment = 0.20 mmHg.
Cell insert used = 5 cc
Permeability = 0.52 scm³.cm/cm².s.(cmHg)



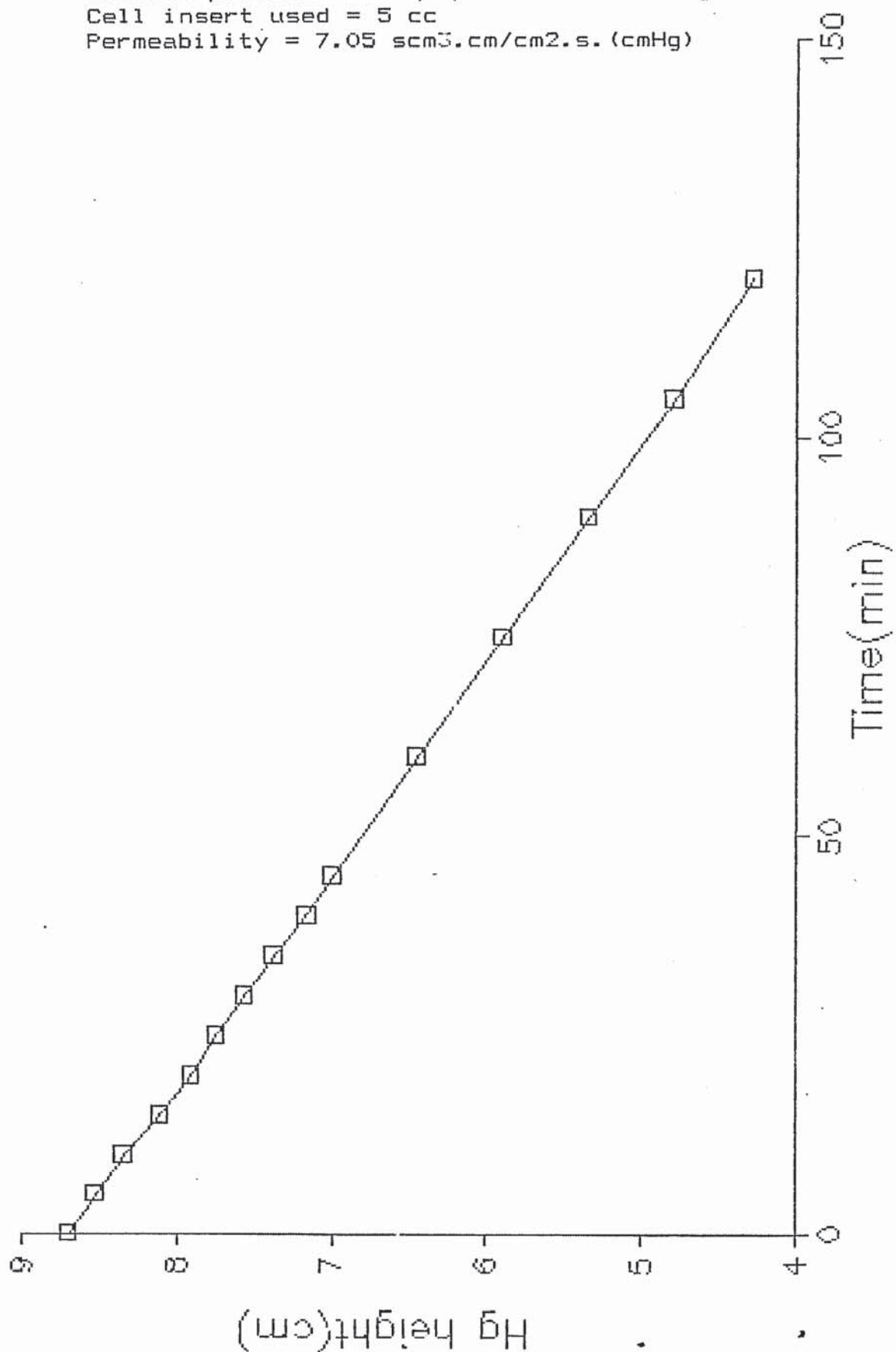
Membrane thickness = 0.05mm
Temperature of experiment = 19 C
Initial pressure of equipment = 0.20 mmHg
Cell insert used = 5 cc
Permeability = 0.016 scm³.cm/cm².s.(cmHg)

CARBON MON-OXIDE/POLYIMIDE(TYPE R)



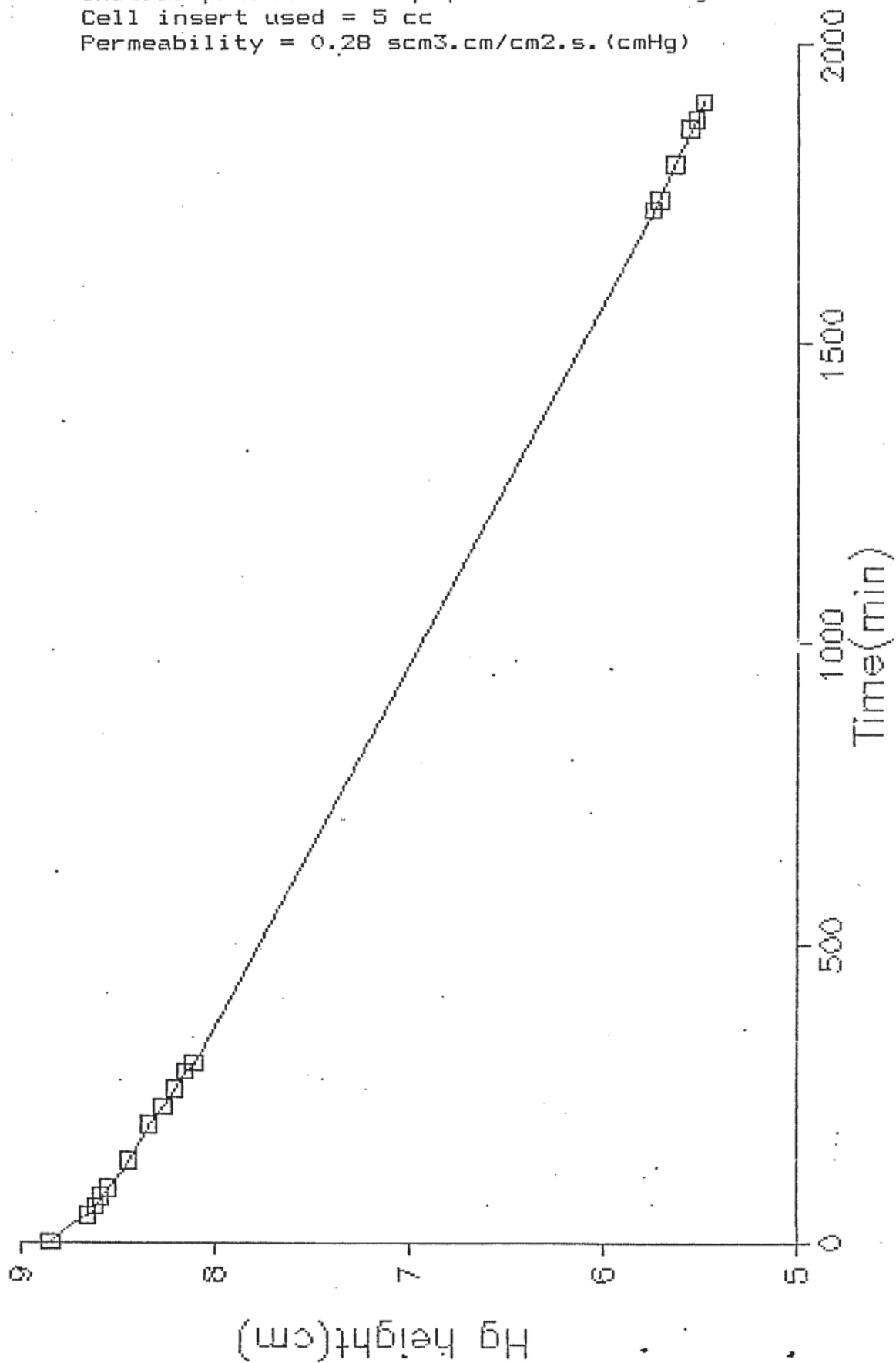
Membrane thickness = 0.31mm
Temperature of experiment = 20 C
Initial pressure of equipment = 0.25 mmHg
Cell insert used = 5 cc
Permeability = 7.05 scm³.cm/cm².s.(cmHg)

HYDROGEN/POLYCARBONATE



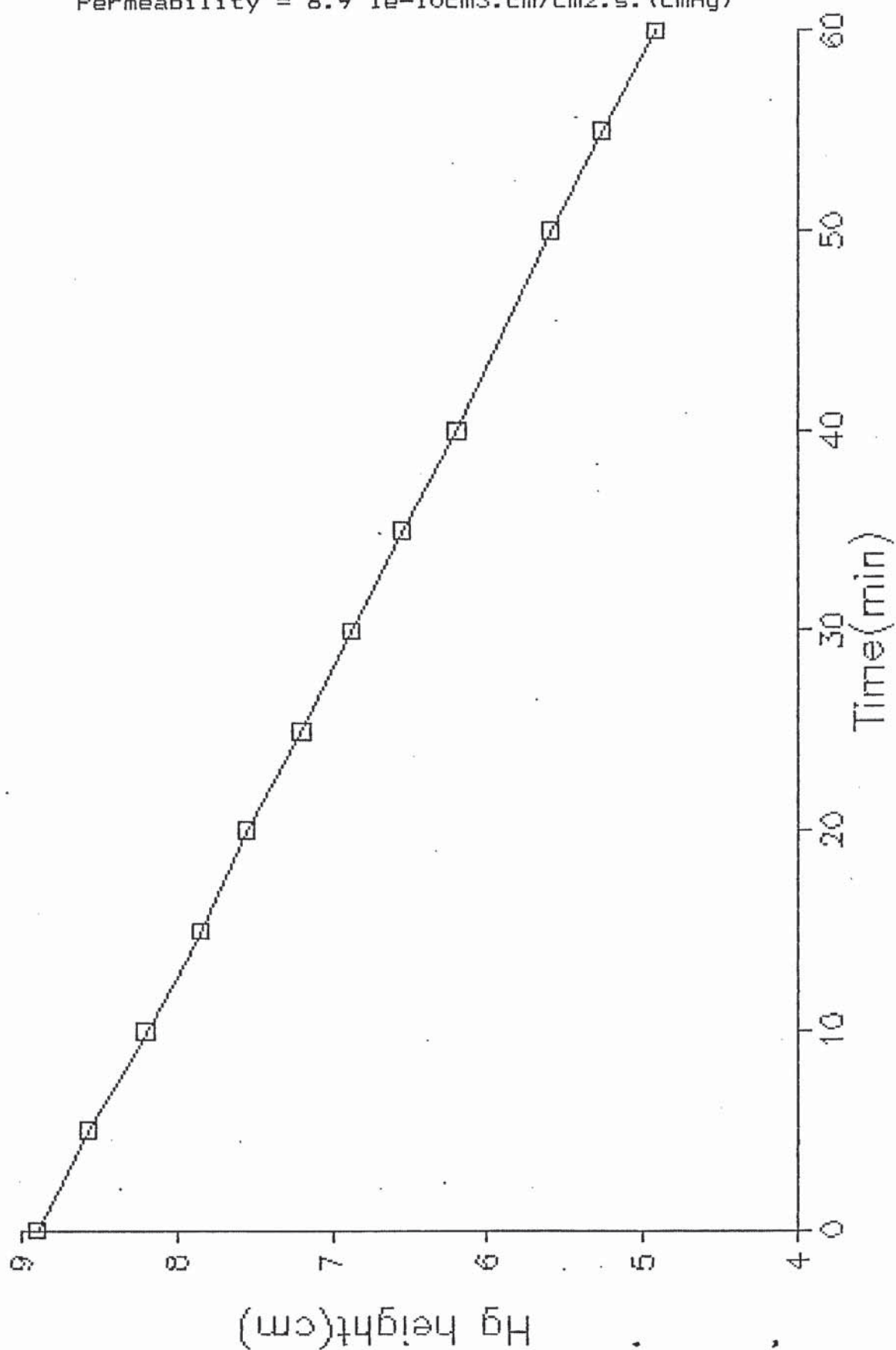
CARBON MON-OXIDE/POLYCARBONATE

Membrane thickness = 0.31mm
Temperature of experiment = 20 C
Initial pressure of equipment = 0.35 mmHg
Cell insert used = 5 cc
Permeability = 0.28 scm³.cm/cm².s.(cmHg)



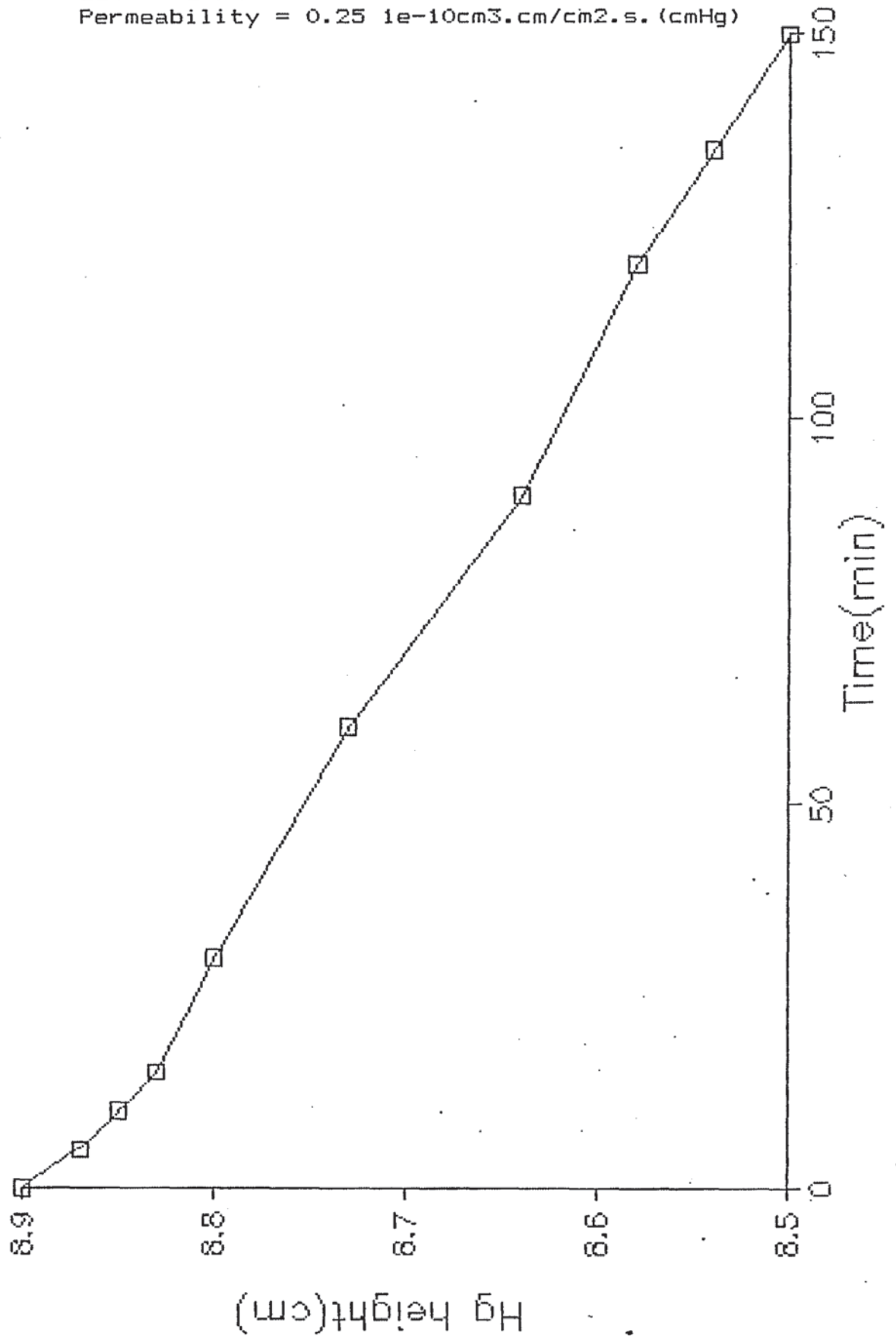
Membrane thickness = 0.085mm
Temperature of experiment = 16 C
Initial pressure of equipment = 0.95 mmHg
Cell insert used = 10 cc
Permeability = $6.9 \times 10^{-10} \text{ cm}^3 \cdot \text{cm} / \text{cm}^2 \cdot \text{s} \cdot (\text{cmHg})$

HYDROGEN/PMMA



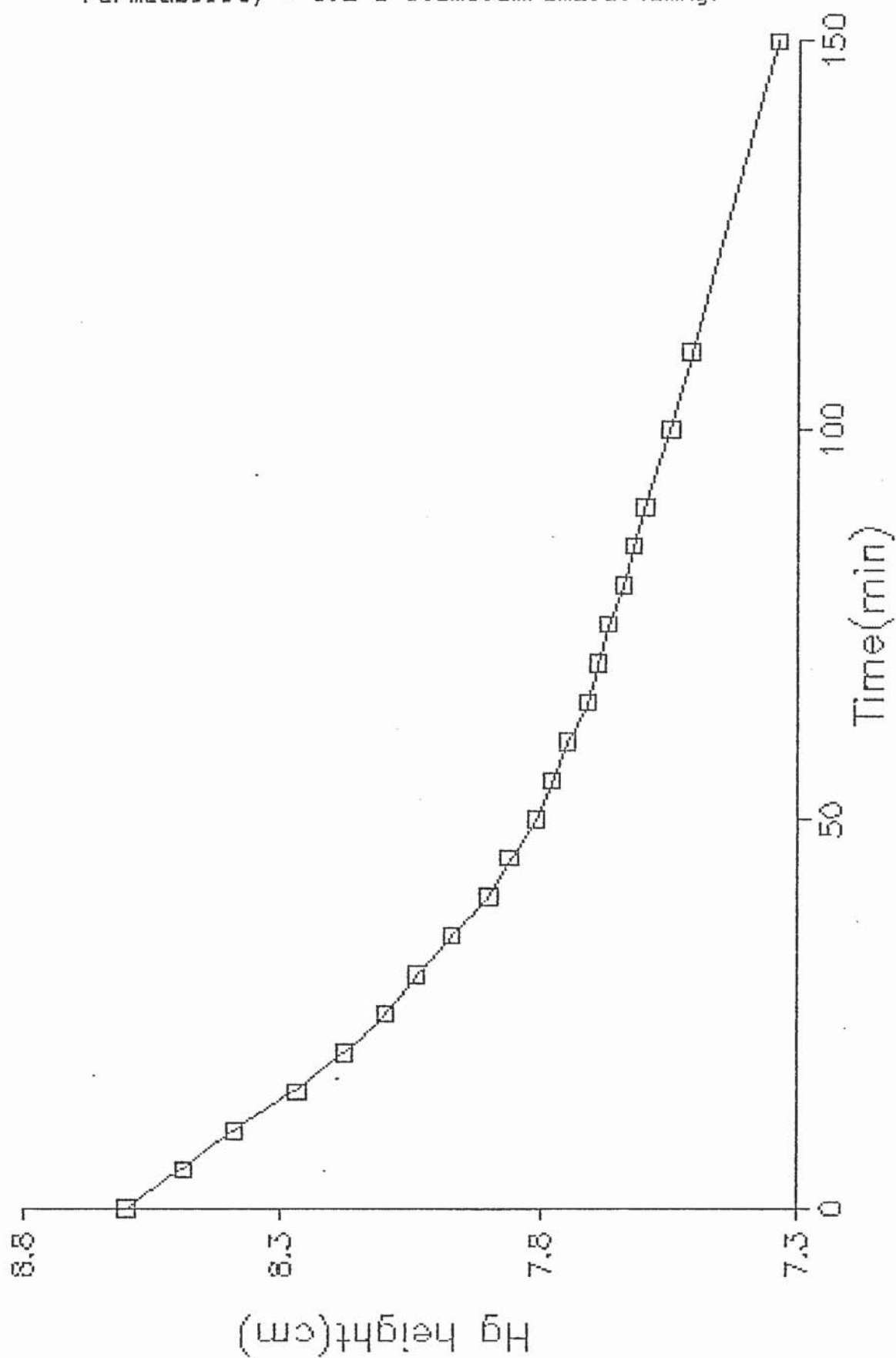
Membrane thickness = 0.085mm
Temperature of experiment = 16 C
Initial pressure of equipment = 0.95 mmHg
Cell insert used = 10 cc
Permeability = $0.25 \times 10^{-10} \text{ cm}^3 \cdot \text{cm} / \text{cm}^2 \cdot \text{s} \cdot (\text{cmHg})$

CARBON MON-OXIDE/PMMA



CARBON MON-OXIDE/MMA-SILOXY COPOLYMER

Membrane thickness = 1.05 mm
Temperature of experiment = 17 C
Initial pressure of equipment = 0.40 mmHg
Cell insert used = 5 cc
Permeability = $3.2 \times 10^{-10} \text{ cm}^3 \cdot \text{cm} / \text{cm}^2 \cdot \text{s} \cdot (\text{cmHg})$



Membrane thickness = 0.012mm

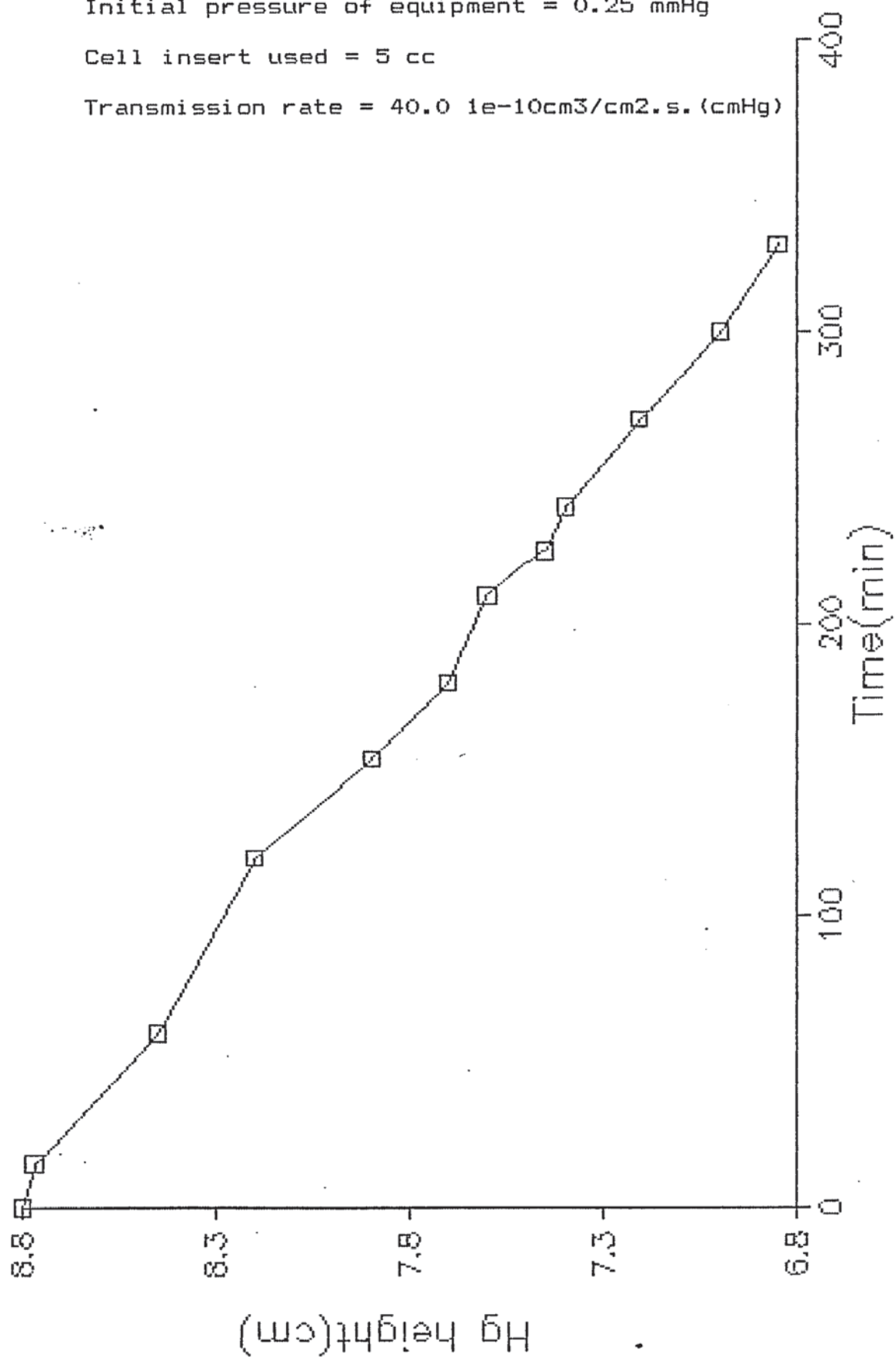
Temperature of experiment = 22 C

Initial pressure of equipment = 0.25 mmHg

Cell insert used = 5 cc

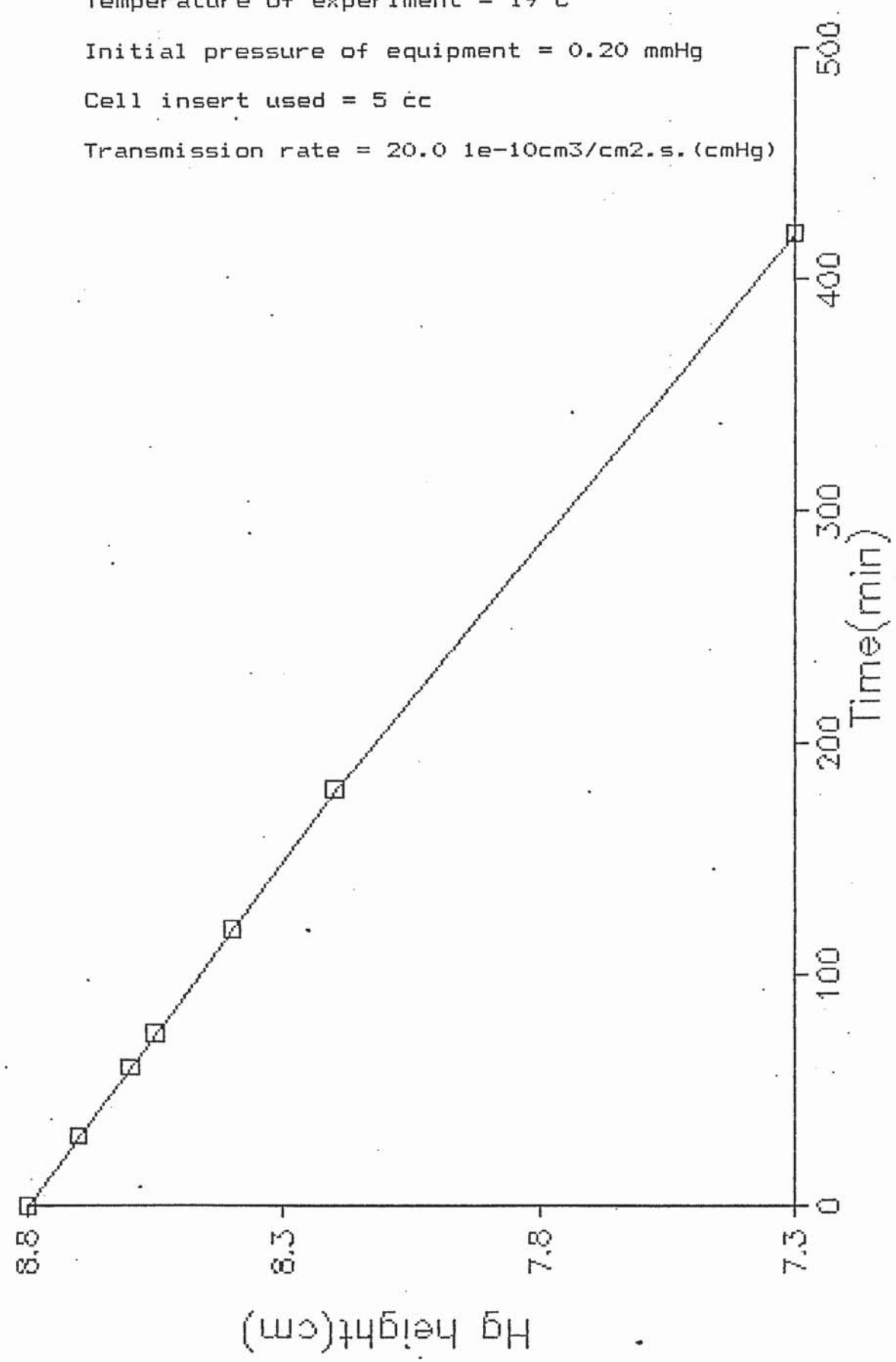
Transmission rate = $40.0 \times 10^{-10} \text{ cm}^3/\text{cm}^2 \cdot \text{s} \cdot (\text{cmHg})$

HYDROGEN/METALLISED PET



CARBON MON-OXIDE/METALLISED PET

Membrane thickness = 0.012mm
Temperature of experiment = 19 C
Initial pressure of equipment = 0.20 mmHg
Cell insert used = 5 cc
Transmission rate = $20.0 \times 10^{-10} \text{ cm}^3/\text{cm}^2 \cdot \text{s} \cdot (\text{cmHg})$



REFERENCES

1. Akagi, K., Shirakawa, H., Araya, K., Mukoh, A., Narahara, T., Polymer J. 19 (1) 185 (1987).
2. Allen, D. H., Page, R. C., Chem. Eng. pp 142 3rd March 1975.
3. Amerongen, van G. J., J. Appl. Phys. 17 972 (1946).
4. Amerongen, van G. J., J. Polymer Sci. 2 381 (1947).
5. Amerongen, van G. J., Rubb. Chem. Technol. 37 1065 (1964).
6. Amerongen, van G. J., J. Polymer Sci. 5 307 (1950).
7. Antonson, C. R., Gardener, R. J., King, C. F., Ko, D.Y., Ind. Eng. Chem. Proc. Des. Dev. 16 463 (1977).
8. Assink, R. A., J. Polymer Sci. Polymer Phys. Ed. 13 1665 (1975).

9. Aston University. Department of Chemical Engineering and Applied Chemistry, booklet on "Safety". 1/10/89.
10. Backhouse, I. W., Proceedings of the 4th B.O.C. Priestley Conference. Sept. 1986 pp 265-280.
11. Backhurst, J.R., Harker, J.H., "Process plant design." Heinemann Educational Books (London) 1973.
12. Baldus, W. and Tillman, D., Proceedings of the 4th B. O. C. Priestley Conference Sept. 1986. pp 26-42.
13. Barrer, R. M., Barrie, J. A., Slater, J., J. Polymer Sci. 27 177 (1958).
14. Barrer, R. M., Barrie, J. A., J. Polymer Sci. 28 377 (1958).
15. Barrer, R. M., Barrie, J. A., J. Polymer Sci. 23 315 (1957).
16. Barrer, R. M., Barrie, J. A., J. Polymer Sci. 23 311 (1957).
17. Barrer, R. M., Barrie, J. A., Slater, J., J. Polymer Sci. 27 177 (1958).
18. Barrer, R. M. & Chio, H. T., J. Polymer Sci. C10, 136 (1965).

19. Barrer, R. M., Chio, H. T., J. Polymer Sci. C10 111 (1966).
20. Barrie, J. A., Proceedings of the 4th B. O. C. Priestley Conference Sept. 1986 pp 89-113.
21. Barton, A. F. M., "Solubility Parameters". Chemical Reviews 75 731 (1975).
22. Battino, R., Clever, H. L., Chemical Reviews 66 395 (1966).
23. Battino, R., Evans, F. D., Danforth, W. F., Wilhelm, E., J. Chem. Thermodyn. 3 743 (1971).
24. Biegler, L. T., Grossmann, I. E., Reviews in Chem. Eng. 3 (1) 1 (1985).
25. Blaisdell, C. T., Kammermeyer, K., Chem. Eng. Sci. 28 1249 (1973).
26. Bolinger. et. al., Chem. Eng. Prog. 78 (10) 27 (1982).
27. Borneman, Z., Van't Hoff, J. A., Smolders, C. A., Van Veen, H. M., Proceedings of the 4th B. O. C. Priestley Conference Sept. 1986 pp 145-157.

28. Boucif, N., Majumdar, S., Sirkar, K. K., Ind. Eng. Chem. Fundam. 23 470 (1973).
29. Brandrup and Immergut. (Ed.) Polymer Handbook. 5th edition.
30. B.P. Chemicals. A5 project mass balance.
31. B. P. Chemicals cost curves.
32. B.P. Chemicals. File note S/NPB/FN/24/83 B. P. Chemicals.
33. Cifuentes, M., Lee, C. L., Chapman, H., Lee, K., Ulman, K., "Investigation of Structure-Permeability Relationships in Silicone Polymers".
34. Chern, R. T., Koros, W. J., Fedkiw, P. S., Ind. Eng. Chem. Proc. Des. Dev. 24 1015 (1985).
35. Chern, R. T., Koros, W. J., Sanders, E. S., Chen, S. H., Hopfenberg, H. B., "Industrial Gas Separations". pp 47-73 American Chemical Society (1983).
36. Chern, R. T., Koros, W. J., Sanders, E. S., Yui, R., J. Membrane Sci. 15 157 (1983).

37. Coady, A. B. et. al., Chem. Eng. Prog. 78 (10) 45 (1982).
38. Cooper, D. R., Law, A. M. G., & Tighe, B. J., Br. Polymer J. 5 163-182 (1973).
39. Coulson, J.M., Richardson, J.F., "Chemical Engineering." Vol. 2 and 3 3rd Edition. Pergamon Press 1978.
40. Cowie, J. M. G., "Polymers : Chemistry and Physics of Modern Materials". Intertext Books (1973).
41. Gas Permeability Apparatus, Serial No. GP 468/44, Davenport (London) Ltd., Welwyn Garden City, Herts.
42. Dubinin, M. M., Prog. Surf. Membrane Sci. 9 1 (1975).
43. East, G. C., McIntyre, J. E., Rogers and Senn, S. C., Proceedings of the 4th B. O. C. Priestley Conference Sept. 1986 pp 130-144.
44. Fedors, R. F., Polymer Eng. and Sci. 14 147 (1974).
45. Fedors, R. F., Polymer Eng. and Sci. 14 472 (1974).

46. Fenelon, P. J., *Polymer Eng. Sci.* 13 440 (1973).
47. Fleming, G. K. Koros, W. J., *Macromolecules.* 19 2285 (1986).
48. Gantzel, P. K., Merten, U., I and E. C. *Proc. Des. Dev.* 9 331 (1970).
49. Garder, R. J., Crane, R. A., and Hannan, J. F., *Chem. Eng. Prog.* 73 (11) 76 (1977).
50. Hakuta, T., Haraza, K., Obata, K., Shindo, Y., Ito, N., and Yoshitome, H., *Proceedings of the 4th B.O.C. Priestley Conference.* Sept. 1986 pp 281-290.
51. Haraya, K., Sindo, Y., Ito, N., Obata, K., Hakuta, T., Yoshitome, H., "Development of Hydrogen Separation Membranes for C1 Chemistry in Japan". *Membranes and Membrane Processes. Stresa Conference.*
52. Haraya, K., Hakuta, T., Yoshitome, H., *Sep. Sci. Technol.* 20 403 (1985).
53. Haselden, G. C., *Proceedings of the 4th B.O.C. Priestley Conference.* Sept. 1986 pp 201-217.
54. Hayduk, W., Buckley, W. D., *Can. J. Chem. Eng.* 49 667 (1971).

55. Hayduk, W., Cheng, S. C., Can. J. Chem. Eng. 48 93 (1970).
56. Henis, Tripodi, Sepn. Sci. and Technol. 15 1059 (1980).
57. Hercules Solubility Parameters.
58. Hirschfelder, J. O., Curtis, C. F., & Bird, R. B., "Molecular Theory of Gases and Liquids". John Wiley & Son Inc. N. Y. (1954).
59. Hogsett, J. E., Mazur, W. H., Hydrocarbon Processing. 52-54 Aug. (1983).
60. Holland, F.A., "Fluid Flow for Chemical Engineers." Edward Arnold. (1973)
61. Permeability of Plastic Films and Coatings to Gases, Vapours and Liquids. Edited by Hopfenberg, H. B., Plenum Press 1974.
62. Huckins, H. E., Kammermeyer, K., Chem. Eng. Prog. 49 294 (1953).
63. Hwang, S. T., Sep. Sci. 4 (2) 167-170 (1969).

64. Hwang, S. T., Yuen, K. H., Thorman, J. M., Sep. Sci. Technol. 15 1069 (1980).
65. Iler, L., Koros, W. J., Yang, K. K., Yui, R., "Sorption and transport of physically and chemically interacting penetrants in Kapton polyimide. Polyimides: Synth., Charact., Appl., (Proc. Tech. Conf. Polyimides). 1st Meeting 1982 Vol. 1. pp 443-460.
66. Iler, L., Koros, W. J., Hopfenberg, H. B., Am. Chem. Soc., Div. Polym. Chem. 24 (1) 102 (1983).
67. Iler, L., Koros, W. J., Yang, K. K., Yui, R., Polyimides: Synth. Charact. Appl. (Proc. Tech. Conf. Polyimides) 1st Meeting Date 1982 Vol 1 443-460 Edited by Mittal, K. L., Plenum, N. Y.
68. Ingeleby, S., Rossiter, A. P., Douglas, J. M., Chem. Eng. Res. Dev. 64 241 (1986).
69. International Critical Tables.
70. Jeffrey, A., "Mathematics for Engineers and Scientists." Nelson 1971.
71. Katayama, T., Nitta, T., J. Chem. Eng. Data. 21 194 (1976).

72. Kirkby, N. F., Proceedings of the 4th B.O.C. Priestley Conference. Sept. 1986 .pp 218-229.
73. Koros, W. J., J. Polymer Sci. Polymer Phys. Ed. 18 981-993 (1980).
74. Koros, W. J., Chern, R. T., Stannett, V., Hopfenberg, H. B., J. Polymer Sci. Polymer Phys. Ed. 19 1513 (1981).
75. Koros, W. J., J. Polymer Sci. Polymer Phys. Ed. 23 1611-1628 (1985).
76. Koros, W. J., Paul, D. P., "Current aspects of membrane based separation of gases". 16th annual international symposium. Michigan Molecular Inst., Midland, Aug. 1984.
77. Koros, W. J., Paul D. R., Rocha, A. A., J. Polymer Sci. Polymer Phys. Ed. 14 687 (1976).
78. Koros, W. J., Paul, D. R., J. Polymer Sci. Polymer Phys. Ed. 16 1947 (1978).
79. Krishne, R., Proceedings of the 4th B. O. C. Priestley Conference Sept. 1986 pp 64-88.

80. Kummins, C.A., (Ed.) "Transport Phenomena Through Polymer Films." Polymer Symposia 41. Wiley Interscience. (1973).
81. Industrial Processing with Membranes. Edited by Lacey, R. E., Loeb, S., Wiley Interscience. 1972.
82. Lane, V. O., Hydrocarbon Processing. pp. 58. Aug. 1983.
83. Lee, C. L., Chapman, H. L., Lifuentes, M. E., Lee, K. M., Merrill, L. D., Ulman, K. C., and Venkutaranan. Proceedings of the 4th B.O.C. Priestley Conference. Sept. 1986 pp 364-381.
84. Lonsdale, H. K., J. Membrane Sci. 10 81 (1982).
85. Loverly, B. W., and O'Hair, J. G., Proceedings of the 4th B.O.C. Priestley Conference. Sept. 1986 pp 291-310.
86. MacLean, D. L., and Graham, T. E., Chem. Eng. 87 (4) 54 (1980).
87. Maclean, D. L., Proceedings of the 4th B.O.C. Priestley Conference Sept. 1986 pp 382-398.
88. McCandless, F. P., J. Membrane Sci. 24 15 (1985).

89. McCandless, F. P., *Ind. Eng. Chem. Proc. Des. Dev.* 11 (4) 470 (1972).
90. McReynolds, K. B., *Proceedings of the 4th B.O.C. Priestley Conference*
Sept. 1986 pp 342-350.
91. Matson, S. L., Lopez, J., Quinn, J. A., *Review Article No. 13*, 503-524.
92. Mazur, W. H. et. al., *Chem. Eng. Prog.* 78 (10) 38 (1982).
93. Mears, P., *J. Am. Chem. Soc.* 76 3415 (1954).
94. Meares, P., *Trans. Faraday Soc.* 53 101 (1957).
95. Meares, P., *Proceedings of the 4th B. O. C. Priestley Conference.*
16th-18th September 1986. pp 1-25.
96. Mercea, P., Muresan, L., Mecca, V., Silipas, D., *J. Membrane Sci.* 35
291 (1988).
97. Michaels, A. S., Vieth, W. R., Barrie, J. A., *J. Appl. Phys.* 34 1 (1963).
98. Michaels, A. S., Vieth, W. R., Barrie, J. A., *J. Appl. Phys.* 34 13 (1963).

99. Michaels, A. S., Bixler, H., "Progress in Separation and Purification".
Vol 1 pp 143-185 Edited by Perry, E. S., Interscience (1968).
100. Michaels, A. S., Bixler, H. J., J. Polymer Sci. 50 413 (1961).
101. Moore, W.J., "Physical Chemistry." 5th Edition. Longman. (1972).
102. Nakamura, A., Hotta, M., Chem. Economy and Eng. Review 17 (No. 7-8)
42 (1985).
103. Nakaqawa, T., Proceedings of the 4th B.O.C. Priestley Conference Sept.
1986 pp 351-363.
104. Naylor, R. W., Backer, P.O., A.I.Ch.E. Journal. 1 95-99 (1955).
105. Norton, F. J., J. Appl. Polymer Sci. 7 1649 (1963).
106. O'Brien, K. C., Koros, W. J., Barbari, T. A., Sanders, E. S., J. Membrane
Sci. 29 229 (1986).
107. O'Brien, K. C., Koros, W. J., Barbari, T. A., Sanders, E. S., J. Membrane
Sci. 29 229 (1986).

108. Ogden, I. K., Richards, R. E. and Rizvi, A. A., Proceedings of the 4th B.O.C. Priestly Conference Sept. 1986 pp 114-129.
109. Ohno, M., Heki, H., and Ozaki, O., J. Nucl. Sci. Technol. 15 (9) 516 (1978).
110. Pan, C. Y., A.I.Ch.E. Journal. 29 545 (1983).
111. Pan, C. Y., Habgood, H. W., Can. J. Chem. Eng. 56 210 (1978).
112. Pastemak, R. A., Christenson, M. V., Heller, J., Macromolecules 3 366 (1970).
113. Pearce, D., Cooper, G. B., Holford, R., & Fogg, P. H., "Carbon Mon-oxide : A Study of Manufacture and Technology". B. P. Chemicals report number CH/200/292.
114. Peinemann, K. V., Ohlnogge, K., and Knauth, H. D., Proceedings of the 4th B.O.C. Priestley Conference Sept. 1986 pp 329-341.
115. Perry, R. H. and Chilton, C. H., (Ed.) Chemical Engineers Handbook. Section 14. 5th Edition. McGraw-Hill.
116. Perry, R. H. and Chilton, C. H., (Ed.) Chemical Engineers Handbook. Section 17. 5th Edition. McGraw-Hill.

117. Perry, R. H. and Chilton, C. H., (Ed.) Chemical Engineers Handbook. Section 25. 5th Edition. McGraw-Hill.
118. Polymer Eng. & Sci. 27 603 (1987).
119. Porter, K. E., & Jenkins, J., Distillation Supplement. TCE pp 23-27 (Sept. 1987).
120. Powell, T. E., Chemical Engineering. pp 187 Nov. 1985.
121. Pye, D. G., Hoehn, H. H., Panar, M., J. Appl. Polymer Sci. 20 287 (1976).
122. Pye, D. G., Hoehn, H. H., Panar, M., J. Appl. Polymer Sci. 20 1921 (1976).
123. Ranade, G., Stannett, V. T., Koros, W. J., J. Appl. Polymer Sci. 25 (10) 2179 (1980).
124. Rautenbach, R., Dahm, W., Chem. Eng. Process. 21 141 (1987).
125. Rogers, C. E., "Solubility and Diffusivity". Physics and Chemistry of the Organic Solid State. Vol. 2 Ch. 6. Interscience (1965).

126. Permselective Membranes. Edited by Rogers, C. E., Marcel-Dekker Inc., N. Y. 1971.
127. Russel, F. G., Hydrocarbon Processing. pp. 55. Aug. 1983.
128. Salame, M., Polymer Eng. and Sci. 26 (22) 1543 (1986).
129. Salame, M., S. P. E. Transactions. Oct. 1961. pp 153-163.
130. Saltonstall, C. W., J. Membrane Sci. 32 185 (1987).
131. Sanders, E. S., Koros, W. J., Hopfenberg, H. B., Stannett, V. T.
J. Membrane Sci. 18 53 (1984).
132. Sanders, E. S., Koros, W. J., J. Polymer Sci. Polymer Phys. Ed. 24 175
(1986).
133. Sanders, E. S., Koros, W. J., Hopfenberg, H. B., Stannett, V. T.,
J. Membrane Sci. 18 53 (1984).
134. Sanders, B., Skjold-Jordensen, S., Rasmussen, P., Fluid Phase
Equilibria 11 105 (1983).
135. Schell, W. J. et. al., Chem. Eng. Prog. 78 (10) 33 (1982).

136. Schendel, R. L. et. al., Hydrocarbon Processing 62 (8) 58 (1983).
137. Schendal, R. L., Proceedings of the 4th B.O.C. Priestly Conference. Sept. 1986 pp 311-328.
138. Simril, V. L., Herschberger, A., Modern Plastics. 27 (11) 95 (1950).
139. Sirkar, K. K., Sep. Sci. Technol. 13 165 (1978).
140. Sithiosoth, S., PhD. Thesis "The Molecular Design of a New Solvent for the Absorption of Carbon Dioxide." Aston University (Sept. 1986).
141. Sourirajan, S., "Reverse Osmosis". Logos Press, London. pp 580 (1970).
142. Stallworthy, E. A., T. C. E. pp 182 June 1970.
143. Stanley, M., Proceedings of the 4th B. O. C. Priestley Conference. Sept. 1986 pp 161-174.
144. Stannett, V. T., Szwarc, M., J. Polymer Sci. 16 89 (1955).

145. Stannett, V., "Diffusion in Polymers". pp 41-73 Edited by Crank, J. and Park, G. S., Academic Press (1968).
146. Stern, S. A., Walawender, W. P., Sep. Sci. 4 129 (1969).
147. Stern, S. A., De Meringo, A. H., J. Polymer Sci. Polymer Phys. Ed. 16 735 (1978).
148. Stern, S. A., "Gas Permeation Processes". Industrial Processing With Membranes. Ch. 13. Edited by Lacey, R. E. and Loeb, S., Wiley-Interscience (1972).
149. Stern, S. A., Sen, S. K., Rao, A. K., J. Macromol. Sci. Phys. B10 (3) 507 (1974).
150. Stern, S. A., Frisch, H. L., Ann. Rev. Mater. Sci. 11 523 (1981).
151. Stern, S. A., Shah, V. M., and Hardy, B. J., Proceedings of the 4th B. O. C. Priestley Conference. Sept. 1986 pp 158-160.
152. Taylor, G.A., "Organic Chemistry." 2nd Edition. Longman. (1978).
153. Tennent, R.M., "Science Data Book." Oliver and Boyd. (1971).

154. Thorman, J. M., Hwang, S. T., Chem. Eng. Sci. 33 15 (1978).
155. Thorman, J. M., Rhim, H., Hwang, S. T., Chem. Eng. Sci. 30 751 (1975).
156. Tighe, B. J., Lecture Course : "Structure/Property Relations of Polymers". Aston University (Oct. to Dec. 1987).
157. Tighe, B. J., & Kishi, M., Contact Lens Monthly. pp 21-28 (5/8/1988).
158. Toi, K., Morel, G., Paul, D. R., J. Appl. Polymer Sci. 27 2297 (1982).
159. Vieth, W. R., Alcalay, H. H., Frabetti, A. J., J. Appl. Polymer Sci. 8 2125 (1964).
160. Vieth, W. R., Eilenberg, J. A., J. Appl. Polymer Sci. 16 945 (1972).
161. Walawender, W. P., Stern, S. A., Sep. Sci. 7 553 (1972).
162. Ward, W. J. et. al., J. Membrane Sci. 1 99 (1976).
163. Warn, J.R.W., "Concise Chemical Thermodynamics." Von Nostrand Reinhold. (London). (1969).

164. Waters, J. A., Mortimer, G. A., Clement, H. E., J. Chem. Eng. Data. 15 174 (1970).
165. Weller, S., Steiner, W. A., Chem. Eng. Prog. 46 585 (1950).
166. Werner, U., Proceedings of the 4th B. O. C. Priestley Conference. Sept. 1986. pp 43-63.
167. Wilcock, R. J., Battino, R., Danforth, W. F., Wilhelm, E., J. Chem. Thermodyn. 10 817 (1978).
168. Wilhelm, E., Battino, R., "Thermodynamic functions of the solubilities of gases in liquids at 25°C. Chemical Reviews 73 (Feb. 1973).
169. Wilson, G.T., Brit. Chem. Eng. and Proc. Tech. 16 (10) 931 (1971).
170. Yang, D. K., Koros, W. K., Hopfenberg, H. B., Stannett, V. T., J. Appl. Polymer Sci. 30 1035 (1985).
171. Yang, D. K., Koros, W. J., Hopfenberg, H. B., Stannett, V. T., J. Appl. Polymer Sci. 31 1619 (1986).
172. Yasuda, H., Rosengren, K., J. Appl. Polymer Sci. 14 1839 (1970).
173. Zevnik, F. C., Buchanan, R. L., Chem. Eng. Prog. 59 (2) 70 (1963).